UNIVERSITY OF ICELAND

Ph.D. Thesis

in Earth Sciences

The Effects of Long-term Cessation of Grazing on Carbon Dynamics in Icelandic Grassland and Heathland

Christian Klopsch

June 2026

FACULTY OF EARTH SCIENCES

The Effects of Long-term Cessation of Grazing on Carbon Dynamics in Icelandic Grassland and Heathland

Christian Klopsch

Dissertation submitted in partial fulfilment of a
Philosophiae Doctor degree in Earth Sciences

Ph.D. Committee
Anna Guðrún Þórhallsdóttir
Áslaug Geirsdóttir
Björn Þorsteinsson
René van der Wal
Richard D. Bardgett

Opponents
Sari Stark
Thomas C. Parker

Faculty of Earth Sciences
School of Engineering and Natural Sciences
University of Iceland
Reykjavik, June 2026

The Effects of Long-term Cessation of Grazing on Carbon Dynamics in Icelandic Grassland and Heathland
Dissertation submitted in partial fulfilment of a *Ph.D.* degree in Earth Sciences

Faculty of Earth Sciences
School of Engineering and Natural Sciences
University of Iceland
Askja, Sturlugata 7
101, Reykjavik
Iceland

Telephone: 525 4000

Bibliographic information:
Christian Klopsch, 2026, *The Effects of Long-term Cessation of Grazing on Carbon Dynamics in Icelandic Grassland and Heathland*, PhD dissertation, Faculty of Earth Sciences, University of Iceland, 205 pp.

Author ORCID: 0009-0007-3750-3954
ISBN: 978-9935-9877-2-3

Printing: Háskolaprent
Reykjavik, Iceland, June 2026

Abstract

Large herbivores are increasingly recognised as key regulators of terrestrial carbon cycling, yet empirical evidence on how long-term cessation of grazing alters carbon dynamics and storage remains limited. The aim of this PhD research is to investigate how multi-decadal cessation of grazing influences carbon fluxes and storage in sub-arctic grassland and heathland ecosystems. The study uses a network of grazer exclosures established 20-83 years ago across 34 sites in Iceland, with paired continuously grazed land. Growing-season CO_2 exchange was quantified through extensive chamber-based flux measurements and NDVI data, and carbon storage and pathways in the plant–soil system were assessed using 201 soil profiles to 60 cm depth. The study results show that across sites, long-term cessation of grazing was associated with a 37% lower growing-season net CO_2 uptake and lower vegetation greenness relative to grazed land. In topsoil (0–10 cm), soil organic carbon stocks were 8% lower in exclosures, accompanied by 21% lower fine-root biomass, while root functional traits remained largely unchanged. Grazed grassland retained both the highest net CO_2 uptake and largest SOC stocks. Cessation of grazing caused a transition toward heathland at several grassland sites, associated with lower productivity and carbon sequestration while it had more limited effects in long-established heathlands. Collectively, the findings demonstrate that sustained extensive grazing maintains higher carbon turnover, enhances below-ground carbon inputs, and supports long-term SOC storage in sub-arctic grassland. This dissertation provides comprehensive empirical evidence that grazing can function as a nature-based solution for preserving carbon sinks in sub-arctic ecosystems.

Útdráttur

Áhrif langtíma beitarfriðunar á kolefnisbúskap graslendis og mólendis í íslenskum láglendisúthaga.

Rannsóknir og áhugi á áhrifum og mikilvægi stórra grasbíta í kolefnishringrás vistkerfa hefur aukist verulega á undanförnum árum, þó beinar rannsóknir á áhrifum langtímabeitar hafi skort, einkum á norðlægum slóðum. Á Íslandi hefur úthagabeit lengi verið umdeild og áhersla lögð á að friða land, þrátt fyrir að rannsóknir á áhrifum beitarfriðunar hafi verið takmarkaðar. Markmið þessarar rannsóknar var að skoða áhrif langtíma beitarfriðunar á kolefnisbúskap íslensks láglendisúthaga. Kolefnishringrás langtíma beitarfriðunar (20-83 ár) var rannsökuð og borin saman við kolefnishringrás samliggjandi beitarsvæða á 34 völdum svæðum víðs vegar um landið. Gerðar voru meira en 2400 mælingar á CO_2-flæði og blaðgrænu (NDVI). Kolefnisferli í jarðveginum var rannsakað út frá magni jarðvegskolefnis (SOC), köfnunarefni, rótarmagni og rótareiginleikum í 201 jarðvegssniði (0-60 cm). Niðurstöðurnar sýna að beitarfriðun leiddi til minni (-37%) kolefnisupptöku yfir vaxtartímann og var munurinn meiri í graslendi en mólendi. Magn jarðvegskolefnis var einnig minna (-8%) auk þess sem magn fínna róta, sem mælikvarði á uppsöfnun jarðvegskolefnis, var 21% minna á meðan rótabygging hélst svipuð í beittum og friðuðum svæðum. Beitarfriðun hafði almennt meiri áhrif í graslendi en mólendi og sérstaklega þar sem langtíma beitarfriðun leiddi til gróðurbreytinga, frá graslendi til mólendis. Þegar á heildina er litið sýna þessar niðurstöður að beit örvar kolefnisupptöku og eykur kolefnisbindingu í jarðvegi graslendis og mólendis í íslenskum láglendisúthaga.

Preface

This dissertation builds on the conceptual foundation of the research project ‘ExGraze’, led by Anna Guðrún Þórhallsdóttir. The ExGraze project originally developed the methodological framework to map and explore how grasslands and heathlands are changing in long-term grazer exclosures which was then applied and refined in this dissertation. Thanks to the knowledge and resources that were assembled in the ExGraze project, it was possible to identify the study sites, my dissertation is based on. Raw data and analysis scripts generated throughout this PhD project have been made publicly available in the ZENODO data repository, see Klopsch *et al.* (2026a).

Table of Contents

List of Figures

List of Tables

List of Publications and planned Submissions

Article 1: Klopsch, C., Thorhallsdottir, A.G., van der Wal, R., Bardgett, R.D., Thorsteinsson, B., Geirsdottir, A., 2026. Long-term cessation of grazing reduces net carbon uptake in northern grassland and heathland. Agriculture, Ecosystems & Environment 407, 110441. https://doi.org/10.1016/j.agee.2026.110441

Contribution of the author in Article 1: I drafted the original manuscript, co-organised and conducted the field data collection, let the formal data analysis, curate the data and contributed to funding acquisition. The conceptualisation and methodology of the study was developed by Anna Guðrún Þórhallsdóttir in the context of the ExGraze project. Anna Guðrún Þórhallsdóttir, Björn Þorsteinsson and I organised and conducted the study site selection and developed the methodology for the field data collection. All co-authors contributed with validation of the methodology and reviewing and editing of the original manuscript, and I revised the final version.

Article 2: Klopsch, C., Thorhallsdottir, A.G., Thorsteinsson, B., Gudmundsson, J., Bardgett, R., Van Der Wal, R., Geirsdottir, A.: Upscaling of net CO_2 flux with ground-based and satellite-derived NDVI in Icelandic grassland, *in prep.*

Contribution of the author in Article 2: I drafted the original manuscript, co-organised and conducted the field data collection, let the formal data analysis, curate the data and contributed to funding acquisition. Anna Guðrún Þórhallsdóttir, Björn Þorsteinsson and I organised and conducted the study site selection and prepared the methodology for the field data collection. Jón Guðmundsson contributed additional data to the study. All co-authors contributed with validation of the methodology and reviewing and editing of the original manuscript, and I revised the final version.

Article 3: Klopsch, C., Thorhallsdottir, A.G., Thorsteinsson, B., Bardgett, R., Van Der Wal, R., Geirsdottir, A.: Sustained grazing is essential for soil carbon sequestration and ecosystem stability in sub-arctic grassland, Global Change Biology Communications, *in review*.

Contribution of the author in Article 3: I drafted the original manuscript, organised and conducted the sample processing in the laboratory, let the formal data analysis, curate the data and contributed to funding acquisition. The conceptualisation and methodology of the study was developed by Anna Guðrún Þórhallsdóttir in the context of the ExGraze project. Anna Guðrún Þórhallsdóttir, Björn Þorsteinsson and I organised and conducted the study site selection, methodology and the field data collection. Richard Bardgett provided facilities for carbon and nitrogen analysis. All co-authors contributed with validation of the methodology and reviewing and editing of the original manuscript, and I revised the final version.

Article 4: Klopsch, C., Thorhallsdottir, A.G., Thorsteinsson, B., Bardgett, R., Van Der Wal, R., Geirsdottir, A.: Grazing abandonment in Iceland: unearthing the consequences for root biomass and community-level root functional traits, Plant and Soil, *in review*.

Contribution of the author in Article 4: I drafted the original manuscript, organised and conducted the sample processing in the laboratory, let the formal data analysis, curate the data and contributed to funding acquisition. The study was conceptualised by Anna Guðrun Þórhallsdóttir, me and Richard Bardgett. Anna Guðrún Þórhallsdóttir, Björn Þorsteinsson organised and conducted the study site selection, methodology and the field data collection. Richard Bardgett provided facilities for root scanning. All co-authors contributed with validation of the methodology and reviewing and editing of the original manuscript, and I revised the final version.

Abbreviations and Glossary

AGBM	Above-ground biomass
AMF	Arbuscular mycorrhizal fungi
BGBM	Below-ground biomass
BUE	Biomass use efficiency
C	Carbon
ER	Ecosystem respiration
GHG	Greenhouse gas
GPP	Gross primary production
LUE	Light use efficiency
MAOC(M)	Mineral-associated organic carbon (matter)
M_{soil}	Soil moisture
N	Nitrogen
NDVI	Normalised Difference Vegetation Index
NEE	Net ecosystem exchange
PAR	Photosynthetically active radiation
POC(M)	Particulate organic carbon (matter)
RD	Root diameter
RLD	Root length density
RMF	Root mass fraction
RTD	Root tissue density
SOC	Soil organic carbon
SRA	Specific root area
SRL	Specific root length
T_{soil}	Soil temperature
C sink / source	Uptake of atmosphere CO_2 is higher/lower than emission of CO_2 into atmosphere
Cessation of grazing	Actively halted grazing of large mammalian herbivores from a previously grazed area (= grazer exclusion/grazing cessation)
Grazer exclosure	Fenced land where access for herbivores is restricted
Herbivore	Large mammalian grazing animal with adult bodyweight > 45 kg (= grazer)
Nature-based solution	Actions to protect, sustainably manage, and restore natural and modified ecosystems that address mitigation of climate change.

Acknowledgements

I am deeply grateful and would like to thank all of those who helped and supported me during the past years in my graduate studies. First and foremost, my deepest thanks to my advisor Anna Guðrún Þórhallsdóttir, who conceptualised and administrated the ExGraze project which forms the foundation of this dissertation. It has been a joy and a big adventure to work with you and to learn about Iceland, the beautiful world of grazing and grazers and how to read the landscape through space and time through your eyes. Thank you sincerely for being so patient and generous with me and bringing me to Hólar í Hjaltadalur. Thank you also to my administrative supervisor at University of Iceland, Áslaug Geirsdóttir, who supported and guided me through the graduated studies and enabled it that I could do my studies in Hólar in the countryside and graduate with the University of Iceland. Thank you also to my committee members Björn Þorsteinsson, Rene van der Wal and Richard Bardgett. I deeply appreciate the sincerity with which you dedicated time and thought to my research. The ways in which to contemplate about the English language, opening my eyes for the reader's perspective, planting ideas, directions and critical question marks into my thoughts have shaped my dissertation tremendously. Björn Þorsteinsson I want to thank further for infecting me with his admiration for plants and species, maintenance and routines. A special thanks to Richard Bardgett for hosting me for three months in the Soil and Ecosystem Ecology Lab at Manchester University. I would also like to thank Jón Guðmundsson, project partner in the ExGraze project. Jón introduced me to the CO_2 measurements, gave advice and inspiration, supported us in the field work and facilitated laboratory work at the Agricultural University of Iceland, thank you very much.

Thank you to Gesine Kliesch who endured with endless patience and support my endeavour and countless hours I have spent in on this work. Without your support and faith in my capabilities, my self-doubts certainly would have made aborting the dissertation. Gesine also contributed tremendously to the field work, root washing and root scanning. Without your support this elephant would never have been eaten up completely and the root washing procedure would have been a hopeless endeavour. Thank you so much.

I would also like to thank wonderful colleagues I have met in Hólar University: Paul Debes, for his great company, strong scientific mind, guidance in statistical approaches and inspirational discussions about almost everything; Broddi Reyr Hansen, for assistance in all technical issues in Hólar, inspirational discussion in the library and shared joy for the outdoors and snow in Hólar, Marie Delbasty for being such a great and uplifting company in Hólar who always spreads so much enthusiasm, for sharing great time with me skiing, hiking and running through the mountains and for giving me access to laboratory facilities in Hólar, Gudny Zoega and John Steinbeck for sharing their custom-made root washing barrel with me that facilitated the root washing procedure in the first year greatly, Ingibjörg Sigurðardóttir, head of the rural tourism department at Hólar University, who supported and helped me in all administrative circumstances which facilitated my studies in Hólar. I further want to thank the whole Soil and Ecosystem Ecology lab at Manchester University for welcoming and including me during my three months stay, it has been a great experience; a special thanks thereby to Henry Birt for hosting me in his house, for helping to orientate in the university and the lab and for taking me on excursions and to Deborah Ashworth for

supervising me in the laboratory, introducing the root scanning procedure and elemental analysis to me and for conducting the elemental analysis of C and N of all the small cubes I formed. Further, I would like to thank all colleagues from the Agricultural University in Hvanneyri and Kednaholt who supported me and facilitated my field and laboratory work there: Jofiður Leifsdóttir and Jónina Svavarsdóttir for providing laboratory, drying and storage facilities in Hvanneyri; without these spaces, it would have been hardly possibly to maintain control over the myriads of samples we brought from the field. María Svavarsdóttir for giving me access to the soil laboratory in Kednaholt and conducting elemental analysis of the first batch of soil samples, Hafdis Jóhannsdóttir for providing accommodation in Ásgarður for such generous long time and helped in all housing issues, Johann Þórsson for helping with a spare EGM-5 infrared gas analyser in the middle of the field season when our instrument crashed. I further want to thank Sveinbjörn Steinþórsson from the University of Iceland for the great help with sending samples to Manchester, Guðmundur Gunnarsson for providing field laboratory facilities in Möðruvellir—it was a great adventure to use this place, Brian Cusack for giving a truly inspirational workshop in scientific writing that greatly improved my writing and thinking about writing, Katharina Bremer for being a great friend in Hólar and Kópavogur, providing me a lot mental support. A special thank also to Sverre Davidsen, without your sheep and the time I have spent with you, I probably would never have started to think about the role of grazing animals in carbon cycling. You are a wonderful person. I also want to thank the members of the Eurasian Dry Grassland Group (EDGG) for introducing me to diverse and precious grasslands, grassland plant species and efficient vegetation mapping during excursions, conferences and field workshops.

My research would not have been possible without the generous support of a number of funding sources. I am deeply grateful for Anna Guðrún Þórhallsdóttir as principal investigator of the ExGraze project that funded large parts of this research, thanks to the project grant 217920-051 of the Icelandic Centre for Research (Rannís). My PhD project was further funded by Rannís through the Doctoral student grant of the Ministry of the Environment, Energy and Climate of Iceland (grant number 239629-051). The University of Iceland Research Fund funded a one-year extension for my project (grant number RSJ2025-96440) which enabled me to finish this dissertation. The International Association for Vegetation Science (IAVS), EDGG, the Erasmus+ fund and my labour union (Félag íslenskra nátturufræðinga) supported me with funding for the participation at conferences, summer schools and field excursions and the research stay in Manchester. I am eternally grateful for all the support.

Thank you also to all farmers and landowners that permitted, supported and facilitated our work on their land, who shared their knowledge about past and present land use and who pointed to potential further study sites that we could use. Without this great local knowledge, in many cases accumulated over generations, and the great support, our work would not have been possible. Finally, I also want to thank my family and friends for their love, encouragement and support over the years that kept me going on this journey. Thank you for being with me.

1 Chapter I: Introduction

1.1 Climate Change and the Terrestrial Carbon Cycle

Recent atmospheric CO_2 concentrations are approaching 430 ppm due to human disruptions of the carbon cycle, an increase by more than 50% compared to the pre-industrial level (~ 280 ppm), and far higher than throughout the evolutionary history of humans (Lisiecki 2010, Rae *et al.* 2021, Steinthorsdottir *et al.* 2021). This rapid rise in CO_2 strengthens the greenhouse effect and increases heat retention within the Earth system (IPCC 2021). The resulting energy imbalance is driving major climate changes, including widespread warming, altered precipitation patterns, substantially reduced snow and ice cover, and more frequent extreme events such as droughts, floods, and storms (IPCC 2023). This novel climate jeopardises the 'safe operating space' for humans and many other species (Rockström *et al.* 2021, 2024). Urgent action is therefore required to both reduce emissions and remove CO_2 from the atmosphere (IPCC 2023, Smith *et al.* 2025).

Nature-based solutions are increasingly emphasized for their potential to lower atmospheric CO_2, particularly through restoring or enhancing carbon (C) sinks and C sequestration in terrestrial ecosystems (Griscom *et al.* 2017, Bossio *et al.* 2020, Lal *et al.* 2021, Buckley *et al.* 2024). The terrestrial C cycle is driven primarily by the circulation of C between the atmosphere, vegetation and soil. The main fluxes are the absorption of atmospheric CO_2 by plants through photosynthesis (~142 Pg C $year^{-1}$), and the emission of CO_2 to the atmosphere through plant autotrophic and soil heterotrophic respiration (~136.7 Pg C $year^{-1}$; (IPCC 2021). Animals have largely been ignored in terrestrial C cycle models due to their minor direct contributions (Schmitz *et al.* 2014). However, growing evidence shows that animals exert important indirect effects on major C pools and fluxes, and animal impacts have been increasingly emphasised as potential nature-based solution for climate change mitigation (Schmitz *et al.* 2018, 2023, Kristensen *et al.* 2022, Borer and Risch 2024).

1.2 Herbivores in the Terrestrial Carbon Cycle

Prior to human colonisation, most terrestrial ecosystems were shaped by a diverse guilt of megaherbivores, present on every continent except Antarctica (Sandom *et al.* 2014, Fricke *et al.* 2022). According to the megaherbivore hypothesis (Owen-Smith 1987, Vera 2000, Hyvarinen *et al.* 2021), the activities of the animals created and maintained some of the most C rich ecosystems on Earth, such as the mammoth steppe in Eurasia, the great plains of North America or the savannas of southern Africa and India (McNaughton 1985, Frank *et al.* 1998, Blinnikov *et al.* 2011, Zimov *et al.* 2012, Koltz *et al.* 2022, Hyvarinen *et al.* 2023, Geremia *et al.* 2025). Recent theoretical modelling shows that large herbivores directly affect vegetation and soil through defoliation, trampling and defecation which in turn indirectly alters the C cycle between the atmosphere and the plant-soil system and can promote

sequestration of C in soil (Rizzuto *et al.* 2024). These new perspectives stimulated efforts to better understand how grazing animals influence C cycling and the mechanisms through which they could strengthen C sequestration (Kristensen *et al.* 2022, Malhi *et al.* 2022, Schmitz *et al.* 2023).

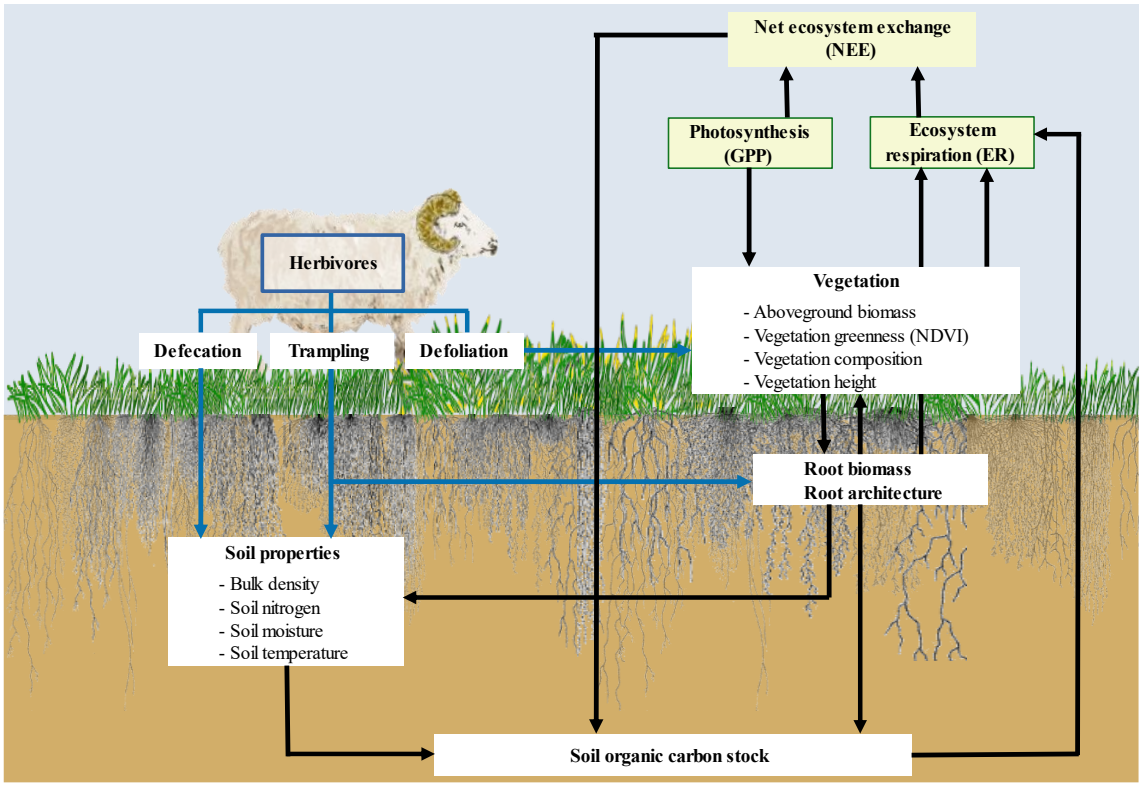

Figure 1-1: Theoretical framework of my research project. Proposed associations between herbivores, vegetation and soil (blue arrows) are outlined with further effects on the soil carbon pool and CO_2 fluxes (black arrows).

Herbivores can modify C cycling through the plant-soil system primarily through the combined activities of grazing, trampling and defecation (Figure 1-1). Herbivores impact vegetation through shifts from closed to open canopy vegetation in temperate and warm climates (Bond 2019) and from moss, lichen or shrub-dominated to graminoid vegetation in cold climates through selection for grazing-tolerant vegetation (Van der Wal 2006, Da Silveira Pontes *et al.* 2015). Grasses are particularly adapted to grazing with basal meristems, located below typical grazing height which allow rapid recovery and compensatory regrowth following defoliation events (Briske 1991, Blair *et al.* 2014). Palaeoecological research suggests that the mutualistic co-evolution with herbivores facilitated the global spread of grasses and grasslands (McNaughton 1979, Frank *et al.* 1998, Strömberg 2011). Also, many shade-intolerant forbs benefit from competition exclusion and canopy opening due to grazing (Bråthen *et al.* 2021, Søndergaard *et al.* 2025). Shrubs and woody species are, on the other side, more vulnerable to grazing, with typically reduced sapling recruitment (Smit *et al.* 2015, Salisbury *et al.* 2023). Many of these species have developed strategies to escape grazing pressure either through chemical or physical defence strategies or growth height (Bond 2019). In colder climates, slow-growing mosses and lichens, sensible to the trampling

and defoliation of herbivores, are replaced by graminoids with increasing grazing intensity (Van der Wal 2006). Herbivores also prevent litter accumulation on the surface and moss layer depth, which enhances light availability on the surface and topsoil temperatures, both benefitting grass growth (Van der Wal and Brooker 2004, Borer *et al.* 2014, Jessen *et al.* 2023).

Grasses and forbs, the major growth forms that prosper under grazing, allocate the majority of photosynthetic assimilated C into fast growing fibrous roots with short life cycles (Figure 1-1; Ottaviani *et al.* 2020). Thus, they quickly release C and nutrients from plant biomass into the soil food web, rather than storing it in biomass (Da Silveira Pontes *et al.* 2015, Linder *et al.* 2018). Consequently, 90 % of organic C in grassland is found below-ground, mostly as soil organic carbon—SOC (Qi *et al.* 2019, Zhou *et al.* 2025). In the presence of herbivores, plants constantly must respond and adjust to grazing events. Typically, root growth is inhibited immediately after defoliation events, as plants reallocate resources into compensatory growth of new photosynthetic tissue (Irving 2015). To supply new growing tissue with water and nutrients, fine roots regrow rapidly (Garcia-Pausas *et al.* 2011, Xiang *et al.* 2025). Hence, roots are frequently discarded, replaced and renewed and both living and decaying roots are an important C source for the soil food web (Bardgett *et al.* 2014, Malhotra *et al.* 2025). Besides C, herbivores supply the soil also with other key nutrients via dung and urine (Van der Wal *et al.* 2004, Doughty *et al.* 2016, Barthelemy *et al.* 2018). Through defoliation, digestion and defecation, herbivores transform relatively slowly decomposing plant material into labile, rapidly decomposing organic matter that is much faster available for the soil food web compared to above-ground plant litter, particularly in cold climates (Sitters *et al.* 2017, 2020; He *et al.* 2020). Thus, herbivores can stimulate soil activity by both increased supply of organic C and nutrients (Figure 1-1). Both are essential for the formation of stable soil organic matter associated with mineral surfaces and improve soil fertility with positive feedback for plant growth (Sokol, *et al.* 2019b, Cotrufo and Lavallee 2022).

Model studies have shown, that through increased circulation of C from the atmosphere through the plant-soil system and back to the atmosphere (C turnover of photosynthesis and respiration), more C can accumulate in the soil (Zhu *et al.* 2018, Ferraro *et al.* 2022, Rizzuto *et al.* 2024). Photosynthetically assimilated C is transferred into the soil through roots and mycorrhizal fungi (Jackson *et al.* 2017, Hawkins *et al.* 2023, Bunn *et al.* 2024). Through root exudation and decay of roots and fungal mycelia, labile C compounds leach from the vegetation into the soil food web (Sokol, *et al.* 2022a). More C inputs can sustain a larger soil microbial community that processes the organic C while reproducing and decaying in fast cycles (Angst *et al.* 2021). The dead microbial matter (i.e. necromass) of soil microorganisms (bacteria and fungi) is now thought to be the main resource of soil organic matter formation (Liang *et al.* 2019, Buckeridge *et al.* 2022, Cotrufo and Lavallee 2022, Sokol, *et al.* 2022a). Microbial necromass is bound to mineral surfaces of charged clay particles or incorporated into mineral soil aggregates as mineral-associated organic matter (MAOM) and protected from further decomposition over time periods relevant for climate change mitigation (Lavallee *et al.* 2020, Angst *et al.* 2021). This ‘soil microbial carbon pump’ (Liang and Zhu 2021) effectively transfers photosynthetically assimilated C into the soil and creates SOC reservoirs from microbial necromass over time (Figure 1-1). However, the accumulation and stability of the SOC depends on a sufficient supply of new photosynthetically assimilated C into the soil due to the constant breakdown of organic matter by soil organisms. When supply is halted, microorganisms may decompose

previously accumulated SOC, known as ‘priming’ (Liu, X. *et al.* 2020). In grazed ecosystems, grazing of large herbivores has been proposed to accelerate C transfer below-ground, thereby sustaining the microbial C pump and SOC formation (Ritchie *et al.* 1998, Bardgett and Wardle 2010).

1.3 European Grassland and Heathland

1.3.1 Replacement of Wild with Domestic Herbivores

In Europe, most wild large herbivores went extinct with the colonisation of humans and the ranges of the remaining species were greatly reduced (Svenning, *et al.* 2024b). Following these dramatic changes in herbivore distributions, human pastoralists partly replaced the ecological function of the vanished wild herbivores (Bocherens 2018). For millennia, most grasslands in Europe have been maintained by traditional livestock grazing and hay making (Pärtel *et al.* 2005, Hejcman *et al.* 2013, Janišová *et al.* 2025). Therefore, these grasslands are commonly referred to as semi-natural grasslands (Dengler *et al.* 2014). Semi-natural grasslands are valued for their high biodiversity, heterogeneity and SOC stocks (Bengtsson *et al.* 2019, Janišová *et al.* 2023, Lindborg *et al.* 2023, Lockwood *et al.* 2026, Widmer *et al.* 2026). On more acidic or less productive soils, particularly in coastal and northern ecosystems in Europe, heathlands, dominated by plants from the *Ericeae* family, developed under natural and livestock grazing disturbance (Beier *et al.* 2009, Newton *et al.* 2009, Rosa García *et al.* 2013, Rupprecht *et al.* 2016).

Like grassland, heathland is vulnerable to overgrowth of canopy-forming taller species without disturbances such as wildfire or grazing (Ward *et al.* 2007, Rosa García *et al.* 2013, Løvschal and Damgaard 2022, Rittl *et al.* 2025). Research on the key heath-forming plant, *Calluna vulgaris*, has shown that heath responds with strong rejuvenating regrowth to such disturbances (Schellenberg and Bergmeier 2022). Therefore, traditional use of heathlands as grazing lands contributed largely to the maintenance of these valuable semi-natural habitats (Newton *et al.* 2009, Rosa García *et al.* 2013). Long-established heathlands often accumulate a thick organic topsoil layer, derived from fragmented slowly decomposing shoot and root litter (Quin *et al.* 2015, Duddigan *et al.* 2024). Thus, SOC accumulates predominantly in particulate organic matter (POM), which is typically less persistent than microbial-derived MAOM and more vulnerable to loss through land use change or microbial mineralisation (Ward *et al.* 2007, Friggens *et al.* 2020, Angst *et al.* 2021, Housego *et al.* 2025).

1.3.2 Abandonment of Livestock Grazing

With technological innovation and socio-economic changes over the last century, traditional livestock grazing practices have been abandoned in large parts of Europe (Plieninger *et al.* 2016, Schils *et al.* 2022). Agricultural intensification on suitable land and abandonment of less accessible land that had been maintained by grazing for centuries, led to a sharp decline of semi-natural grassland and heathland, often with negative consequences for biodiversity and provision of ecosystem functioning, including storage of SOC (Cousins *et al.* 2015, Bengtsson *et al.* 2019, Herzon *et al.* 2021, Fagúndez and Pontevedra-Pombal 2022,

Duddigan *et al.* 2024, Malek *et al.* 2024). In northern Europe, a mosaic of semi-natural grassland and heathland, reflecting past land use patterns, was preserved for longer time due to climatic limitation of crop cultivation (Normand *et al.* 2017, Maliniemi *et al.* 2018, Dengler *et al.* 2020). However, also in northern Europe, livestock grazing abandonment has accelerated over the last decades, mirroring patterns from other parts of the continent (Cousins *et al.* 2015, Aune *et al.* 2018, Stoessel *et al.* 2022). Consequences of this abandonment are colonisation of shrubs, heath and trees, such as birch, in these traditional open landscapes (Vowles and Björk 2019, Mekonnen *et al.* 2021, Parker *et al.* 2021) and afforestation of abandoned grazing land as alternative land use (Friggens *et al.* 2020, Tau Strand *et al.* 2021, Aslaksen *et al.* 2025).

As natural grazing on uncultivated land has been emphasised as potential contribution to land-based SOC sequestration, a better understanding of the consequences of ceased traditional livestock grazing for C dynamics is needed (Dangal *et al.* 2020, Bardgett *et al.* 2021, Borer and Risch 2024, Pillar and Winck 2026). Responses of C dynamics to cessation of grazing in comparison to continued grazing have been classically studied with fenced exclosures, restricting the access of herbivores to an experimental unit within grazed land (Stark *et al.* 2015, Frank *et al.* 2018, Forbes *et al.* 2019). Meta-analyses and syntheses that analysed studies on grazed and ungrazed land globally showed often inconsistent results with both positive, negative and neutral effects of grazing for C uptake and SOC storage (McSherry and Ritchie 2013, Abdalla *et al.* 2018, Forbes *et al.* 2019, Qu *et al.* 2024, Niu *et al.* 2025). One repeatedly drawn conclusion stresses that short-term vs. long-term grazer exclusion may have different effects on C uptake (Stanley *et al.* 2024, Jia *et al.* 2026). Often, experimental grazer exclusion initially increases C uptake. However, most of such exclusion treatments are applied on a short time scale (< 10 years) in grassland or heathland that co-developed with herbivores for centuries to millennia (Price *et al.* 2022). A long grazing history leaves a legacy in the ecosystem (Milchunas and Lauenroth 1993). For example, nutrient availability and vegetation composition are typically modified towards more productive plants and soils (Valls Fox *et al.* 2015, Ferraro *et al.* 2024). In the short-term, a productive plant community can response with enhanced C uptake to the release from grazing. Such effects are relatively well documented and such short-term treatments can improve recovery of grasslands that have been overused or degraded (Hu *et al.* 2016, Bardgett *et al.* 2021).

1.4 Long-term Perspective

With increasing time since grazing ceased, different outcomes may evolve, although empirical evidence of long-term effects is much weaker due to a low number of available studies (Saccone and Virtanen 2016, Stanley *et al.* 2024, Niu *et al.* 2025). In the long-term, such as after multiple decades, nutrient availability may fade without additional inputs from animal faeces and urine (Bardgett and Wardle 2003, Van der Wal *et al.* 2004, Barthelemy *et al.* 2018). Plant litter accumulation, expanding moss cover or colonisation of tall shrubs and trees can modify light availability, soil temperatures, soil moisture and soil microbial activity with cascading effects for gross primary production and ecosystem respiration (Van der Wal and Brooker 2004, Van der Wal 2006, Christie *et al.* 2015, Te Beest *et al.* 2016, Jiang *et al.* 2024). For example, several long-term studies have found negative responses of plant and soil biodiversity that did not unfold in the short-term (Porensky *et al.* 2020, Price *et al.* 2022, Schrama *et al.* 2023, Shu *et al.* 2024). Some studies that applied a multi-decadal to centennial

perspective of grazing impact showed that areas with more intensive traditional use have a higher productivity than the surrounding, less intensively used, landscape as a historical land use legacy (Foster *et al.* 2003). Such 'islands of fertility' (Allington and Valone 2014) have been identified in such contrasting ecosystems as abandoned reindeer herding pens in arctic Scandinavia (Freschet *et al.* 2014, Egelkraut, *et al.* 2018a, Stark *et al.* 2019, Castaño *et al.* 2023), or preferred resting places of nomadic pastoralists in Mediterranean grasslands (Vidaller *et al.* 2022) and African savanna (Marshall *et al.* 2018). Similar to the results of Egelkraut *et al.* (2018a), introduction of reindeer (*Rangifer tarandus*) on the previously herbivore-free sub-arctic Aleutian islands caused a shift in dominance from shrubs to graminoids at preferred foraging spots, thereby improving foraging resources of the established reindeer population (Ricca *et al.* 2016). Few other studies have studied either SOC dynamics or CO_2 fluxes in grazer exclosures that have been maintained for multiple decades. These long-term perspectives indicated that the short-term benefits for C uptake associated with cessation of grazing are only temporal and C uptake in the long-term is fading relative to continued grazed land, including arctic tundra (Lara *et al.* 2017), alpine grassland (Welker *et al.* 2004), steppe grassland (Krzic *et al.* 2014, Hu *et al.* 2016, Bork *et al.* 2023), *Calluna* heathland (Li *et al.* 2023; cut not grazed), boreal forest understory (Kantola *et al.* 2024) or sub-arctic grassland (Thorhallsdottir and Gudmundsson 2023). Despite an increasing number of studies, more data beyond single sites are needed to understand the consequences for C cycling associated with the ongoing livestock grazing abandonment and extirpation of wild herbivores in natural and semi-natural grassland and heathland (Atwood *et al.* 2020, Pillar and Winck 2026). The FAO declared 2026 to the 'International Year of Rangelands and Pastoralists', emphasising the timely need to better understand the ecological implications of these systems (Briske *et al.* 2026).

1.5 Iceland as a Model System

In a pilot study, Thorhallsdottir & Gudmundsson (2023) outlined unique conditions in Iceland to comprehensively study long-term effects of grazing and cessation of grazing for C cycling. Iceland is one of the last remaining regions in Europe with extensive semi-natural grassland and heathland that have been maintained by traditional livestock grazing in the lowlands (below 200 m a.s.l.) for a millennium (Figure 1-2; Helgadóttir *et al.* 2014; Ross *et al.* 2016; Dengler *et al.* 2020). Approximately 35% of the Icelandic lowlands are natural and semi-natural grassland and heathland which are, to a large degree, still used for livestock grazing (Table 1-1; Ottoson *et al.* 2016). Due to climatic limitations, most land has never been cultivated or otherwise altered by human activities, except for the introduction of livestock grazing approximately 1100 years ago (Ross *et al.* 2016). Most grassland and heathland are grazed by free-roaming sheep (*Ovis aries*) during the summer months. Closer to farms, also fenced pastures exist where sheep, horses (*Equus ferus caballus*) and cattle (*Bos taurus*) graze for shorter periods between spring and autumn (Defourneaux *et al.* 2024). Commonly, horses are kept outside all year round and graze on fenced pastures during winter. Although, livestock grazing in Iceland is still more common than in other parts of Europe, animal numbers have declined over the last decades, resulting in expanding areas where grazing is abandoned. For example, relative to 1980, sheep numbers and active sheep farms have declined by more than 50%, with area used for grazing continuously declining (Johannesson 2025; StatIce 2024, Table 1-2).

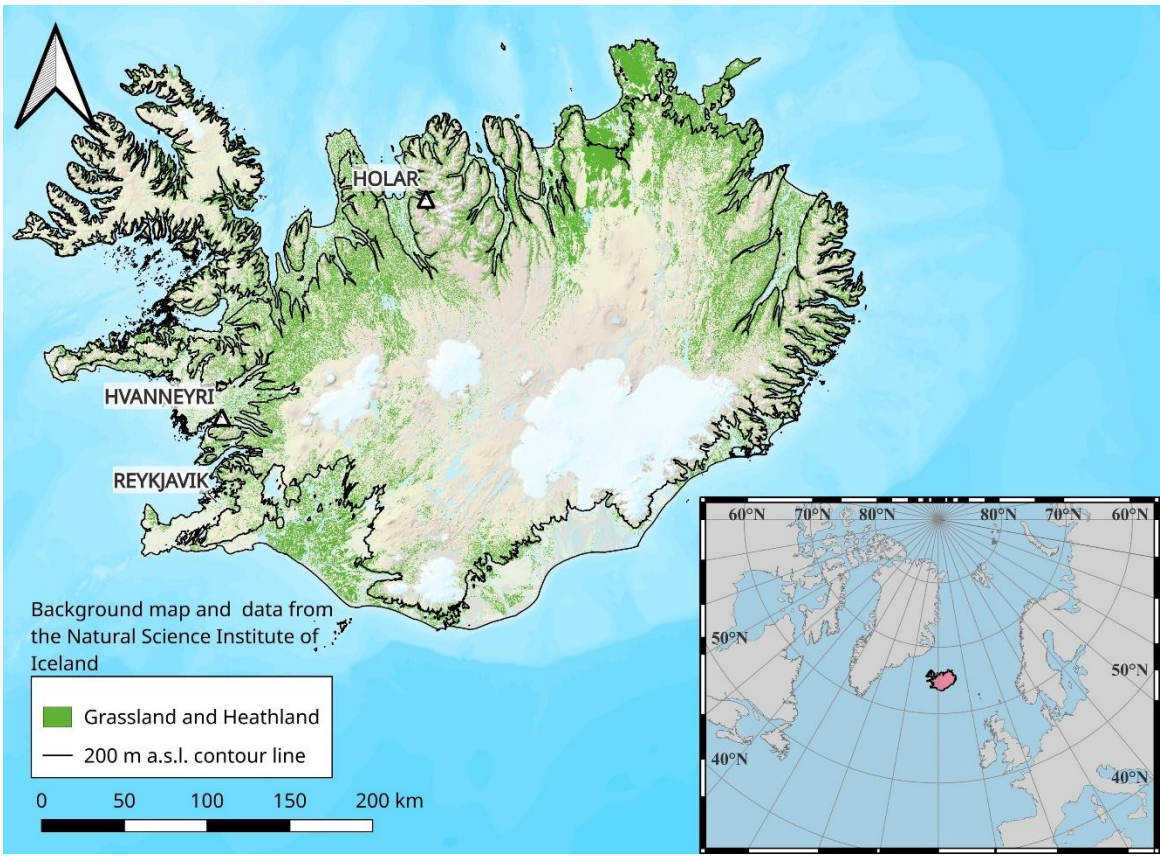

Figure 1-2: Distribution of grassland and heathland in Iceland. The map is based on data from the habitat types map of the Natural Science Institute of Iceland. Reykjavik is marked as the capital of Iceland and Hólar and Hvanneyri as research bases of this project. See the map in the lower right corner for the location of Iceland in the North (red quare).

As part of the Palaearctic biogeographic realm (Dengler *et al.* 2014), plants that have colonised Iceland after the last glacial maximum share a long grazing history with herbivores from Europe (Willerslev *et al.* 2014, Alsos *et al.* 2021, Thorhallsdottir 2021). Prior to human colonisation, Icelandic ecosystems developed without mammalian grazers. Paleo-ecological research indicates that the fully vegetated lowlands were likely a dynamic mosaic of open birch woodlands, heathlands, grasslands and peatlands, frequently disturbed and re-configured by volcanic eruptions (Geirsdóttir *et al.* 2020, Edwards *et al.* 2021). Although the extent of pre-settlement ecosystems is still highly debated (Geirsdóttir *et al.* 2020, Harning *et al.* 2025, Kjær *et al.* 2025), grasslands likely expanded with the introduction of livestock, analogue to graminoid proliferation in grazed tundra and with recent introduction of reindeer to the sub-arctic Aleutian islands (Van der Wal 2006, Ricca *et al.* 2016, Stark *et al.* 2023).

Table 1-1: Area distribution of Icelandic habitat classes across the lowlands below 200 m a.s.l. (24.4% of total land area). Different grassland and heathland habitat types are further detailed (in italic). Habitat class names and data are based on the Icelandic habitat types map, curated by the Natural Science Institute of Iceland (https://vistgerdakort.ni.is/ [accessed 22.02.2026]).

Habitat class	**Area (km^2)**	**Proportion of lowland (%)**
< 200 m a.s.l.	25,105.6	-
Iceland total	102,715.1	-
Northern boreal Festuca grasslands	84.0	0.3
Wavy hair-grass grasslands	123.7	0.5
Icelandic Festuca grasslands	366.2	1.5
Insular Nardus-Galium grasslands	96.9	0.4
Boreo-subalpine Agrostis grasslands	863.3	3.4
Boreal tufted hairgrass meadows	380.1	1.5
Icelandic Carex bigelowii grasslands	481.7	1.9
Grasslands	**2,395.8**	**9.54**
North Atlantic boreo-alpine heaths	2,281.8	9.1
Icelandic lichen Racomitrium heaths	248.4	1.0
Icelandic Empetrum Thymus grasslands	545.8	2.2
Oroboreal moss-dwarf willow snowbed communities	104.7	0.4
N. Atlantic Vaccinium-Empetrum-Racomitrium heaths	1,330.1	5.3
Icelandic Racomitrium grass heaths	525.8	2.1
Arctic Dryas heaths	135.4	0.5
Icelandic Carex bigelowii heaths	386.7	1.5
Oroboreal willow scrub	551.2	2.2
Icelandic Salix lanata/S. phylicifolia scrub	144.9	0.6
Heathlands	**6,254.7**	**24.91**
Wetlands	3,464.3	13.80
River plains	2,074.4	8.26
Lavafields	1,721.7	6.86
Mosslands	1,511.3	6.02
Icelandic birch woods	1,204.6	4.80
Freshwater	1,173.2	4.67
Disturbed gravel and sand land	1,077.0	4.29
Coastlands	904.0	3.60
Artificial habitats	565.8	2.25
Scree slopes	501.7	2.00
Mixed forestry plantations	429.5	1.71
Regularly or recently cultivated agricultural	1,757.0	0.07
Icelandic exposed andic soils	5.6	0.02
Glaciers	61.4	0.00
Geothermal land	0.3	0.00

Currently, land use is reported as the most important contributor to greenhouse gas (GHG) emissions in the latest National Inventory Report of Iceland, with grazed land as a significant GHG source (Keller *et al.* 2026). In previous studies, free-roaming sheep grazing has been consistently associated with large-scale land degradation and C losses (Marteinsdóttir *et al.* 2017, Barrio *et al.* 2018). However, data documenting grazing effects on the C storage of grazed land are highly limited, acknowledged as major uncertainty by Keller *et al.* (2026) (p. 357-361). So far, it has not been addressed how cessation of grazing affects C storage in Icelandic grassland and heathland that have been used for livestock grazing over long time, despite their large spatial extent. Following emerging theory about herbivore-plant-soil interactions, grazed grassland and heathland could be significant but overlooked C sinks, accumulating SOC with time (Figure 1-1; Kristensen *et al.* 2022; Norderhaug *et al.* 2023; Thorhallsdottir and Gudmundsson 2023; Bardgett 2025).

Previous surveys have found that mineral soils in the Icelandic lowlands store vast SOC stocks even though they have been used for livestock grazing over centuries (Óskarsson *et al.* 2004). The soils of Iceland are of volcanic origin, termed Andosols (Arnalds 2015). Andosols are typically rich in SOC due to the high availability of small-textured mineral surfaces that can bind organic C, especially with sufficient nitrogen supply (Matus *et al.* 2014, Leblans *et al.* 2017). With frequent aeolian deposition of fresh, rapidly-weathering parent material from volcanic eruptions, andosols are typically less likely to become saturated with MAOC, and hence provide a strong opportunity to study grazing effects for SOC sequestration, without constraining saturation effects (Dahlgren *et al.* 2004, Dec *et al.* 2012, Parada *et al.* 2024).

Table 1-2: Livestock numbers for whole Iceland. Data are shown from 1980 to 2020 (according to yearly autumn reports) and number of active sheep farms between 1990 and 2025, adopted from Johannesson (2025) and StatIce (2026).

Year	Sheep	Horse	Cattle	Sheep farms[†]
1980	827,927	52,346	59,933	-
1990	548,508	71,693	74,889	3192 (1993)
2000	465,777	73,995	72,135	-
2010	479,841	77,164	73,781	2785 (2008)
2020	401,022	58,466	80,643	~1500 (2025)

[†] Reference year in parentheses

Natural woodland cover in Iceland is low, approximately 5 % of the lowland area (Table 1-1). Following incentives to promote tree cover, afforestation exclosures were erected within grazed land on many farms all around Iceland during the last decades. Most of these exclosures were never fully planted and provide multi-decadal fence contrasts between grazed and ungrazed grassland or heathland (Thorhallsdottir and Gudmundsson 2023). Within the ExGraze project, sites with fenced exclosures adjacent to continuously grazed land have been mapped all around Iceland. For my dissertation, I used such long-term fence contrasts as unintentional experimental sites to study long-term changes in C uptake and C storage associated with cessation of grazing. The sub-arctic climate and low woodland cover limit tree colonisation of ungrazed land in Iceland and ungrazed exclosures remain often as open grassland for decades (Frigo *et al.* 2023, Behrend *et al.* 2025). Instead of tree succession, encroachment of heathland (including ericaceous shrubs, mosses, lichen) and deciduous shrubs (e.g. *Betula nana*) into abandoned grassland has been reported (Alfreðsson

2018, García Criado *et al.* 2025, Ryde *et al.* 2025). Such state transitions have also been documented from graminoid tundra shifting into shrub or moss and lichen tundra in the absence of herbivores (Van der Wal 2006, Te Beest *et al.* 2016, Stark *et al.* 2023). Such vegetation changes could have further cascading effects on plant-soil interactions and C dynamics over time, including shifting C allocation pattern, nutrient cycling, root dynamics and mycorrhizal associations (Deslippe and Simard 2011, Sørensen, *et al.* 2018a, Mekonnen *et al.* 2021, Parker *et al.* 2021, Castaño *et al.* 2023). Thus, to reveal how C cycling through the plant-soil system differs in grazed and ungrazed land, long-term perspectives are needed (Saccone and Virtanen 2016).

1.6 Scope and Aims of this Dissertation

With the dissertation thesis, I aim to gather empirical data from a broad range of sub-arctic grassland and heathland sites to elucidate how the cessation of grazing affects C cycling in these key sub-arctic ecosystems in the long-term to expand evidence gathered from short-term treatments. I use both grassland and heathland as two contrasting vegetation types that are both widespread and used as grazing land in Iceland and other sub-arctic regions, thus findings from this thesis can have implication beyond our study region (Myers-Smith *et al.* 2011, Wang, *et al.* 2016a, Boulanger-Lapointe *et al.* 2022, Defourneaux *et al.* 2024). Grassland and heathland can co-exist in similar abiotic conditions and one or the other might dominate as a result of land use practices or small-scale difference in soil properties (Te Beest *et al.* 2016, Vowles, *et al.* 2017b, Egelkraut, *et al.* 2018b). Following the proposed aim, this thesis is guided by four major objectives that are addressed in separate chapters:

(i) I aim to understand how grazing vs. long-term cessation of grazing influences growing season CO_2 fluxes between the land and the atmosphere (GPP and ER) in grassland and heathland as a measure for the C sink strength, measured as the net ecosystem exchange of CO_2 (NEE) (Chapter III).

With this objective, I provide a quantitative assessment over a broad range of study sites in grassland and heathland about the C sink strength in grazed and ungrazed land for these two major sub-arctic plant communities. Following findings of a global synthesis of grazing effects on grassland greenhouse gas fluxes (Dangal *et al.* 2020) and a synthesis of arctic CO_2 flux studies (See *et al.* 2024), I expect that Icelandic grassland and heathland are overall net sinks for atmospheric CO_2. In grassland, specifically, I expect reduced net CO_2 uptake (NEE) and photosynthetic activity (GPP) due to self-shading of accumulating litter and reduced tillering of photosynthetic active shoots in the absence of grazing (Blair *et al.* 2014, Metcalfe and Olofsson 2015, Malhi *et al.* 2022). Contrary, in heathland, I expect taller growth of heath and shrubs with increased green biomass in the absence of grazing, resulting in higher net CO_2 uptake compared to grazed heathland (Sørensen, *et al.* 2018a, Sundqvist *et al.* 2020, Min *et al.* 2021).

(ii) I aim to analyse to what extent direct measurement of CO_2 fluxes can be substituted by remote-sensed NDVI as a cost- and time-efficient means with the potential to upscale point measurements from our study sites towards the wider landscape (Chapter IV).

I expect that GPP and NEE can be estimated using ground-based NDVI, measured on the same scale as the direct CO_2 fluxes (Street *et al.* 2007, Siewert and Olofsson 2020). Further, I expect that ground-based measurements of NDVI and CO_2 fluxes can be calibrated with satellite-derived NDVI and upscaled to the regional scale for comparable land cover types (Williams *et al.* 2008, Nestola *et al.* 2016, Juutinen *et al.* 2017, Bazzo *et al.* 2023).

(iii) I aim to quantify the distribution of SOC in grassland and heathland soils and the long-term effect cessation of grazing on the SOC stocks. Although, baseline SOC data prior to cessation of grazing are missing from the sites, I further aim to determine how SOC sequestration differs between grazed and ungrazed land (Chapter V).

Following the hypothesis of Kristensen *et al.* (2022) that grazing can enhance the formation of persistent SOC in grassland, I expect to find higher SOC stocks in grassland than in heathland and in grazed land than in ungrazed land, driven by a higher transfer of photosynthetically assimilated C below-ground and higher soil microbial activity in grazed grassland compared to other land (Bai and Cotrufo 2022, Franzluebbers 2022, Stanley *et al.* 2024). Further, I expect to find enhanced soil nitrogen (N) availability in grazed relative to ungrazed land from dung and urine which is an important driver of microbial-derived SOC accumulation in mineral-associated organic matter (Piñeiro *et al.* 2010, Schrama, Veen, *et al.* 2013, Soussana and Lemaire 2014, Lavallee *et al.* 2020).

(iv) I aim to quantify how the root systems in grazed versus long-term ungrazed vegetation types differ and how the density, distribution and morphology of roots relate to SOC dynamics (Chapter VI).

As the major pathway of photosynthetically assimilated C into the soil is through roots rather than from above-ground biomass, I expect that root traits can help to explain the distribution of SOC in the study sites (Jackson *et al.* 2017). I expect that the vegetation allocates more C above-ground in the absence of grazing to escape self-shading and competition of neighbouring plants together with less root turnover, when N availability is limited without inputs from grazing animals, indicated by a lower fine root density and a more conservative rooting strategy (Van der Wal *et al.* 2004, Gough *et al.* 2012, Oñatibia *et al.* 2017, Eskelinen *et al.* 2022, Ren *et al.* 2024).

2 Chapter II: Study Site Selection and Methodology

2.1 Study Sites

The study sites for this PhD project were spread across the Icelandic lowlands below 200 m a.s.l. in grassland and heathland used for livestock grazing. The limit of 200 m a.s.l. was not predetermined, but it is commonly considered as the limit of permanent settlement and active land use, thus long-term exclosures within grazed land were typically distributed below this elevation. With the aim to study long-term fence contrasts of grazed and ungrazed land, digital surveying of historical and recent aerial photographs was used to map potential grazer exclosures. Most potential sites were thereby identified as afforestation exclosures that were only partly planted and included substantial open, treeless land within the exclosure, as visible from aerial photographs. The used image databases were publicly available through the Natural Science Institute of Iceland (loftmyndasja.gis.is; natt.is) and Loftmyndir ehf. (map.is). A database of active sheep farms in Iceland was used to pre-select continuous grazed land adjacent to grazer exclosures (accessible through map.is). In addition to this, land use information was gathered from local landowners to locate suitable sites. Suitable study sites were selected according to a set of criteria to ascertain that environmental conditions were comparable between grazed and ungrazed land prior to the establishment of the grazer exclosures (Table 2-1). Due to this careful study site selection, I am confident that differences in C dynamics between grazed and ungrazed land are primarily related to the presence or absence of grazing and not to confounding site-specific factors unrelated to grazing.

Table 2-1: Criteria for study site selection. Conditions that had to be met (☑) and conditions that could not be present (☒) are outlined.

Criteria for study site selection
☑ > 20 years of grazer exclusion
☑ Grazed and ungrazed land directly adjacent to each other, just divided by a fence
☑ Known and consistent land use history prior and after cessation of grazing
☑ Permanent exclusion of grazers since cessation of grazing
☑ Equal abiotic conditions in grazed and ungrazed land (topography, aspect, hydrology)
☒ Measurement plot in exclosure not planted by trees
☒ No other human alteration than grazing (ploughing, fertiliser, drainage)
☒ No organic soils (peat)
☑ Full vegetation cover in grazed and ungrazed land
☑ Located in lowlands below 200 m a.s.l.

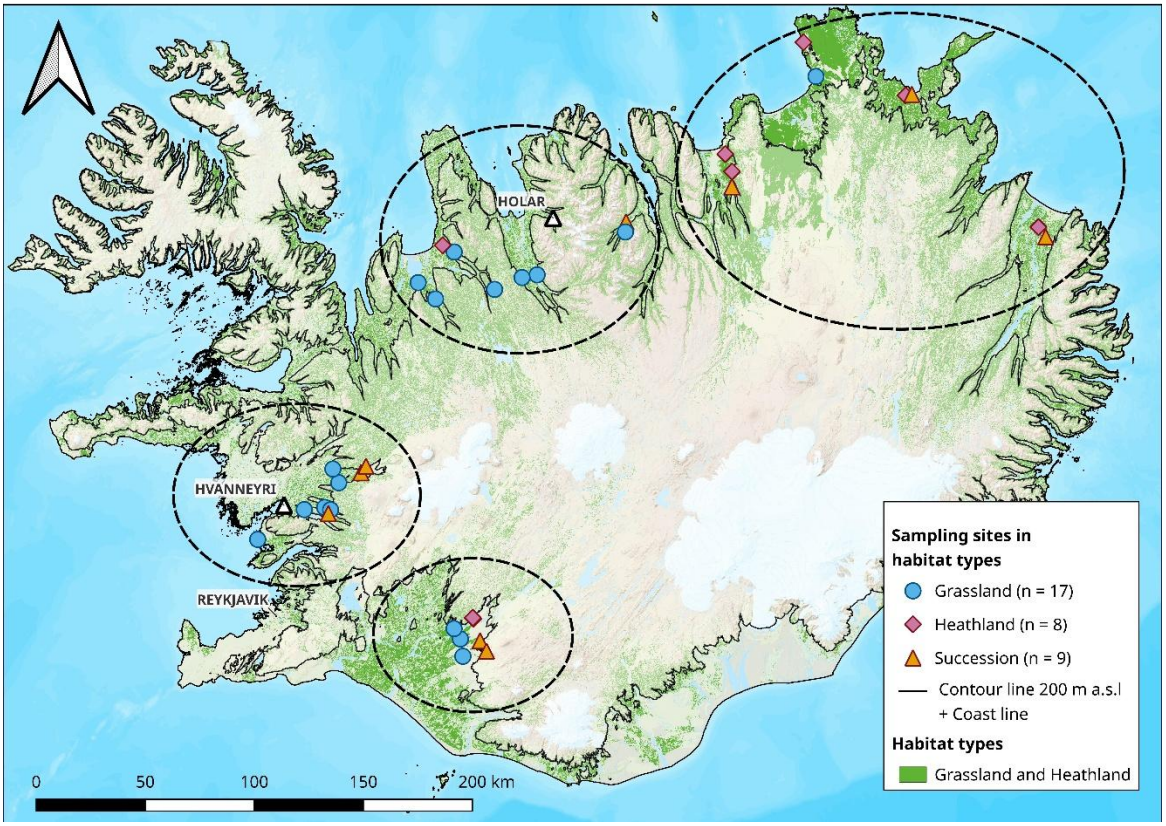

Figure 2-1: Study sites across Iceland in different dominant vegetation types. The sites were clustered in the eastern, northern (around Hólar), western (around Hvanneyri) and southern part of Iceland (broken-line ellipses). Hólar and Hvanneyri are marked as research stations from where the data collection at the sites was operated. The black line marks the 200 m a.s.l. contour line.

Eventually, 34 sites across Iceland met the criteria and were used in this thesis (Figure 2-1). All studied sites consist of long-established (> 20 years) fence contrasts, with paired continuously grazed land on one side and land where grazing ceased multiple decades ago on the other side of the fence. The selection included relatively young (20-30 years, n = 9), medium-to-old (31-50 years, n = 13) and old (51-83 years, n = 12) exclosures (Table 2-2). They span an elevation gradient from 5 to 198 m a.s.l. The climate across the study sites is sub-arctic, according to Köppen-Geiger classification. At the closest meteorological station (within 30 km from individual study sites), mean annual temperatures range from 2 to 4.5 °C with a mean 3.2 °C (summer: 7.4 °C – 10.3 °C) and mean annual precipitation range from 470 to 1234 mm with a mean of 733 mm (summer: 95 mm – 274 mm) for the time periods 1961 – 1990 or 1981 – 2000 (Table 2-2). On the grazed land, animal densities and grazing regimes will have varied between sites and over time, but all locations had been grazed throughout time, confirmed by landowners (before and after grazer exclosures were erected). Most of the sites were grazed by sheep or horses on the grazed land, but some sites were also grazed by cattle or a combination of them (Figure 2-2, Table 2-2). According to landowners, both sides were managed identically prior to cessation of grazing, i.e. both sides were equally grazed. Thus, the grazed land is treated throughout the whole thesis as reference control and the long-term fenced-out land as grazer exclusion treatment.

Table 2-2: Summary information of the selected study sites for the dissertation. The names of the study sites refer to the farm associated with the site. Throughout the thesis, the site ID is used for site identity instead of the study site name.

Region	Study site	ID	Latitude	Longitude
E	Gunnarsstaðir	Gun	66.154	-15.431
E	Hjaltalundur	Hja	65.517	-14.236
E	Holt	Holt	66.152	-15.496
E	Leirhöfn	Lei	66.404	-16.491
E	Presthólar	Pho	66.260	-16.396
E	Presthvammur	Phv	65.830	-17.311
E	Reykjarhóll	Reyk	65.892	-17.299
E	Skarðaborg	Skb	65.966	-17.359
E	Viðastaðir	Vid	65.560	-14.296
N	Álfgeirsvellir	Alf	65.493	-19.439
N	Bergsstaðir	Ber	65.446	-19.713
N	Geitaskarð	Gsk	65.604	-20.107
N	Lárusarlundur	LL	65.411	-20.298
N	Miðhóp	Mh	65.478	-20.466
N	Örlygsstaðir	Orl	65.502	-19.289
N	Röðull	Rod	65.632	-20.218
N	Skriða	Skr	65.707	-18.387
N	Syðri-Bægisá	SB	65.666	-18.398
S	Haukadalur	Hau	63.975	-19.965
S	Hólar1943	H43	63.986	-19.934
S	Hólar1960	H60	63.988	-19.935
S	Hvammur	Hva	64.048	-20.126
S	Skarðlóð	Skl	64.019	-20.074
S	Skarfanes1940	Sk40	64.055	-19.992
S	Skarfanes1990	Sk90	64.055	-19.992
W	Gilsbakki	Gil	64.724	-20.986
W	Hóll	Holl	64.528	-21.345
W	Lundur	Lun	64.555	-21.386
W	Melaleiti	Mel	64.419	-22.017
W	Oddsstaðir	Odd	64.539	-21.305
W	Steindórstaðir	Stein	64.655	-21.242
W	Stóri-Ás	SA	64.697	-21.033
W	Þorgautsstaðir	Thor	64.712	-21.304
W	Vatnsendi	Vatn	64.544	-21.577

Region: E = East, N = North, S = South, W = West

ID	Days	Elevation m a.s.l.	MAT	MST (JJA) °C	MAP	MSP (JJA) mm	Ref. period
Gun	2	5	3.1	8.7	561.5	133.9	1984-2004
Hja	1	6	2.3	8.8	516.9	127.6	1966-1998
Holt	2	52	3.1	8.7	561.5	133.9	1984-2004
Lei	2	20	2	7.4	732.4	145.0	1961-1990
Pho	2	25	2.7	8.3	563.8	174.7	1961-1990
Phv	2	45	2.1	9	629.5	134.0	1962-1991
Reyk	1	198	2.1	9	629.5	134.0	1962-1991
Skb	2	52	3.4	9.6	721.8	155.5	1961-1990
Vid	1	41	2.3	8.8	516.9	127.6	1966-1998
Alf	6	186	2.4	8.8	469.5	128.9	1961-1990
Ber	6	190	2.4	8.8	469.5	128.9	1961-1990
Gsk	6	67	3.1	9.1	476.5	123.3	1982-2001
LL	5	32	3.1	9.1	476.5	123.3	1982-2001
Mh	5	48	3.1	9.1	476.5	123.3	1982-2001
Orl	6	40	2.4	8.8	469.5	128.9	1961-1990
Rod	5	118	3.1	9.1	476.5	123.3	1982-2001
Skr	6	70	3.2	9.9	489.6	95.4	1961-1990
SB	5	174	3.2	9.9	489.6	95.4	1961-1990
Hau	3	102	4.5	10.3	1234.4	274.3	1961-1990
H43	2	110	4.5	10.3	1234.4	274.3	1961-1990
H60	2	95	4.5	10.3	1234.4	274.3	1961-1990
Hva	3	76	3.6	9.9	1105.8	274.2	1961-1990
Skl	3	144	3.6	9.9	1105.8	274.2	1961-1990
Sk40	2	165	4.5	10.3	1234.4	274.3	1961-1990
Sk90	2	165	4.5	10.3	1234.4	274.3	1961-1990
Gil	7	183	3.2	9.3	733.5	169.1	1957-1986
Holl	7	74	3.2	9.3	733.5	169.1	1957-1986
Lun	7	67	3.2	9.3	733.5	169.1	1957-1986
Mel	4	13	4.3	9.7	792	172.6	1965-1987
Odd	7	64	3.2	9.3	733.5	169.1	1957-1986
Stein	7	63	3.2	9.3	733.5	169.1	1957-1986
SA	7	98	3.2	9.3	733.5	169.1	1957-1986
Thor	7	59	3.2	9.3	733.5	169.1	1957-1986
Vatn	6	122	3.3	9.6	904.6	173.1	1963-1994

Days: Measurement days for CO_2 fluxes

Climate: MAT = Mean annual temperature, MST = Mean summer temperature (JJA = June, July, August), MAP = Mean annual precipitation, MSP = Mean summer precipitation (June, July, August), Ref. period = time period for climate data from nearest meteorological station with sufficient time series (< 30 km)

(continued)

ID	Dominant vegetation		Vegetation type category	Exclosure age (years)	Grazing animals
	Grazed	Exclosure			
Gun	Grassland	Heathland	Succession	34	Sheep/Horse
Hja	Grassland	Heathland	Succession	80	Cattle
Holt	Heathland	Heathland	Heathland	30	Sheep
Lei	Heathland	Heathland	Heathland	72	Sheep
Pho	Grassland	Grassland	Grassland	22	Horse
Phv	Grassland	Heathland	Succession	42	Horse
Reyk	Heathland	Heathland	Heathland	42	Sheep
Skb	Heathland	Heathland	Heathland	42	Sheep
Vid	Heathland	Heathland	Heathland	22	Horse
Alf	Grassland	Grassland / Heathland	Grassland / Succession	52	Sheep/Horse
Ber	Grassland	Grassland	Grassland	42	Sheep/Horse
Gsk	Grassland	Grassland	Grassland	22	Sheep/Horse
LL	Grassland	Grassland	Grassland	52	Horse
Mh	Grassland	Grassland	Grassland	27	Horse
Orl	Grassland	Grassland	Grassland	52	Sheep
Rod	Heathland	Heathland	Heathland	52	Horse
Skr	Grassland	Grassland / Heathland	Grassland / Succession	66	Horse
SB	Grassland	Grassland	Grassland	60	Sheep/cattle
Hau	Grassland	Grassland	Grassland	33	Sheep
H43	Grassland	Birch woodland	Succession	80	Sheep
H60	Grassland	Birch woodland	Succession	63	Sheep
Hva	Grassland	Grassland	Grassland	23	Horse
Skl	Grassland	Grassland	Grassland	33	Sheep/horse/cattle
Sk40	Heathland	Heathland	Heathland	83	Sheep/Horse
Sk90	Heathland	Heathland	Heathland	33	Sheep/Horse
Gil	Grassland	Heathland	Succession	33	Sheep
Holl	Grassland	Heathland	Succession	45	Sheep/Horse
Lun	Grassland	Grassland	Grassland	68	Sheep/Horse
Mel	Grassland	Grassland	Grassland	28	Horse
Odd	Grassland	Grassland	Grassland	43	Sheep
Stein	Grassland	Grassland	Grassland	23	Horse
SA	Grassland	Grassland / Heathland	Grassland / Succession	23	Sheep/Horse
Thor	Grassland	Grassland	Grassland	43	Sheep
Vatn	Grassland	Grassland	Grassland	71	Sheep

Grazing animal = dominant herbivores during the measurement period

(continued)

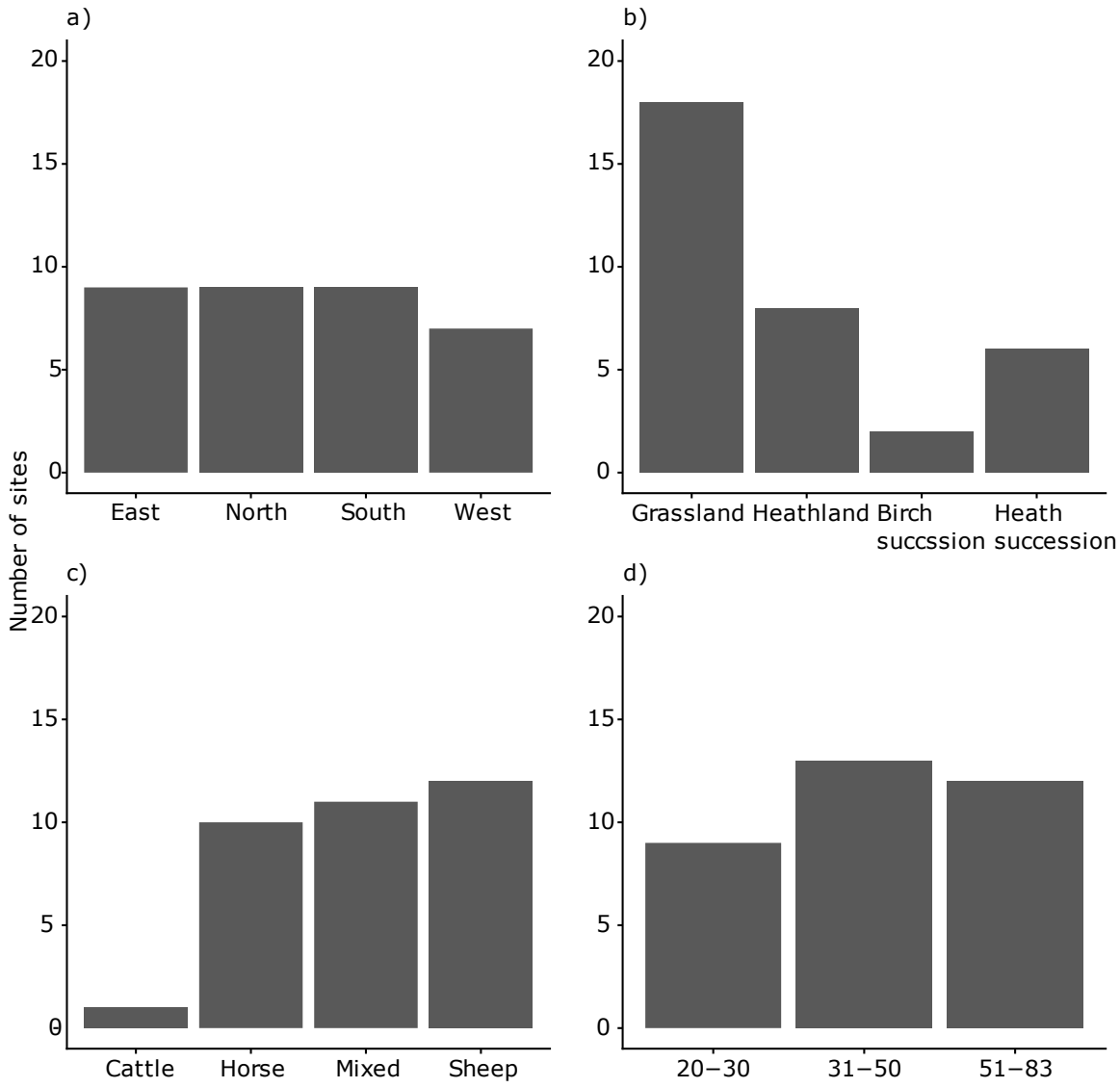

Figure 2-2: Distribution of study site characteristics. The sites were evenly distributed across the Icelandic lowlands (a) and most were in grassland (grazed and ungrazed) and fewer in heathland or succession from grassland (grazed) into heathland or birch woodland (ungrazed) (b). Most sites were grazed during the measurement period by sheep, horse or both; one sites was grazed exclusively by cattle (c). Exclosure age was evenly distributed over relatively young (20-30 years), medium-to-old (31-50 years) and old (51-83 years) exclosures (d).

The study sites were located both in grassland, heathland and transitional vegetation (Figure 2-2). The vegetation type was defined according to the dominant vegetation on the grazed part (control) as this represents the vegetation before grazer exclosures were established. Most sites were grassland (n = 26), dominated by graminoid and/or other herbaceous plants (Figure 2-3a-d). The most common grassland species were *Agrostis capillaris, Anthoxanthum odoratum, Avenella flexuosa, Bistorta vivipara, Carex bigelowii, C. vaginata, Deschampsia cespitosa, Equisetum arvense,*

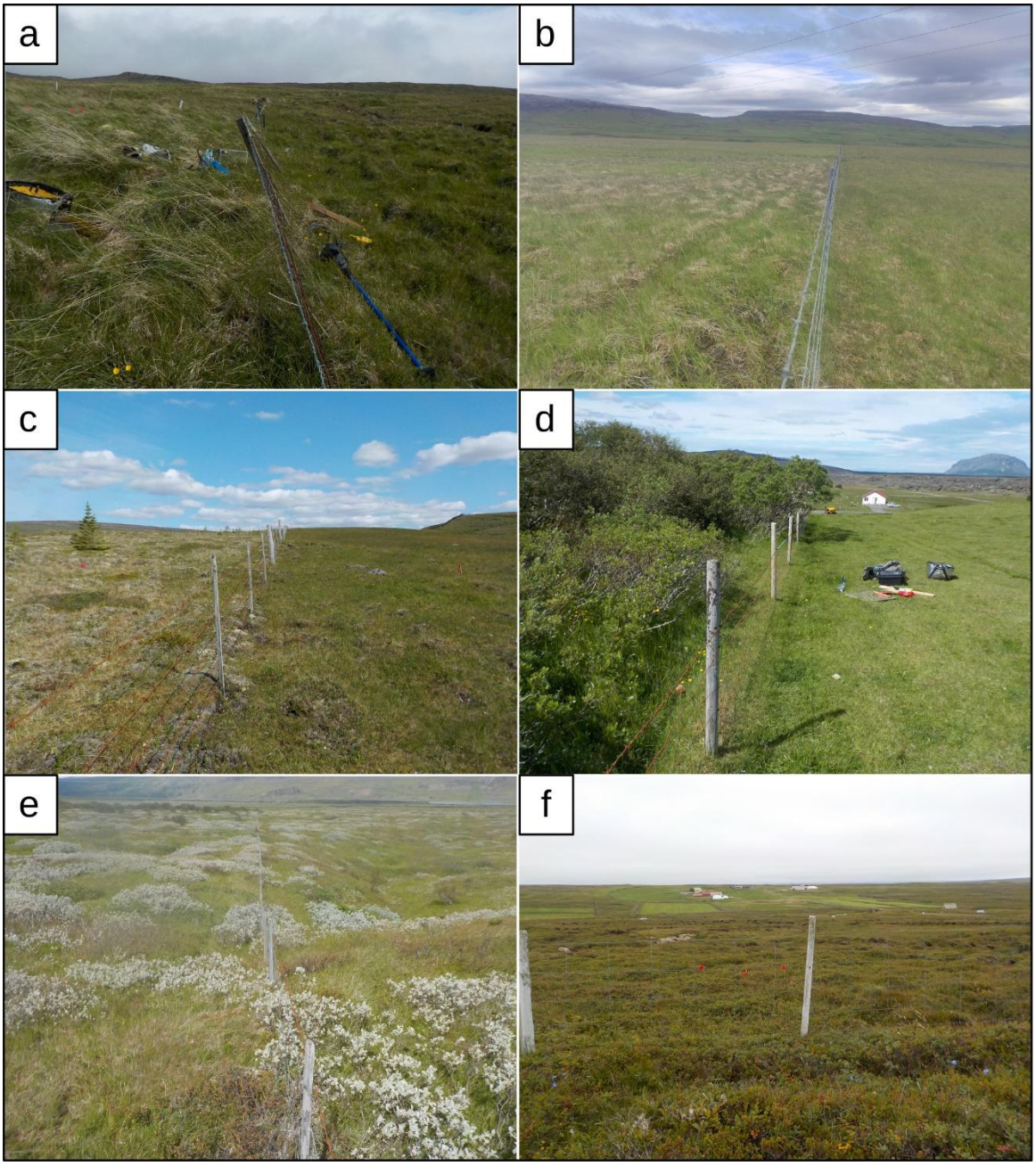

Figure 2-3: Examples for study sites in different major vegetation types. In a-e the grazer exclosure is on the left side and the grazed land on the right side of the image. in f, the picture is taken from inside the grazer exclosure facing into the grazed land behind the fence. The vegetation types represented in the photographs are Grassland in slopes (a) and flat land (b), Succession from grazed grassland into heathland (c) and birch forest (d), Heathland, dominated by deciduous shrubs (e) and Ericaceae (f). All photographs were taken by Christian Klopsch.

E. pratense, Festuca rubra, F. vivipara, Galium verum, Poa pratensis and *Ranunculus acris.* Most grassland sites were dominated by grassland vegetation in both the grazed and ungrazed side of the fence (n = 18; Figure 2-3a-b). Several grassland sites shifted from grassland on the grazed part to either heathland (n = 6) or natural birch woodland (n = 2) on the ungrazed part, either partly or completely, following cessation of grazing (Figure 2-3c-

d). These sites were collectively termed ‘Succession’ and treated either as a sub-group of the grassland sites (Chapter 3 and 4) or as an own vegetation category (Chapter 5 and 6). At three sites, the ungrazed plots did not shift consistently from grassland into heathland and one (Gunnarsstaðir, Stóri-Ás) or two (Skriða) sub-plots were defined as grassland, and the other as heathland succession. At one site (Álfgeirsvellir), the landowner re-introduced grazing in the ungrazed plot right before the start of the measurement period. Consequently, the ungrazed plot for CO_2 flux measurements (Chapter 3 and 4) was moved to the next field that was also not grazed for the same period and soil sampling (Chapter 5 and 6), not affected by the recent re-introduction, was conducted on the original plot. However, the moved plot for CO_2 measurements was in a heathland succession (developed on grassland after grazing ceased), thus Álfgeirsvellir is defined as ‘Succession’ in Chapter 3 and 4, but the original plot for soil sampling was in grassland and Álfgeirsvellir was defined as ‘Grassland’ in Chapter 5 and 6. Most of the heathland sites were in the eastern part of Iceland and dominated by heathland vegetation on both the grazed and the ungrazed side of the fence (n = 8). Heathland sites were either dominated by deciduous shrubs (Figure 2-3e) or by *Ericaceae* (Figure 2-3f). The most common heathland species were *Betula nana, Calluna vulgaris, Dryas octopetala, Empetrum nigrum, Salix herbacea*, *Salix sp.* and *Vaccinium uliginosum*.

2.2 Study Design

At each site, one paired fence contrast was defined in an open and dry terrain patch (> 50 × 50 m on mineral soil) in equal topography on both sides of the fence with a uniform measurement scheme (Figure 2-4a-b). In the ungrazed exclosure plot, three sub-plots were randomly selected in 5-20 m distance from the fence and from the neighbouring sub-plot mirrored in comparable terrain position (elevation, slope, aspect, distance) in the grazed plot. Around each sub-plot, three permanent measurement points were defined in an equilateral triangle with 1 m distance to the centre of the sub-plot (Figure 2-4c). For Chapter 3 (CO_2 flux measurements), 32 out of the 34 sites were used. The two sites, where grassland transitioned into mature birch woodland (canopy height > 5 m) following cessation of grazing were excluded because it was impossible to measure CO_2 fluxes of the whole vegetation in the exclosures using the chamber-based approach. For Chapter 4 (interaction of NDVI and CO_2 flux), 17 out of the 34 sites were used. For this analysis, only grassland sites with four or more sampling days were included. These sites were clustered in the western part (around Hvanneyri) and the northern part (around Hólar) of Iceland (Figure 2-1). For Chapter 5 and 6 (soil and root analysis), all 34 sites were included.

Data collection was conducted between July-September over two years; in 2022 in northern and eastern parts of Iceland and 2023 in western and southern parts of Iceland. For Chapter 3 and 4, I performed all measurements during July and August, considered as peak growing season (CO_2 flux, NDVI and complementary measurements). For logistical reasons, the data collection was split into sites that were measured once every 1-2 weeks and sites that were measured less frequently. In all sites in the vicinity of Hólar (northern part) and Hvanneyri (western part), from where the field campaigns were operated (n = 18, see encircled sites around the two places in Figure 2-1), measurements were taken on four to seven days at variable times between 8 AM and 7 PM, capturing a broad range of light and temperature conditions to represent average conditions during the growing season (Appendix 1: Supplemental Figure 8-2, Appendix 3: Supplemental Figure 8-12 and Supplemental Figure 8-13). Depending on distance from the respective fieldwork base (range 175-350 km), the

less frequently visited sites were measured once (eastern Iceland, 190-350 km, n = 3), twice (eastern and southern Iceland, 175-300 km, n = 8) or three times (southern Iceland, 175 km, n = 3) during the study (Table 2-2). During each measurement day, I recorded vascular plant species richness (presence/absence) in a 5 m radius around each sub-plot of grazed and ungrazed plots at each site. The plant species list for each site is available in Appendix 1: Supplemental Table 8-1 (nomenclature following Wąsowicz 2020). As a general pattern, mean, maximum and minimum species richness were larger in grazed plots compared to ungrazed plots, both in grassland, heathland and transitional vegetation between grassland and heathland/birch woodland (Table 2-3). Across all sites, mean vascular plant species richness was 37 in grazed plots (range 14-59 species) and 29 in ungrazed plots (range 11-49 species).

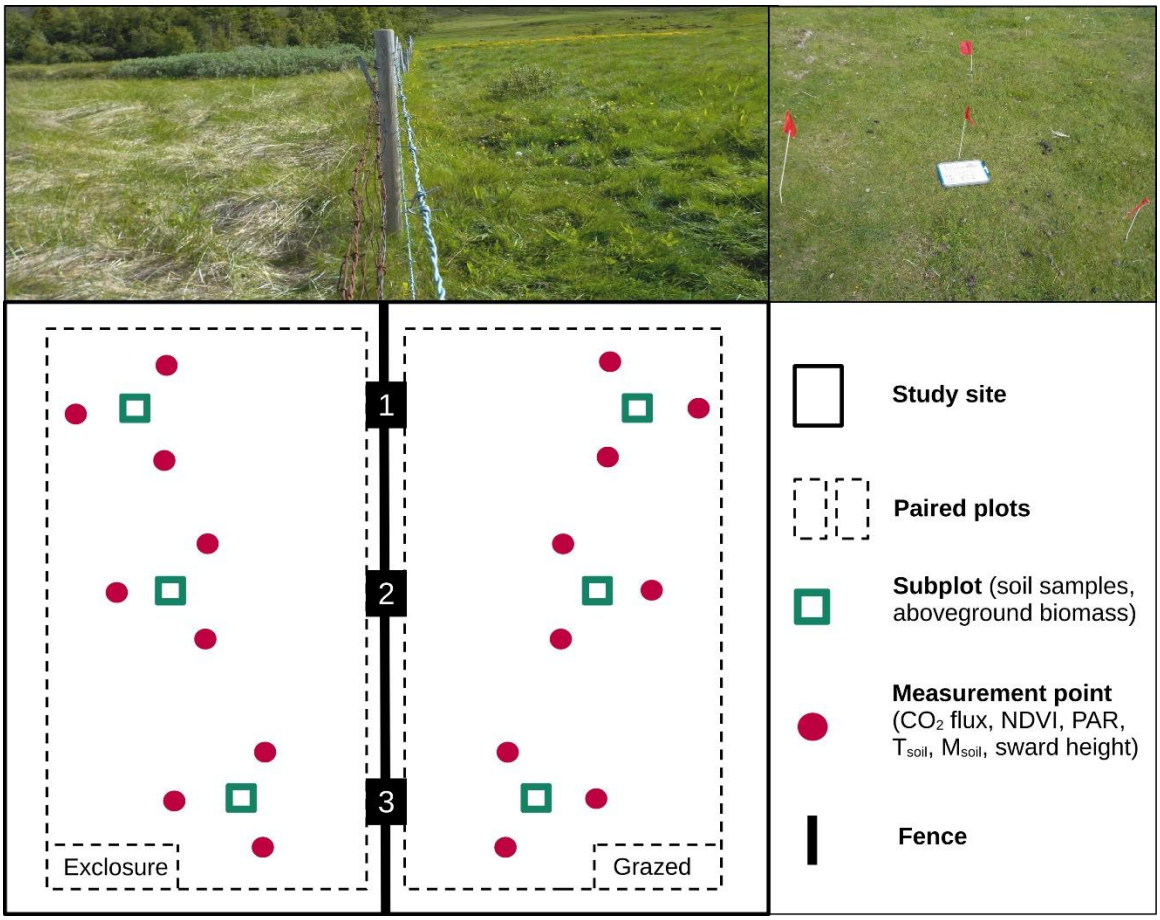

Figure 2-4: Uniform sampling design at each study site. Each study site was divided into a paired grazed and exclosure plot by a fence, erected more than 20 years ago (a). The same sampling design was applied within three sub-plots in 5-20 m distance between each other and the fence in the grazed and exclosure plot (b). Permanent measurement points for repeated CO_2 flux measurements were installed in 1 m distance around the sub-plot in an equilateral triangle (c). All photographs were taken by Christian Klopsch.

After the completion of CO_2 flux measurements, soil samples for Chapter 5 and 6 were collected from soil profiles from late August to late September in 2022 and 2023 in collective field campaigns, organised by the ExGraze project.

Table 2-3: Vascular plant species richness across the study sites. For all sites combined, and each of the regions and vegetation types mean, maximum and minimum species richness are shown (n indicated number of sites per category).

Region	Vegetation type	Plot	n	Species richness of vascular plants		
				Mean	Max	Min
ALL	ALL	Grazed	34	37	59	14
ALL	ALL	Exclosure	34	29	49	11
ALL	Grassland	Grazed	16	34	53	14
ALL	Grassland	Exclosure	16	26	42	11
ALL	Heathland	Grazed	8	41	57	32
ALL	Heathland	Exclosure	8	32	41	23
ALL	Succession	Grazed	8	45	59	35
ALL	Succession	Exclosure	8	37	49	26
E	Grassland	Grazed	1	37	37	37
E	Grassland	Exclosure	1	28	28	28
E	Heathland	Grazed	5	41	49	32
E	Heathland	Exclosure	5	34	41	29
E	Succession	Grazed	3	46	55	37
E	Succession	Exclosure	3	39	49	29
N	Grassland	Grazed	6	45	53	40
N	Grassland	Exclosure	6	35	42	24
N	Heathland	Grazed	1	57	57	57
N	Heathland	Exclosure	1	40	40	40
N	Succession	Grazed	2	36	37	35
N	Succession	Exclosure	2	31	36	26
S	Succession Birch	Grazed	2	23	24	21
S	Succession Birch	Exclosure	2	17	21	13
S	Grassland	Grazed	3	16	19	14
S	Grassland	Exclosure	3	16	21	11
S	Heathland	Grazed	2	32	32	32
S	Heathland	Exclosure	2	25	26	23
W	Grassland	Grazed	6	31	45	19
W	Grassland	Exclosure	6	22	34	13
W	Succession	Grazed	3	50	59	43
W	Succession	Exclosure	3	39	44	32

2.3 Methodological Approaches to Measure Ecosystem Carbon Dynamics

2.3.1 CO_2 Flux Measurements

To effectively apply the concept of nature-based solutions for climate change mitigation, it is critical to quantify C sink and source dynamics of ecosystems and associated land uses (Borer and Risch 2024). One approach to evaluate C sinks is to measure CO_2 fluxes between terrestrial C pools and the atmosphere, whereby a net flux from the atmosphere into the plant-soil-system corresponds to C sink and vice versa (Gilmanov *et al.* 2007, Pumpanen *et al.* 2010). On the other hand, changes of terrestrial C pools, such as vegetation or soil, can be measured directly, whereby net increases over time correspond to C sinks and vice versa (Kutsch *et al.* 2009, Lal 2018). In this thesis, both approaches are combined to determine the current seasonal net C flux and the resultant cumulative C pool of the past decades in relation to cessation of grazing.

CO_2 flux chambers are the major method to determine the net CO_2 exchange between the atmosphere and the plant-soil system in low vegetation when a large sample size and specific land uses and vegetation communities are targeted (Williams *et al.* 2006, Virkkala *et al.* 2018, Virkkala, *et al.* 2025b). The CO_2 flux is measured from changes in CO_2 concentration over time in the air over a small patch of land that is enclosed by the chamber, typically using an infra-red gas analyser (Pumpanen *et al.* 2004). Compared to other methods, CO_2 flux chambers are cheap, mobile, flexible in size and allow for replicated measurements. These features make them particularly useful in heterogeneous natural communities and small-scale experimental treatments such as the fence contrasts between grazed and ungrazed land in this thesis. Trade-offs of chamber-based flux measurements include a low temporal and spatial resolution, high labour and time costs and potential erroneous measurement in high wind or precipitation.

I used a closed dynamic chamber system to measure CO_2 fluxes for this dissertation, composed of a custom-built acrylic chamber (35 × 35 × 25 cm) with a sharpened aluminium frame at the open end to efficiently seal the chamber with the soil surface (Appendix 1: Supplemental Figure 8-1a,b). The chamber was connected to an infrared gas analyser which measured CO_2 concentration at one second intervals and calculated CO_2 fluxes directly based on CO_2 concentration change over time within the volume of the chamber (EGM 5, PP systems, Amesbury, USA; Pumpanen *et al.* 2010). Each CO_2 flux measurement consisted of two paired CO_2 flux measurement series, performed on the same measurement point (Figure 2-4) with an acclimation period in between to normalise CO_2 concentration in the chamber; one in ambient light (transparent chamber), to calculate net ecosystem exchange (NEE) and one with all incoming radiation excluded (chamber covered with an opaque hood), to calculate ecosystem respiration (ER; vegetation + soil respiration). Simultaneously with each NEE measurement series, incoming photosynthetically active radiation (PAR; µmol m^{-2} s^{-1}), volumetric soil moisture (M_{soil}; 0 - 100 % saturation) and soil temperature (T_{soil}; ˚C) in the topsoil (0-8 cm) were recorded, using a PAR probe and a soil sensor attached to the EGM-5 (TRP-3, PP-systems, Amesbury, USA; Hydra Probe II, Stevens Water Monitoring Systems, Portland, USA). Additionally, sward height was measured at nine random vegetation patches around each sub-plot on each sampling day, using a A4 writing blotter (160 g) placed on top of the sward and a folding ruler (Stewart *et al.* 2002). In total,

2442 measurements of ER and NEE, together with environmental measurements were performed during the measurement period.

2.3.2 NDVI Measurements

A complementary approach to estimate the net C exchange of an ecosystem is to use remote sensing (Beamish *et al.* 2020). Remote sensing products are constantly improving in spatial and temporal resolution with large publicly available databases (Gorelick *et al.* 2017, Andreatta *et al.* 2022). Using biophysical responses of vegetation to different spectral wavelengths, various vegetation indices have been developed to analyse land cover and land condition time-efficiently on large spatial and temporal scales (Bannari *et al.* 1995, Yan *et al.* 2025). As the most widely used vegetation index the Normalised Difference Vegetation Index (NDVI) provides information about the greenness (i.e. chlorophyll content) of vegetation (Pettorelli 2013, Huang *et al.* 2021). It is based on the ratio between incoming and reflected red and near-infrared light and returns a value between -1 and 1. Unvegetated land has principally a value < 0 and increasingly dense and green vegetation has increasing values towards 1. The biophysical basis of the index is that green, chlorophyll-rich plant tissue reflects less of the red light while it reflects more of the infra-red light compared to non-photosynthetic vegetation or unvegetated ground (Pettorelli 2013). NDVI can be assessed on a wide spectrum of pixel sizes – ranging from cm^2, using hand-held spectral instruments over m^2, using drones to km^2, using satellite sensors (Siewert and Olofsson 2020).

A major trade-off associated with larger spatial resolution are a lower temporal resolution. For assessing the net C balance, previous research showed that NDVI can be a proxy for GPP, and partly for NEE and ER in grassland and heathland when measured on a similar scale and calibrated with direct measurements of CO_2 fluxes such as chamber-based measurements (Nestola *et al.* 2016, Argenti *et al.* 2022, Guðmundsson *et al.* 2026). With NDVI as indirect proxy for net C exchange, spatial and temporal limitations of chamber-based methods can be resolved and CO_2 fluxes up-scaled to a larger area, such as similar vegetation types (Street *et al.* 2007, Guðmundsson *et al.* 2026). However, with increasing pixel size precision of upscaled CO_2 fluxes decreases due to land cover heterogeneity (Assmann *et al.* 2020, Siewert and Olofsson 2020). Thus, the applicability of NDVI is limited for the magnitude of CO_2 fluxes, but it can be a powerful indicator to define thresholds for C sinks and sources in different vegetation types and land uses.

Before each CO_2 flux measurement, I measured NDVI from 1.5 m above each measurement point, covering the same vegetation patch as the subsequent CO_2 flux measurement with a ground area of 0.35 m^2. A hand-held pole and two channel sensors connected to a SpectroSence 2+ data logger (SKR1849D/SS2, SKR1840ND/SS2, SKL906, Skye Instruments, Llandrindod Wells, UK) were used to measure incoming and reflected red (RED; 650 nm) and near-infrared (NIR; 800nm) radiation. NDVI was calculated automatically within the data logger as NDVI = (NIR – RED) / (NIR + RED). In total, 2536 ground-based NDVI measurements were performed during the measurement period. Additionally, satellite-derived NDVI data ($NDVI_{Sentinel\text{-}2}$) with a 10 m resolution were derived for the same period and area as the ground-based measurements (July-August 2022 and 2023) and for all of Iceland for July-August 2023 from band 4 (RED, 665 nm) and band 8 (NIR, 842 nm) of the Sentinel-2 satellite image library, using Google Earth Engine (Gorelick *et al.* 2017). $NDVI_{Sentinel\text{-}2}$ was calibrated with the ground-based NDVI, using the

$NDVI_{Sentinel-2}$ value of the GPS locations of each measurement point. $NDVI_{Sentinel-2}$ and the calibration with ground-based NDVI were further used to estimate average summer NDVI and net C balance of the Icelandic lowland grasslands.

2.3.3 SOC Measurements

Both direct measurements of CO_2 fluxes and NDVI reveal only the instantaneous exchange of CO_2 between the plant-soil system and the atmosphere during the measurement; they cannot determine whether C is ultimately stored or lost in the ecosystem over time. Through other pathways, C may enter or leave the system, for example as lateral leaching of dissolved organic C in the soil solution or by bioturbation by soil organisms (Soussana *et al.* 2010; Kindler *et al.* 2011; Howison *et al.* 2017; Nakhavali *et al.* 2021; Don *et al.* 2024). Also, interannual variability limits extrapolation of measurements from one year to the other (Baldocchi *et al.* 2018). Therefore, assessing actual C accumulation or loss over time is more reliable by quantifying ecosystem C stocks (Rodeghiero *et al.* 2010, Poeplau *et al.* 2011).

As noted above, in grassland and heathland ecosystems most C is stored below-ground as SOC, rather than as plant biomass (Jobbágy and Jackson 2000, Scharlemann *et al.* 2014). Typically, SOC accumulation is slow, compared to C accumulation in biomass and detecting reliable changes in SOC stocks requires long-term comparisons of contrasting treatments (Stockmann *et al.* 2013, Rumpel *et al.* 2020, Stanley *et al.* 2023). For example, to evaluate net SOC sequestration, baseline SOC values prior to the long-term treatment are needed (Don *et al.* 2024). However, such reference values are often unavailable in long-term comparative studies—typically the treatments were not originally established with SOC accounting in mind. This limitation applies also for the sites selected in this thesis. Consequently, a space-for-time substitution approach was applied for the land use contrasts, assuming equal conditions and equal SOC prior to the cessation of grazing – an approach widely used to infer long-term ecosystem development, such as in studies of primary succession (Walker and del Moral 2003, Walker *et al.* 2010). Differences in SOC stocks between paired grazed and ungrazed land can, therefore, be interpreted as SOC change associated with cessation of grazing either by SOC loss or sequestration (Franzluebbers 2021, Silveira *et al.* 2024).

To quantify C stocks in vegetation and soil and for root analysis, above-ground biomass and soil samples were taken from each sub-plot in all study sites following a standard protocol (Appendix 1: Supplemental Figure 8-1c): First, a soil profile was excavated on each sub-plot to a soil depth of 60 cm, except for three profiles with shallower soils until bedrock started (n = 201, Sk40 and Sk90 shared that same grazed plot with three soil profiles, but separate exclosure plots á three soil profiles with different exclosure age) . Then, the boundary of the soil profile was defined as the upper limit consisting of mineral material, following WRB guidelines (IUSS Working Group WRB 2022). Above the soil profile boundary, total above-ground biomass was sampled using a 10 cm ×10 cm metal frame, driven into the vegetation, cut off at the soil surface and stored in paper bags, in total 200 samples (one sample missing). Above-ground biomass samples included live green biomass, dead standing biomass, woody biomass (if present) and detached plant litter on the soil surface and were air-dried after sampling. Subsequently, soil profiles were described for the percentage amount of coarse fraction (parent material > 20 mm) and visual characteristics, including colour, texture, tephra layers (ash deposits of volcanic eruptions) and iron oxidation zones (indicating

groundwater influence) in each soil horizon. Then, soil samples for bulk density, C and N analysis and root analysis were collected (Appendix 1: Supplemental Figure 8-1c).

Three or more bulk density samples were collected from each soil profile with at least one sample from 0-10 cm, 10-30 cm and 30-60 cm. If variation in the profile was larger, the number of samples was adjusted accordingly. Samples were collected using a metal cylinder with sharp edges of 5 cm diameter and 5 cm depth pressed horizontally into the soil layer and cut off from above. When the soil was too coarsely textured or too loosely packed to use the soil cylinder, a soil block of predetermined volume was cut with a knife. At least four samples for C and N analysis were collected from the 0-60 cm soil profile, according to previously defined soil horizon depth as complete blocks of 5 cm × 5 cm × sample depth. Sample depth ranged between 4 and 30 cm, but for most samples either 10 or 20 cm. All soil samples were air-dried after sampling and in total 710 bulk density samples and 893 samples for C and N analysis were collected from 201 soil profiles.

Root samples were collected from every soil profile in four predetermined depth intervals: 0-10 cm, 10-20 cm, 20-40 cm and 40-60 cm, in total 802 samples from 201 soil profiles. Every root sample was taken as complete block with a defined soil volume of 5 cm × 5 cm × sample depth. After sampling, root samples were stored in plastic bags at 4˚C until root samples were washed off from bulk soil (no later than 14 days after sampling and typically within 7 days). Cleaned root samples were scanned using a flatbed scanner to obtain community-level root morphological traits, using digital image analysis of the root scans (Freschet, *et al.* 2021b, Seethepalli *et al.* 2021). After scanning, fresh and dry root biomass was determined.

2.3.4 Application of the collected Data in this Dissertation

The data, generated through the field sampling campaigns, were used as the basis for the four following chapters in this thesis and further sample and data processing, specific for each chapter, are outlined in each chapter. The CO_2 flux data were processed in Chapter 3 to establish whether grazed and ungrazed plots of the study sites were C sinks or sources during the measurement period. NDVI data together with CO_2 flux data of the grassland sites measured in greater detail (n = 17) were processed in Chapter 4to examine the predictability of CO_2 fluxes from NDVI. Soil C and N data were processed in Chapter 5 to quantify SOC stocks in grazed and ungrazed plots of the study sites. Root biomass and root trait data were processed in Chapter 6 to assess the density, distribution and morphology of community-level root systems at our sites. These data form a basis to study how long-term cessation of grazing influences C cycling through the plant-soil system compared to continuous grazed land and provide useful baseline measurements for future studies at these sites concerning further questions of C cycling or other ecological responses to long-term cessation of grazing. To facilitate future research, all data and data analysis scripts are stored and publicly available in Klopsch *et al.* (2026a).

3 Chapter III: Long-term Cessation of Grazing Reduces Net Carbon Uptake in sub-arctic Grassland and Heathland

Abstract: In northern grassland and heathland, livestock grazing has historically been the main land use. Today, traditional grazing is diminishing and ceased in many places with so far unknown long-term effects for ecosystem carbon cycling due to the scarcity of long-term studies. We compared CO_2 fluxes in exclosures where grazing was ceased multiple decades ago (20-83 years) with adjacent grazed land across a broad range of semi-natural grassland and heathland in Iceland. All 32 study sites, both grazed plots and the exclosures, were net carbon sinks during the growing season. However, long-term grazing cessation led to considerable changes in ecosystem CO_2 fluxes, with overall 37% less net CO_2 uptake (NEE_{600}) in the exclosures ('Exclosure effect'). Grassland was a substantially larger carbon sink and had a stronger 'Exclosure effect' than heathland. Across all sites, calculated Light Use Efficiency and Biomass Use Efficiency were 22% and 66% lower, respectively, in the exclosures compared to grazed plots. At several grassland sites, grazing cessation led to a shift in vegetation to heathland. At these sites, NEE_{600} was 72% lower in the exclosures. The greatest reductions in NEE_{600} occurred in the first 20-30 years following grazing cessation, and further reductions with advancing age of the exclosures (> 50 years) were found when grassland shifted into heathland. Our results showed that long-term grazing cessation results in a reduced carbon sink strength, highlighting the key role of grazing animals for vegetation dynamics and carbon cycling in grassland and heathland.[1]

3.1 Introduction

Grassy ecosystems, including grassland and heathland, cover about 40% of the Earth´s surface and are vital for biodiversity, climate regulation and global biogeochemical cycles (Bengtsson *et al.* 2019, Stevens *et al.* 2022). Due to extensive degradation, driven by land-use change, overgrazing, abandonment of traditional pastoral practices, and declining wild herbivore populations, these ecosystems are threatened globally (Bardgett *et al.* 2021, Buisson *et al.* 2022). In a global synthesis, Dangal *et al.* (2020) showed that grassland, when grazed extensively, is typically a net carbon (C) sink and soils of grazed grassland store substantial organic C despite regular biomass removal (Roy and Bagchi 2022). Therefore, soil organic carbon (SOC) sequestration through improved grazing management and herbivore-plant-soil interactions have been proposed as promising but neglected nature-based solutions for climate change mitigation (Conant *et al.* 2017, Schmitz *et al.* 2018, Borer and Risch 2024, Stanley *et al.* 2024). However, most C cycling models ignore the role of

[1] A version of this chapter is published:
Klopsch, C., Thorhallsdottir, A.G., van der Wal, R., Bardgett, R.D., Thorsteinsson, B., Geirsdottir, A., 2026. Long-term cessation of grazing reduces net carbon uptake in northern grassland and heathland. Agriculture, Ecosystems & Environment 407, 110441. https://doi.org/10.1016/j.agee.2026.110441.

grazing animals, limiting predictions of C cycling and C sequestration in grazed ecosystems (Viglizzo *et al.* 2019, Roe *et al.* 2021, Rizzuto *et al.* 2024).

In general, mammalian herbivores influence CO_2 fluxes between vegetation, soil and the atmosphere indirectly above- and below-ground through grazing activities (Rizzuto *et al.* 2024, Trepel *et al.* 2024). Above-ground, grazing promotes herbaceous vegetation over mosses, lichen and woody vegetation, thereby maintaining open ecosystems (Van der Wal 2006, Olofsson and Post 2018). Below-ground, grazing modifies soil microclimate and nutrient cycling (Van der Wal *et al.* 2004, Doughty *et al.* 2016, Li *et al.* 2024). These effects are particularly relevant in northern ecosystems, where cold climate and short growing seasons limit nutrient availability and turnover rates (Petit Bon *et al.* 2020). Together, these grazing effects influence photosynthetic activity and respiration and control net ecosystem exchange (NEE), i.e. the net C sink or source strength of the ecosystem (Dangal *et al.* 2020, Malhi *et al.* 2022).

Particularly in northern Europe, traditional grazing created mosaics of (semi-natural) grassland and heathland, with grassland typically dominating where grazing activities are relatively high and heathland, often dominated by *Calluna vulgaris*, developing under less fertile conditions (Rosa García *et al.* 2013, Ross *et al.* 2016, Vowles, *et al.* 2017b, Norderhaug *et al.* 2023, Rittl *et al.* 2025). Long-established grassland and heathland have been shown to be important C sinks that can accumulate large amounts of SOC (Quin *et al.* 2015, Sørensen, *et al.* 2018b, Duddigan *et al.* 2024, Lockwood *et al.* 2026). However, without disturbance, such as grazing, productivity is often diminishing in both grassland and heathland (Li *et al.* 2023, Norderhaug *et al.* 2023). Linked to grazing cessation and climate warming, shrub expansion is a widely described phenomenon across northern ecosystems (Myers-Smith *et al.* 2011, Mekonnen *et al.* 2021), with erect deciduous shrubs such as *Salix sp*., or stress-tolerant evergreen shrubs such as *Empetrum nigrum* expanding into abandoned grassland and heathland (Vowles, *et al.* 2017a, Maliniemi *et al.* 2018). Productive deciduous shrubs can modify microclimate and enhance both uptake and emission of CO_2 while low-productive evergreen shrubs may reduce total C cycling (Sørensen, *et al.* 2018b, Vowles and Björk 2019, Parker *et al.* 2021, Myrsky *et al.* 2024). In grassland on the other side, self-shading and reduced tillering from basal meristems through litter accumulation may reduce productivity when left ungrazed over extended periods (Borer *et al.* 2014, Eskelinen *et al.* 2022, Thorhallsdottir and Gudmundsson 2023).

Long-term effects of grazing cessation for the CO_2 flux balance of northern ecosystems remain poorly understood because most studies maintained grazing cessation for < 10 years (Forbes *et al.* 2019, Niu *et al.* 2025). Such short-term interventions often reflect legacy effects of previous grazing, such as altered nutrient availability, vegetation composition and structure which can promote net C uptake in the short-term (Egelkraut, *et al.* 2018b, Wu *et al.* 2025). Our study addresses this gap by comparing CO_2 fluxes in exclosures where grazing was ceased multiple decades ago with adjacent grazed land across a broad range of semi-natural grassland and heathland in Iceland. In the long-term, CO_2 fluxes may respond fundamentally different to grazing cessation due to different growth strategies in grassland and heathland and soil processes unfolding on different temporal scales relative to above-ground processes (Ward *et al.* 2014, Wang, J. *et al.* 2024). Iceland still retains extensive semi-natural grassland and heathland in contrast to other parts of Northern Europe (Helgadóttir *et al.* 2014, Cousins *et al.* 2015, Aune *et al.* 2018), historically maintained by free-roaming sheep without further cultivation (Ross *et al.* 2016). In Iceland, land use changes are now also leading to accelerated grazing cessation, abandoned grassland and

shrub expansion. The sub-arctic climate and low woodland cover facilitates long-term comparisons of CO_2 fluxes between grazed and ungrazed grassland and heathland, as succession into closed-canopy woodland is limited in Iceland (Behrend *et al.* 2025). Specifically, we addressed the following research questions:

(i) How does long-term cessation of grazing affect CO_2 fluxes and the net carbon balance (NEE) during the growing season?

(ii) How does time since cessation of grazing influence CO_2 fluxes in grassland and heathland, respectively?

(iii) How are vegetation structure and soil microclimate, factors that could influence CO_2 fluxes, modified by the long-term cessation of grazing?

3.2 Methods

3.2.1 Study Design

In the Icelandic lowlands (< 200 m a.s.l.), approximately 35 % of land is semi-natural grassland or heathland and used for livestock grazing, either free-roaming or in fenced pastures closer to the farms during the growing season (Marteinsdóttir *et al.* 2017, Defourneaux *et al.* 2024). During the last century, livestock exclosures (hereafter 'exclosures') were fenced off at many farms across the country following incentives to promote afforestation (Thorhallsdottir and Gudmundsson 2023). Many of these exclosures were never fully planted and provide long-term fence contrasts in grassland and heathland, without the confounding effects of forest succession (Thorhallsdottir *et al.* 2013).

Local knowledge of land use from landowners and digital surveying of historical and recent aerial photographs were used to map sites with exclosures, adjacent to continuous grazed land. All sites were semi-natural, unfertilised grassland and heathland below 200 m a.s.l. Sites were selected according to the following criteria: known time of grazing cessation and reliable land use information with confirmed historical grazing for the last centuries; similar abiotic conditions on the grazed and ungrazed section of the fence; complete vegetation cover; and no known human alteration of the land except for the introduction of livestock. While originally aiming for 40 sites, 32 sites across Iceland eventually met the criteria (Figure 3-1). The selection included young (20-30 years, n = 9), medium-to-old (31-50 years, n = 12) and old (51-83 years, n = 11) exclosures (Appendix 2: Supplemental Table 8-2). Animal densities and grazing regimes will have varied, but all locations had been grazed throughout time. Thus, we used grazed land as control and long-term fenced-out exclosures as grazing cessation treatment.

At each site, a grazed and ungrazed patch were matched and defined as paired plots (n = 2 × 32). Three sub-plots were randomly positioned in each ungrazed plot and duplicated in similar elevation, topography and distance to the fence in each associated grazed plot (n = 2 × 32 × 3 = 192; Figure 3-1). Around each sub-plot, three permanent measurement points were marked out at 1 m distance to the sub-plot centre, in the shape of an equilateral triangle (n = 3 × 192 = 576). At these measurement points, CO_2 flux, abiotic parameters, NDVI and sward height were assessed on each measurement day.

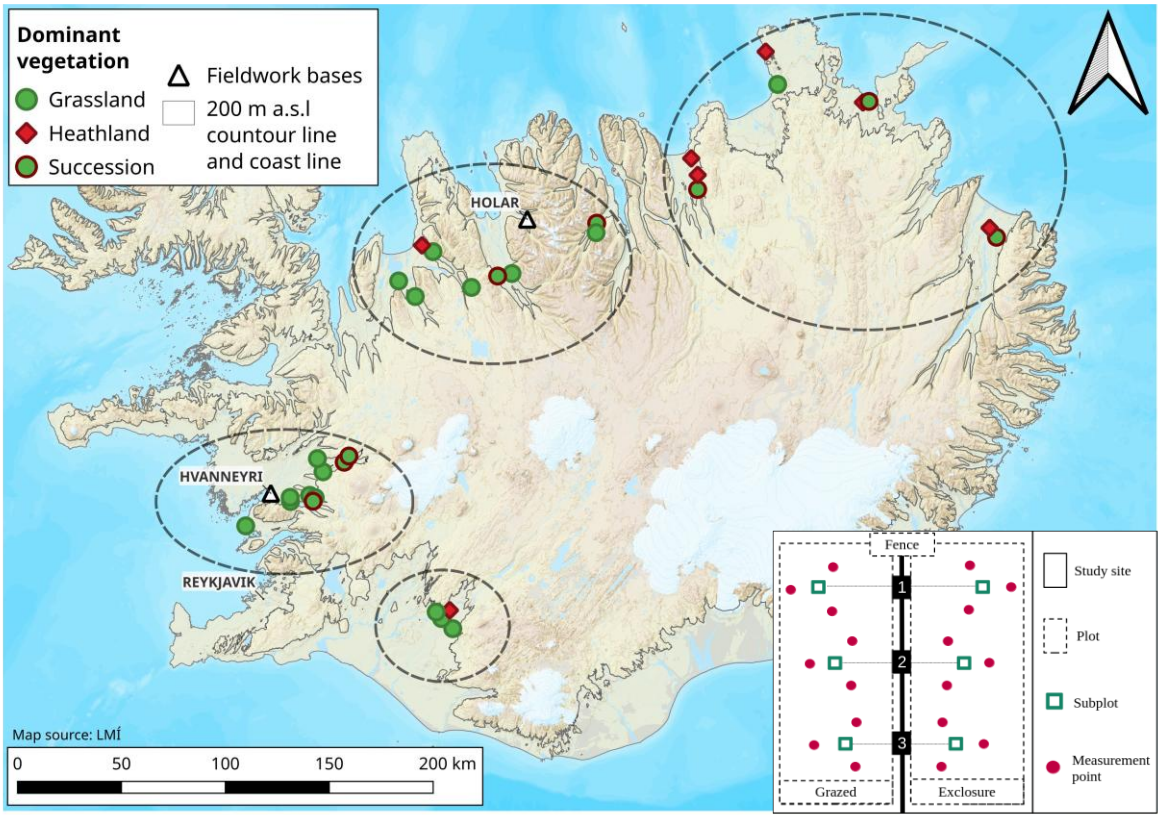

Figure 3-1: Overview map of the 32 sites used in this study. The sites were located in the northern, eastern, western and southern part of Iceland below < 200 m a.s.l. The site symbols refer to the dominant vegetation. The general study design was composed of three sub-plots surrounded by three permanent measurement points per grazed and ungrazed plot in each site (see box in the lower right).

The 32 sites were classified into two groups based on dominant vegetation in the grazed land (Figure 3-1): 'grassland', dominated by graminoid or other herbaceous vegetation (n = 24) and 'heathland", dominated by deciduous or evergreen shrub or heath vegetation (n = 8). Within the 'grassland' group, an additional sub-group 'succession' was classified where a shift from grassland-dominated vegetation in the grazed plot to heathland-dominated vegetation in the exclosure occurred (n = 8). The most common grassland species were *Agrostis capillaris, Anthoxanthum odoratum, Avenella flexuosa, Bistorta vivipara, Carex bigelowii, C. vaginata, Deschampsia cespitosa, Equisetum arvense, E. pratense, Festuca rubra, F. vivipara, Galium verum, Poa pratensis* and *Ranunculus acris.* The most common heathland species were *Betula nana, Calluna vulgaris, Dryas octopetala, Empetrum nigrum, Salix herbacea* and *Vaccinium uliginosum.*

3.2.2 Data Collection

CO_2 flux measurements

A closed dynamic chamber system was used to measure CO_2 fluxes, composed of a custom-built acrylic chamber (35 × 35 × 25 cm) with a fan for continuous air mixing. The chamber was connected to an infrared gas analyser which measured CO_2 concentration at one second

intervals for 120 seconds (EGM 5, PP systems, Amesbury, USA; Pumpanen *et al.* 2010). At the end of the 120 seconds measurement series, the CO_2 flux was automatically calculated over the 120 individual measurements and used further as CO_2 flux measurement. Two paired CO_2 flux measurement series were performed at the same point with an acclimation period in between to normalise CO_2 concentration in the chamber; one in ambient light (transparent chamber), measuring net ecosystem exchange (NEE) and one with all incoming radiation excluded (chamber covered with an opaque hood), measuring ecosystem respiration (ER; plant and soil respiration). Simultaneously with each NEE measurement series, incoming photosynthetically active radiation (PAR; µmol m^{-2} s^{-1}), volumetric soil moisture (M_{soil}; 0-100 % saturation) and soil temperature (T_{soil}; °C) in the topsoil (0-8 cm) were recorded, using a PAR probe and a soil sensor attached to the EGM-5 (TRP-3, PP-systems, Amesbury, USA; Hydra Probe II, Stevens Water Monitoring Systems, Portland, USA).

Measurements were performed during July and August. For logistical reasons, we worked in 2022 in the northern and eastern parts of Iceland and in 2023 in the western and southern parts. At all sites in the vicinity of Hólar (northern part) and Hvanneyri (western part), from where the field campaigns were operated (n = 18, see encircled sites around the two places in Figure 3-1), measurements were taken on four to seven days at variable times between 8 AM and 7 PM, in variable light conditions to capture a wide range of environmental conditions. Depending on distance from their respective fieldwork base (150-400 km), distant sites in eastern and southern Iceland were measured once (n = 3), twice (n = 8) or three times (n = 3) during the study (Appendix 2: Supplemental Table 8-2).

NDVI and Sward Height Measurements

Before the CO_2 flux measurements, NDVI, as a proxy for photosynthetically active biomass, was measured from 1.5 m above each measurement point, covering a ground area of 0.35 m^2. A hand-held pole and two channel sensors connected to a SpectroSence 2+ data logger (SKR1849D/SS2, SKR1840ND/SS2, SKL906, Skye Instruments, Llandrindod Wells, UK) were used to measure incident and reflected red (RED; 650 nm) and near-infrared (NIR; 800nm) radiation. NDVI was calculated automatically within the data logger from Eq. 3-1

$$NDVI = (NIR - RED) / (NIR + RED), \qquad \textit{Eq. 3-1}$$

returning values between -1 to +1. Values below 0 generally indicate unvegetated ground and values between 0 and 1 represent successively greener (i.e. chlorophyll-richer) vegetation (Pettorelli 2013). Additionally, height of the sward was measured at nine random vegetation patches around each sub-plot on each sampling day, using a A4 writing blotter (160 g) placed on top of the sward and measured with a folding ruler (Stewart *et al.* 2002).

3.2.3 Data Processing

All CO_2 flux values were converted into µmol m^{-2} s^{-1} and reported from an atmospheric perspective, i.e. negative values correspond to absorption from the atmosphere and positive values correspond to emissions into the atmosphere. Environmental variables (PAR, T_{soil} and M_{soil}) were averaged across each 120 seconds NEE measurement series. In 2023, PAR and T_{soil} were higher ($p < 0.05$) than in 2022 but without systematic bias between the grazing contrasts (i.e. 'year'×'grazing cessation' not significant, Appendix 2: Supplemental Table 8-3).

Gross Primary Production (GPP)

Gross primary production (GPP) was calculated as GPP = NEE – ER. Actual GPP is primarily driven by incoming PAR (Ruimy *et al.* 1995), which varied between 51 and 1789 µmol m^{-2} s^{-1}, with a mean of 695 µmol m^{-2} s^{-1}. To improve comparisons under variable light conditions among sites and days, GPP was standardised to a common irradiance of 600 µmol m^{-2} s^{-1} using a light response curve (LRC) modelling approach (Shaver *et al.* 2007). Four seasonal community LRCs were modelled: two for grassland (maximum GPP > 20 µmol m^{-2} s^{-1}, maximum GPP < 20 µmol m^{-2} s^{-1}) and two for heathland (maximum GPP > 10 µmol m^{-2} s^{-1}, maximum GPP < 10 µmol m^{-2} s^{-1}; Appendix 2: Supplemental Figure 8-3, Supplemental Table 8-2). The LRCs were calculated according to Eq. 3-2, adapted from Strimbeck et al. (2019), using a self-starting non-linear least-squares regression that fitted model parameters with the lowest residual sum of squares as

$$GPP_{raw} = (GPP_{max} \times PAR) \,/\, (k + PAR), \qquad Eq.\ 3\text{-}2$$

where GPP_{raw} = NEE – ER, GPP_{max} = rate of light saturated photosynthesis, and k = half saturated constant of photosynthesis. With the model parameters, a seasonal community GPP at PAR = 600 µmol m^{-2} s^{-1} and at each measurement PAR was calculated. The ratio between both was then used as a correction factor in Eq. 3-3 to estimate GPP_{600} (Strimbeck *et al.* 2019) as

$$GPP_{600} = GPP_{raw} \times ((GPP_{max} \times 600) \,/\, (k + 600)) \,/\, ((GPP_{max} \times PAR) \,/\, (k + \mathrm{PAR})). \qquad Eq.\ 3\text{-}3$$

Ecosystem Respiration (ER)

Ecosystem respiration (ER) is commonly directly influenced by soil temperature (T_{soil}; Tjoelker *et al.* 2001). During the measurement periods, T_{soil} ranged between 8.4 and 31.7 °C, with a mean of 15.8 °C, and was positively correlated with ER ($\rho_{2434} = 0.40$, $p < 0.001$; Appendix 2: Supplemental Figure 8-4). Hence, to improve comparisons, ER was standardised to a common T_{soil} of 15 °C using Eq. 3-4, following the temperature dependent Q_{10} approach of Tjoelker *et al.* (2001) that describes the increase in respiration per 10 °C increase in soil temperature as

$$ER_{15} = ER \times Q_{10}^{((15 - Tsoil)/10)}, \qquad Eq.3\text{-}4$$

where ER_{15} = standardised ER to T_{soil} = 15 °C and Q_{10} = 3.22 - 0.046 * T_{soil} (Tjoelker *et al.* 2001). A standardised NEE_{600} was then re-calculated as the difference between GPP_{600} and ER_{15} for each measurement, representing net ecosystem exchange at an average PAR of 600 µmol m^{-2} s^{-1} and T_{soil} of 15 °C.

Carbon uptake efficiency

To analyse the C uptake efficiency of vegetation, the ecological light use efficiency (LUE) was calculated (Eq. 3-5), reflecting the capability of the vegetation to use incoming radiation to absorb C (Gilmanov *et al.* 2007), as

$$LUE = GPP_{raw} \,/\, PAR. \qquad Eq.3\text{-}5$$

To reflect the capability of the vegetation to use the standing biomass to absorb CO_2, biomass use efficiency (BUE) was calculated (Eq. 3-6) as

$$BUE = GPP_{600} / Sward\ height, \qquad Eq.3\text{-}6$$

where sward height was used as proxy for above-ground biomass and GPP_{600} was used as average CO_2 absorption, unconfounded by differences in PAR. Both C uptake efficiencies are reported from the plant's perspective, i.e. all values are positive.

3.2.4 Statistical Analysis

The effect of grazing cessation, i.e. 'Exclosure effect', on GPP_{600}, R_{15}, NEE_{600}, NDVI, sward height, T_{soil}, M_{soil}, PAR, LUE and BUE was tested, using linear mixed effects models (LMM) to account for the structure of the study design. As random effects, 'sub-plot' nested in 'site' and 'measurement day' nested in 'year' were consistently specified. As fixed effects, 'grazing cessation', 'dominant vegetation' (grass or heath) and, when significant, the interaction between both were specified. The effect size and level of significance of predictor variables were retrieved from least-squares post-hoc tests. The 'succession' sub-group of the 'grassland' sites (n = 8), where grassland shifted into heathland following cessation of grazing, was specifically addressed in a separate LMM, using the same model structure and response variables as above and 'grazing cessation' as sole fixed effect.

Spearman's rank correlation was used to analyse correlations between vegetation and soil parameters and CO_2 fluxes in grassland and heathland. Further, linear regression was used with a mixed effect model structure with the same random effects as described above, to analyse how sward height was associated with ecosystem respiration. Sward height was used as a proxy for grazing intensity in the grazed part or for biomass accumulation in the ungrazed (Appendix 2: Supplemental Figure 8-5).

To explore the trend of CO_2 fluxes over the measurement season, the dataset was subsampled to all sites with at least 5 measurement days (n = 17). Flux values were summarised into five weekly intervals during the measurement period. Mean fluxes with their 95 % confidence intervals were plotted along the timeline of the measurement period. Differences between aggregated fluxes from grazed and ungrazed plots for each weekly interval were tested using ANOVA with 'grazing cessation', 'weekly interval' and 'dominant vegetation' as independent factors, followed by a least-squares means post-hoc test to determine the significance of the 'Exclosure effect'.

From the contrast values, retrieved from post-hoc tests, an 'Exclosure effect' was calculated as the percent change from Grazed (G) to Exclosure (E) either per plant community or across all data using the Eq. 3-7

$$Exclosure\ effect\ (\%) = (G - E) / G \times 100, \qquad Eq.3\text{-}7$$

where negative percentages indicate a lower value, and positive percentages indicate a higher value associated with ungrazed relative to grazed land.

The effect of increasing time since grazing cessation relative to the grazed reference on CO_2 fluxes was analysed using LMM. For this analysis, all measurements were pooled and reclassified to four categories of 'years since grazing cessation' ('years'): 'grazed' (all

measurements from grazed plots), ‘20-30 years’, ‘31-50 years’ and ‘51-83 years’. Then, ‘years’, ‘dominant vegetation’ and their interaction were used as fixed effects within the same random effect model structure as described above. Significant differences between ‘years’ for each vegetation group were tested with least-squares means post-hoc tests.

All data processing and statistical analyses were performed using R statistical software, version 4.2.1 (R Core Team 2024) with the additional packages nls (Baty *et al.* 2015), lme4 (Bates *et al.* 2015), lmerTest (Kuznetsova *et al.* 2017), emmeans (Lenth 2023) and multicomp (Hothorn *et al.* 2008).

Table 3-1: Model diagnostics for effects of cessation of grazing. F-statistics from ANOVA of fixed effects from linear mixed effects models (LMM) across all sites for responses of CO_2 fluxes, Light and Biomass Use Efficiency (LUE,BUE) and environmental parameters with ‘Grazing cessation’ and ‘Dominant vegetation’ (grassland/ heathland) and the interaction between both as fixed effects (Significance indicated with bold numbers and asterisks). Random effects in each LMM were ‘sub-plot’ nested in ‘site’ and ‘day of year’ nested in ‘year’. For the sub-group of sites that shifted from grassland into heathland following grazing cessation (‘succession’) the same LMMs were performed but without ‘dominant vegetation’ as fixed effect. T_{soil} = Soil temperature, M_{soil} = Soil moisture

Dataset	Response	Grazing cessation (G)		Dominant vegetation (V)		G × V	
		F		*F*		*F*	
All Sites (n = 32)	NEE_{600}	**63.0**	***	**7.5**	*	**9.0**	**
	GPP_{600}	**79.9**	***	**11.0**	**	**15.4**	***
	ER_{15}	2.5		**6.4**	*	**6.6**	*
	LUE	**55.3**	***	**12.6**	**	**5.5**	*
	BUE	**839.3**	***	**13.1**	***	**78.4**	***
	NDVI	**83.0**	***	1.3		**176.6**	***
	Sward height	**1293.1**	***	1.1		**72.2**	***
	T_{soil}	**68.3**	***	0.7		**8.6**	**
	M_{soil}	**206.9**	***	**13.0**	**	**7.4**	**
Succession sites (n = 8)	NEE_{600}	**313.9**	***	-		-	
	GPP_{600}	**551.5**	***	-		-	
	ER_{15}	**194.2**	***	-		-	
	LUE	**436.9**	***	-		-	
	BUE	**1138.0**	***	-		-	
	NDVI	**752.9**	***	-		-	
	Sward height	**674.7**	***	-		-	
	T_{soil}	**131.5**	***	-		-	
	M_{soil}	**105.5**	***	-		-	

Significance levels; *** < 0.001; ** < 0.01; * < 0.05

3.3 Results

3.3.1 The Effect of Grazing Cessation on Ecosystem CO_2 Fluxes in Grassland and Heathland

There was a clear and significant 'Exclosure effect' on all fluxes with 'grazing cessation' explaining most variation in the models for net CO_2 uptake (NEE_{600}) and gross primary production (GPP_{600}; Table 3-1). Across all sites, NEE_{600} was 37% lower in the exclosures ($p < 0.001$), with 20 % lower gross CO_2 uptake (GPP_{600}; $p < 0.001$) but no differences in CO_2 emission from ecosystem respiration (ER_{15}; $p = 0.119$) relative to grazed plots (Table 3-2).

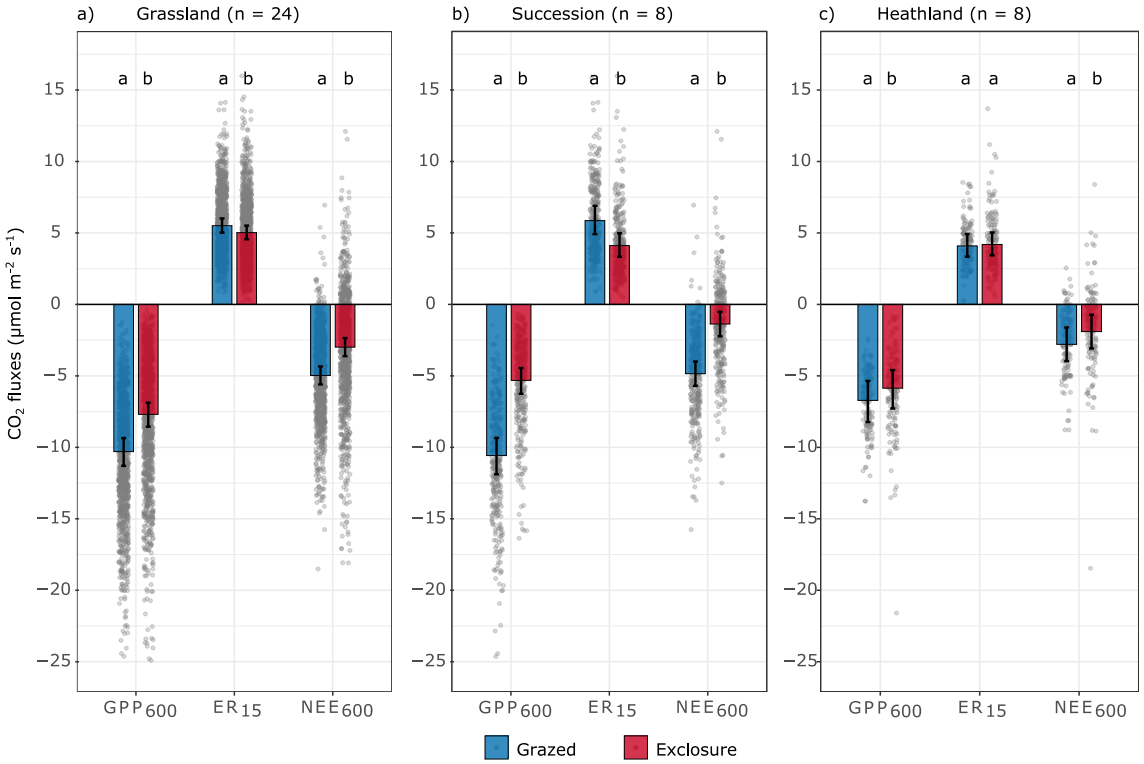

Figure 3-2: Standardised CO_2 fluxes in grazed and ungrazed land. Mean GPP_{600}, ER_{15}, and NEE_{600} are shown for (a) grassland sites (n = 24), (b) succession sites that shifted from grassland into heathland without grazing (sub-group of grassland sites, n = 8) and (c) heathland sites (n = 8), derived from linear mixed effects models. Error bars represent 95 % confidence intervals. Different letters represent significant differences between grazed and exclosure plots in each category following pairwise comparisons post-hoc tests. Grey dots represent individual measurements.

All CO_2 fluxes responded significantly to 'dominant vegetation' and the interaction of 'grazing cessation' × 'dominant vegetation' (Table 3-1). Independent of grazed or not, post-hoc tests showed that GPP_{600} and NEE_{600} (t = 2.7, $p = 0.010$) were more negative (t = 3.5, $p = 0.001$) and ER_{15} was more positive (t = 2.6, $p = 0.013$) at grassland sites compared to heathland sites, indicating higher productivity and C turnover in grassland compared to heathland (Figure 2). Overall, grazed and ungrazed grassland (NEE_{600} = -4.97 and -2.99

µmol m^{-2} s^{-1}, respectively) and heathland sites (-2.79 and -1.90 µmol m^{-2} s^{-1}, respectively) were net C sinks during the growing season.

Table 3-2: CO_2 fluxes and exclosure effect across sites and dominant vegetation types. Mean values ± standard error (SE) and change from grazed to ungrazed ('Exclosure effect' in % ± SE) with p-values retrieved from pairwise comparisons post-hoc test for GPP_{600}, R_{15}, NEE_{600} (all fluxes in µmol m^{-2} s^{-1}), Light Use Efficiency (LUE in µmol $mmol^{-1}$), and Biomass Use Efficiency (BUE in µmol µmol^{-1} cm^{-1}) from separate linear mixed models (LMMs) for all sites together, grassland and heathland sites, and succession sites only. Significant effects of grazing cessation are highlighted in bold.

Dominant vegetation	Response	Grazed (G)	Exclosure(E)	Exclosure effect†		
		Mean ± SE	Mean ± SE	% ± SE	*t*	*p*
All sites (n = 32)	GPP_{600}	-8.41 ± 0.47	-6.75 ± 0.42	-19.9±1.5	-8.7	**<0.001**
	ER_{15}	4.77 ± 0.25	4.60 ± 0.25	-3.7 ± 2.3	-1.6	0.119
	NEE_{600}	-3.88 ± 0.35	-2.45 ± 0.35	-37.1 ± 4.6	-7.9	**<0.001**
	LUE	0.016 ± 0.001	0.012 ± 0.001	-21.6 ± 1.7	-12.9	**<0.001**
	BUE	0.109 ± 0.008	0.037 ± 0.003	-66.2 ± 4.6	-14.1	**<0.001**
Grassland (n = 24)	GPP_{600}	-10.30 ± 0.48	-7.69 ± 0.42	-25.3 ± 1.5	-16.6	**<0.001**
	ER_{15}	5.51 ± 0.25	5.02 ± 0.24	-8.8 ± 1.4	-5.7	**<0.001**
	NEE_{600}	-4.97 ± 0.31	-2.99 ± 0.31	-39.9 ± 2.6	-15.3	**<0.001**
	LUE	0.017 ± 0.001	0.013 ± 0.001	-22.5 ± 2.1	-11.5	**<0.001**
	BUE	0.125 ± 0.008	0.040 ± 0.003	-68.3 ± 4.7	-14.6	**<0.001**
Heathland (n = 8)	GPP_{600}	-6.71 ± 0.72	-5.86 ± 0.67	-12.7 ± 4.8	-2.7	**0.011**
	ER_{15}	4.09 ± 0.39	4.20 ± 0.40	+2.5 ± 4.7	0.5	0.601
	NEE_{600}	-2.79 ± 0.59	-1.90 ± 0.59	-32.0 ± 12.2	-2.6	**0.011**
	LUE	0.010 ± 0.001	0.009 ± 0.001	-16.7 ± 5.9	-2.8	**0.007**
	BUE	0.060 ± 0.007	0.033 ± 0.004	-45.8 ± 6.9	-6.6	**<0.001**
Succession†† (n = 8)	GPP_{600}	-10.58 ± 0.56	-5.31 ± 0.40	-49.7 ± 2.6	-19.2	**<0.001**
	ER_{15}	5.86 ± 0.44	4.12 ± 0.37	-29.9 ± 2.4	-12.2	**<0.001**
	NEE_{600}	-4.85 ± 0.38	-1.37 ± 0.38	-71.8 ± 4.1	-17.7	**<0.001**
	LUE	0.016 ± 0.002	0.008 ± 0.001	-48.8 ± 3.5	-7.9	**<0.001**
	BUE	0.140 ± 0.018	0.033 ± 0.004	-76.5 ± 10.3	-7.6	**<0.001**

†Exclosure effect was calculated as percent change from G to E to the basis of G, with *t*-ratio and *p*-values derived from least-squares mean post-hoc tests

††Succession is a sub-group of Grassland

Across all grassland sites, GPP_{600}, ER_{15} and NEE_{600} were 25%, 9%, and 40% lower in ungrazed relative to grazed plots, respectively ($p < 0.001$; Figure 3-2a, Table 3-2). At the heathland sites, the 'Exclosure effect' was weaker than at grassland sites (Figure 3-2c). In ungrazed plots, GPP_{600} (- 13%, $p < 0.05$) and NEE_{600} (-32%, $p < 0.05$) were lower compared to grazed plots (Table 2). For ER_{15}, no 'Exclosure effect' was found (+2,5%, $p = 0.601$).

In the sub-group of succession sites, with a vegetation shift from grassland in the grazed plots to heathland in the ungrazed plots, we found the strongest 'Exclosure effect'. With

grazing cessation, net CO_2 uptake (NEE_{600}) was 72% lower with 50% lower GPP_{600} and 30% lower ER_{15} compared to the reference grazed plots ($p < 0.001$; Figure 3-2b). Overall, CO_2 flux rates in grazed plots were comparable to CO_2 fluxes in all other grazed grassland and the ungrazed plots had comparable flux magnitudes to other heathland sites (Table 3-2).

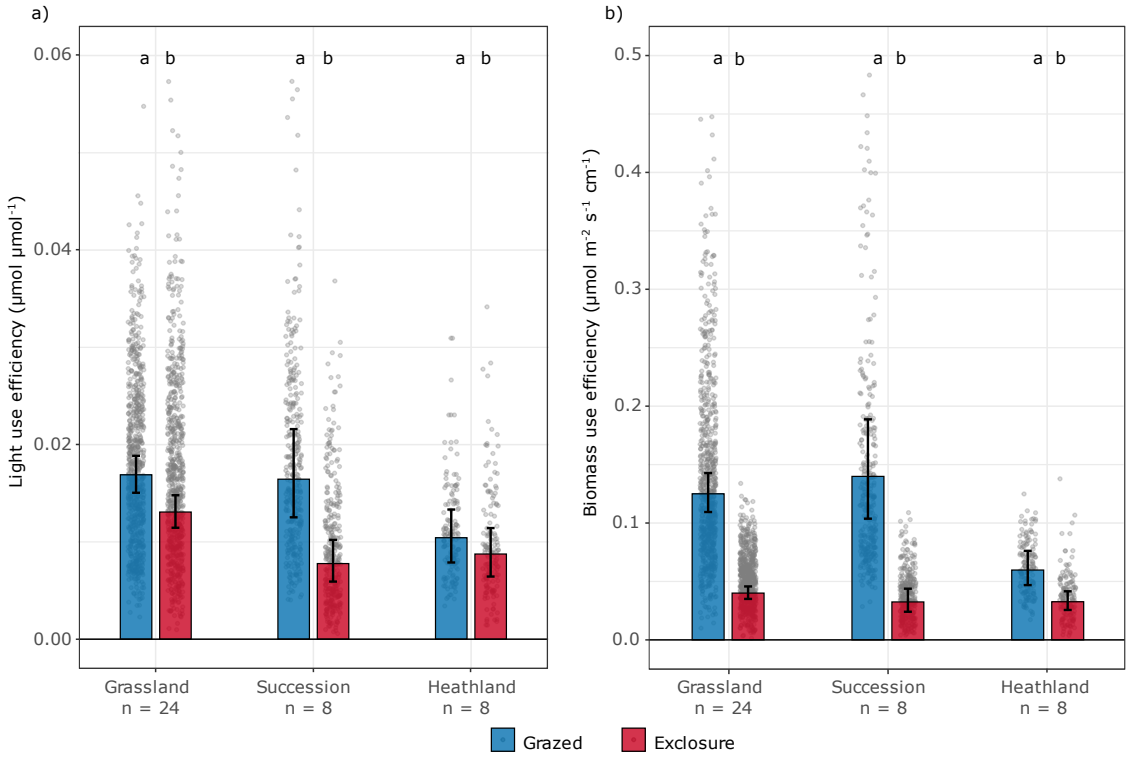

Figure 3-3: Light Use Efficiency (LUE, a) and Biomass Use Efficiency in grazed and ungrazed land (BUE, b). LUE represents C uptake efficiency per incoming radiation and BUE represents the C uptake efficiency per vegetation height at grassland, succession from grassland to heathland (sub-group of grassland) and heathland sites, derived from linear mixed effects models. Error bars represent 95 % confidence intervals. Different letters represent significant differences between grazed and exclosure plots in each category following pairwise comparisons post-hoc tests. Grey dots represent input data points.

3.3.2 Impacts of Grazing Cessation on Light and Biomass Use Efficiency

Across all sites, Light Use Efficiency (LUE) was 22% lower and Biomass Use Efficiency (BUE) was 66% lower in the ungrazed relative to the grazed plots ($p < 0.001$; Table 3-2). In both responses, 'grazing cessation', 'dominant vegetation' and their interaction had significant effects (Table 3-1). In general, C uptake efficiency (both LUE and BUE) and the 'Exclosure effect' were higher in grassland compared to heathland (Figure 3-3). As it was for CO_2 fluxes, the 'Exclosure effect' was largest in the 'succession' sub-group (LUE -49%; BUE -77%, $p < 0.001$) with typical grassland LUE and BUE values in grazed plots and typical heathland values in ungrazed plots (Figure 3-3).

3.3.3 Growing Season CO_2 Flux Balance

At each weekly interval, NEE_{600} was negative (i.e. net CO_2 uptake) over the whole season (Figure 3-4a-c). At the grassland sites, NEE_{600} and GPP_{600} were constantly more negative in grazed compared to ungrazed plots ($p < 0.05$), without a trend of reduced C uptake towards the end of the measurement season (Figure 3-4a,d). Values of ER_{15} were consistently around 5 µmol m^{-2} s^{-1} in grazed and ungrazed plots over the measurement period without notable trends.

In the 'succession' sub-group, NEE_{600}, GPP_{600} and ER_{15} were far lower in ungrazed plots in each weekly interval over the measurement period ($p < 0.05$) compared to grazed plots (Figure 3-4b,e). Notably, net CO_2 uptake (NEE_{600}) increased over the course of the measurement season, particularly ungrazed plots, with fully photosynthetic active vegetation still in late August (week 35).

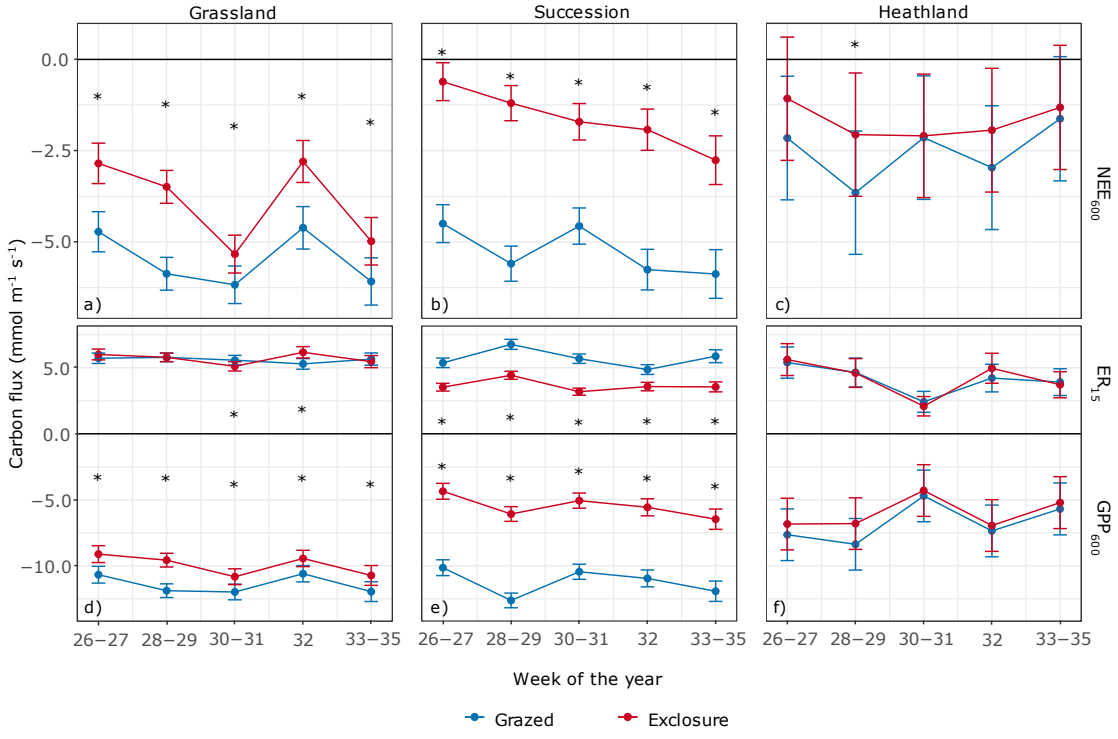

Figure 3-4: Weekly CO_2 fluxes over the growing season in grazed and exclosure plots. Standardised CO_2 fluxes ± 95 % confidence intervals are presented for grassland (a, d), succession from grassland to heathland (sub-group of grassland; b, e), and heathland (c, f). Only sites with ≥ 5 measurement days were included (n = 17). Lines represent the trend over the measurement period. Asterisks represent significant differences ($p < 0.05$) between grazed and exclosure plots per week interval, derived from Tukey post-hoc tests following ANOVA.

For heathland, CO_2 fluxes did not differ between grazed and ungrazed plots during most of the season, had large confidence intervals due to a small sample size and were generally of a similar magnitude as ungrazed plots at succession sites (Figure 3-4c,f).

3.3.4 The Relation of ER_{15} with Sward Height

Mean sward height was 112 %, 55 % and 75 % higher in ungrazed plots (range 108-246 mm) of grassland, heathland and succession sites, respectively, than in grazed plots (range 20-163 mm; Table 3-3, Appendix 2: Supplemental Figure 8-5).

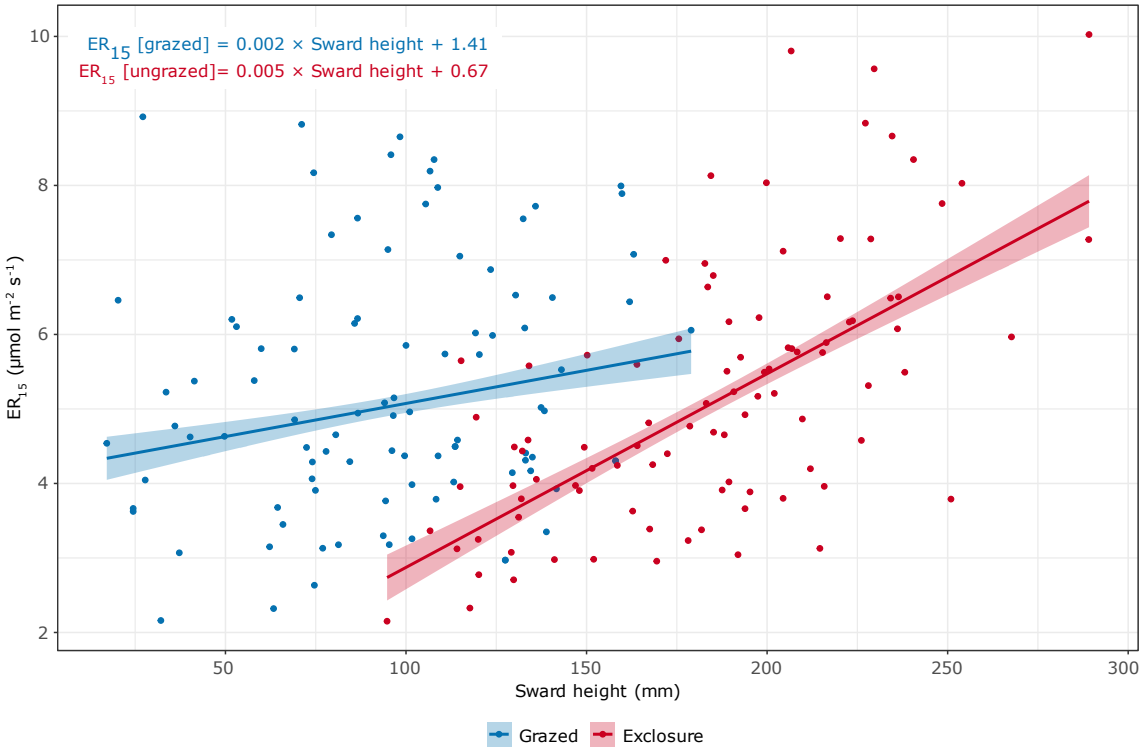

Figure 3-5: Linear regression between standardised ecosystem respiration (ER_{15}) and sward height. Values were averaged over the season for each sub-plot (n = 192). The interaction between 'grazing cessation' and 'sward height' was significant, hence both slope and intercept differed between grazed and exclosure plots.

Sward height ($F_{1, 168}$ = 51.8, p < 0.001) affected ER_{15} differently in grazed and ungrazed plots (interaction 'sward height' × 'grazing cessation': $F_{1,165}$ = 9.1, p = 0.002; Figure 3-5). In general, ER_{15} increased linearly with increasing sward height (i.e. decreasing grazing intensity at grazed or increasing biomass accumulation at ungrazed plots; Appendix 2: Supplemental Figure 8-5). In the exclosures, ER_{15} increased more than twice as much with increasing sward height (ER_{15} = 0.005 × *Sward height* + 0.67) relative to the grazed land (ER_{15} = 0.002 × *Sward height* + 1.41).

Table 3-3: Environmental factors in response to cessation of grazing. Mean values ± standard error (SE) and change from grazed to ungrazed ('Exclosure effect' in % ± SE) with p-values retrieved from least-squares means post hoc tests for vegetation and soil parameters in grassland, heathland and succession (sub-group of grassland). The number of sites in the respective category is given by n. Significant effects of grazing cessation are highlighted in bold. T_{soil} = Soil temperature, M_{soil} = Soil moisture.

Dominant vegetation	Response	Grazed (G)	Exclosure(E)	Exclosure effect††		
		Mean ± SE	Mean ± SE	% ± SE	*t*	*p*
Grassland (n = 24)	NDVI	0.75 ± 0.01	0.66 ± 0.02	-10.7 ± 0.4	-30.5	**<0.001**
	Sward height (mm)	85.3 ± 4.7	180.5 ± 6.8	+111.8 ± 2.9	36.1	**<0.001**
	T_{soil} (°C)	15.7 ± 0.6	14.5 ± 0.6	-7.4 ± 0.6	-13.4	**<0.001**
	M_{soil} (%)	40.4 ± 1.4	33.1 ± 1.4	-17.9 ± 0.7	-23.9	**<0.001**
Heathland (n = 8)	NDVI	0.72 ± 0.02	0.73 ± 0.02	+2.2 ± 1.0	2.3	**0.031**
	Sward height (mm)	111.9 ± 9.6	173.6 ± 11.9	+55.1 ± 4.2	12.9	**<0.001**
	T_{soil} (°C)	16.2 ± 1.0	15.6 ± 1.0	-3.7 ± 1.2	-2.8	**0.007**
	M_{soil} (%)	30.3 ± 2.4	25.3 ± 2.4	-16.3 ± 2.6	-6.2	**<0.001**
Succession† (n = 8)	NDVI	0.77 ± 0.02	0.64 ± 0.02	-17.7 ± 0.0	-27.4	**<0.001**
	Sward height (mm)	92.8 ± 13.4	161.9 ± 13.4	+74.6 ± 2.9	26.1	**<0.001**
	T_{soil} (°C)	15.7 ± 0.5	14.4 ± 0.5	-8.1 ± 0.8	-10.8	**<0.001**
	M_{soil} (%)	43.1 ± 1.9	37.5 ± 1.9	-12.9 ± 1.3	-10.3	**<0.001**

†Succession is a sub-group of Grassland

††Exclosure effect was calculated as percent change from G to E to the basis of G with *t*-ratio and *p*-values derived from least-squares mean post-hoc tests

3.3.5 CO_2 Flux Response to Years since Grazing Cessation

We found a significant effect of 'years since grazing cessation' on all CO_2 fluxes, LUE and BUE with distinctive trends at grassland, succession and heathland sites, respectively (significant interaction 'dominant vegetation' × 'years since grazing cessation'; Table 3-4). The largest changes in all CO_2 fluxes occurred during the first 20-30 years since the cessation of grazing with a halving of NEE_{600} in ungrazed relative to grazed land across vegetation types (Figure 3-6a-c). At the succession sites, NEE_{600} ($p > 0.05$) and GPP_{600} ($p < 0.05$) declined further with longer time since the cessation of grazing for up to 80 years. After 50 years since grazing cessation, both grassland and heathland had a substantially lower C uptake efficiency (both LUE and BUE, $p < 0.05$), with continued decline in the oldest exclosures in grassland (particularly at the succession sites) but not in heathland (Figure 3-6d,e).

Table 3-4: Diagnostics for Exclosure age models. F-statistics and degrees of freedom (df) from ANOVA are shown for the fixed effects 'years since grazing cessation' ('Grazed'; '20-30 years'; '31-50 years'; '51-83 years'), 'dominant vegetation' ('grassland', 'heathland', 'succession') and their interaction from linear mixed effects models. Random effects in each model were 'sub-plot' nested in 'site', and 'day of year' nested in 'year'.

	Years since grazing cessation (Y)			**Dominant vegetation (V)**			**Y × V**		
Response	***df***	***F***		***df***	***F***		***df***	***F***	
NEE_{600}	3, 2723	**79.8**	***	2, 348	**8.8**	***	6, 2822	**9.5**	***
GPP_{600}	3, 2994	**126.3**	***	2, 279	**15.5**	***	6, 2974	**25.1**	***
ER_{15}	3, 2936	**21.1**	***	2, 285	**8.1**	***	6, 2917	**13.5**	***
LUE	3, 3000	**98.4**	***	2, 296	**17.3**	***	6, 2979	**20.7**	***
BUE	3, 2974	**689.8**	***	2, 284	**9.8**	***	6, 2956	**44.2**	***
NDVI	3, 3146	**183.5**	***	2, 221	**9.8**	***	6, 3119	**58.9**	***

Significance levels; *** < 0.001; ** < 0.01; * < 0.05

3.3.6 Impacts of Grazing Cessation on NDVI and Soil Microclimate

Both, NDVI, soil temperature and soil moisture were different in grazed vs. ungrazed plots ($p < 0.001$) with a significant interaction between 'grazing cessation' and 'dominant vegetation' (Table 3-1). In ungrazed plots, NDVI (i.e. vegetation greenness) was 11 % and 18 % lower at grassland and succession sites and 2 % higher at heathland sites, respectively, relative to grazed plots ($p < 0.05$; Table 3-3). With extended grazing cessation, NDVI responded differently in the three vegetation groups (Figure 3-6f). In grassland, NDVI showed a sharp decline within the first 20-30 years since grazing cessation with continued decline in progressively older exclosures at succession sites ($p < 0.05$), but without further changes in other grassland. In heathland, NDVI increased in the exclosures for the first 20-30 years since grazing cessation after which no difference was found between grazed land and > 30 years old exclosures.

Soil temperatures were on average 7 %, 4 % and 8 % lower in ungrazed plots at grassland, heathland and succession sites, respectively, relative to grazed plots. Soil moisture was 18 %, 17 % and 9 % lower in ungrazed plots at grassland, heathland and succession sites, respectively, relative to grazed plots and generally higher in grassland (35.6 %) compared to heathland (26.5 %; $t = 3.8$, $p < 0.001$).

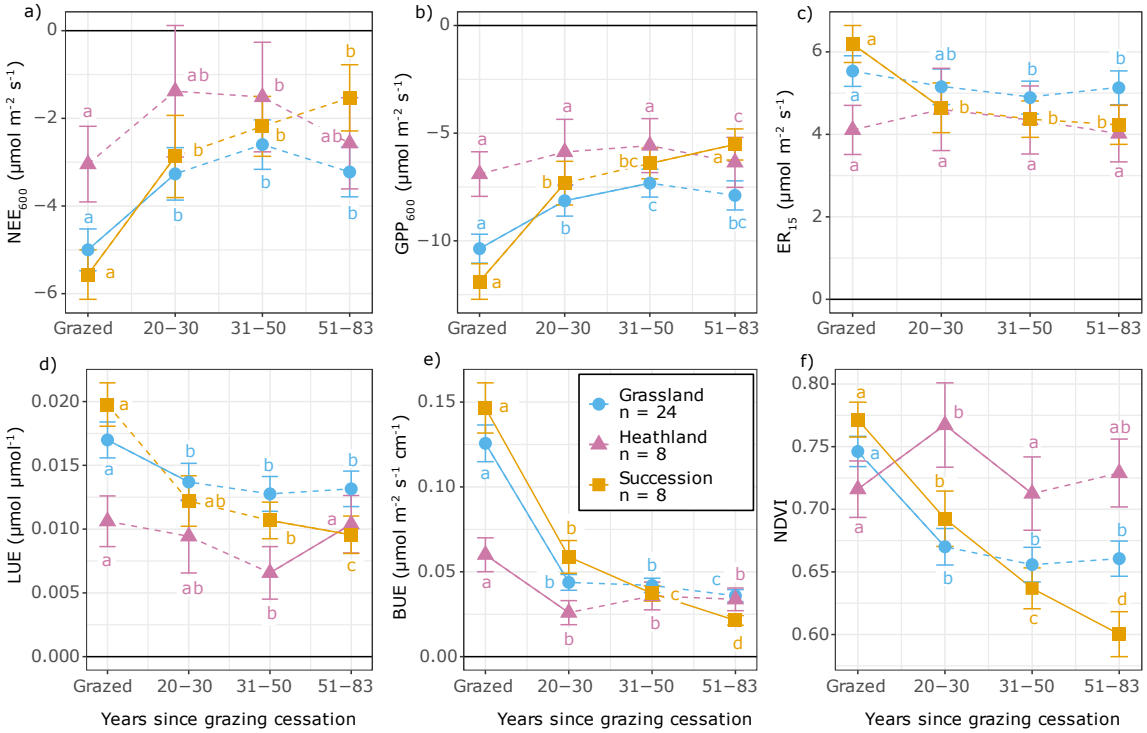

Figure 3-6: Effects of Exclosure age on CO_2 fluxes. Changes in NEE_{600} (a), GPP_{600} (b), ER_{15} (c), LUE (d), BUE (e) and NDVI (f) from grazed (n = 32) to three levels of years since grazing cessation: 20-30 years (n = 9), 31-50 years (n = 12), 51-83 years (n = 11), separated for grassland, succession from grassland into heathland (sub-group of grassland) and heathland. Values are presented as mean ± 95 % confidence intervals. Different letters and solid lines represent significant differences between 'years since grazing cessation' categories in each vegetation group following pairwise comparisons post-hoc tests

NDVI and soil microclimate were also directly related to raw CO_2 fluxes, possibly influencing flux responses to grazing cessation differently at grassland and heathland sites (Table 3-5). Spearman's correlation tests showed that in grassland NDVI and soil temperature were negatively correlated with GPP and NEE (i.e. larger uptake with increase in correlated parameter) and positively correlated with ER ($p < 0.01$, n = 683). In heathland, soil temperature was negatively correlated with GPP and soil temperature and NDVI were positively correlated with ER ($p < 0.01$, n = 102). Soil moisture was generally unrelated to CO_2 fluxes.

Table 3-5: Spearman's rank correlation coefficients of environmental conditions. Correlations are shown between raw CO_2 fluxes (NEE, GPP, ER) and soil temperature, soil moisture and NDVI averaged over the measurement season. In grassland, 683 data points from 24 sites were included and in heathland, 102 data points from 8 sites were included. Significant correlations are highlighted in bold ($p < 0.01$).

Dominant vegetation		Soil temperature	Soil moisture	NDVI
Grassland	NEE	**-0.26**	**0.10**	**-0.46**
	GPP	**-0.42**	0.04	**-0.64**
	ER	**0.42**	0.08	**0.58**
Heathland	NEE	-0.28	0.12	0.09
	GPP	**-0.70**	0.18	-0.24
	ER	**0.62**	-0.20	**0.38**

3.4 Discussion

3.4.1 Cessation of Grazing reduces C Turnover and Net C Uptake

Growing evidence shows that herbivores can play an important role in mitigating climate change by influencing C capture and storage in ecosystems (Cromsigt *et al.* 2018, Kristensen *et al.* 2022, Malhi *et al.* 2022, Schmitz *et al.* 2023). Rizzuto et al. (2024) proposed a theoretical model showing that herbivore presence could increase ecosystem C capture two- to threefold, primarily through enhanced primary productivity. Consistent with this model, our findings showed that net CO_2 uptake (NEE_{600}) declined by 37% in long-term exclosures (-2.45 µmol m^{-2} s^{-1}) compared to grazed land (-3.88 µmol m^{-2} s^{-1}), with markedly reduced CO_2 fluxes (primarily GPP_{600}) in the absence of herbivores. Geremia *et al.* (2025) recently showed how free-ranging bison grazing at Yellowstone National Park stimulates plant regrowth and nutrient cycling and maintains productive vegetation composition with positive feedback for the C sink strength. Our study revealed comparable effects for extensive livestock grazing in Iceland. C use efficiency was markedly lower in ungrazed vegetation relative to grazed vegetation, both in relation to light (LUE, -22%) and standing biomass (BUE, -66%). This indicates that one major effect of grazing is more efficient plant C uptake, consistent with previous findings from arctic-alpine ecosystems and recent reviews, highlighting the crucial role of herbivores to maintain ecosystem functioning in arctic ecosystems (Susiluoto *et al.* 2008, Schmitt *et al.* 2010, Koltz *et al.* 2022, Barbero-Palacios *et al.* 2024).

In general, our study provides robust evidence that semi-natural grassland and heathland in Iceland are net C sinks during the growing season, supporting findings from circumpolar arctic-alpine grass- or heath-dominated ecosystems (Eze *et al.* 2018, Sørensen, *et al.* 2018b, Fischer *et al.* 2022, See *et al.* 2024, Virkkala, *et al.* 2025a). While most CO_2 flux chamber studies in northern regions are based on relatively small data sets (Virkkala *et al.* 2018), our dataset includes approximately 2500 NEE and ER measurements during daytime hours in peak growing season (weeks 26–35) across 32 sites of paired grazed and exclosure plots. To

our knowledge, few studies have examined grazing cessation effects on CO_2 fluxes in northern ecosystems with comparable detail (Schmitt *et al.* 2010, Fischer *et al.* 2022). Net CO_2 uptake remained stable from early July to late August (Figure 3-4), indicating an extended growth season (Blume-Werry *et al.* 2016). See *et al.* (2024) synthesized more than 300 flux chamber estimates from northern high latitudes spanning the last three decades and concluded that non-permafrost ecosystems are typically net C sinks with summer C balances representative of the annual C sink strength. This suggests that our growing season C sinks were also representative for the annual balance. Moreover, their timeseries showed that the net C sink increased over the last decades in non-permafrost regions, with stronger increases in GPP than ER in response to climate warming (Maes *et al.* 2024, See *et al.* 2024). As GPP was the main driver of differences in net CO_2 uptake between grazed and ungrazed land in our study, we hypothesise that warming will further amplify the C sink strength in grazed land although further testing is needed (Väisänen *et al.* 2014).

3.4.2 Grassland versus Heathland

In Iceland, like in sub-arctic tundra in Scandinavia, more intensive grazing typically results in dense grass swards, whereas reduced grazing promotes mosses and dwarf shrubs, shifting vegetation from grassland to heathland (Van der Wal 2006, Egelkraut, *et al.* 2018b, Egelkraut *et al.* 2020). In our study, CO_2 fluxes in both grassland and heathland declined with cessation of grazing, reducing C turnover and the capacity of the land to function as net C sink, consistent with findings of Schmitt *et al.* (2010) at mountain grasslands. In grassland, NEE_{600} was -4.93 µmol m^{-2} s^{-1} in grazed land and -2.92 µmol m^{-2} s^{-1} in exclosures (-40 %) and in heathland, NEE_{600} was -2.74 µmol m^{-2} s^{-1} in grazed land and -1.80 µmol m^{-2} s^{-1} in exclosures (-32 %). In a comparable study, Sørensen et al. (2018a) studied how grazing cessation influenced CO_2 fluxes in alpine meadow and heath in Norway. After two years of grazing cessation, they did not yet measure differences in CO_2 fluxes. Consistent with our study, they found that NEE_{600} was markedly lower in the heath (-1.65 to -2.25 µmol m^{-2} s^{-1}) than in the meadow (-2.71 to -3.01 µmol m^{-2} s^{-1}). The fluxes of our heathland sites were within the range of values reported by Sørensen et al. (2018a) and of other heath and tundra ecosystems across the northern hemisphere (Susiluoto *et al.* 2008, Cahoon *et al.* 2012, Quin *et al.* 2015, Li *et al.* 2023, Wang, J. *et al.* 2024). The C sink strength of our grazed grassland on the other hand was higher than values reported from northern ecosystems (Fischer *et al.* 2022).

The markedly enhanced GPP_{600} and NEE_{600} of grazed grassland is probably reflecting the ability of grasses for compensatory regrowth of photosynthetic active tillers as response to defoliation (Briske 1996, Irving 2015, Linder *et al.* 2018). When grazed, grasses are more productive and efficient to utilise the short but high light growing season to assimilate C, as indicated by LUE and BUE, contributing to the large net CO_2 uptake in our grazed grassland with cascading effects on plant-soil interactions and whole ecosystem metabolism (Francini *et al.* 2014; Kytöviita and Olofsson 2021; Fischer *et al.* 2022). In ungrazed grassland, soil temperatures and NDVI were considerably lower than in grazed grassland, likely due to higher litter accumulation and moss depth, insulating soil and reducing light availability (Van der Wal and Brooker 2004, Valkó *et al.* 2018, Kantola *et al.* 2024). These factors further hinder regrowth of photosynthetically active tissue, as reflected by strong correlations of GPP with NDVI and soil temperature (Jessen *et al.* 2023).

Slow-growing heathland shrubs, by contrast, have a low LUE and BUE and thus a lower uptake capacity during the growing season relative to grassland (Strimbeck *et al.* 2019, Juutinen *et al.* 2022). Contrary to grassland, studies from shrub tundra have reported increased CO_2 uptake following grazing cessation, with shrubs growing taller and greener (Cahoon *et al.* 2012, Metcalfe and Olofsson 2015, Sundqvist *et al.* 2019, Min *et al.* 2021). This was partly confirmed by our study, with both NDVI (i.e. green vegetation) and sward height reaching higher values inside exclosures (Table 3-3). Unexpectedly, GPP_{600} and NEE_{600} were lower inside exclosures, challenging previous findings. Several studies indicated that expanding deciduous shrubs such as *Salix sp.* drive increasing CO_2 uptake relative to graminoid or heath (*Ericaceae*) vegetation (Street *et al.* 2007, Cahoon *et al.* 2016, Sørensen, *et al.* 2018a). Our heathland sites were more dominated by *Ericaceae*, with less potential to increase productivity (Li *et al.* 2023). With lower soil temperatures and limited nutrient return in the absence of herbivores, ungrazed heathland productivity was probably reduced and counterbalanced higher vegetation growth, indicated by lower BUE (Van der Wal *et al.* 2004, Liu *et al.* 2016, Barthelemy *et al.* 2018). Further, a higher and more closed shrub canopy developing without grazing, could limit photosynthetic activity of understory vegetation, such as grasses, contributing to the reduced GPP_{600} (Schoenecker *et al.* 2022).

3.4.3 Succession from Grassland to Heathland

Grazing cessation had the strongest impact on CO_2 fluxes and net CO_2 uptake at successional sites where vegetation composition shifted from grassland to heathland. In contrast to shrub expansion into graminoid tundra—which typically increases CO_2 uptake and plant respiration (Cahoon *et al.* 2016, Mekonnen *et al.* 2021, Min *et al.* 2021)—our succession sites exhibited a reduction of > 70 % in NEE_{600} and > 30 % in ER_{15} after 50 years since grazing cessation (Figure 3-6). Moreover, NEE_{600} was substantially lower in such successional heathland (-1.37 µmol m^{-2} s^{-1}) relative to long-established ungrazed heathland (-1.90 µmol m^{-2} s^{-1}), indicating that successional heathland was still a smaller C sink than long-established heathland. While long-established heathland had a typically closed dwarf shrub canopy, successional heathland was more open with larger patches of cryptogams, litter and grasses between low-growing shrubs, probably contributing to the smaller C sink capacity (Street *et al.* 2011, Falk *et al.* 2015, Sundqvist *et al.* 2020). Like our succession sites, grassland, established by previous intensive use, prevailed for more than 100 years at fertile sites of historical reindeer milking grounds in northern Sweden, while along a gradient of decreasing legacy of historical use, grassland gradually shifted into less productive heathland (Egelkraut *et al.* 2018a; Stark *et al*. 2019). Therefore, we hypothesise that reduced soil fertility following grazing cessation was driving the vegetation shift and reduced CO_2 exchange of our succession sites (Van der Wal and Brooker 2004, Van der Wal *et al.* 2004, Christie *et al.* 2015). This supports ecological theory positing that functioning and continuity of grassland ecosystems is driven by disturbance such as grazing (Bond 2019). The analysis of SOC and nutrient dynamics at our sites will help clarifying these trajectories (Chapter 5), as soil fertility is a key factor determining ecosystem functioning above-ground (Bardgett and Wardle 2003).

3.4.4 The Importance of Long-term Studies of Grazing Cessation

Most published exclosure studies span 2-10 years and often report increased CO_2 uptake after short-term grazing cessation (Forbes *et al.* 2019, Niu *et al.* 2025). However, several studies have shown that exclosure effects can differ markedly in the long-term (Kitti *et al.*

2009, Väisänen *et al.* 2014, Lara *et al.* 2017, Kantola *et al.* 2024). Our study revealed that after 20 years, clearly negative effects of grazing cessation prevailed for net CO_2 uptake, confirming results from a pilot study in western Iceland with 40 years exclosure age (Thorhallsdottir and Gudmundsson 2023). In our study, even after more than 80 years since grazing cessation, C turnover and net CO_2 uptake remained clearly and persistently lower relative to grazed grassland (Figure 3-6a-c). This is in line with few other multi-decadal exclosure studies; Lara *et al.* (2017) showed that 50+ years of exclusion of lemming grazing in the tundra notably reduced net CO_2 uptake and even turned a wet tundra C sink into a net C source. Similarly, Fischer *et al.* (2022) showed that 22 years after re-introduced grazing, C turnover strongly increased compared to adjacent ungrazed land in Siberian wet tundra. In other tundra sites, net CO_2 uptake was unchanged, despite larger above-ground biomass in land ungrazed for multiple decades, i.e. reduced BUE (Susiluoto *et al.* 2008, Petit Bon *et al.* 2023).

Such long-term effects have been linked to changes in soil properties, vegetation composition and litter accumulation that unfold over time (Johnson *et al.* 2011, Ylänne and Stark 2019). For example, legacy effects of grazing can alter soil nutrient stoichiometry and vegetation composition in the ecosystem (Egelkraut *et al.* 2018b; Sitters *et al.* 2017). In the short-term, vegetation benefit from grazing cessation and respond with increased CO_2 uptake (Chen *et al.* 2015). However, after multiple decades without grazing, the legacy of previous grazing diminishes, productivity declines and vegetation changes are becoming more likely (Vuorinen *et al.* 2021), such as from grassland into heathland as shown at our succession sites or by expanding shrubs into graminoid tundra in the study of Lara *et al.* (2017), reversing the short-term gains. Thus, the duration of grazing cessation is crucial for more realistic predictions how grazing abandonment is affecting C cycling in grazed ecosystems (Bürgi *et al.* 2017, Niu *et al.* 2025, Lockwood *et al.* 2026).

3.5 Conclusion and Implications

Based on our large-scale dataset of CO_2 fluxes from grassland and heathland in Iceland, we showed that the cessation of grazing substantially reduced ecosystem C turnover (GPP and ER) and the net CO_2 uptake (NEE). Thus, our study provides empirical evidence for increased ecosystem metabolism and CO_2 uptake driven herbivore-plant-soil-interactions with more pronounced contrasts in grassland than in heathland due to physiological differences in dominant plant species. At several sites, heathland replaced grassland multiple decades after grazing cessation. Such regime shift led to a sharp decline of CO_2 fluxes and net CO_2 uptake. For that reason, we emphasise the value of long-term studies, as many processes associated with CO_2 exchange between the atmosphere and the ecosystem respond differently to grazing cessation in the short-term and the long-term (Kantola *et al.* 2024).

Our findings have important implications for land use management, since most grazing activity in northern grassland and heathland, including Iceland, is livestock management. Grazing, as practiced at our sites, may serve as role model for a more sustainable livestock management to prevent grassland degradation (Bardgett *et al.* 2021). Grassland and heathland in Iceland have been maintained by grazing for centuries (Thorhallsdottir *et al.* 2013) and are, as shown in our study, a C sink. This grazing-mediated C sink likely contributes to sustained SOC sequestration, which has cumulated in high SOC stocks, typical of Icelandic grassland soils (Óskarsson *et al.* 2004, Leblans *et al.* 2017, Thorhallsdottir and

Gudmundsson 2023). With grazing cessation over multiple decades C turnover (GPP and ER) and the C sink strength were consistently smaller throughout the measurement period, which may result in lower SOC sequestration in the long-term (Chapter 5). Thus, our study supports recent hypotheses postulating that SOC sequestration can be enhanced and mediated by grazing animals (Kristensen *et al.* 2022, Rizzuto *et al.* 2024). We, therefore, conclude that low-input grazing in semi-natural grassland and heathland, can contribute to mitigate greenhouse gas emissions associated with livestock agriculture and has a larger potential as nature-based solution for climate change mitigation than grazing cessation (Chang *et al.* 2021, Roe *et al.* 2021, Borer and Risch 2024).

3.6 Acknowledgements

This research was supported by the Icelandic Centre for Research (Rannis, grant numbers 239629-051 and 217920-051) and the University of Iceland Research Fund (grant number RSJ2025-96440). We thank Jon Gudmundsson and Gesine Kliesch for guidance and support during field work, Johann Thorsson for technical support with a spare infrared gas analyser and Paul Debes for assistance in data analysis. We further gratefully acknowledge the permission of all landowners to work on their land and share land use information.

4 Chapter IV: Upscaling of Summer Net CO_2 Flux of Sub-arctic Grassland with Ground-based and Satellite-derived NDVI in Iceland

Abstract: Sub-arctic grasslands are important carbon sinks, yet quantifying their net CO_2 flux under grazed versus ungrazed conditions remains challenging. We investigated whether the Normalized Difference Vegetation Index (NDVI) can serve as a proxy for ecosystem CO_2 fluxes in sub-arctic grassland and enable upscaling from plot to landscape scale. Across 17 sites in Iceland, we measured ground-based NDVI and chamber-based CO_2 fluxes (gross primary production (GPP), ecosystem respiration (ER), and net ecosystem exchange (NEE)) in grazed and ungrazed grassland during two peak growing seasons (2022–2023). Ground-based NDVI was a strong predictor for GPP and NEE (R^2 up to 0.81 for seasonal aggregated GPP), but less for ER, reflecting its closer link to photosynthetic activity. Our models indicate that grassland starts net emitting CO_2 during daytime when ground-based NDVI drops below 0.55. The cessation of grazing had negative effects on NDVI and CO_2 fluxes, but without affecting the NDVI-CO_2 flux relationship. Ungrazed land exhibiting 11 % lower NDVI and 28% lower NEE compared to grazed land with total July-August NEE averaging −0.44 Mg C ha^{-1} in grazed and −0.07 Mg C ha^{-1} in ungrazed grassland. Calibration of ground-based NDVI with Sentinel-2 NDVI (10 m resolution) enabled upscaling to Icelandic lowland grasslands (<200 m a.s.l., 10% of lowland area). Despite moderate fits for satellite-based models, NDVI proved effective for estimating seasonal NEE and detecting grazing cessation impacts. Our findings highlight NDVI as a rapid, scalable indicator of grassland carbon uptake with the potential to substitute ground measurements.[2]

4.1 Introduction

To mitigate anthropogenic climate change, it is becoming increasingly important to evaluate how land use change influence the carbon (C) sink strength of ecosystems (Beillouin *et al.* 2022). However, in grazed grassland it remains challenging to quantify and verify net gains or losses of C in relation to cessation of grazing. This is because most C is stored as soil organic carbon (SOC) with reference values prior to land use change often missing. Thus, a change in C storage is difficult to quantify, compared to above-ground C storage in plant biomass. Soils are heterogenous and complex, interconnected ecosystems, not visible from above, making it difficult to establish a causation between land use change and SOC change and to extrapolate detected changes to the wider landscape (Smith *et al.* 2020, Stanley *et al.* 2023, 2025). Finally, large uncertainties persist how grazing, as the major land use in grassland, affects the grassland C sink strength (e.g. Liu *et al.* 2016; Eze *et al.* 2018; Sørensen *et al.* 2018a; Dangal *et al.* 2020; Niu *et al.* 2025).

[2] A version of this chapter is in preparation for submission:
Klopsch, C., Thorhallsdottir, A.G., Thorsteinsson, B., Gudmundsson, J., Bardgett, R., Van Der Wal, R., Geirsdóttir, A.: Upscaling of net CO_2 flux with ground-based and satellite-derived NDVI in Icelandic grassland, *in prep.*

Chamber-based CO_2 flux measurement is a widely used method to measure the net ecosystem CO_2 flux as an estimate for SOC sequestration and the C sink or source strength in northern treeless ecosystems (See *et al.* 2024, Virkkala *et al.* 2024, Virkkala, *et al.* 2025b). Flux chambers are flexible to use over multiple sites and treatments and in different environmental conditions to estimate average flux rates linked with varying land use (Jespersen *et al.* 2023). For example, Virkkala *et al.* (2024) demonstrated in a very fine-grained CO_2 flux chamber study in northern Finland that northern grassland is typically a strong C sink and that the sink strength may weaken when shrubs encroach into grassland. In agreement with Virkkala *et al.* (2024), we found a comparable growing season C sink for sub-arctic grassland in Iceland, when continuously (Klopsch *et al.* 2026b). With cessation of grazing, the C sink strength faded, particularly when heathland encroach into ungrazed grassland. However, measuring CO_2 uptake and emission with chambers is labour and time intensive and restricted to point measurements, limiting the potential to upscale such point measurements in heterogeneous natural ecosystems (Virkkala *et al.* 2021, Wang *et al.* 2022, Guðmundsson *et al.* 2026). Rapid assessments, accessible to land managers, are needed to evaluate effects of land use change on C uptake or losses (Smith *et al.* 2020, Nevalainen *et al.* 2022).

Remote sensing can help overcoming time and labour-related limitations and low spatial and temporal resolution of chamber measurements (Street *et al.* 2007, Guðmundsson *et al.* 2026). By calibrating point measurements of C uptake with remote sensed multispectral indices which can be scaled over large areas to estimate ecosystem productivity (Shaver *et al.* 2013, Balzarolo *et al.* 2015, Wang *et al.* 2022). One of the most frequently used vegetation indices to estimate photosynthetic activity is NDVI (Nestola *et al.* 2016, Del Grosso *et al.* 2018). NDVI is the ratio between incoming and reflected red and near-infrared light and reflects the amount of green (photosynthetic active) tissue within the vegetation patch (Pettorelli 2013). Ground-based NDVI typically matches gross primary production (GPP) measured with chambers under average light conditions (Street *et al.* 2007). This allows for locally specific calibrations of NDVI with absorbing (GPP) and emitting (ecosystem respiration, ER) CO_2 fluxes and their net ratio (net ecosystem exchange, NEE; Jespersen *et al.* 2023). Further calibrating of ground-based NDVI with NDVI products from satellite sensors over the growing season can be used to scale the C uptake potential of a point measurement to the wider landscape (Gargiulo *et al.* 2023). Today, prediction of GPP that is based on remotely sensed spectral data is still imprecise, making ground measurements of C uptake still inevitable (Chen *et al.* 2021). Particularly for comparisons between land use changes, such as the cessation of grazing within grazed land, ground-based calibrations are key to upscale effects from small-scale experimental sites to the landscape scale (Del Grosso *et al.* 2018, Karlsen *et al.* 2018).

Previous research in arctic tundra showed that CO_2 fluxes and NDVI have specific relationships for different vegetation types (Street *et al.* 2007, Shaver *et al.* 2013, Petit Bon *et al.* 2025). For high-latitude grassland which is typically more productive than tundra in similar climate (Van der Wal 2006, Olofsson and Post 2018), the relationship between NDVI and GPP or net ecosystem exchange (NEE) is less well established (Street *et al.* 2007, Juutinen *et al.* 2017). In particular, how grazing, as the dominant land use of high-latitude grassland, affects the relation between NDVI and GPP is insufficiently understood (Beamish *et al.* 2020). Grazing has strong and long-lasting effects on productivity and stability of grassland (Egelkraut, *et al.* 2018a, Fischer *et al.* 2022, Castaño *et al.* 2023, Klopsch *et al.* 2026b). On the one side, grazing removes substantial amount of photosynthetic active tissue

which can reduce NDVI and GPP. On the other side, grazing can stimulate compensatory regrowth, nutrient cycling and litter removal with positive effects on NDVI and GPP. Further, grazing can have variable effects on ecosystem respiration by modifying plant biomass and soil microbial activity. Thus, the effects of grazing on the relation between NDVI and CO_2 flux can be locally distinct and change when grazing is ceased in historically grazed grassland (Cahoon *et al.* 2012, Mipam *et al.* 2019, Jiang *et al.* 2024).

The aim of this study was to use our extensive dataset of spatially and temporally matched NDVI and CO_2 flux measurements to compare how NDVI is linked to CO_2 fluxes in grazed versus ungrazed Icelandic grassland. This is an important basis to upscale C uptake and emission rates of ground-based CO_2 flux measurements (Smith *et al.* 2020, Virkkala *et al.* 2021). We used fenced enclosures that inhibit grazing since multiple decades, within grazed sub-arctic grassland in Iceland. Extensive livestock grazing is still widespread in Iceland, but animal numbers and active farms are declining in the last decades (StatIce 2026). Grassland, historically shaped by livestock grazing, is an important land cover in the Icelandic lowlands, covering approximately 10 % of the land < 200 m a.s.l. (Ottoson *et al.* 2016). Thus, we consider Iceland as a field laboratory to study how the ongoing livestock grazing abandonment affects the relationship between NDVI and CO_2 fluxes in sub-arctic grassland. Our research questions were:

(i) How is NDVI linked with gross primary production (GPP), ecosystem respiration (ER) and net CO_2 flux (NEE) in grazed and ungrazed grassland when measured on the same scale?
(ii) How reliable is satellite-derived NDVI to upscale the net CO_2 flux (NEE) from ground-based measurements to the landscape scale of Icelandic grasslands?

4.2 Materials and Methods

4.2.1 Study Sites

For this study, 17 sites were selected in northern (n = 8) and western (n = 9) Iceland in uncultivated grassland on mineral soils below 200 m a.s.l. to measure CO_2 fluxes and ground-based NDVI during July and August 2022 and 2023 (Figure 4-1, Appendix 3: Supplemental Figure 8-6). All sites were associated with active farms and included a fence contrast with continued grazing on uncultivated land on one side (hereafter ‘grazed land’) and a patch of uncultivated land, where livestock grazers were excluded for more than 20 years on the other side of the fence (hereafter ‘grazer exclosures’). All grazed land was dominated by grasses, but in 4 of the 17 grazer exclosures we recorded an expansion of heath into the former grassland (Appendix 3: Supplemental Table 8-4, Supplemental Figure 8-7). According to information of land use history gathered from landowners the heath expanded following the cessation of grazing. Thus, the grazed land was treated as the reference condition, as the land was maintained by livestock grazing for centuries, and the grazer exclosures as treatment.

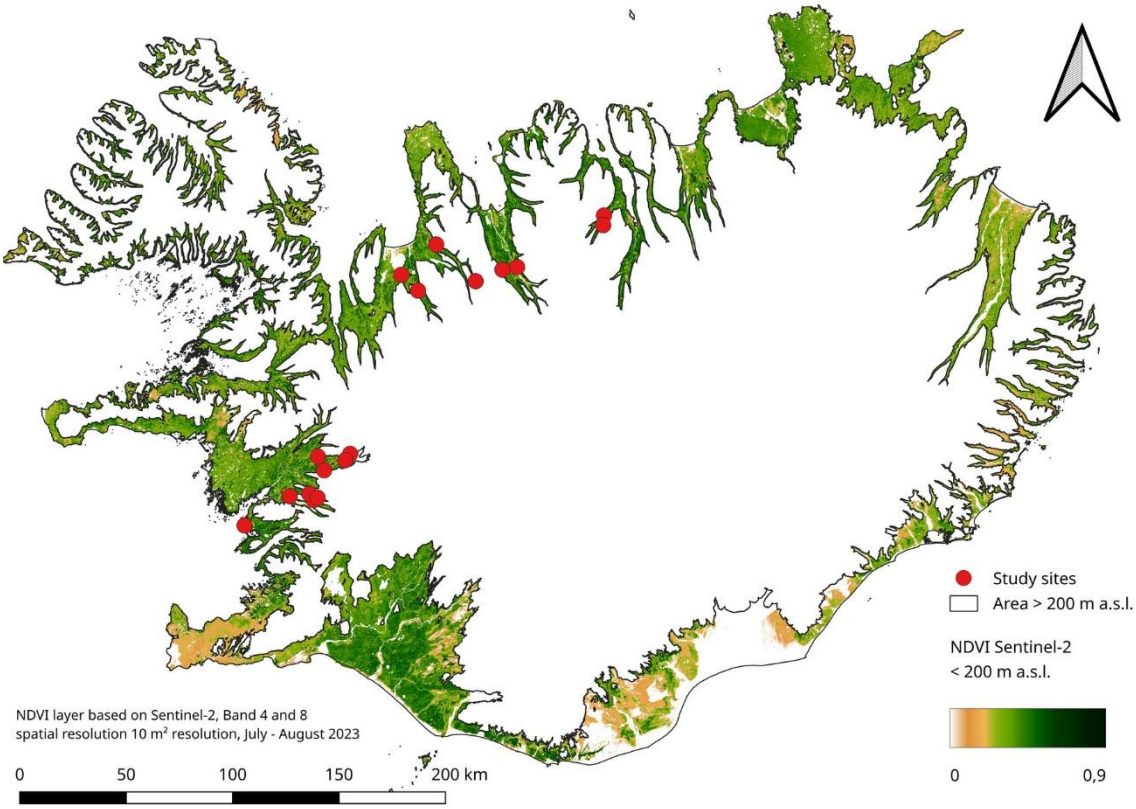

Figure 4-1: Map of Iceland with composite NDVI in the lowlands < 200 m a.s.l. Map data are derived from Sentinel-2 satellite images between July-August 2023, with the 17 study sites for field measurements.

The study design has been described in detail in Chapter 3; briefly, at each site, 3 sub-plots were randomly defined in the grazer exclosures in 5-20 m distance from the fence and in 5-20 m distance between sub-plots and mirrored on the grazed land in similar slope, elevation and aspect. Only fully vegetated patches were considered. When this requirement was not met due to large rocks on the surface, for example, the sub-plot location was moved by 5 m further away from the fence. Animal densities and grazing regimes varied between the sites but were not further defined and all grazed land was treated equally, simply as grazed.

4.2.2 Field Data

Each site was visited 4-7 times; once every one or two weeks on variable times of the day between 8 AM and 6 PM. The sites in northern Iceland were measured during July-August 2022 and in western Iceland during July-August 2023. Around each sub-plot, three measurements were performed within 1 m distance from the sub-plot centre and pooled together as one composite sub-plot measurement per measurement day. Measurement points were marked during the first measurement, and at each consecutive measurement day the same vegetation patch was measured. Each measurement consisted of one measurement of (i) ground-based NDVI, (ii) net ecosystem exchange, and (iii) ecosystem respiration on the same vegetation patch.

Ground-based NDVI was measured from 1.5 m above the surface and covered approximately 0.35 m² surface area. For the measurement, a hand-held pole was used with

two-channel sensors, directed perpendicular upwards and downwards, attached to a data logger (SKR1849D/SS2, SKR1840ND/SS2, SKL906, Skye Instruments, Llandrindod Wells, UK). The sensors measured incoming and reflected red (RED_{650}; 650 nm) and near-infrared (NIR_{800}; 800 nm) radiation and automatically calculated NDVI = (NIR_{800} - RED_{650}) / (NIR_{800} + RED_{650}). NDVI values range between -1 to +1, where values below 0 generally indicate unvegetated surface and values between 0 to +1 indicate successively greener (i.e. chlorophyll-richer) vegetation (Pettorelli 2013).

Following NDVI measurements, CO_2 flux measurements were performed using a closed custom-built acrylic chamber (35 cm × 35 cm × 25 cm, 0.1225 m²) with a fan, connected to an infrared gas analyser which recorded CO_2 levels continuously at one second intervals and run for 120 seconds after an acclimation period (EGM 5, PP systems, Amesbury, USA; Pumpanen *et al.* 2010). First, net ecosystem exchange (photosynthesis + ecosystem respiration; NEE_{raw}) was determined in ambient light from the net change of CO_2 over 120 seconds. This was followed by a second measurement on the same patch with all incoming radiation excluded, using an opaque hood covering the chamber, to determine ecosystem respiration (ER_{raw}) exclusively. During each NEE_{raw} measurement, incoming photosynthetic active radiation (PAR; µmol m^{-2} s^{-1}) and soil temperature in 0-10 cm (T_{soil}; ˚C) were measured simultaneously (TRP-3, PP-systems, Amesbury, USA; Hydra Probe II, Stevens Water Monitoring Systems, Portland, USA). Additionally, community sward height was measured at nine vegetation patches around each sub-plot randomly at each sampling day using an A4 writing pad (160 g) placed on top of the sward and measured with a folding ruler (Stewart *et al.* 2002).

4.2.3 Satellite Data

Satellite images were extracted from the Sentinel-2 library with 10 m resolution using Google Earth Engine (Gorelick *et al.* 2017). To calibrate ground-based NDVI (hereafter '$NDVI_{ground}$') with Sentinel-2 NDVI (hereafter '$NDVI_{sentinel}$'), band 4 (RED_{665}; 665 nm) and band 8 (NIR_{842}; 842 nm) of composite Sentinel-2 satellite images were extracted covering the two regions of our study sites. The composite satellite image for northern Iceland was composed of 13 images between 6.7.2022 – 4.9.2022 with < 2 % cloud cover and the composite satellite image for western Iceland was composed of 6 images from 8.7.2023 – 13.8.2023 with < 1% cloud cover. For each pixel, a value between -1 to +1 was automatically calculated as $NDVI_{sentinel}$ = (NIR_{842} – RED_{665}) / (NIR_{842} + RED_{665}). A $NDVI_{sentinel}$ value for each sub-plot GPS point was then extracted as the seasonal average value using the *rastersampling* tool in QGIS (version 3.3434, (QGIS Development Team 2025)).

In the next step, Sentinel-2 NDVI images (band 4,8) were extracted for whole Iceland < 200 m a.s.l. for the period July-August 2023, representing peak growing season conditions, with < 5 % cloud cover. The elevation limit of 200 m a.s.l. was chosen, because it is commonly considered as agricultural limit in Iceland and all our sites were below 200 m a.s.l. The total area < 200 m a.s.l. was derived from a 10 m resolution digital elevation model, extracted from Google Earth Engine, using *raster terrain analysis tools* in QGIS. The $NDVI_{sentinel}$ raster layer was subsequently cut to the area < 200 m a.s.l. (Figure 4-1).

To estimate $NDVI_{sentinel}$ for all Icelandic lowland grassland, the spatial coverage of all habitat types in the habitat class grasslands (L9) < 200 m a.s.l. was extracted from the Icelandic habitat type raster map 1:25000, curated by the Icelandic Institute of Natural History

(https://www.natt.is/en/resources/geospatial-data/habitat-types [accessed 25.02.2026]). In QGIS, the habitat-types raster file was vectorised and polygons of grassland habitat types were extracted and merged into a single multi-polygon for each of the grassland habitat types. With the 'NDVI$_{sentinel}$ < 200 m a.s.l.' raster and the 'grassland habitat < 200 m a.s.l.' vector layer as input data sets, the area of grassland covered by the NDVI$_{sentinel}$ layer, mean and standard deviation of NDVI$_{sentinel}$ for July-August 2023 in grassland were calculated based on all NDVI$_{sentinel}$ pixel values within the grassland vector layers, using the *zonal statistics* tool in QGIS.

Table 4-1: PAR and T_{soil} during the measurement period. Average daylength, photosynthetic active radiation (PAR) and soil temperatures (T_{soil}) during July-August based on 30-minute average PAR data series from two sites over two years (2002-2003, Guðmundsson et al. 2026) and PAR and soil temperature measurements of this study.

	July	**August**	**Average**	**Calculation**	**Dataset**[†]
Daytime hours	16.3	14.1	15.4	Hours PAR > 50	A
Nighttime hours	7.7	9.9	8.6	Hours PAR < 50	A
∑ (daytime hours)	505	436	953	Hours PAR > 50 × 62 days	A
∑ (nighttime hours)	239	308	535	Hours PAR < 50 × 62 days	A
PAR day	453	439	446	mean PAR of all measure-ments with PAR > 50	A
PAR day	712	487	626	mean PAR of all measurements	B
T_{soil} day grazed	17.2	15.1	15.8	mean T_{soil}	B
T_{soil} day ungrazed	15.8	14.4	14.6	mean T_{soil}	B
T_{soil} night grazed	13.2	10.3	10.7	mean T_{soil} between 8:00 - 9:00 AM	B
T_{soil} night ungrazed	11.9	9.39	10.0	mean T_{soil} between 8:00 - 9:00 AM	B
T_{soil}-ratio grazed	-	-	0.675	T_{soil} night / T_{soil} day	B
T_{soil}-ratio ungrazed	-	-	0.681	T_{soil} night / T_{soil} day	B

[†] A = 30-minute average PAR data for July-August 2002 and 2003 from two sites in western Iceland (Guðmundsson *et al.* 2026); B = PAR and T_{soil} measurements during CO_2 flux measurements in the 17 sites of this study

4.2.4 GPP Calculation and Flux Adjustments

From the field CO_2 flux measurements, the values of NEE_{raw} and ER_{raw} were automatically calculated from the change in CO_2 concentration over the 120 seconds measurement. From these values, gross primary production (GPP_{raw}) was calculated as $GPP_{raw} = NEE_{raw} - ER_{raw}$. During the measurement period, environmental conditions varied widely with direct effects on instantaneous CO_2 fluxes, but not on NDVI (Appendix 3: Supplemental Figure 8-8 - Supplemental Figure 8-13). For this reason, CO_2 fluxes were adjusted to represent average environmental conditions during the measurement period, which also makes values more comparable between sites and measurement days. Incoming radiation (PAR) ranged between 67 and 1918 µmol m^{-2} s^{-1} with a mean PAR of 626 µmol m^{-2} s^{-1} and soil temperature ranged between 8.5 and 31.7 °C with a mean of 15.8 °C in grazed land and 14.6 °C in grazer exclosures (Table 4-1). Average environmental conditions during the measurement period were defined as PAR = 600 µmol m^{-2} s^{-1} and T_{soil} = 16 °C in grazed and T_{soil} = 15 °C in ungrazed land, similar as used previously in arctic environments (Shaver *et al.* 2007, Strimbeck *et al.* 2019).

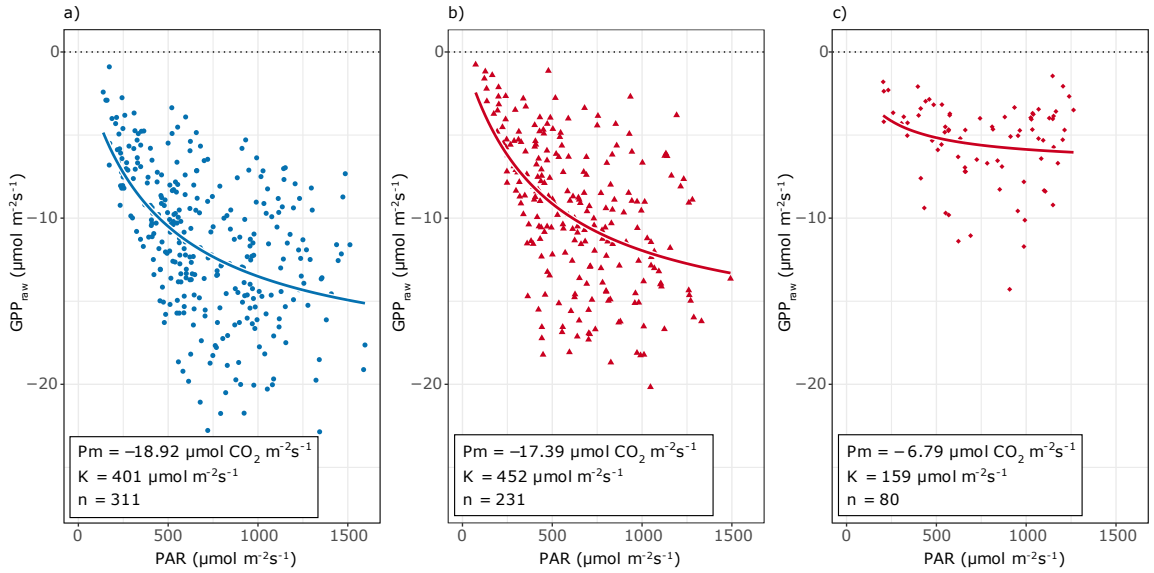

Figure 4-2: Community light response curves for the three classes used in the study: grassland-grazed (a), grassland-exclosure (b), heath expansion-exclosure (c). The light response curves were fitted with a non-linear regression using a Michaelis-Menten equation, fitting the parameters Pm = rate of light-saturated photosynthesis and K = half-saturated constant of photosynthesis with measured GPP and PAR (Eq. 4-1).

GPP_{raw} was adjusted to PAR = 600 µmol m^{-2} s^{-1} using a light response curve (LRC) modelling approach (Shaver *et al.* 2007). Three community LRCs were modelled, one for grazed grassland, one for ungrazed grassland and one for heath (12 sub-plots in grazer exclosures at 5 sites, Appendix 3: Supplemental Figure 8-7) due to strong differences in responses in GPP_{raw} to increasing light in grass and heath vegetation (Figure 4-2).

The LRCs were calculated using a self-starting non-linear least-squares regression that fitted model parameters (k and GPP_{max}) with the lowest residual sum of squares, using the Eq. 4-1, adopted from Strimbeck *et al.* (2019) as

$$GPP_{raw} = (GPP_{max} \times PAR) / (k + PAR), \quad \textit{Eq. 4-1}$$

where $GPP_{raw} = NEE_{raw} - ER_{raw}$, GPP_{max} = rate of light saturated photosynthesis, and k = half saturated constant of photosynthesis (Figure 4-2). A community GPP at PAR = 600 µmol m^{-2} s^{-1} and at each measured PAR was calculated with the fitted model parameters. The ratio between both (Eq. 4-2) was then used as adjustment factor to estimate GPP_{adj}:

$$GPP_{600} = GPP_{raw} \times ((GPP_{max} \times 600) / (k + 600)) / ((GPP_{max} \times PAR) / (k + \mathrm{PAR})). \quad \textit{Eq. 4-2}$$

Soil temperatures and ER_{raw} were positively correlated (Appendix 3: Supplemental Figure 8-10,Supplemental Figure 8-14a), and ER_{raw} was adjusted to a common soil temperature of 16 °C in grazed and 15 °C in ungrazed land, using a Q_{10} approach (Eq. 4-3; Tjoelker *et al.* 2001). We used a Q_{10} = 2, which has been shown previously to be representative for grasslands to model soil respiration (Gilmanov *et al.* 2004, Meyer *et al.* 2018) and calculated an adjusted ER (ER_{adj}) as

$$ER_{15} = ER \times Q_{10}^{((16(15) - Tsoil)/10)}, \quad \textit{Eq.4-3}$$

From GPP_{adj} and ER_{adj}, an adjusted NEE ($NEE_{adj} = GPP_{adj} + ER_{adj}$) was calculated as net ecosystem exchange under average environmental conditions during the measurement period. If not stated otherwise, fluxes were converted into µmol CO_2 m^{-2} s^{-1} and reported from an atmospheric perspective, i.e. negative values correspond to absorption from the atmosphere and positive values correspond to emissions into the atmosphere. A seasonal value for the net ecosystem exchange during July-August, representing peak growing season conditions, was calculated with Eq. 4-4 as

$$NEE_{July\text{-}August} = (NEE_{daytime} + ER_{night}) \times 62 \text{ days}, \quad \textit{Eq. 4-4}$$

where $NEE_{daytime}$ is the net ecosystem exchange for daytime hours (defined as PAR > 50 µmol m^{-2} s^{-1}), calculated with Eq. 4-5, and ER_{night} is the nighttime respiration, calculated with Eq. 4-6 as

$$NEE_{daytime} = GPP_{450} + ER_{adj} \times Daylength, \quad \textit{Eq. 4-5}$$

where GPP_{450} is GPP adjusted to PAR = 450 µmol m^{-2} s^{-1}, using Eq. 4-2, as average PAR for daytime (defined as PAR > 50 µmol CO_2 m^{-2} s^{-1}), based on two July-August 30-minutes PAR measurement series from western Iceland for 2002 and 2003 (Data from Guðmundsson *et al.* 2026), ER_{adj} is ecosystem respiration during daytime (Eq. 4-3) and daylength represents average daylength (PAR > 50 µmol m^{-2} s^{-1}) during July and August (Table 4-1, Appendix 3: Supplemental Figure 8-12);

$$ER_{night} = ER_{adj} \times T_{soil}\text{-}ratio, \quad \textit{Eq. 4-6}$$

where T_{soil}-ratio is the ratio between mean soil temperatures between 8:00 – 19:00 (daytime) and mean soil temperatures between 8:00 – 9:00 AM (nighttime), variable for grazed and

ungrazed land (Table 4-1, Appendix 3: Supplemental Figure 8-13). Seasonal fluxes were then converted from µmol CO_2 m^{-2} s^{-1} into Mg C ha^{-1}. By integrating equations retrieved from linear regression models between $NDVI_{ground}$ and NEE_{adj} and $NDVI_{ground}$ and $NDVI_{Sentinel-2}$ into Eq.4-4, $NEE_{July-August}$ values based on NDVI were estimated.

4.2.5 Statistical Analysis

Relationships between CO_2 fluxes and NDVI were analysed with linear or exponential regression using linear mixed effects models. Dependent on the data aggregation (all sub-plots on all measurement days / all sub-plots over the season / all sites over the season), 'Day of year' (i.e. measurement day) nested in 'Sub-plot' nested in 'Site' / 'Sub-plot' nested in 'Site' / 'Site' were used as random factors. The best regression model was determined from the minimum residual sum of squares and the highest R^2 value.

To analyse how the NDVI-CO_2 flux relationship responded to the cessation of grazing, the mean difference between grazed and ungrazed sub-plots on each measurement day or aggregated over the season were calculated as $\Delta x = x_{ungrazed} - x_{grazed}$, where x is the respective adjusted flux or NDVI. The retrieved Δ-variables were subsequently analysed with linear mixed effects regression models with 'Day of year' and 'Sub-plot' nested in 'Site' or 'Site' as random effect to test if NDVI and fluxes respond differently to the cessation of grazing.

Ground-based $NDVI_{ground}$ was calibrated with Sentinel-2 $NDVI_{sentinel}$ using a linear mixed-effects regression model with 'Site' as random factor. This calibration model was further integrated into the regression model of $NDVI_{ground}$ and NEE_{adj} to calculate average NEE values for all grassland area in the Icelandic lowlands < 200 m a.s.l., based on $NDVI_{sentinel}$ values. Additionally, a $NEE_{July-August}$ based on $NDVI_{ground}$ and $NDVI_{sentinel}$ was calculated by integrating linear regression equations for NEE_{adj} ~ $NDVI_{ground}$ and $NDVI_{ground}$ ~ $NDVI_{Sentinel-2}$ into Eq.4 to compare modelled and calculated seasonal NEE. Differences between grazed and ungrazed land in seasonal NEE, $NDVI_{ground}$ and $NDVI_{sentinel}$ were tested with linear mixed effects models with 'Site' as random effect. The effect size and significance between grazed and ungrazed land for the respective response variable were retrieved from least squares means post-hoc tests.

All statistical analyses were performed using R statistical software, version 4.2.1 (R Core Team 2024) with the additional packages nls (Baty *et al.* 2015), lme4 (Bates *et al.* 2015), lmerTest (Kuznetsova *et al.* 2017) and emmeans (Lenth 2023).

4.3 Results

4.3.1 Relationship between CO_2 Fluxes and $NDVI_{ground}$ per Measurement Day

First, we analysed the relationship between CO_2 fluxes with ground-based NDVI for each sub-plot per site and each measurement day. We found that measured ground-based NDVI ($NDVI_{ground}$) and all raw and adjusted CO_2 fluxes were strongly correlated ($p < 0.001$, Appendix 3: Supplemental Figure 8-14). With the regression analysis, we found that both GPP_{raw} and ER_{raw} followed an exponential regression with $NDVI_{ground}$ (larger flux with larger $NDVI_{ground}$) while for NEE_{raw}, a negative linear regression with $NDVI_{ground}$ (more

negative NEE (larger net C uptake) with larger $NDVI_{ground}$) explained most variation in the data (Figure 4-3a-c). As expected, there was a stronger relation between $NDVI_{ground}$ and raw gross primary production (GPP_{raw}) than with ecosystem respiration (ER_{raw}) and net ecosystem exchange (NEE_{raw}). Generally, the data showed a high variability in the raw CO_2 fluxes and the grazing treatment had no effect on the relationship between fluxes and $NDVI_{ground}$ ($p > 0.05$). In the adjusted CO_2 fluxes (PAR = 600 µmol m^{-2} s^{-1}, soil temperature = 16 °C/15 °C), variability due to environmental factors was reduced. The exponential regression models between $NDVI_{ground}$ and adjusted GPP (GPP_{adj}) and adjusted ER (ER_{adj}) and the linear regression with adjusted NEE (NEE_{adj}) explained more variation than the model for raw fluxes (R^2_{adj} = 0.54, 0.36 and 0.27 vs. R^2_{raw} = 0.41, 0.32 and 0.22, respectively; Figure 4-3d-f). $NDVI_{ground}$ ranged between 0.5 – 0.9, raw and adjusted GPP between -1 and -24, raw and adjusted ER between 0.5 and 15 and raw and adjusted NEE between -15 and +6 µmol m^{-2} s^{-1} between sub-plots and measurement days. In those sites, where heath expanded into grassland following the cessation of grazing, NDVI and CO_2 fluxes were overall lower than in grazed or ungrazed grass-dominated grassland (Figure 4-3).

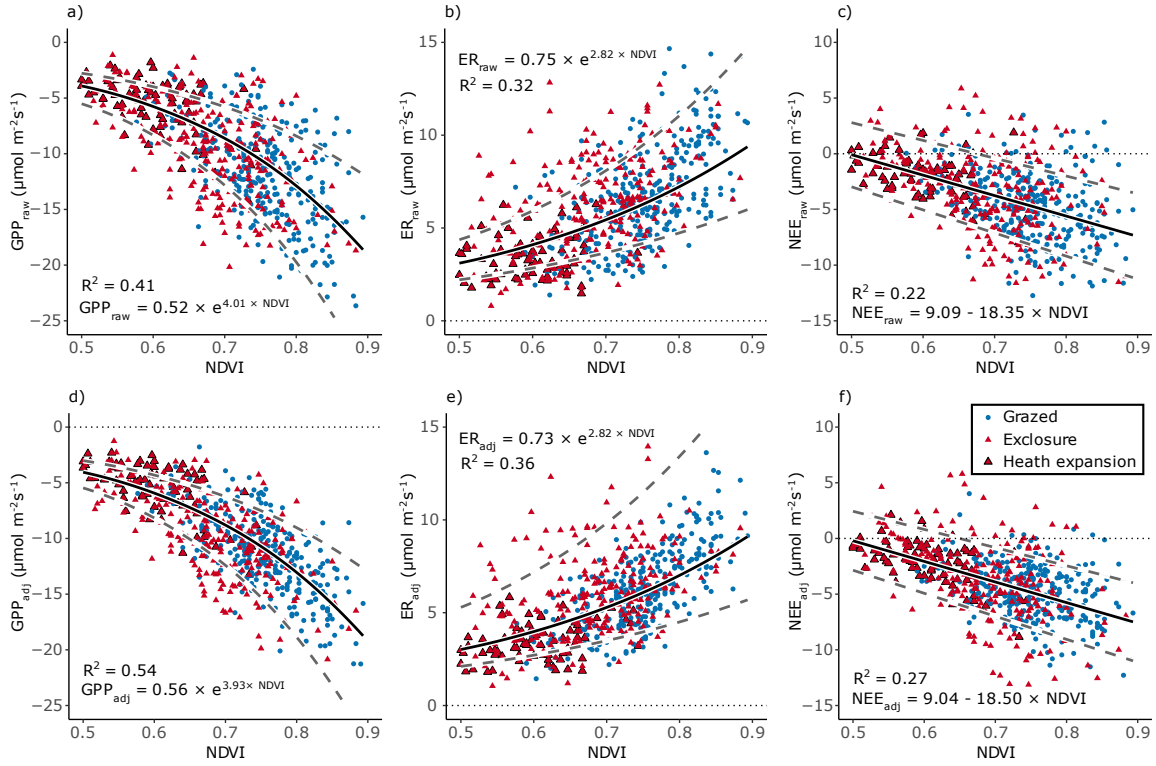

Figure 4-3: Relationships between measured NDVI and raw and adjusted CO_2 fluxes per sub-plot and measurement day. Regression curves and equations are derived from exponential or linear regression in linear mixed effects models with 'Day of year' and 'Sub-plot' nested in 'Site' as random factors for raw GPP (a), ER (b), NEE (c), and adjusted GPP (d), ER (e) and NEE (f). R^2 indicates the variance explained in each model and dashed lines represent 95 % confidence intervals. GPP = Gross primary production, ER = Ecosystem respiration, NEE = Net ecosystem exchange.

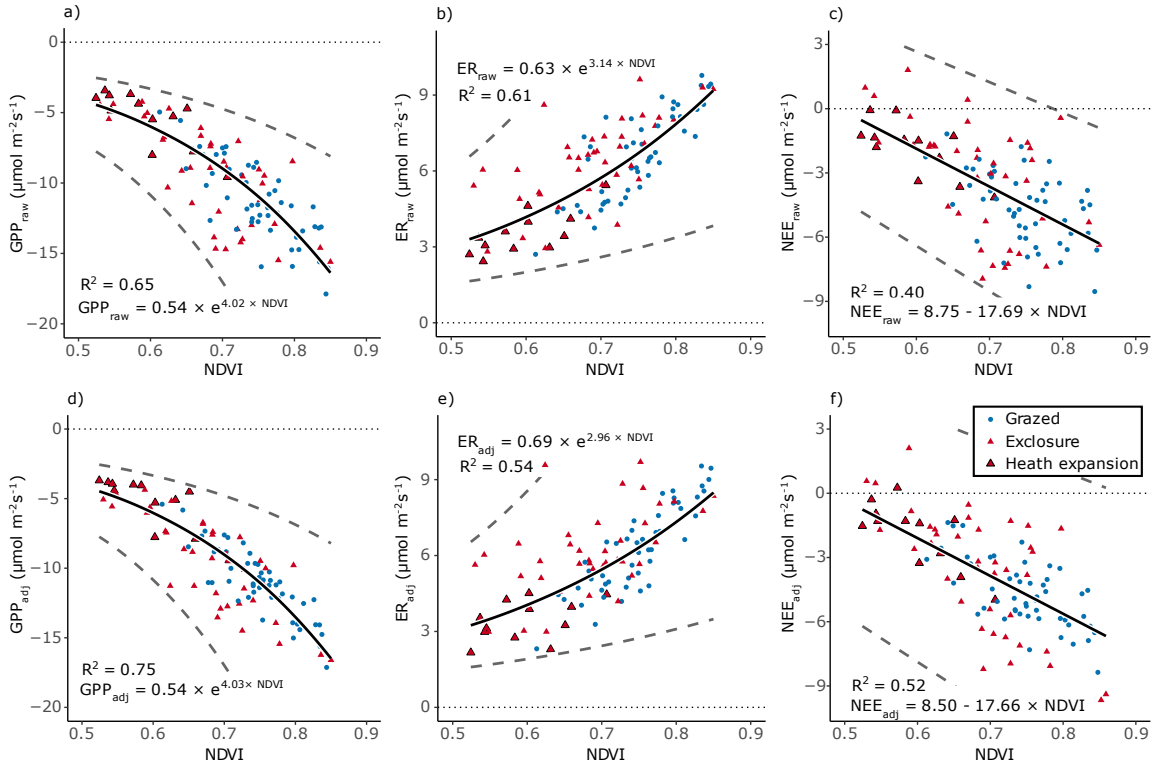

Figure 4-4: Relationships between mean NDVI and raw and adjusted CO_2 fluxes per sub-plot over the measurement period. Regression curves and equations are derived from exponential or linear regression in linear mixed effects models with 'Sub-plot' nested in 'Site' as random factors for raw GPP (a), ER (b), NEE (c), and adjusted GPP (d), ecosystem respiration (e) and NEE (f). R^2 indicates the variance explained in each model and dashed lines represent 95 % confidence intervals. GPP = Gross primary production, ER = Ecosystem respiration, NEE = Net ecosystem exchange.

4.3.2 Relationship of CO_2 Fluxes and $NDVI_{ground}$ over the Measurement Period

We aggregated raw and adjusted CO_2 fluxes and $NDVI_{ground}$ to mean values per sub-plot over the measurement period, cumulating to 11-24 individual datapoints per seasonal sub-plot value. This improved the strength of the regression between fluxes and $NDVI_{ground}$, as indicated by higher R^2 values compared to values per measurement day, but to the cost of wider confidence intervals due to smaller sample sizes and larger error terms (Figure 4-4). Again, the best models for GPP_{raw}, GPP_{adj}, ER_{raw} and ER_{adj} followed exponential regressions with $NDVI_{ground}$ while NEE_{raw} and NEE_{adj} followed linear regressions with $NDVI_{ground}$. The adjustment improved both the model fit of $NDVI_{ground}$ with GPP and NEE (R^2_{adj} = 0.75 and 0.52 vs. R^2_{raw} = 0.65 and 0.40, respectively; Figure 4-4a,c,d,f), but for ER, the model fit was higher for ER_{raw} (R^2 = 0.61) than for ER_{adj} (R^2 = 0.54; Figure 4-4b,e). Seasonal $NDVI_{ground}$ was significantly lower in ungrazed grassland than in grazed grassland and all replicates with $NDVI_{ground}$ < 0.6 were in grazer exclosures ($F_{1,89}$ = 5.2, p = 0.024), and most of them associated with expanding heath into ungrazed grassland. With $NDVI_{ground}$ < 0.6 the likelihood of a net neutral (NEE = 0 µmol m^{-2} s^{-1}) or net emitting (NEE > 0 µmol m^{-2} s^{-1}) seasonal C balance increased strongly (Figure 4-4c,f).

When aggregated to a single seasonal mean grazed and ungrazed value per site, the best models for all fluxes were linear regressions with $NDVI_{ground}$ (Figure 4-5). The strength of the relationship was further improved for GPP_{raw}, GPP_{adj}, NEE_{raw} and NEE_{adj} compared to the less aggregated models (R^2_{adj} = 0.81 and 0.61 vs. R^2_{raw} = 0.71 and 0.45, respectively; Figure 4-5a,c,d,f). Each aggregated value represented the mean of 35 – 66 individual measurements over a two-month period. This additional aggregation did not improve the model fit for the regression between $NDVI_{ground}$ and ER_{raw} and ER_{adj} and ER_{raw} (R^2 = 0.61) had still a better model fit than ER_{adj} (R^2 = 0.52; Figure 4-5b,e). The strongest model was for GPP_{adj} and $NDVI_{ground}$ with 81 % of the variation explained by the linear regression (Figure 4-5d). Despite the moderate model fit for ER_{adj} (R^2 = 0.52), 61 % of the variation in NEE_{adj} was explained by $NDVI_{ground}$. This model indicated that, on average, grassland turns into a net C source during daytime with $NDVI_{ground}$ < 0.55 due to low GPP (Figure 4-5f).

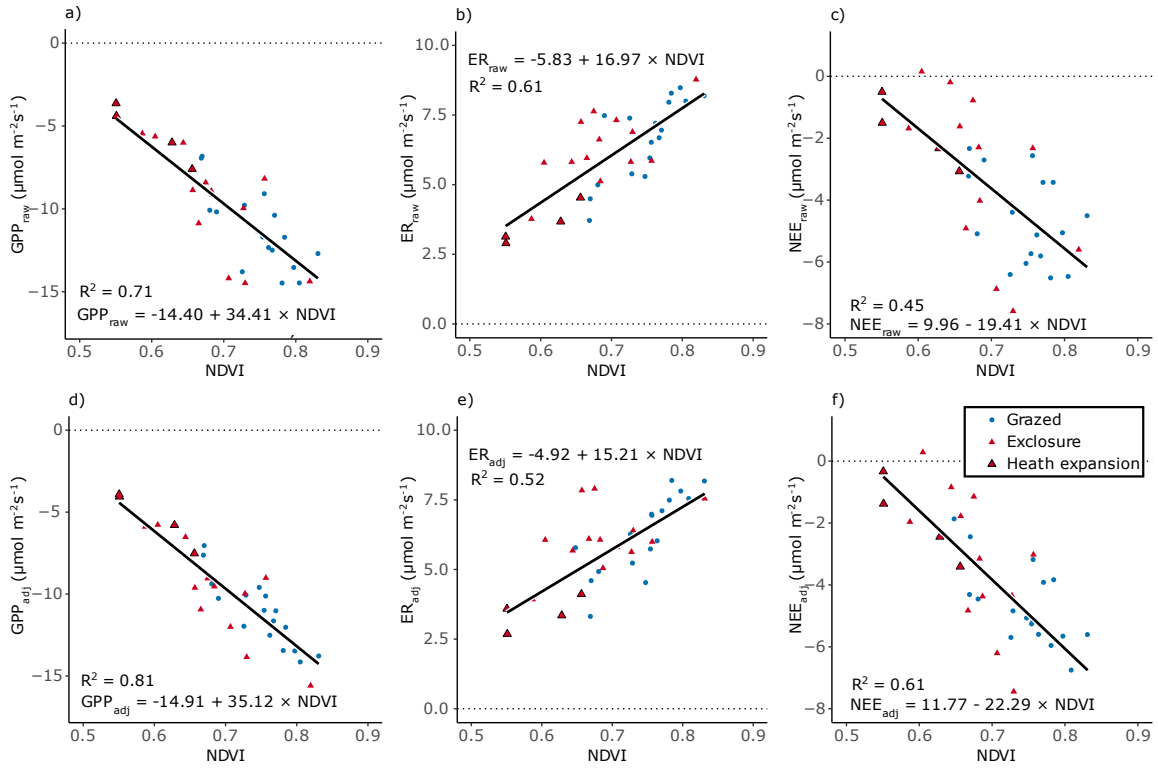

Figure 4-5: Relationships between mean NDVI and raw and adjusted CO_2 fluxes over the measurement period (July-August). Regression curves and equations are derived from linear regression in linear mixed effects models with 'Site' as random factor for raw GPP (a), ER (b), NEE (c), and mean adjusted GPP (d), ER (e) and NEE (f). R^2 indicates the variance explained in each model and dashed lines represent 95 % confidence intervals. GPP = Gross primary production, ER = Ecosystem respiration, NEE = Net ecosystem exchange.

4.3.3 How do $NDVI_{ground}$ and Adjusted CO_2 Fluxes Change with Cessation of Grazing?

Grazing cessation significantly affected CO_2 fluxes and NDVI, as shown by linear mixed effect models (Table 4-2). $NDVI_{ground}$ was consistently lower in ungrazed land during each week over the measurement period compared to grazed land (Appendix 3: Supplemental Figure 8-15). Raw and Adjusted GPP and ER were lower in ungrazed grassland compared to grazed grassland with a stronger reduction in GPP than in ER ($p < 0.001$). Consequently, the net C balance (raw and adjusted NEE) was also less negative (lower net C uptake) in ungrazed compared to grazed grassland (Table 4-2). The lowest NDVI values and CO_2 fluxes were associated with the grazer exclosures where heath expanded into grassland following cessation of grazing (Figure 4-5 – Figure 4-5).

Table 4-2: Effect of grazing cessation on raw and adjusted CO_2 fluxes and NDVI. F-statistics degrees of freedom (df) are derived from linear mixed effects model with 'Day of Year' and 'Sub-plot' nested in 'Site' as random effects and 'Grazing cessation' as fixed effect. Contrast values and t-statistics were derived from post-hoc tests. GPP = Gross primary production, ER = Ecosystem respiration, NEE = Net ecosystem exchange.

	Grazing cessation			**Difference Grazed – Ungrazed**[†]		
Response	***df***	***F***	***p***	**Contrast**	***t***	***p***
GPP_{raw}	1, 308	117.4	<**0.001**	-3.04 ± 0.28 µmol $m^{-2}s^{-1}$	10.8	<**0.001**
GPP_{adj}	1, 308	111.6	<**0.001**	-2.79 ± 0.26 µmol $m^{-2}s^{-1}$	10.6	<**0.001**
Er_{raw}	1, 308	59.0	<**0.001**	-1.14 ± 0.15 µmol $m^{-2}s^{-1}$	7.7	<**0.001**
ER_{adj}	1, 299	44.4	<**0.001**	-0.99 ± 0.15 µmol $m^{-2}s^{-1}$	6.7	<**0.001**
NEE_{raw}	1, 306	84.5	<**0.001**	-1.89 ± 0.21 µmol $m^{-2}s^{-1}$	9.2	<**0.001**
NEE_{adj}	1, 299	61.8	<**0.001**	-1.64 ± 0.21 µmol $m^{-2}s^{-1}$	7.9	<**0.001**
$NDVI_{ground}$	1, 570	341.0	<**0.001**	-0.09 ± 0.004	18.5	<**0.001**

[†] *t*-statistics and *p*-value derived from least-squares means post-hoc test

Beyond the overall negative effect of grazing cessation, both $NDVI_{ground}$ and all adjusted CO_2 fluxes shifted in concert with grazing cessation compared to grazed land (Figure 4-6). We found significant correlations ($p < 0.001$) between the mean difference of ungrazed - grazed pairs in $NDVI_{ground}$ (ΔNDVI) and the mean difference in GPP_{adj} (ΔGPP), ER_{adj} (ΔER) and NEE_{adj} (ΔNEE; Appendix 3: Supplemental Figure 8-14d). Mean differences in fluxes and $NDVI_{ground}$ between grazed and ungrazed land followed a linear regression both on each measurement day (Figure 4-6a-c) and aggregated over the measurement period (Figure 4-6d-f). As expected from the linear mixed effect models testing the effect of grazing cessation, in most grazer exclosures both $NDVI_{ground}$ and CO_2 fluxes were smaller than in grazed land (negative Δ values). Generally, the regression models for aggregated mean differences over the measurement period explained more variation than the models for each sampling day. The strongest linear regression model was for ΔGPP, averaged over the measurement period with 75 % of variation explained by ΔNDVI. Less variation was explained for ΔER (R^2 = 0.47) and ΔNEE (R^2 = 0.52). The lower model fit was partly attributed to the sub-plots with positive ΔER (higher ecosystem respiration in grazer exclosures compared to grazed land; Figure 4-6b,e).

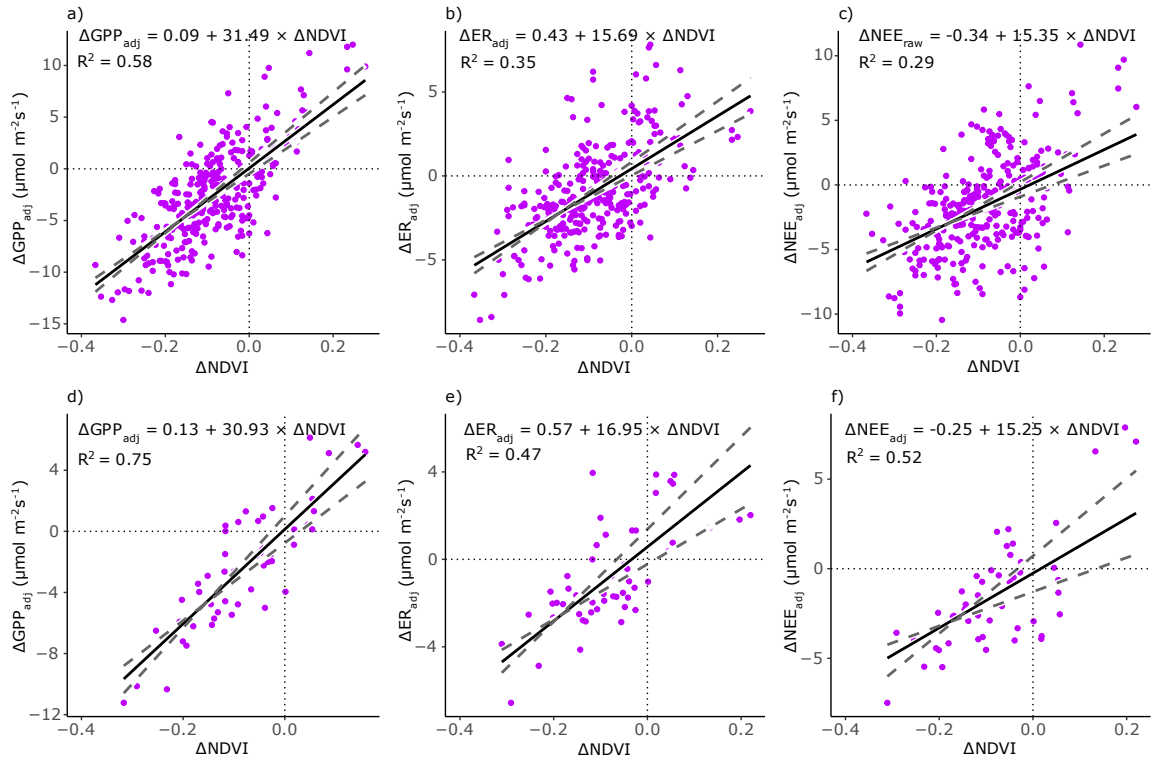

Figure 4-6: Linear regression of mean difference in NDVI and fluxes between grazed and ungrazed plots (Δ). Regression between ΔNDVI in adjusted ΔGPP, ΔER, and ΔNEE is shown for each sub-plot and sampling day (a-c) and summarised for each sub-plot over the measurement period (d-f). Regression curves and equations are derived from linear mixed effects regression models with 'Sampling day' and 'Site' (a-c) or 'Site' (d-f) as random factors. R² indicates the variance explained in each model and dashed lines represent 95 % confidence intervals. GPP = Gross primary production, ER = Ecosystem respiration, NEE = Net ecosystem exchange.

We found that the high variation in ΔER was partly related to differences in sward height (ΔSward; Figure 4-7). ΔER shifted from negative to positive when ΔSward exceeded 100 mm for data aggregated to sites over the measurement period (mean sward height > 100 mm higher in grazer exclosures compared to grazed land). With ΔSward > 100 mm, ER was higher in ungrazed compared to grazed land (positive ΔER) and increased linearly with increasing ΔSward. With ΔSward < 100 mm, ΔER was negative and weakly related to ΔSward (Figure 4-7).

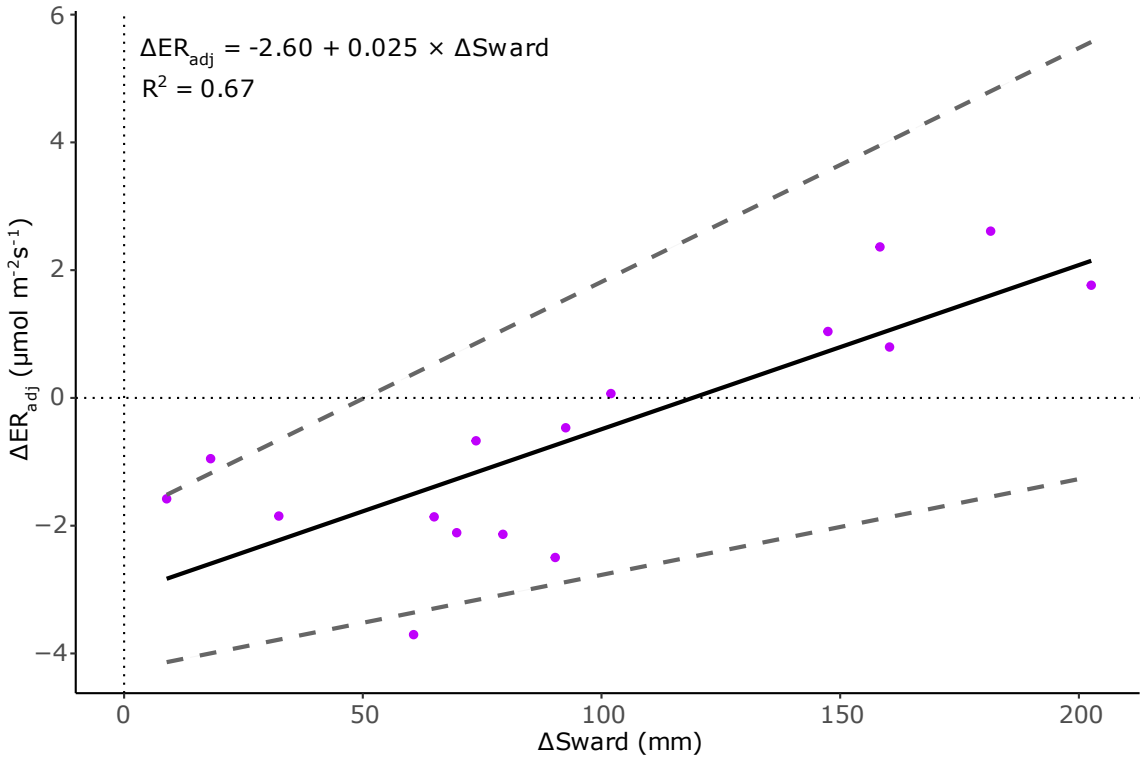

Figure 4-7: Linear regression between ΔSward and $ΔER_{adj}$. Differences between grazed and ungrazed plots (ΔSward and $ΔER_{adj}$) are summarised per site and over the measurement period. Regression equation and R² are derived from simple linear regression. Dashed lines represent 95 % confidence intervals.

4.3.4 How do Ground-based NDVI Measurements Correspond to Satellite-derived NDVI?

We found a positive correlation between the seasonal $NDVI_{ground}$ (mean of all sampling days) and NDVI derived from Sentinel-2 satellite data (r = 0.64, p < 0.01; Appendix 3: Supplemental Figure 8-14c). Sentinel-2 NDVI ($NDVI_{Sentinel}$) values were lower compared to $NDVI_{ground}$ measurements due to the coarser resolution (100 m² vs. 0.35 m²). Using linear regression, we calibrated $NDVI_{ground}$ with $NDVI_{Sentinel}$ with a moderate model fit (R^2 = 0.41; Figure 4-8). The cessation of grazing did not affect the $NDVI_{ground}$ - $NDVI_{Sentinel}$ relationship, but the lower $NDVI_{ground}$ values in grazer exclosures compared to grazed land were reproduced in $NDVI_{Sentinel}$, although with smaller contrasts. Two grazed sub-plots were removed from the model as outliers, due to low $NDVI_{Sentinel}$ values, probably related to a large proportion of surface rocks in the pixel area, when checked on aerial photographs.

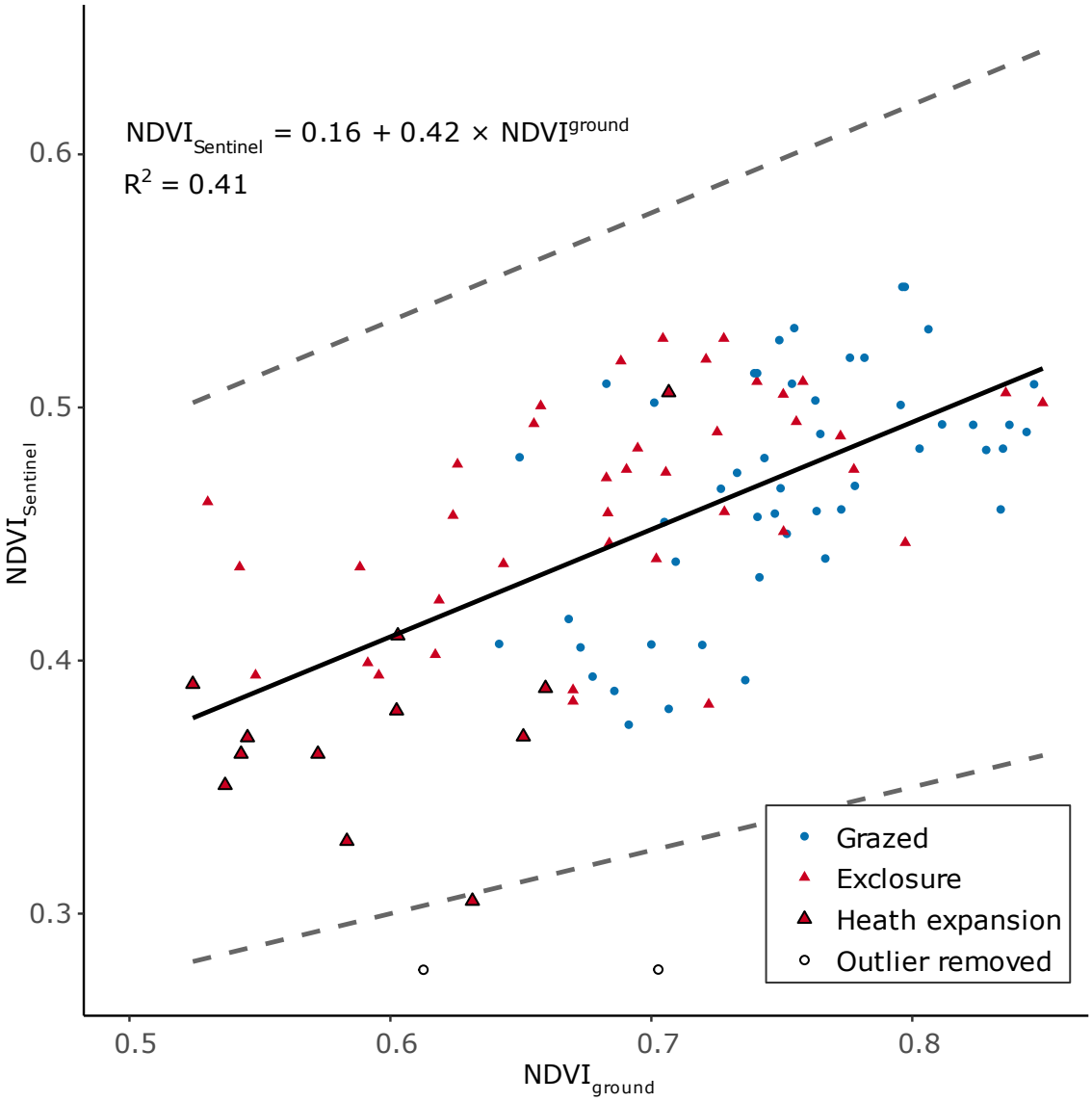

Figure 4-8: Calibration between ground-based NDVI ($NDVI_{ground}$) and NDVI derived from Sentinel-2 satellite data ($NDVI_{Sentinel}$). A linear regression models was used for the calibration for each sub-plot as the average over the measurement period (July-August). Two points were removed from the regression model as outliers and are highlighted with empty dots. Dashed lines represent 95 % confidence intervals.

We further integrated the resultant regression equation between $NDVI_{ground}$ and $NDVI_{Sentinel}$ into the regression equation between $NDVI_{ground}$ and NEE_{adj} and modelled average NEE values over the measurement period based on $NDVI_{ground}$ and $NDVI_{Sentinel}$. We used a linear regression model to calibrate modelled and adjusted NEE which gave a moderate model fit (R^2 = 0.35 for NEE modelled from $NDVI_{Sentinel}$; R^2 = 0.51 for NEE modelled from $NDVI_{ground}$; Figure 4-9).

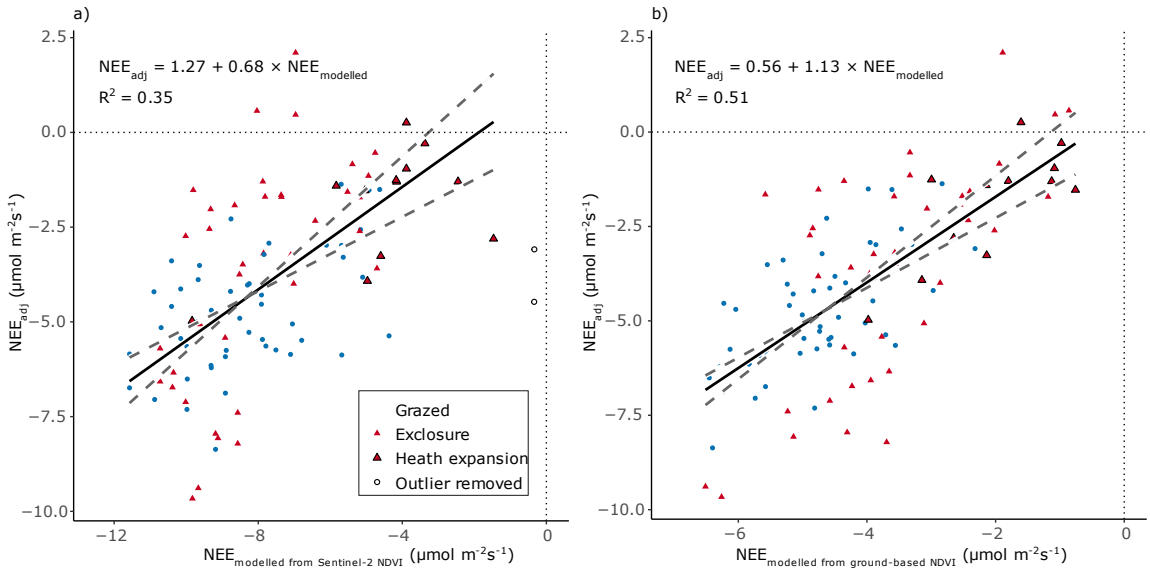

Figure 4-9: Calibration models for adjusted and modelled NEE based on $NDVI_{Sentinel}$ (a) and $NDVI_{ground}$ (b). Data are averaged per sub-plot and over the measurement period with regression equation and R^2 derived from linear mixed effects regression models with 'Site' as random effect. Modelled NEE from $NDVI_{Sentinel}$ was calculated from integrating the regression equation between $NDVI_{ground}$ and $NDVI_{Sentinel}$ into the regression equation of adjusted NEE and $NDVI_{ground}$. Dashed lines represent 95 % confidence intervals. The two removed outliers in a) are the same as in Figure 4-8.

4.3.5 What is the Net CO_2 Flux of Icelandic Lowland Grassland over the Measurement Period?

Based on GPP adjusted to PAR = 450 µmol m^{-2} s^{-1} and adjusted ER, the net daytime ecosystem exchange over the 62-day peak growing season (NEE_{day}) cumulated to -1.40 ± 0.14 Mg C ha^{-1} in grazed and -0.93 ± 0.14 Mg C ha^{-1} in ungrazed grassland with significantly higher NEE_{day} in grazed compared to ungrazed land ($p < 0.001$; Table 4-3). Nighttime respiration (ER_{night}) for the same period cumulated to 0.96 ± 0.05 Mg C ha^{-1} in grazed and 0.85 ± 0.05 Mg C ha^{-1} in ungrazed grassland with significantly higher ER_{night} in grazed compared to ungrazed land ($p = 0.019$; Table 4-3). Together, grazed grassland was a net C sink for July-August with $NEE_{July\text{-}August}$ = -0.44 ± 0.14 Mg C ha^{-1} while grazer exclosures were net C neutral during July-August with $NEE_{July\text{-}August}$ = -0.07 ± 0.14 Mg C ha^{-1} (Table 4-3). The net C uptake was in total larger in grazed than ungrazed land ($t = -3.0$, $p = 0.007$). Similarly, $NDVI_{ground}$ was larger in grazed grassland compared to ungrazed grassland (0.75 vs. 0.67, $p < 0.001$). This difference decreased with the coarser resolution of $NDVI_{Sentinel}$, but it was still significantly higher in grazed compared to ungrazed grassland (0.47 vs. 0.44, $p = 0.001$). The cumulated $NEE_{July\text{-}August}$ modelled from $NDVI_{ground}$ was larger than the average $NEE_{July\text{-}August}$ based on measured fluxes (Table 4-3). $NEE_{July\text{-}August}$, modelled from $NDVI_{ground}$, was significantly lower in grazer exclosures (-0.30 ± 0.07 Mg C ha^{-1}) than in grazed grassland (-0.77 ± 0.07 Mg C ha^{-1}). Modelled $NEE_{July\text{-}August}$, based on $NDVI_{Sentinel}$ and corrected with the calibration equation between $NDVI_{ground}$ and $NDVI_{Sentinel}$ (Figure 4-8), also overestimated the net C uptake and was similar to $NEE_{July\text{-}August}$ predicted from $NDVI_{ground}$ (-0.69 ± 0.15 Mg C ha^{-1} in grazed and (-0.33 ± 0.15 Mg C ha^{-1} in ungrazed

grassland, respectively), but differences with grazing cessation were still significant (p = 0.001; Table 4-3).

Table 4-3: Mean ± standard error values cumulated NEE and mean NDVI. Parameters were calculated for July-August (62 days) daytime and nighttime net CO_2 flux, the cumulated net C balance ($NEE_{July-August}$), ground-based and Sentinel-2 NDVI and modelled July-August NEE using $NDVI_{ground}$ and $NDVI_{Sentinel}$ based on 108 measurement points from 17 sites. Values, t-statistics and p-values are derived from least-squares mean post-hoc tests following significant ($p < 0.05$) linear mixed effect models with 'Site' as random factor. $NDVI_{Sentinel}$ and NEE for all grassland in the Icelandic lowlands were estimated based on grassland distribution according to the habitat map of Iceland. ER = Ecosystem respiration, NEE = Net ecosystem exchange.

Parameter†	**Grazed**	**Ungrazed**	**Grazed - Ungrazed**	**df**	***t***	***p***
Daytime NEE (Mg C ha^{-1})	-1.40 ± 0.14	-0.93 ± 0.14	-0.48 ± 0.13	84	-3.6	**0.001**
Nighttime ER (Mg C ha^{-1})	0.96 ± 0.05	0.85 ± 0.05	-0.11 ± 0.05	84	2.4	**0.019**
$NEE_{July-August}$ (Mg C ha^{-1})	-0.44 ± 0.14	-0.07 ± 0.14	-0.37 ± 0.13	84	-3	**0.007**
Average $NDVI_{ground}$	0.75 ± 0.01	0.67 ± 0.01	-0.08 ± 0.01	84	6.8	**<0.001**
NEE modelled from $NDVI_{ground}$ (Mg C ha^{-1})	-0.77 ± 0.07	-0.30 ± 0.07	-0.48 ± 0.07	84	-7.0	**<0.001**
Average $NDVI_{Sentinel}$	0.47 ± 0.01	0.44 ± 0.01	-0.03 ± 0.01	82	3.4	**0.001**
NEE modelled from $NDVI_{Sentinel}$ (Mg C ha^{-1})	-0.69 ± 0.15	-0.33 ± 0.15	-0.36 ± 0.01	82	-4	**0.001**
Mean $NDVI_{Sentinel}$ of grassland (± SD)	0.42 ± 0.08††		-	-	-	-
$NEE_{July-August}$ of grassland (Mg C)	-8228.5††		-	-	-	-

† cumulated flux or mean NDVI over July-August (62 days)
†† estimated for 2351.3 km^2 of grassland in Icelandic lowlands

Following the same procedure we extrapolated a $NEE_{July-August}$ to the total area of Icelandic grassland below 200 m a.s.l. Following the Icelandic habitat types map, grassland covers 2395.8 km² or 9.5 % of the land below 200 m a.s.l. The suitable Sentinel-2 satellite images covered 98.1% of the grassland area during the selected period between July-August 2023 or 2351.3 km². Average $NDVI_{Sentinel}$ of the total grassland during July-August 2023 was 0.42 ± 0.08. Based on this NDVI, the estimated mean $NEE_{July-August}$ was -0.035 Mg C ha^{-1} and extrapolated to the total area -8228.5 Mg C for July-August 2023 (Table 4-3). This value can

only serve of coarse estimate of NEE in Icelandic lowland grassland during July-August, due to the relatively low model fits of the regression models between $NDVI_{ground}$ and $NDVI_{Sentinel}$ with modelled and adjusted fluxes, carrying large error terms.

4.4 Discussion

4.4.1 NDVI as a Proxy for Ecosystem CO_2 Fluxes in Sub-arctic Grassland

In this study, we asked to what extent ground-measured NDVI can substitute CO_2 flux measurements during the growing season in sub-arctic grassland in Iceland and how this relation is influenced by differences in above-ground vegetation due to the cessation of grazing. Previous studies from northern ecosystems have found that NDVI can be applied as ground-truthing tool of C sink or source activity in low vegetation (Shaver *et al.* 2013, Karlsen *et al.* 2018, Jespersen *et al.* 2023). Consistent with these studies, our findings show that ground-based NDVI is an effective proxy for daytime gross (GPP) and net C uptake (NEE) in sub-arctic grassland during peak growing season conditions (July-August). NDVI correlates strongest with GPP, because NDVI reflects chlorophyll content (Del Grosso *et al.* 2018, Badgley *et al.* 2019, Jespersen *et al.* 2023). This makes NDVI particularly useful for comparing photosynthetic activity under different management practices, such as continued grazing versus cessation of grazing (Petit Bon *et al.* 2025). However, directly measured CO_2 fluxes are strongly controlled by instantaneous environmental conditions, whereas NDVI is not (Appendix 3: Supplemental Figure 8-9 – Supplemental Figure 8-11; Strimbeck *et al.* 2019). Therefore, adjusting GPP to average incidental radiation (GPP_{adj}) markedly improved the NDVI-based prediction, both per measurement day and as aggregates over the measurement period. In our study, NEE_{adj} was more driven by GPP_{adj} than by ecosystem respiration (ER_{adj}; see correlations in Appendix 3: Supplemental Figure 8-14), enabling a prediction of daytime NEE_{adj} from NDVI during the peak growing season with precision comparable to other arctic studies (Shaver *et al.* 2013, Jespersen *et al.* 2023, Petit Bon *et al.* 2025). NDVI thus serves as a rapid indicator of average peak growing season net C uptake but is less suited for fluxes under variable weather conditions, consistent with findings from the tundra (Street *et al.* 2007, Shaver *et al.* 2013). According to findings of See *et al.* (2024), the peak growing season net C balance is a strong predictor for the annual net C balance in northern non-permafrost ecosystems.

The NDVI–ER relationship was weaker and more variable compared to GPP, consistent with other arctic studies (Jespersen *et al.* 2023, Petit Bon *et al.* 2025). This is reflecting that ER is a composite of autotrophic and heterotrophic respiration, only partly linked to plant productivity, and thus NDVI (Jin *et al.* 2024). Autotrophic respiration is typically proportional to photosynthetic uptake, thus follows a similar relationship to NDVI as GPP (Schmitt *et al.* 2010). In contrast, heterotrophic (microbial) respiration is less aligned with NDVI because microbial activity depends more on resource availability (e.g. litter), temperature and moisture (Sjögersten *et al.* 2012, Meyer *et al.* 2018, Jian *et al.* 2022). However, the moderate fit of the NDVI-ER regression in our study suggests a covariation of microbial activity, root respiration and plant productivity, possibly related to general soil fertility (Barneze *et al.* 2024, Maes *et al.* 2024). Conversely to C uptake, adjusting ER to average soil temperatures (ER_{adj}) reduced model fits with NDVI. In several ungrazed sub-

plots, ER was markedly higher than expected from NDVI. This separation further amplified with ER adjustments to soil temperatures and aggregation over the measurement period. We speculate that decomposition of accumulated grass litter at these sub-plots contributed to enhanced respiration, poorly reflected in NDVI (Strimbeck *et al.* 2019, Wang *et al.* 2021).

4.4.2 Grazing Cessation and NDVI–CO_2 Flux Dynamics

Grazing cessation was associated with substantially reduced CO_2 fluxes (raw and adjusted), net ecosystem exchange and NDVI, consistent with previous results from the same study system, including more sites (Klopsch *et al.* 2026b) and from other high latitude studies (Falk *et al.* 2015, Lara *et al.* 2017, Fischer *et al.* 2022, Thorhallsdottir and Gudmundsson 2023). Overall, NDVI–CO_2 flux relationships were equal in grazed and ungrazed land during the measurement period. NDVI differences (ΔNDVI) >0.1 reliably predicted proportional changes in CO_2 fluxes and NEE_{600} during our measurement period. Differences below this threshold yielded poor predictions, likely due to biomass composition. In grazed grassland, most standing biomass is green and photosynthetic active (i.e. high NDVI), but total photosynthetic biomass can be low (Miao *et al.* 2021, Vaieretti *et al.* 2021). Contrary, in ungrazed grassland litter is accumulating, reducing NDVI despite high photosynthetic biomass and GPP (Jespersen *et al.* 2023).

Above-ground biomass composition and litter accumulation likely also influenced the ΔNDVI – ΔER relationship (Parker *et al.* 2021). When sward height differences exceeded 100 mm, ER was generally higher in exclosures and ΔER increased linearly with ΔSward. A positive ΔER was partly caused by relatively low ER under intensive grazing (low sward, low litter; Klopsch *et al.* 2026b; Li *et al.* 2024), and by increased ER in long-term exclosures with high litter accumulation (high sward, high litter; Wang *et al.* 2020, 2021), both not strongly reflected in NDVI (Huang *et al.* 2019). Smaller ΔSward (< 100 mm) had less influence on ΔER, and ER was generally higher grazed land and more linearly controlled by NDVI and thus plant productivity.

Overall, our results show that NDVI is useful for estimating CO_2 fluxes and grazing cessation-induced changes of CO_2 fluxes in sub-arctic grassland, which could provide a basis for monitoring C sink responses to land use practices (Nevalainen *et al.* 2022). Predictions could be improved by better accounting for total photosynthetic biomass and litter, which are poorly reflected by ground-based NDVI (Jespersen *et al.* 2023) and by analysing ER components separately with NDVI and complementary remote-sensing indices (Ge *et al.* 2017, Azevedo *et al.* 2021, Argenti *et al.* 2022). For example, emerging approaches such as Solar-Induced Chlorophyll Fluorescence (SIF) is directly linked to photosynthetic activity and could enhance GPP prediction accuracy (Sun *et al.* 2017, Chen *et al.* 2021, Zhao *et al.* 2024). Including other indices could advance remote-sensed substitution of direct CO_2 flux measurements further at scales relevant for land management (Argenti *et al.* 2022).

4.4.3 Upscaling from Point Measurements to the Landscape

Our second question concerned the suitability to upscale the net ecosystem exchange from our ground measurement plots to the Icelandic lowland grasslands over July-August. Overall, seasonally aggregated ground-based $NDVI_{ground}$ and satellite-derived peak season $NDVI_{Sentinel}$ were linearly related, enabling upscaling of seasonal net C flux estimates (Nestola *et al.* 2016). In line with previous research, our results showed that the 10 m

resolution of $NDVI_{Sentinel}$ captured small-scale differences in above-ground vegetation between adjacent grazed and ungrazed grassland (Raynolds *et al.* 2015, Cicuéndez *et al.* 2024, Kodl *et al.* 2024). However, two outliers (both from the same site 'LL') in our calibration model indicated that more rigorous calibration is needed to account for landscape heterogeneity (Nestola *et al.* 2016). For example, non-vegetated patches, such as surface rocks or bare soil, which were included in $NDVI_{Sentinel}$, but avoided by $NDVI_{ground}$ measurements. This probably caused overestimated $NDVI_{ground}$ in rocky grasslands (as in the case of the two outliers), consistent with findings of (Siewert and Olofsson 2020) and (Kodl *et al.* 2024) in heterogenous tundra in Iceland and Fennoscandia. Although our findings, based on a single peak season, provide a snapshot of the magnitude of the C sink strength across Icelandic grasslands, they should not be extrapolated without accounting for inter-annual variability in temperature, precipitation and grazing regime (Falk *et al.* 2015). Therefore, it is essential to further improve NDVI-NEE and ground-to-satellite-NDVI calibrations to extrapolate grassland C dynamics temporally and in response to changing land-use (Beer *et al.* 2010, Baldocchi *et al.* 2018).

We estimated daytime net ecosystem exchange and nighttime respiration over the 62-day measurement period (July-August) as –1.40 Mg C ha^{-1} and +0.96 Mg C ha^{-1} in grazed grassland and –0.93 Mg C ha^{-1} and +0.85 Mg C ha^{-1} in ungrazed grassland, respectively (Table 4-3). Combined, the net flux indicated that grazed grassland was a net C sink (-0.44 ± 0.14 Mg C ha^{-1}) while grazer exclosures were net C neutral (-0.07 ± 0.14 Mg C ha^{-1}). Seasonal dynamics beyond the measurement period were not considered in this study but will likely reduce annual C sink strength (See *et al.* 2024). Complementary soil analyses indicated a 0.15 Mg C ha^{-1} yr^{-1} lower sequestration rate in the top 10 cm of soil in exclosures since grazing ceased, cumulating to approximately 4 Mg C ha^{-1} lower topsoil SOC stocks in ungrazed compared to grazed grassland (Chapter 5). This sequestration rate difference is slightly smaller than the calculated $NEE_{July\text{-}August}$ difference of 0.37 Mg C ha^{-1}, suggesting that CO_2 efflux outside the growing season reduce the C sink strength more in grazed than ungrazed grassland (Gong *et al.* 2014, Petit Bon *et al.* 2020). Root and microbial respiration persist far longer than above-ground activity in the Arctic (Blume-Werry *et al.* 2016, Wang *et al.* 2017). Root biomass of our grazed grassland was approximately twice that of ungrazed land (Chapter 6), suggesting that root and soil respiration will also differ in grazed and ungrazed grassland beyond the growing season, which requires further research. These findings indicate that the C sink function of our sub-arctic grassland sites fades without continued grazing, underscoring that the C storage function of northern grassland is linked to grazing activity which could have implications for land-use related climate change mitigation of these ecosystems (Rizzuto *et al.* 2024, Ylänne and Stark 2025).

Interestingly, NEE estimates for July-August, modelled from ground-based and Sentinel-2 NDVI, resembled NEE calculated from measured fluxes, even though the NDVI-NEE relationship showed high variability on individual days and across the season, despite extensive ground measurements. For broader applications and time series, substituting extensive ground-based measurements with high-resolution airborne remote sensing would be preferable (Bazzo *et al.* 2023). Although $NDVI_{Sentinel\text{-}2}$ estimates reproduced general C uptake and grazing effects on C uptake, the satellite-derived estimates were less accurate than $NDVI_{ground}$. A finer resolution than 10 m would improve detection of management impacts. For example, drone-based NDVI offers higher spatial detail and has proven effective in precision agriculture and vegetation monitoring (Assmann *et al.* 2019, Gargiulo *et al.* 2023, Qi *et al.* 2025). Drones can capture detail missed by satellites and still cover

large areas, making them highly suitable for small-scale differences such as grazed vs. ungrazed fence contrasts or heterogeneous vegetation mosaics (Assmann *et al.* 2020, Siewert and Olofsson 2020, Kodl *et al.* 2024).

4.5 Conclusion

Our results demonstrate that NDVI can serve as a rapid indicator of C balance differences between grazed versus ungrazed sub-arctic grassland. We found that the predictability of net ecosystem CO_2 exchange (NEE) from NDVI improved with data aggregation from daily to seasonal values and NEE standardisation to average incident radiation and soil temperature. NDVI and NEE were substantially lower with cessation of grazing, while the principal relationship between both remained consistent. We developed a linear calibration curve linking ground-based NDVI to Sentinel-2 NDVI (10 m resolution) and successfully upscaled point-scale measurements to estimate the average July-August net C balance of Icelandic grasslands, comparable to (Del Grosso *et al.* 2018). Although our regression models often showed moderate fits and upscaled estimates carried large uncertainties, these findings reinforce the potential of NDVI as a substitute of CO_2 flux measurements (Jespersen *et al.* 2023). Future work should focus on refining calibration models to more accurately predict C balances of high-latitude grasslands. Improved remote-sensing models could become powerful tools for assessing grassland C sequestration potential, guiding land-use policies that promote management practices to strengthen grasslands as nature-based solutions for climate change mitigation (Norderhaug *et al.* 2023, Guðmundsson *et al.* 2026).

5 Chapter V: Sustained Grazing enhances Soil Organic Carbon Storage in Sub-arctic Grassland

Abstract: Grazing systems remain underrepresented in global carbon cycle models, and grazed grassland is rarely recognised as an active carbon sink. Emerging evidence indicates that grazing can enhance plant carbon allocation below-ground, contributing to soil organic carbon (SOC) sequestration. Yet, longstanding grazing practices are increasingly being abandoned in sub-arctic regions with poorly understood consequences for SOC sequestration. Here, we examined the long-term consequences of abandonment of livestock grazing for SOC in sub-arctic grassland and heathland across 34 sites in Iceland, by comparing paired ungrazed exclosures (20 – 83 years) with adjacent continuously grazed land. Our results show that the cessation of grazing was associated with 8% lower SOC stocks in the topsoil (0-10 cm), but without effect on SOC in deeper soil. Overall, SOC stocks (on average 130 Mg C ha^{-1} in 0-60 cm) were an order of magnitude larger than carbon in total plant biomass, including roots, shoots and litter. With the cessation of grazing, root carbon and nitrogen stocks in the topsoil, as important factors of SOC dynamics, were 29% and 9% lower, respectively. Our findings indicate that soil nitrogen limitation associated with cessation of grazing, promoted vegetation shifts from grassland into heathland or birch woodland at multiple sites. Both heathland and birch woodland were associated with markedly lower SOC stocks in the upper 30 cm of soil compared to grazed grassland. Therefore, we emphasise that sustained extensive grazing is important for maintaining SOC stocks of sub-arctic grassland.[3]

5.1 Introduction

Land use is a major factor controlling carbon (C) uptake and emissions in terrestrial ecosystems (Sanderman *et al.* 2017). As a strategy to mitigate climate change, land use change has gained increasing attention, often under the banner of nature-based solutions (Buckley *et al.* 2024). Nature-based solutions have thus far largely focussed on afforestation. However, in northern high latitudes, such strategies are increasingly questioned (Briske *et al.* 2024, Kristensen *et al.* 2024, Aslaksen *et al.* 2025). Empirical evidence indicates a growing uncertainty of the boreal forest C sink (Virkkala, *et al.* 2025a) and soil C losses associated with afforestation of open ecosystems (Friggens *et al.* 2020, Tau Strand *et al.* 2021, Joly *et al.* 2025). Conversely, soil organic carbon (SOC) in northern grazed grassland is emerging as a promising alternative, although empirical evidence remains limited and more data are needed to address long-term effects of grazing on SOC (Norderhaug *et al.* 2023, Ylänne and Stark 2025, Pillar and Winck 2026).

[3] A version of this chapter is accepted for publication:
Klopsch, C., Thorhallsdottir, A.G., Thorsteinsson, B., Bardgett, R., Van Der Wal, R., Geirsdóttir, A.: Sustained grazing enhances soil organic carbon storage in sub-arctic grassland, Global Change Biology Communications, *in review*.

Driven by recent grazing abandonment and climate change, grassland increasingly develops into shrub-dominated heathland or birch woodland in northern ecosystems, with uncertain consequences for SOC dynamics (Vowles and Björk 2019, Parker *et al.* 2021). Kristensen *et al.* (2022) hypothesised that grazing could improve the persistence of SOC in grassland by promoting the flux and turnover of organic matter through the plant-soil system (Bardgett and Wardle 2003). Stimulated C cycling, together with organic material mixed into mineral soil by trampling and bioturbation could enhance microbial activity and the formation of dead microbial matter (i.e., necromass) and its subsequent mineral protection in persistent SOC fractions (Bai and Cotrufo 2022). Further evidence suggests that grazing can stimulate the below-ground transfer of photosynthetically assimilated C via root exudation and root turnover (Hamilton III and Frank 2001, Roy and Bagchi 2022, Geremia *et al.* 2025, Zhang *et al.* 2025). This propels a positive feedback loop with increased soil microbial turnover and microbial necromass, which is now recognised as the primary source of stable SOC bound to mineral surfaces—provided sufficient silt and clay minerals are present (Angst *et al.* 2021, Bai and Cotrufo 2022, Georgiou *et al.* 2025). This 'microbial carbon pump' is regarded as a central mechanism for SOC sequestration in grazed grassland (Liang and Zhu 2021, Kristensen *et al.* 2022).

In northern ecosystems, herbivores typically promote grassland at the expense of woodland, heathland, and moss/lichen communities (Van der Wal 2006, Metcalfe and Olofsson 2015, Ylänne and Stark 2025). Long-lived above-ground plant biomass stored in woodland and heathland is less accessible to the soil food web, whereas grassland vegetation allocates more C below-ground, facilitating rapid turnover and transfer into soil due to compensatory regrowth of root and photosynthetic tissue following defoliation (Olofsson and Post 2018, Sarquis *et al.* 2019, Ottaviani *et al.* 2020, Penner and Frank 2021). Via defecation, herbivores return organic matter to the soil, thereby making nutrients (e.g. nitrogen) accessible to soil microorganisms (Van der Wal *et al.* 2004, Barthelemy *et al.* 2018). Trampling by large herbivores has also been shown to influence soil bulk density and soil structure, which can affect microbial activity and SOC sequestration (Heggenes *et al.* 2017, Egelkraut *et al.* 2020, Tuomi *et al.* 2021). Thus, grazing-mediated modifications of fine root turnover, soil nutrient return and microbial activity can influence photosynthetic and respiration activity and potentially enhance SOC formation and stabilisation (Wilson *et al.* 2018, Kristensen *et al.* 2022, Du and De Vries 2025).

Generally, the majority of the C assimilated through photosynthesis that cycles through the soil is respired back into the atmosphere, leaving only a fraction sequestered as SOC—primarily in the main rooting zone (Lal 2018, Franzluebbers 2021). Responses of SOC to changes in grazing practices are small per annum and often inconsistent across studies (McSherry and Ritchie 2013, Abdalla *et al.* 2018). Thus, long-term data are essential to understand SOC dynamics and the sequestration potential of grazing systems (Smith *et al.* 2020, Stanley *et al.* 2024, Encarnation *et al.* 2025, Zhou *et al.* 2026). In a space-for-time approach, SOC sequestration can be quantified as the additional SOC in the rooting zone exceeding basal SOC in deeper soil (Villarino *et al.* 2021, Franzluebbers *et al.* 2023). When applied to long-term contrasts of grazed and ungrazed grassland, this can be used to infer consequences for SOC sequestration with changing grazing practises (Franzluebbers 2022).

In Iceland, continued extensive grazing and a well-known land use history enabled us to test how cessation of grazing influences SOC sequestration, potentially serving as a model for sub-arctic regions (Norderhaug *et al.* 2023, Stark *et al.* 2023). For persistent SOC sequestration, sufficient mineral surfaces to bind C are a key limiting factor (Cotrufo and

Lavallee 2022, Encarnation *et al.* 2025). Andosols, the dominant mineral soil type in Iceland developing on volcanic material (Arnalds 2015), have a high SOC accumulation capacity due to rapidly weathering clay minerals and replenishment of mineral material from volcanic eruptions (Óskarsson *et al.* 2012, Kögel-Knabner and Amelung 2021, Matus *et al.* 2024). This makes these soils particularly suitable to study land-use effects on SOC sequestration. The Icelandic lowlands, characterised by a mosaic of grassland and heathland, maintained through a millennium of traditional livestock grazing (Thorhallsdottir *et al.* 2013), are faced with increasing abandonment of livestock grazing and competing new land uses such as afforestation, similar to other sub-arctic regions (Herzon *et al.* 2021, Kristensen *et al.* 2024). Over the past century, fenced enclosures have been erected across the country within the grazed landscape, creating long-term contrasts between grazed and ungrazed land (Thorhallsdottir and Gudmundsson 2023). Using these contrasts, we have shown that grazed land had a larger net CO_2 uptake than ungrazed land during the growing season (Klopsch *et al.* 2026b). Here, we advance on these findings by testing how SOC stocks, as the long-term accumulation of annual flux balances, are related to long-term cessation of grazing in grassland and heathland. Specifically, we addressed the following questions:

(i) How does the long-term cessation of grazing affect SOC storage and sequestration in sub-arctic grassland and heathland?
(ii) How is SOC distributed through the soil profile of grazed and ungrazed sub-arctic grassland and heathland?
(iii) How are nitrogen, root C and bulk density, as drivers of SOC accumulation, affected by the long-term cessation of grazing?

5.2 Materials and Methods

5.2.1 Sampling Site Selection

To analyse how cessation of grazing affects SOC at a landscape scale, 34 sites were selected, clustered in four regions across the agriculturally relevant Icelandic lowlands (5 - 200 m a.s.l.; Figure 5-1). The climate of the Icelandic lowlands is sub-arctic (Köppen-Geiger classification). At our sampling sites, mean annual temperatures ranged between 2 - 4.5 ˚C (summer 7.4 - 10.3 ˚C) and mean annual precipitation ranged between 469.5 - 1234.4 mm (summer 95.4 - 274.3 mm; Appendix 4: Supplemental Table 8-5). All sites were on mineral soils and included a fenced contrast with a paired long-term grazer exclosure of 20 – 83 years and continuous grazing land with soil abiotic, topographical, and climatic factors being equal. Land use history and the year when grazing was ceased were confirmed by landowners. According to landowners, livestock grazing was historically the only anthropogenic alteration of the sites. The fence contrasts at each site were used as unintentional experiments and a uniform sampling design was applied: each site was treated as a pair of one grazed plot and one ungrazed plot, each with three sub-plots from which soil samples were collected (Appendix 4: Supplemental Figure 8-16). The sub-plots were randomly chosen within each exclosure and mirrored in the grazed plot in an equal terrain position and distance to the fence (see Klopsch *et al.* 2026b). Distances between sub-plots and between sub-plot and the fence were generally less than 20 m.

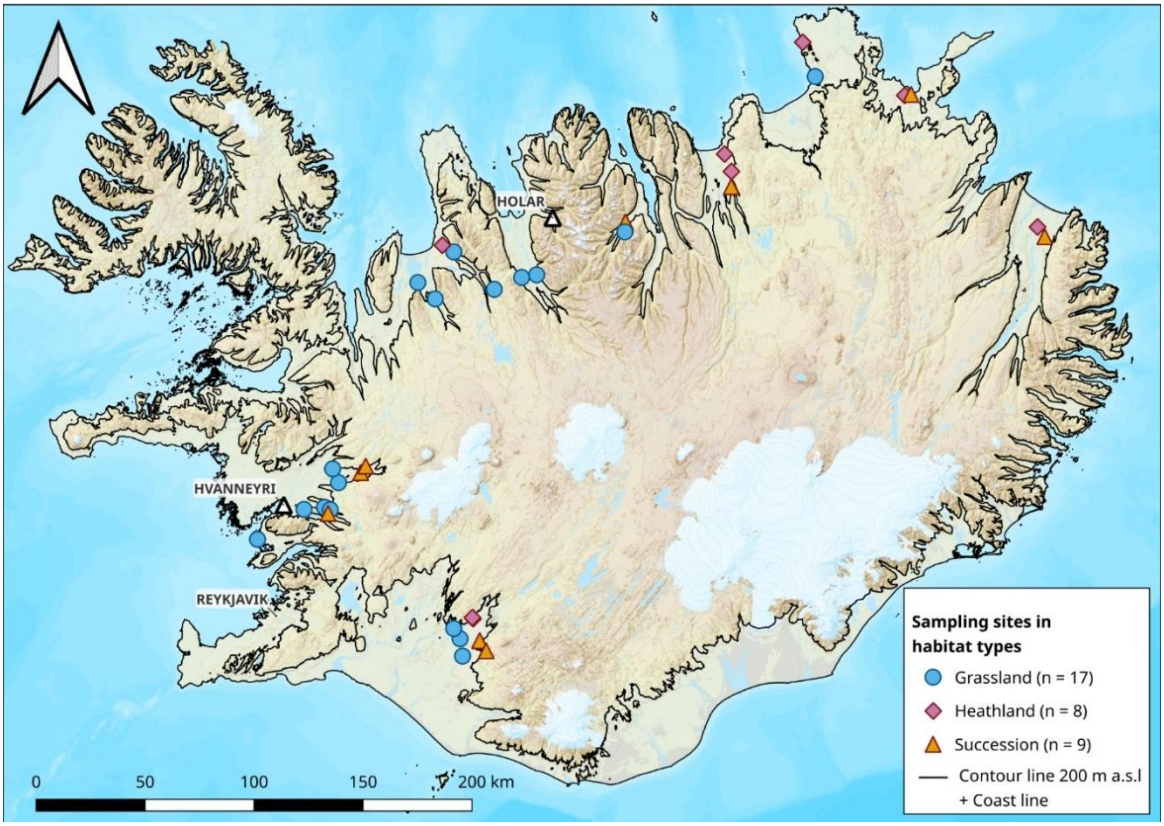

Figure 5-1: Overview map of the 34 soil sampling sites across Iceland. For analysis, the sites were clustered in four regions (eastern, northern, western and southern) and classified in three habitat groups. The background map is sourced from the Natural Science Institute of Iceland (natt.is).

The 34 sites were classified into three vegetation types based on dominant vegetation (Figure 5-1, Appendix 4: Supplemental Table 8-5): 'Grassland', dominated by graminoid or other herbaceous vegetation (n = 17), 'Heathland', dominated by deciduous or evergreen shrub and heath vegetation (n = 8), 'Succession', with shifts from herbaceous vegetation into heath vegetation (n = 7) or birch woodland (n = 2) following the cessation of grazing (total n = 9; Appendix 4: Supplemental Figure 8-17). At one site ('Stori-Ás'), sub-plots were untypically far apart from another (> 100 m) and vegetation composition was inconsistent between sub-plots. This site was divided into one sub-plot, classified as grassland and the two other sub-plots classified as succession.

5.2.2 Soil Sampling

In August and September 2022 and 2023, soil samples were taken at each of the sites following a standard protocol. First, above each soil profile, total above-ground plant biomass was sampled using a 10 cm × 10 cm metal frame, with vegetation being cut off at the soil surface and stored in paper bags. The samples included live green biomass, dead standing biomass, woody biomass and plant litter on the soil surface, but without quantifying offtake from grazing (hereafter 'above-ground samples').

The boundary of the soil profile was defined as the upper limit consisting of mineral material, following WRB guidelines (IUSS Working Group WRB 2022). For each sub-plot, a soil

profile was excavated to the depth of 60 cm, except for three profiles that were shallower than 60 cm (see example in Appendix 4: Supplemental Figure 8-18). Each soil profile was visually assessed to determine soil horizons of different texture or properties. For each horizon, the percentage of solid rock particles with more than 20 mm diameter (coarse fraction) was estimated and visual characteristics, including soil colour and tephra layers (ash deposits of volcanic eruptions), were documented. Following the profile description, separate soil samples were collected for three different purposes: bulk density, carbon and nitrogen analysis (hereafter 'C & N samples'), and root analysis (hereafter 'root samples').

Bulk density samples were collected from at least three depths between 0-10 cm, 10-30 cm and 30-60 cm, using a metal cylinder with sharp edges of 5 cm diameter and 5 cm depth. In case of larger variations in texture or density, the number of bulk density samples was increased accordingly. The cylinder was carefully pressed horizontally into the respective soil layer to not compress the soil and excavated and cut off from above. When soil conditions did not allow for a representative sampling with the cylinder (extensive coarse fraction or extremely loose soil), a soil block of predetermined volume was carefully cut off with a knife. For the C & N samples, sampling depth varied according to determined soil horizons. Horizon depths ranged from 4 to 30 cm, but most samples had a depth of either 10 or 20 cm. At least four individual C & N samples per soil profile were taken along the depth from 0-60 cm as complete soil columns. Both bulk density and C & N samples were stored in paper or canvas bags and air-dried after sampling.

Root samples were collected from each soil profile in four predetermined depth intervals: 0-10 cm, 10-20 cm, 20-40 cm and 40-60 cm. Every root sample was taken as complete soil column with a soil volume of 5 cm × 5 cm and the respective soil depth. After sampling, root samples were stored in plastic bags at 4°C until further processing, but no longer than 14 days to minimise root decomposition.

5.2.3 Sample and Data Processing

Biomass Samples

Above-ground samples were cleaned manually from mineral soil particles and air-dried. Prior to biomass determination, all above-ground samples were additionally oven-dried at 40°C until no further mass loss was recorded and weighted to the nearest 0.01 g.

Root samples were submerged in soap water for several hours to disintegrate roots from soil particles and then washed off from bulk soil using stacked soil sieves with mesh sizes of 2 mm and 0.5 mm in multiple washing circles. For this study, only root samples of the 0-10 cm soil layer were considered, which accounted on average for 72% of total root biomass in the 0-60 cm (Chapter 6). Root samples were oven-dried at 40°C until no further weight loss was recorded and weighted to the nearest 0.01 g.

We estimated the biomass C stocks using conversion factors derived from Ma *et al.* (2018). Specifically, we averaged the leaf and stem biomass values of Ma *et al.* (2018) as conversion factor for above-ground biomass ($C_{above\text{-}ground}$) and the value for root biomass as conversion factor for roots ($C_{root\ 0\text{-}10}$). For herbaceous vegetation we used 0.436 as conversion factor for $C_{above\text{-}ground}$ and 0.425 as conversion factor for $C_{root\ 0\text{-}10}$. For shrub and heath vegetation we used 0.480 as conversion factor for $C_{above\text{-}ground}$ and 0.474 as conversion factor for $C_{root\ 0\text{-}10}$. Both biomass C stocks were converted into Mg ha^{-1}.

Soil Samples

After drying, bulk density and C & N samples were sieved to the fine earth fraction (< 2 mm). In the bulk density samples, weight of the sieved-out coarse fraction > 2 mm was determined to the nearest 0.1 g and the volume as the volume of water replaced by the course fraction in a measuring cylinder to the nearest 0.1 ml. After sieving, bulk density samples were additionally oven-dried at 40 °C until no further mass loss was recorded and weighted to the nearest 0.01 g. Using Eq. 5-1, bulk density of the fine earth fraction was calculated as

$$BD\,[\mathrm{g\ cm^{-3}}] = M_{fe} / (V_t - V_{CF}), \qquad \textit{Eq. 5-1}$$

where BD is the bulk density of the fine earth fraction, M_{fe} is the dry mass of the fine earth fraction, V_t is the total sample volume (cm^3) and V_{CF} is the volume of coarse fraction (particle diameter > 2 mm) within the bulk density sample (McKenzie *et al.* 2002). C & N samples were subsampled after sieving, using a standard riffle splitter and homogenised using a ball mill with three minutes runtime at 400 turns per minute (PM400, Retsch, Haan, Germany). Subsequently, concentrations of C and N were determined by dry combustion, using elemental analysis (vario MAX cube, Elementar, Langenselbold, Germany). As carbonates are very rare in Iceland, we assumed that all C in our samples was organic C, i.e. SOC (Óskarsson *et al.* 2004). Bulk density and concentrations of SOC and N were standardised to 10-cm depth intervals (0-10, 10-20, 20-30, 30-40, 40-50, and 50-60 cm) to make profiles more comparable. Bulk density and the amount of course fraction varied substantially between samples (Appendix 4: Supplemental Figure 8-19). As such, C and N concentrations can be misleading. Therefore, total stocks of SOC and N per soil layer were calculated with Eq. 5-2 as

$$SOC\,/\,N\,stock_i\,[\mathrm{Mg\ ha^{-1}}] = OC_i\,/\,N_i \times BD_i \times (1 - CF_i) \times i \times 0.1, \qquad \textit{Eq. 5-2}$$

where i is the depth of the soil layer, OC_i / N_i is the organic C or N content of the respective soil layer (mg g^{-1} fine earth), BD_i is the bulk density of the respective soil layer, CF_i is the coarse fraction, either derived from visual estimation in the field or from volume determination in bulk density samples (FAO 2020).

SOC Sequestration

To calculate SOC sequestration ($C_{sequest}$), the approach of 'root-zone enrichment', described by Franzluebbers (2021), was adapted (Eq. 5-3). At our sites, 90% of all roots were distributed in the upper 0-20 cm (Chapter 6), thus we defined 0-20 cm as rooting zone where $C_{sequest}$ is related to current land cover and land use and the mean SOC of 20-60 cm as baseline C ($\sum SOC_{20\text{-}60}$ / 4), driven by past processes unrelated to current land use and land cover. $C_{sequest}$ was then calculated as

$$C_{sequest}\,[\mathrm{Mg\ ha^{-1}}] = SOC_i - (\textstyle\sum SOC_{20\text{-}60} / 4), \qquad \textit{Eq. 5-3}$$

where i is the respective soil layer, either 0-10 or 10-20 cm and $C_{sequest}$ returns a value of SOC above the baseline C for each profile.

Reference SOC data prior to land use change were missing, thus it was not possible to calculate annual $C_{sequest}$ rates. Instead, the annual difference in $C_{sequest}$ since grazing ceased was calculated, assuming equal SOC prior to grazing cessation ($\Delta C_{sequest}$; Eq. 5-4), following Hu *et al.* (2016), as

$$\Delta C_{sequest\,i}\ [\text{Mg C ha}^{-1}\ \text{year}^{-1}] = (C_{sequest}(Exc)_i - C_{sequest}(Gr)_i) \ / \ \text{years}, \qquad \textit{Eq. 5-4}$$

where $C_{sequest}$ (Exc) is the C sequestered in the exclosure plot, $C_{sequest}$ (Gr) is the C sequestered in the grazed plot, *i* is the respective depth layer (0-10 cm, 10-20 cm, 0-20 cm) and 'years' are the respective years since grazing ceased.

5.2.4 Data Analysis

Effects of the cessation of grazing on SOC, N, C:N ratio, bulk density, $C_{above\text{-}ground}$, $C_{root\ 0\text{-}10}$, and the proportion of $C_{above\text{-}ground}$ and $C_{root\ 0\text{-}10}$ in total C stock (C_{total} = SOC + $C_{root\ 0\text{-}10}$ + $C_{above\text{-}ground}$) were tested using linear mixed effects models (LMM), accounting for the sampling design. When necessary, response variables were either log- or square-root-transformed, 'region', and 'sub-plot' nested in 'site' were consistently specified as random effects and 'grazing cessation' as fixed effect. To test if the effects of grazing cessation differed among vegetation types, 'vegetation type' and, if significant, the interaction between 'grazing cessation' and 'vegetation type' were included as fixed effects. For SOC, N, C:N ratio and bulk density responses, separate models were performed for the whole soil column (0-60 cm), the upper soil (0-30 cm), the lower soil (30-60 cm) and each of the six 10 cm standardised soil layers. Four out of 200 whole profiles and 16 out of 1208 10-cm soil layers were excluded for models concerning the whole profile or the respective soil layer (Appendix 4: Supplemental Table 8-6). These profiles or soil layers were excluded because of constraining features – including suspicious soil texture and coarse fraction, interpreted as avalanche deposit, suspiciously high subsoil organic matter, interpreted as historical human artefact or a shallow bedrock – that were present in one profile but not in other profiles of the site and thus differences in SOC in the respective profile were unrelated to grazing cessation and mask real effects.

When predictor variables had significant effects ($p < 0.05$, Appendix 4: Supplemental Table 8-7, Supplemental Table 8-8), differences between predictor categories were tested with least-squares means post-hoc tests. Differences in annual $C_{sequest}$ ($\Delta C_{sequest}$) between grazed and ungrazed land were tested using one-tailored t-tests, tested against $\mu = 0$ (= no difference). Relationships between SOC and N, bulk density, coarse fraction or other C stocks were tested with Pearson correlation tests. The relationship between SOC concentration and bulk density was further analysed with a non-linear regression using an exponential decay function, applied to each depth interval. To analyse changes in C pools with increasing time since grazing ceased, a new 'exclosure age' category was created and all values from grazed land were pooled into one class 'Grazed' and all data from ungrazed land into three successive exclosure age classes: '20-30 years', '31-50 years' and '51-83 years'. The effect of 'exclosure age' was tested with 'vegetation type' and the interaction as additional fixed effects using a LMM structure as described above. Differences between exclosure age classes were tested with least-squares means post-hoc tests.

All data processing and statistical analyses were performed using R statistical software, version 4.3.3 (R Core Team 2024) with the packages lme4 (Bates *et al.* 2015), lmerTest (Kuznetsova *et al.* 2017), emmeans (Lenth 2023), multicomp (Hothorn *et al.* 2008).

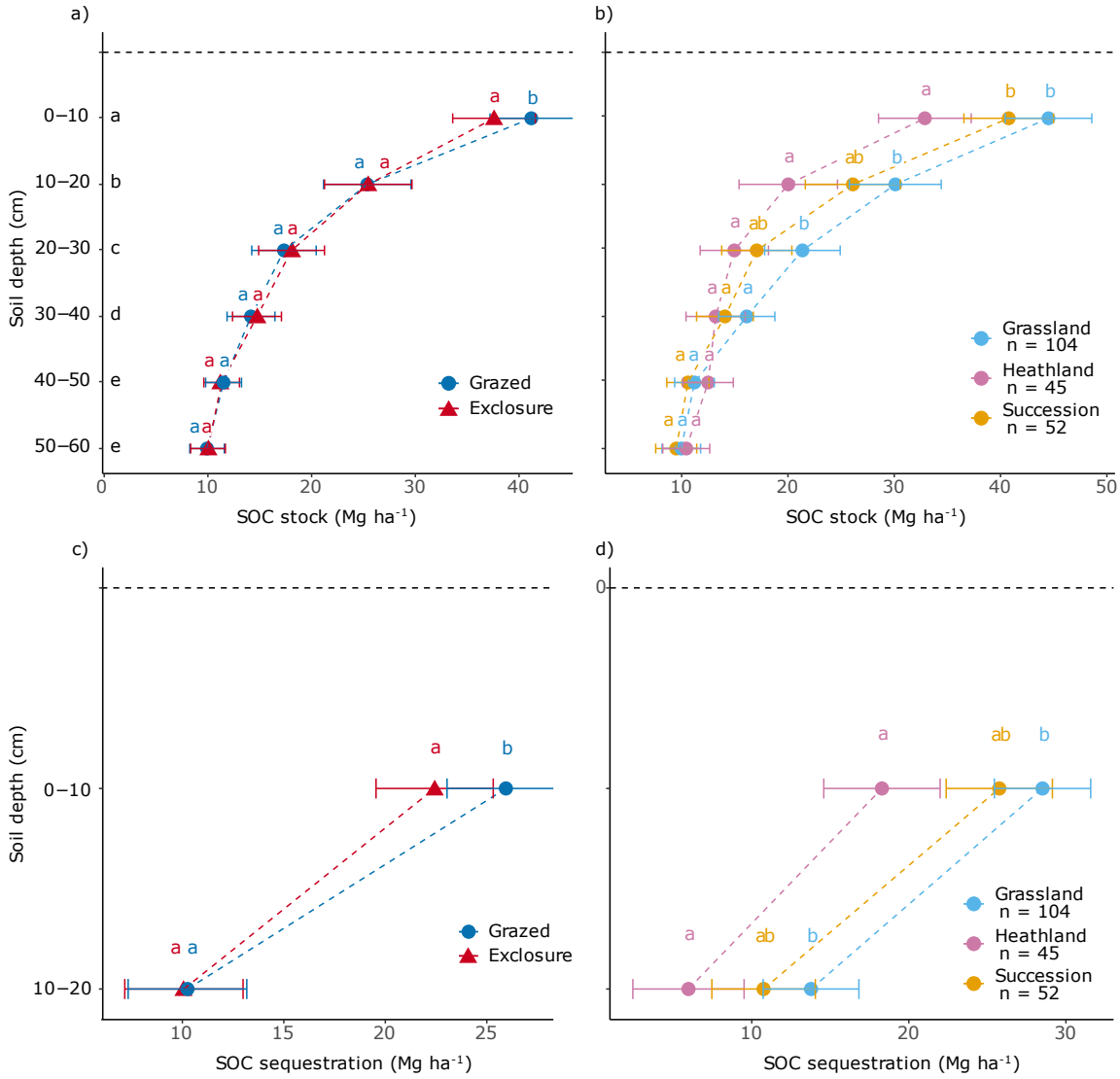

Figure 5-2: Depth distribution of soil organic carbon (SOC) stocks. Depth profiles in 10 cm soil layers for SOC stocks in response to grazing cessation (a) and in each vegetation type (b) for 0-60 cm soil depth and for SOC sequestration above baseline SOC (20-60 cm mean SOC) in 0-10 and 10-20 cm soil in response to grazing cessation (c) and in the three vegetation types (d), based on 201 soil profiles (n = number of soil profiles per vegetation type). For each soil layer an individual linear mixed effect model (LMM) was used, using the same model structure. Different letters in each soil layer indicate significant differences between grazing treatments or vegetation types per soil layer and different letters between soil layers in the y-axis in a) indicate significant differences with depth as derived from least squares means post-hoc-tests following LMM. Error bars represent standard errors

5.3 Results

5.3.1 Effect of Grazing Cessation and Vegetation Type on SOC Stocks, C Sequestration and N Stocks

Soil Organic Carbon

Cessation of grazing had a significant influence on SOC of the uppermost 10 cm of soil, which comprised 32% of the total 0-60 cm SOC stock (Figure 5-2a, Table 5-1). Across sites, ungrazed plots stored less SOC in the 0-10 cm layer than grazed plots, showing an average difference of 8% (40.3 ± 1.2 vs. 43.9 ± 1.8 Mg ha^{-1}, p = 0.002). Similarly, C sequestered in 0-10 cm above the baseline C of the 20-60 cm subsoil ($C_{sequest}$) was 15% lower in ungrazed plots than in adjacent grazed plots (26.1 ± 2.1 vs. 22.3 ± 2.0 Mg ha^{-1}, p = 0.012; Figure 5-2c).

Below 10 cm, the influence of grazing cessation on SOC faded. In all soil layers below 10 cm, SOC stocks did not differ between grazed and ungrazed land and $C_{sequest}$ in 10-20 cm was indistinguishable between grazed and ungrazed land (10.2 ± 2.9 Mg ha^{-1}; Figure 5-2a,c). Instead, SOC declined steadily with every deeper soil layer to 50 cm depth before levelling off in the two lowest soil layers. The subsoil layers (10-30 cm and 30-60 cm) accounted for 36% and 32%, respectively, of the total SOC stock (Table 5-1).

Vegetation type, regardless of grazed or ungrazed (= no interactive effects), exerted a stronger control over SOC distribution than cessation of grazing in the upper soil (0-30 cm) across our sampling sites (Appendix 4: Supplemental Table 8-7). Grassland maintained higher SOC in 0- 30 cm than heathland, +35% in 0-10 cm (p < 0.001), +50% in 10-20 cm (p = 0.002) and +43% in 20-30 cm (p = 0.021), respectively, while succession sites – transitioning between grassland and heathland – had 24% higher SOC in 0-10 cm than heathland (p = 0.011) but were intermediate between grassland and heathland in 10-30 cm (p > 0.05, Figure 5-2b). Grassland had also the highest $C_{sequest}$ above the subsoil baseline C in 0-20 cm, sequestering 56% (p = 0.013) and 130% (p = 0.033) more SOC in 0-10 and 10-20 cm relative to heathland, with succession sites intermediate (p > 0.05, Figure 5-2d).

Two of the succession sites were unique; after more than 50 years without grazing, the vegetation had shifted from grassland to mature birch woodland (Appendix 4: Supplemental Figure 8-17). When analysed separately, these birch succession sites showed a marked difference in $C_{sequest}$: the ungrazed birch woodland held 34% less $C_{sequest}$ in 0–20 cm soil than the adjacent grazed grassland (21.7 ± 4.3 Mg ha^{-1} vs. 33.1 ± 4.3 Mg ha^{-1}, p = 0.046; Figure 5-3).

Table 5-1: Mean soil organic carbon and nitrogen stocks ± standard error (Mg ha^{-1}). Data are presented in relation to cessation of grazing, summed up in four depth intervals and for the total soil column in grassland, heathland and succession. Lower-case letters indicate significant differences between grazed and ungrazed land and upper-case letters indicate significant differences between vegetation types as derived from pairwise least-square mean post-hoc tests.

Soil layer	**Grassland**		**Heathland**		**Succession**	
cm	**grazed**	**ungrazed**	**grazed**	**ungrazed**	**grazed**	**ungrazed**
Soil organic carbon stock (Mg C ha^{-1})						
0-10	47.90 ± 2.61 ^{aA}	43.87 ± 1.63 ^{bA}	36.75 ± 4.14 ^{aB}	32.40 ± 3.38 ^{bB}	41.31 ± 2.67 ^{aAB}	40.30 ± 1.79 ^{bAB}
10-20	28.60 ± 2.21 ^{aA}	30.74 ± 1.92 ^{aA}	22.94 ± 2.43 ^{aB}	20.84 ± 2.41 ^{aB}	28.75 ± 3.61 ^{aAB}	26.41 ± 2.91 ^{aAB}
20-30	20.29 ± 1.64 ^{aA}	23.21 ± 2.53 ^{aA}	19.87 ± 1.80 ^{aA}	18.26 ± 1.95 ^{aA}	20.49 ± 3.25 ^{aA}	19.30 ± 2.47 ^{aA}
30-60	37.11 ± 3.45 ^{aA}	40.64 ± 5.32 ^{aA}	45.19 ± 4.78 ^{aA}	47.14 ± 4.74 ^{aA}	43.76 ± 8.65 ^{aA}	38.64 ± 6.78 ^{aA}
0-60	135.99 ± 5.47 ^{aA}	141.63 ± 7.74 ^{aA}	124.75 ± 7.86 ^{aA}	118.64 ± 6.38 ^{aA}	132.32 ± 13.97 ^{aA}	123.57 ± 11.33 ^{aA}
Soil Nitrogen stock (Mg N ha^{-1})						
0-10	3.69 ± 0.21 ^{aA}	3.50 ± 0.14 ^{bA}	2.08 ± 0.23 ^{aC}	1.80 ± 0.18 ^{bC}	2.89 ± 0.21 ^{aB}	2.61 ± 0.14 ^{bB}
10-20	2.35 ± 0.37 ^{bA}	2.54 ± 0.38 ^{aA}	1.46 ± 0.44 ^{aB}	1.39 ± 0.44 ^{aB}	2.06 ± 0.41 ^{aB}	1.75 ± 0.41 ^{aB}
20-30	1.55 ± 0.27 ^{aA}	1.79 ± 0.29 ^{aA}	1.13 ± 0.29 ^{aB}	1.11 ± 0.28 ^{aB}	1.34 ± 0.28 ^{aB}	1.20 ± 0.27 ^{aB}
30-60	2.88 ± 0.29 ^{aA}	3.16 ± 0.44 ^{aA}	3.13 ± 0.42 ^{aA}	3.26 ± 0.38 ^{aA}	3.24 ± 0.65 ^{aA}	2.82 ± 0.57 ^{aA}
0-60	10.74 ± 0.51 ^{aA}	11.40 ± 0.72 ^{aA}	8.19 ± 0.74 ^{aB}	7.76 ± 0.46 ^{aB}	9.71 ± 1.11 ^{aAB}	i8.61 ± 0.91 ^{bAB}

lower case letters indicate significant differences between grazed and ungrazed land,
upper case letters indicate significant differences between vegetation types

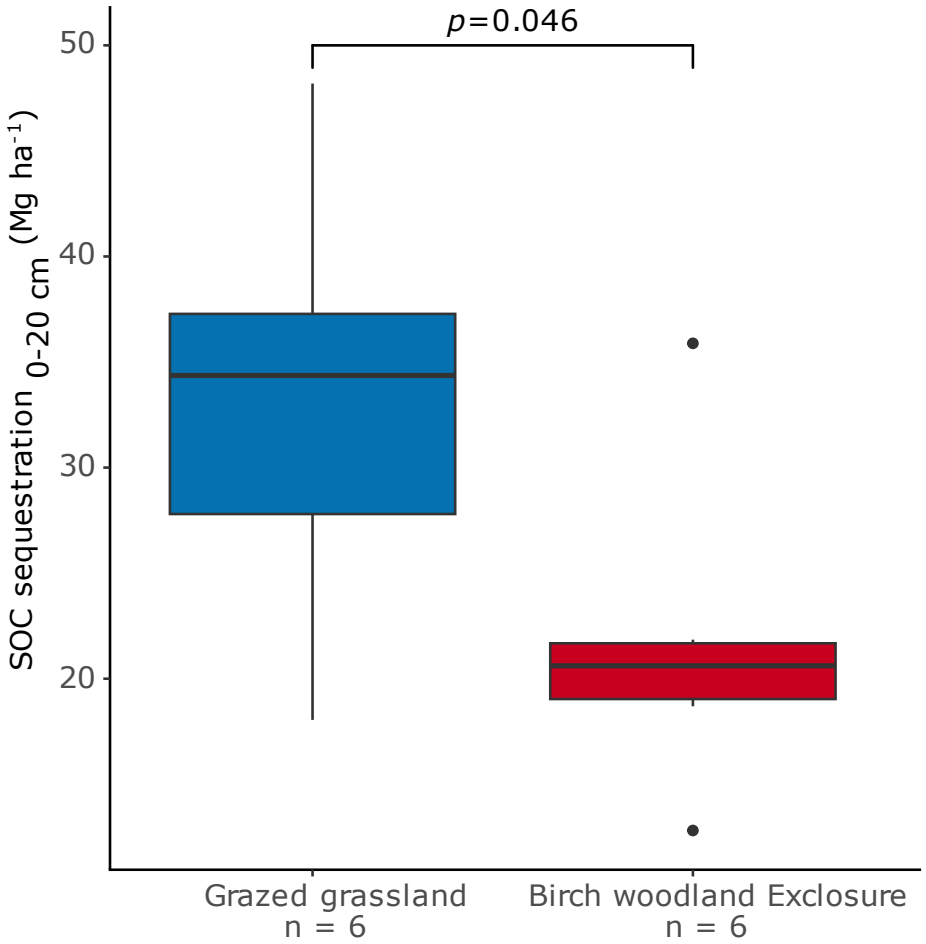

Figure 5-3: Soil organic carbon (SOC) sequestration in 0-20 cm soil following birch woodland succession at two sites with grassland in the grazed land and > 50 years old birch woodland in the exclosures. The significance of the difference between grazed and ungrazed plots is shown by the p-value on top of the graph, as derived from pairwise least-squares means post-hoc tests following a linear mixed effect model ($F_{1,5}$ = 7.0, p = 0.045).

Annual Soil Carbon Sequestration Rate

As the cessation of grazing influenced SOC accumulation in the uppermost soil, we estimated annual differences in $C_{sequest}$ in 0-10 cm between paired grazed and ungrazed land since grazing was ceased (Table 5-2). Ungrazed grassland soils accumulated 0.15 Mg ha^{-1} yr^{-1} less C each year without grazing compared to continued grazed grassland (p = 0.02). Heathland (p = 0.10) and all sites combined (p = 0.08) showed similar, though not significant, annual differences. Succession sites that shifted into heathland following the cessation of grazing showed no annual differences (p = 0.318); however, the two succession sites that had shifted into birch woodland diverged, with ungrazed soils accumulating 0.09 Mg ha^{-1} yr^{-1} less C than the adjacent grazed grassland (p = 0.022).

Table 5-2: Annual differences in soil carbon sequestration (ΔSOC sequestration) between grazed and ungrazed land. Data are shown as mean and 95 % confidence intervals in parentheses with results from one-tailored t-tests (μ = 0 Mg C ha-1 year-1) in the topsoil (0-10 cm) of all sites and of each vegetation type.

Vegetation type	ΔSOC sequestration between grazed and ungrazed land (Mg C ha^{-1} $year^{-1}$)		t-test df	*t*	*p*
All	-0.09	(-0.18, 0.01)	34	-1.8	0.088
Grassland	-0.15	(-0.27, -0.03)	17	-2.6	**0.020**
Heathland	-0.16	(-0.37, 0.04)	7	-1.9	0.096
Succession	0.16	(-0.20, 0.51)	6	1.1	0.318
Birch succession†	-0.09	(-0.13, -0.05)	1	-29.4	**0.022**

†The two birch succession sites were analysed separately from other succession sites.

Soil Nitrogen

Soil nitrogen (N) stocks mirrored SOC to a large degree, as shown by a close correlation between the concentration of C and N (r = 0.97; Appendix 4: Supplemental Table 8-9) and were 9% lower in the uppermost soil layer of ungrazed plots than in adjacent grazed plots, independent of vegetation type (p = 0.002; Table 5-1). By contrast, in 10-20 cm, N was 10% higher in ungrazed grassland (p = 0.05), 15% lower in ungrazed succession (p = 0.07) and not different in heathland (p > 0.05) compared to adjacent grazed plots. Mirroring SOC, N varied more between vegetation types than with cessation of grazing. Overall, grassland maintained substantially larger N stocks than both heathland and succession in every soil layer in 0-30 cm (p < 0.05). Below 30 cm, neither grazing nor vegetation type had a detectable effect on N. Summed up across the full 0-60 cm profile, grassland stored the most N, while heathlands stored the least, without differences between grazed and ungrazed land. In succession sites, though, the cumulative N stock was 11% lower in ungrazed land compared to grazed land (p = 0.04; Table 5-1).

C:N ratio

Variations in SOC and N together shaped distinct C:N ratios across vegetation types (Figure 5-4, Appendix 4: Supplemental Table 8-7). Heathland, with more woody, nutrient-poor vegetation, maintained the highest C:N ratio (~18) in the upper soil. Grassland and succession showed substantially lower ratios, ranging between 13-15. In ungrazed succession sites, the C:N ratio was significantly higher than in grassland, mirroring the vegetation transition from grassland into heathland. This transition was further sharpened in 10-30 cm with grassland vegetation (grazed and ungrazed grassland, grazed succession) exhibited consistently lower C:N ratios (≤ 13) than heathland vegetation (grazed and ungrazed heathland, ungrazed succession; ≥ 14). Below 30 cm, all distinctions faded and the C:N ratio converged around 14, reflecting a homogeneous deeper soil across vegetation types.

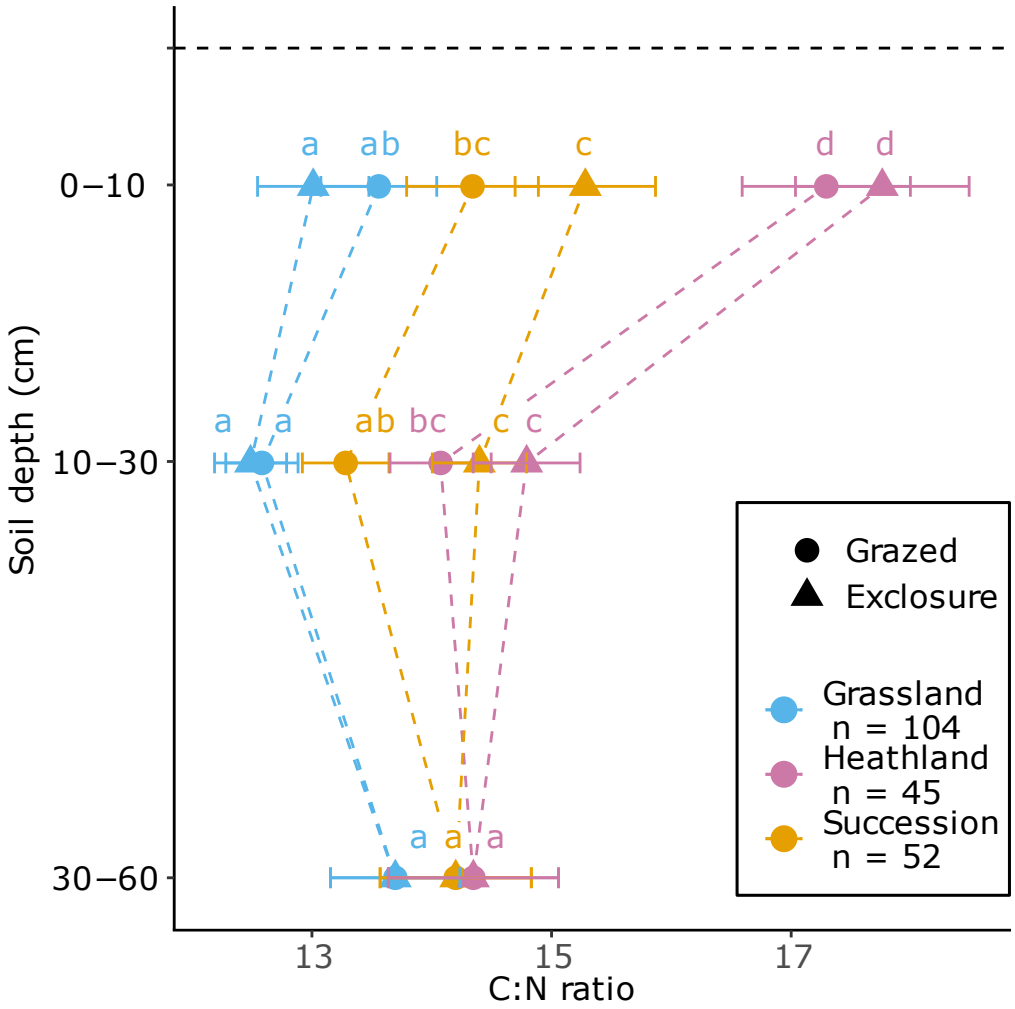

Figure 5-4: Mean C:N ratio ± standard error along the soil profile in three separate soil sections: 0-10 cm (top), 10-30 cm (middle) and 30-60 cm (bottom) in the vegetation types (n = number of soil profiles included). For each section a separate linear mixed-effects model with 'grazing cessation' and 'vegetation type' as fixed effects was performed. Significant differences between grazing cessation and vegetation type in each section are indicated by different letters, as derived from least-squares means post-hoc tests.

5.3.2 Carbon in Above-ground and Below-ground Biomass

Above-ground carbon ($C_{above\text{-}ground}$) responded strongly to the cessation of grazing (Appendix 4: Supplemental Table 8-7). As expected, $C_{above\text{-}ground}$ was higher in ungrazed plots compared to grazed plots (10.3 ± 0.4 Mg ha^{-1} vs. 7.1 ± 0.3 Mg ha^{-1}, $p < 0.001$) of all sites combined and in each of the vegetation types, but without accounting for biomass removed by grazing over the season (Figure 5-5a). Across vegetation types, $C_{above\text{-}ground}$ was larger in heathland than grassland ($p < 0.001$) and succession ($p = 0.003$). Overall, $C_{above\text{-}ground}$ accounted for < 10% of C_{total} ($SOC_{0\text{-}60} + C_{root} + C_{above\text{-}ground}$) and held in each vegetation type a higher fraction of C_{total} in ungrazed plots compared to grazed plots ($p < 0.05$; Appendix 4: Supplemental Figure 8-20a). In heathland-dominated vegetation, $C_{above\text{-}ground}$ was principally a larger fraction of C_{total} compared to grassland-dominated vegetation.

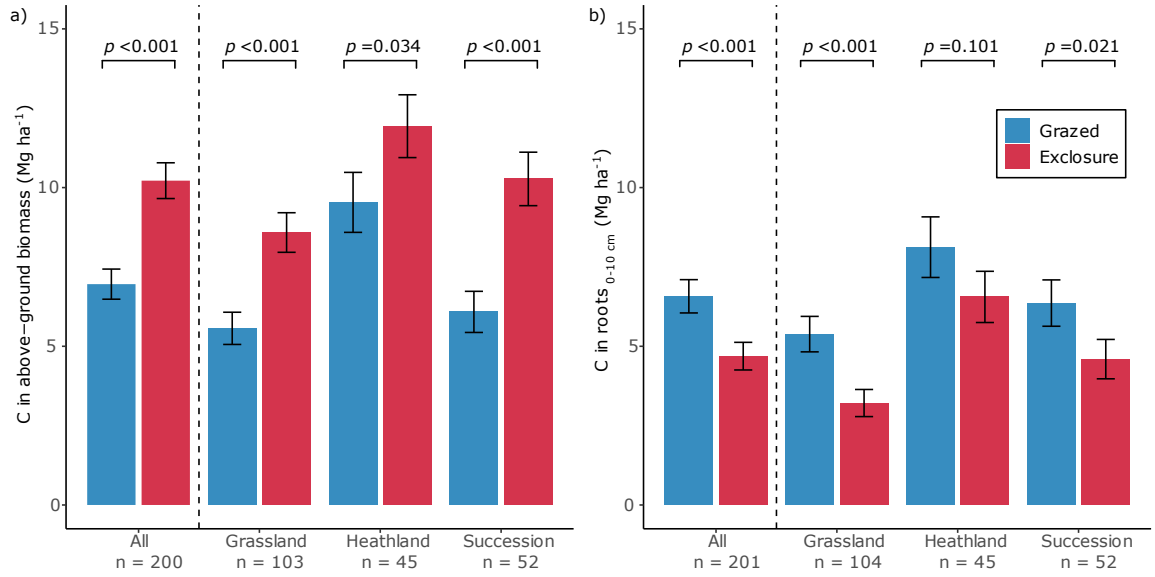

Figure 5-5: Mean carbon (C) in above-ground biomass (a) and in roots in the 0-10 cm soil (b). Data of all sites and each vegetation type are shown for grazed and ungrazed plots, derived from linear mixed effect models (n = number of samples included per category, one above-ground biomass sample was missing). Significant differences with grazing cessation in each of the vegetation types or at all sites are indicated by p-values above the bars, as derived from least-squares means post-hoc tests. Error bars represent standard errors.

Root carbon in the topsoil ($C_{root\ 0\text{-}10}$) exhibited the opposite trend to $C_{above\text{-}ground}$. Across all sites, ungrazed plots contained 29% less $C_{root\ 0\text{-}10}$ than grazed plots (4.7 ± 0.4 Mg ha^{-1} vs. 6.6 ± 0.5 Mg ha^{-1}, $p < 0.001$), with grassland showing the strongest difference (-40%, $p < 0.001$) and heathland showing a tendency only (-19%, $p = 0.101$; Figure 5-5b). These differences translated into a smaller contribution of $C_{root\ 0\text{-}10}$ to C_{total} in ungrazed plots compared to grazed plots, particularly in grassland ($p < 0.001$) and marginally in heathland ($p = 0.07$; Appendix 4: Supplemental Figure 8-20b). Across vegetation types, heathland held larger $C_{root\ 0\text{-}10}$ than grassland ($p < 0.001$) and succession ($p = 0.03$). Overall, we found that in grassland $C_{sequest}$ in 0-10 cm was positively correlated with $C_{root\ 0\text{-}10}$, but negatively correlated with $C_{above\text{-}ground}$, but not in other vegetation types (Appendix 4: Supplemental Table 8-9).

Table 5-3: Diagnostics for exclosure age models. F statistics and degrees of freedom (df) are derived from linear mixed effects models (LMM) for 'exclosure age', 'vegetation type' and their interaction as fixed effects and $SOC_{0\text{-}10\ cm}$, $C_{root\ 0\text{-}10\ cm}$ and $C_{above\text{-}ground}$ as responses. Random effects in each LMM were 'Sub-plot' nested in 'Site' and 'Region'.

Response	Exclosure age (A)		Vegetation type (V)		A × V	
	$df_{num,den}$	*F*	$df_{num,den}$	*F*	$df_{num,den}$	*F*
$SOC_{0\text{-}10}$	3, 124	1.3	2, 113	**11.5*** **	6, 126	1.6
$C_{root\ 0\text{-}10\ cm}$	3, 145	**6.6*** **	2, 98	**14.5*** **	6, 147	**3.4** **
$C_{above\text{-}ground}$	3, 142	**22.2*** **	2, 108	**10.3*** **	6, 148	**2.4** *

Significance codes: '***' < 0.001; '**' < 0.01; '*'< 0.05; '·' < 0.1

5.3.3 Changes in C Pools with Exclosure Age

As shown above, $SOC_{0\text{-}10}$, $C_{root\ 0\text{-}10}$ and $C_{above\text{-}ground}$ were sensitive to cessation of grazing (Figure 5-2, Figure 5-5). We further tested how four levels of 'exclosure age' (Grazed, 20-30, 31-50, 51-83 years) affected these C pools (Table 5-3). With longer exclosure age (> 30 years) more exclosures were added to the succession category, indicating an increasing likelihood of vegetation shifts from grassland into heathland with exclosure age (Figure 5-6). $SOC_{0\text{-}10}$ remained the largest C pool in each vegetation type and each exclosure age class, representing 56-80 % of all C in the topsoil and plant biomass combined, with an overall higher ratio of $SOC_{0\text{-}10}$ to C in vegetation in grassland than heathland.

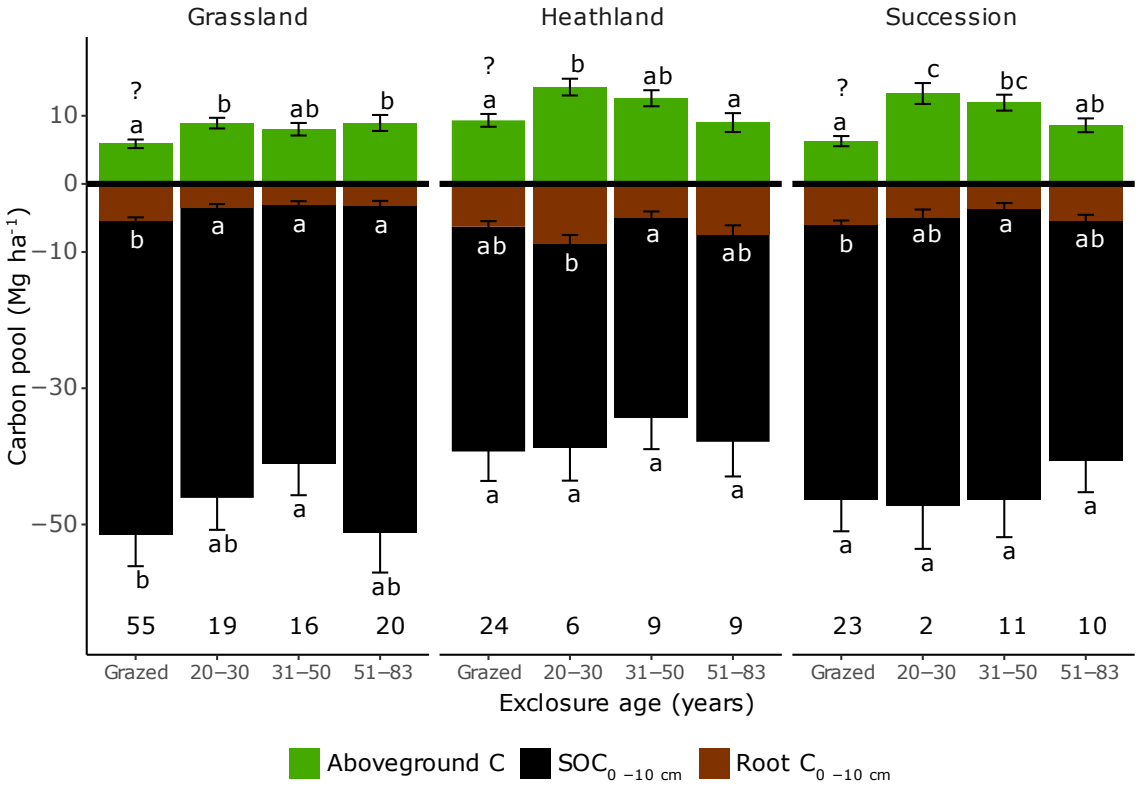

Figure 5-6: Carbon (C) pool differences with exclosure age. C pools (Mg ha^{-1}) of above-ground biomass (green), root biomass in 0 -10 cm (brown) and soil organic carbon (SOC) in 0 - 10 cm (black) are shown for grassland, heathland and succession sites in grazed land and each of three exclosure age classes (20-30 years, 31-50 years, 51-83 years). Error bars represent standard error. Significant differences in each C pool between age classes are indicated by different letters, derived from least-squares means post-hoc tests. Note that on the y-axis positive values represent above-ground C and negative values represent below-ground C. Numbers above the x-axis represent number of soil profiles included in each category. The question marks above grazed above-ground bars indicate that biomass removed by grazing was not measured and is missing from this pool.

In grassland, $SOC_{0\text{-}10}$ was lower in up to 50 years old exclosures (p = 0.011) compared to the grazed reference (Figure 5-6). Exclosures that remained as grassland for more than 50 years were as rich in $SOC_{0\text{-}10}$ as grazed grassland (p = 0.95). $C_{root\ 0\text{-}10}$ halved relative to the

grazed reference in the 20-30 years old grassland exclosures, while $C_{above\text{-}ground}$ increased by 50% in the same period and both C pools remained similar in older exclosures.

By contrast, in heathland and succession, no differences in $SOC_{0\text{-}10\ cm}$ between grazed and any of the three exclosure age classes were found (Figure 5-6). In heathland, both $C_{root\ 0\text{-}10}$ (+42%) and $C_{above\text{-}ground}$ (+52%) peaked initially in 20-30 years old exclosures relative to the grazed reference but declined again in older exclosures until $C_{root\ 0\text{-}10}$ and $C_{above\text{-}ground}$ were indistinguishable from grazed values in the old exclosures. Succession sites followed a similar trajectory as heathland for $C_{above\text{-}ground}$, that more than doubled (+111%) in the 20-30 years old exclosures relative to the grazed reference. $C_{root\ 0\text{-}10}$ on the other hand, was lower than the grazed reference for 50 years following cessation. Interestingly, $C_{above\text{-}ground}$ and $C_{root\ 0\text{-}10}$ in over 50 years old succession exclosures were again as high as the grazed reference, despite the vegetation shift.

Table 5-4: Bulk density (g cm^{-3}) ± standard error, in three soil depth intervals and the whole soil column. Bulk density differed marginally in 0-10 cm and 10-20 cm between grazed and ungrazed plots ($p < 0.1$) and in 0-10 cm significantly between vegetation types. In 20-60 cm, no differences between grazed and ungrazed and between vegetation types were found. For the whole soil column, bulk density was lower in heathland than in grassland and succession. Lower-case letters indicate significant differences between grazed and ungrazed land and upper-case letters indicate significant differences between vegetation types, derived from least-square mean post-hoc tests following LMM.

Soil layer cm	Grassland	Heathland	Succession	All	
				grazed	ungrazed
0 – 10	0.53 ± 0.04^{AB}	0.49 ± 0.04^{A}	0.59 ± 0.04^{B}	0.54 ± 0.03^{a}	0.52 ± 0.03^{a}
10 – 20	0.65 ± 0.06^{A}	0.68 ± 0.07^{A}	0.73 ± 0.07^{A}	0.70 ± 0.06^{a}	0.67 ± 0.06^{a}
20 – 60	0.72 ± 0.03^{A}	0.65 ± 0.05^{A}	0.73 ± 0.05^{A}	0.70 ± 0.03^{a}	0.70 ± 0.03^{a}
0 – 60	0.68 ± 0.02^{B}	0.60 ± 0.03^{A}	0.69 ± 0.03^{B}	0.66 ± 0.03^{a}	0.66 ± 0.03^{a}

Lower-case letters indicate significant differences between grazed and ungrazed land, upper-case letters indicate significant differences between vegetation types

5.3.4 Bulk Density and Soil Properties

Cessation of grazing affected bulk density in the 0-20 cm soil, with marginally less compacted soil in ungrazed plots compared to grazed plots in 0-10 cm (0.52 ± 0.03 vs. 0.54 ± 0.03 g cm^{-3}, $p = 0.094$) and 10-20 cm (0.67 ± 0.06 vs. 0.70 ± 0.06 g cm^{-3}, $p = 0.089$; Table 5-4, Appendix 4: Supplemental Table 8-8). Below 20 cm, no effect of grazing cessation was found and the mean bulk density between 20-60 cm was 0.70 ± 0.03 g cm^{-3}. Overall, topsoil bulk density was lower in heathland (0.49 ± 0.04 g cm^{-3}) compared to succession (0.59 ± 0.04 g cm^{-3}, $p = 0.011$), but not different from grassland (0.53 ± 0.04 g cm^{-3}; $p = 0.406$) and lower in 0-10 cm compared to deeper soil ($p < 0.05$). Bulk density and SOC concentration were inversely correlated ($r_{1201} = -0.63$, $p < 0.001$), following unique exponential decay functions for each soil layer (Appendix 4: Supplemental Figure 8-21): SOC-rich samples (> 10%) had generally low bulk density (< 0.6 g cm^{-3}) while samples with bulk density > 1 g cm^{-3} had generally low SOC concentration (< 2.5 %). Coarse fraction was on average 12 %

of the soil volume without systematic differences between grazed and ungrazed soil profiles ($p > 0.05$, Appendix 4: Supplemental Table 8-5).

5.4 Discussion

Our study revealed that the cessation of grazing over multiple decades was associated with lower topsoil (0-10 cm) C sequestration in Icelandic grassland and heathland, with SOC stocks being on average 8 % lower in ungrazed compared to grazed land. The cessation of grazing was also linked to lower root C and nitrogen (N) stocks in the topsoil, especially in grassland and succession from grassland into heathland. Together, these responses to cessation of grazing likely decrease plant productivity, below-ground transfer of photosynthetic assimilated C into soil, and SOC accumulation (Sokol, *et al.* 2019a, Villarino *et al.* 2021, Cotrufo and Lavallee 2022). By contrast, more C was found above-ground 20-30 years after grazing ceased, but without additional effects of exclosure age, indicating inconsistent responses above- and below-ground to cessation of grazing (Vaieretti *et al.* 2021). Together, our results highlight that the cessation of grazing is not a viable strategy to augment SOC accumulation in sub-arctic open ecosystems.

5.4.1 Soil Organic Carbon in Grazed and Ungrazed Land

The soils of our sampling sites were typical brown andosols, the most common soil type described from Iceland (Arnalds 2015). Across our sites, SOC in the 0-60 cm soil column averaged 130 Mg ha^{-1}, ranging from 70 to 255 Mg ha^{-1}, aligning well with the Icelandic national soil database average of 136 Mg ha^{-1} to 60 cm depth (Óskarsson *et al.* 2004) and global andosol SOC values (Batjes 1996, Kögel-Knabner and Amelung 2021). Similarly, soil bulk density mostly ranged between 0.4 and 1.0 g cm^{-3} across soil layers and followed similar relations with C concentration as described previously for Icelandic and global andosols (Dahlgren *et al.* 2004, Arnalds 2015, Sanchez *et al.* 2025). This indicates our soils were representative for the Icelandic lowlands and that grazing history at these sites contributed to maintaining or augmenting the large SOC stocks of Icelandic brown andosols (Matus *et al.* 2014).

Our results provide empirical support for recent theoretical models on herbivore effects on C cycling (Kristensen *et al.* 2022, Rizzuto *et al.* 2024). For example, Rizzuto *et al.* (2024) demonstrated that herbivores enhance SOC through simultaneous defoliation and defecation, thereby improving plant and microbial performance. However, some recent empirical studies have failed to detect changes in SOC storage after decades of herbivore exclusion in temperate grassland, questioning the role of grazing in SOC dynamics (Medina-Roldán *et al.* 2012, Derner *et al.* 2019, Encarnation *et al.* 2025, but see Zhou *et al.* 2025). However, studies have shown that SOC stocks were maintained under grazing despite substantial biomass removal, interpreted as proportionally greater SOC storage per C input (Roy and Bagchi 2022, Encarnation *et al.* 2025). Moreover, it was recently shown across a network of British grassland sites, comparable to our sampling design, that while long-term grazer exclusion had no impact on total SOC, it is associated with lower mineral-associated organic C, i.e. the more persistent component of SOC (Zhou *et al.* 2026). In our study, we identified the topsoil (0–10 cm) as sensitive to grazing, with lower SOC stocks in long-term exclosures compared to adjacent grazed land, consistent with findings from arctic-alpine long-term studies (Hewins *et al.* 2018, Bork *et al.* 2020, Wu *et al.* 2021, Windirsch *et al.* 2022,

Thorhallsdottir and Gudmundsson 2023). Although not directly measured, we suggest that in grazed soils larger below-ground C input and higher microbial activity contributed to greater SOC accumulation via mineral-bound microbial necromass, as posited by Geremia *et al.* (2025) and Wilson *et al.* (2018).

We found that vegetation type had a stronger influence on total SOC stocks than the cessation of grazing. Grassland stored substantially more SOC (~97 Mg C ha^{-1}) in the 0–30 cm soil layer than heathland (~79 Mg C ha^{-1}) or mature birch woodland (~56 Mg C ha^{-1}), with no differences below 30 cm, possibly reflecting varied historical grazing and C turnover rates over centuries (Parker *et al.* 2015, Egelkraut, *et al.* 2018a). These findings emphasise the need to better protect grassland from land use changes to maintain their long-term SOC storage function (Bardgett *et al.* 2021, Norderhaug *et al.* 2023, Pillar and Winck 2026). Notably, our birch succession sites accumulated over 10 Mg C ha^{-1} less since grazing was ceased compared to adjacent grazed grassland, aligning with markedly lower SOC in 0-30 cm of mature birch woodland (>60 years), found in other studies from Iceland, compared to our grassland soils (Hunziker *et al.* 2019, Sanchez *et al.* 2025). Similar SOC responses following birch colonisation of open land have been observed in Scandinavia and the UK (Parker *et al.* 2015, Housego *et al.* 2025). Emerging evidence has linked shifting mycorrhizal associations to reduced SOC and particularly mineral-associated organic matter with colonising trees and ericaceous shrubs, although this requires further research (Lindahl *et al.* 2021, Parker *et al.* 2021, Ylänne *et al.* 2025, Zhou *et al.* 2026).

5.4.2 Soil Carbon Sequestration

The non-linear decrease of SOC with depth supports our assumption of ongoing SOC sequestration within the rooting zone (Franzluebbers 2021). This is reinforced by CO_2 flux measurements showing our sites acted as net C sinks during the growing season (Klopsch *et al.* 2026b). Using calculations adapted from Franzluebbers (2021), SOC sequestration in the 0-20 cm rooting zone ranged between 1.6 to 91.8 Mg ha^{-1} above the 20-60 cm baseline C at our sites, likely representing C sequestered during the last centuries, comparable to centennial-scale SOC sequestration in the rooting zone of U.S. grassland (Franzluebbers 2021). Since grazing had ceased, on average 0.15 Mg ha^{-1} $year^{-1}$ more C was sequestered in the topsoil of grazed grassland than ungrazed grassland, matching Icelandic data, showing that grassland, N-enriched from bird guano, sequestered 0.14 Mg ha^{-1} $year^{-1}$ more C than N-limited grassland over a 40 years period (Leblans *et al.* 2017). In agreement with Leblans et al. (2017), grazed grassland was also N-enriched in 0-10 cm in our study, emphasising N as limiting factor of long-term SOC sequestration (Piñeiro *et al.* 2010, Schrama, Veen, *et al.* 2013, Bai and Cotrufo 2022).

We could not determine annual SOC sequestration rates due to a lack of reference data prior to land use change—a crucial gap for climate change mitigation schemes (Bossio *et al.* 2020). Sequestration rates for sub-arctic grassland are scarce, but the Icelandic National Inventory Report estimated rates of 0.3-0.9 Mg C ha^{-1} yr^{-1} for eroded soils during restoration and 0.11 Mg C ha^{-1} yr^{-1} for mineral soils in grassland, based on expert judgements (Keller *et al.* 2026). Considering these estimates, we interpret a 0.15 Mg C ha^{-1} yr^{-1} difference in the unknown annual sequestration rate as substantial. Other studies estimated that birch woodland growing on barren or C-depleted land in Iceland sequesters 0.4-0.7 Mg C $ha^{-1}yr^{-1}$ (Hunziker *et al.* 2019, Sanchez *et al.* 2025). By contrast, the birch woodland in our study, established on previously grazed grassland, showed markedly lower SOC sequestration

compared to adjacent grazed grassland (-0.09 Mg C ha^{-1} yr^{-1}), providing empirical support for grazer-enhanced grassland SOC sequestration, as proposed by Rizzuto *et al.* (2024).

5.4.3 Drivers of Change in SOC

Nitrogen

We identified differences in N stocks linked to grazing cessation and vegetation types as one key driver of SOC changes. Our results showed that grassland and heathland N responded differently to cessation of grazing down to 30 cm. Grazing animals return N directly to the soil through defecation, typically lowering the topsoil C:N ratio, thereby improving productivity (Peco *et al.* 2017, Sitters *et al.* 2020, Defourneaux *et al.* 2024). Grassland that persisted for decades after cessation of grazing was characterised by high N and low C:N ratios, particularly in the 10-30 cm soil, likely reflecting historical intensive grazing (Egelkraut, *et al.* 2018a). This high N, as high or higher compared to grazed grassland, maintained productivity in these ungrazed grasslands despite reduced N inputs (Barthelemy *et al.* 2015, Castaño *et al.* 2023). Conversely, grassland with lower N storage and higher C:N ratio in the topsoil, despite continued grazing, faced mounting N limitation with prolonged grazing cessation and developed into heathland, similar to findings from abandoned subalpine grassland (Gavrichkova *et al.* 2022). Although SOC stocks of succession sites were unaffected by grazing cessation in 10-30 cm soil, N stocks diminished, likely causing N-demanding grassland species to be outcompeted by slower- growing shrubs (Egelkraut, *et al.* 2018b, Sørensen, *et al.* 2018b). Generally, heathland exhibited the lowest N and highest C:N ratios in 0-30 cm soil, indicating long-term N limitation favouring heath species that produce nutrient-poor, slowly decomposing litter with a high C:N ratio and low accumulation of SOC (Weintraub and Schimel 2005, Mekonnen *et al.* 2021). Low N in both grazed and ungrazed heathland suggest their long-time persistence over centuries, contrasted with the more recent heathland establishment in ungrazed grassland (decades) with relatively higher N, possibly reflecting historically low grazing activity (Te Beest *et al.* 2016).

Above-ground and Root Carbon

At our grassland sites, SOC was positively linked to root C but negatively to above-ground C. We interpret this as a result of partitioning of photosynthetic-assimilated C in above-and below-ground plant biomass, mediated by grazing (Sarquis *et al.* 2019, Fossum *et al.* 2022). When released from grazing, more C stays above-ground as litter, taller-growing shoots and taller plant species e.g. shrubs (Mekonnen *et al.* 2021, Wang *et al.* 2021, Stark *et al.* 2023). With a larger portion of above-ground C as litter in ungrazed land, photosynthetic activity is hampered by shading and cooler soils and more photosynthetically assimilated C is respired back to the atmosphere before cycling through the soil, thereby reducing soil C input (Sokol, *et al.* 2019a, Su and Xu 2021, Jessen *et al.* 2023).

Following offtake by grazing, grasses respond typically with compensatory regrowth (Frank and Fridley 2025). This likely enhanced photosynthetic C assimilation and below-ground transfer of C at our sites, which influences SOC sequestration more than total biomass (McNaughton 1983, Jackson *et al.* 2017, Ritchie and Penner 2020, Klopsch *et al.* 2026b). This is in line with the conclusion of Encarnation *et al.* (2025), positing a greater C storage per unit C input from plant biomass under grazing.

Our results suggest that differences in topsoil root C of grassland following cessation of grazing better explain differences in SOC, supporting the findings of Franzluebbers *et al.* (2023) who showed that land management impacts SOC sequestration within grassland rooting zones. At our grassland sites, root C was markedly reduced following the cessation of grazing, offsetting above-ground biomass gains and likely changing plant-soil interactions (Villarino *et al.* 2021). As roots are the primary pathway for C into soil, likely more SOC accumulated under grazing (Sarquis *et al.* 2019, Yang *et al.* 2021). Grazed grassland, specifically, feature dense fibrous root systems with rapid turnover, releasing organic matter to soil microorganisms and thus promoting microbial-derived SOC sequestration (Chapter 5; Sokol *et al.* 2019a; February *et al.* 2020; Malhotra *et al.* 2025). With less roots in ungrazed grassland, less C is exuded into the soil, hampering further SOC sequestration.

Heathland contained more total root C than grassland, but heath roots tend to be coarser and longer-lived, likely exuding less C and accumulating C mainly in labile particulate organic matter derived from root litter (Wang, *et al.* 2016b, Arndal *et al.* 2018, Angst *et al.* 2021). With succession from grassland to heathland, root C declined for 50 years after grazing ceased, likely reflecting reduced fibrous grassy root growth (Rodríguez *et al.* 2007, Ylänne *et al.* 2018). However, SOC only tended to decline in the oldest exclosures (50+ years), indicating a time-lagged response of SOC to changing grazing pressure, as long-term result of plant responses to grazing (Bardgett and Wardle 2003).

Bulk density

Grazing animals compact soil through trampling and thereby increase bulk density (Heggenes *et al.* 2017). Andosols typically have low bulk density and high resilience to compaction (Arnalds 2015), and we found no indication of soil compaction that limited aeration or infiltration at our sites (Howison *et al.* 2017). Consistent with previous studies, bulk density was higher in grazed than ungrazed land within the 0-10 cm soil layer (Byrnes *et al.* 2018, Lai and Kumar 2020). However, within the range observed in our study, a slightly more compacted topsoil may even help stabilising soil, especially in very loose heathland topsoil with large amounts of unconsolidated particulate organic matter and improving N mineralisation by enhancing water retention in the topsoil (Schrama, Heijning, *et al.* 2013, Tuomi *et al.* 2021, Meyer and Leroux 2024). Together, we consider N recycling, root density and soil compaction in the topsoil, stimulated by grazing, trampling and defecation as key drivers contributing to higher SOC under grazing at our sites (Heggenes *et al.* 2017, Leblans *et al.* 2017, Malhotra *et al.* 2025).

5.4.4 Implications and Future Directions

Large uncertainties exist regarding how grazing animals influence SOC storage and sequestration, despite numerous studies on the subject (Bai and Cotrufo 2022, Stanley *et al.* 2024, Bardgett 2025, Zhou *et al.* 2026). Yet, cessation of grazing is often regarded as cost-efficient intervention to enhance C sequestration (Abdalla *et al.* 2018, Qu *et al.* 2024). Challenging this assumption, our results provide robust evidence that cessation of grazing over multiple decades is associated with less topsoil SOC in grassland and heathland across the Icelandic lowlands (together 35 % of land < 200 m a.s.l.). Several long-term studies and meta-analyses support our findings, indicating the need to factor in the treatment duration as SOC sequestration rates tend to shift from positive to neutral or negative with extended periods without grazing (McSherry and Ritchie 2013, Hu *et al.* 2016, Derner *et al.* 2019, Silveira *et al.* 2024). We examined cessation of grazing as a constant treatment, though

grazing intensity varied across our grazed plots—from permanent grazing to lightly grazed summer pastures—adding variability across sites (Klopsch *et al.* 2026b). In line with Stanley et al. (2024), future research should account for grazing frequency, timing, duration, and intensity when assessing grazing impacts. As SOC stocks were higher under grazing, we infer that grazing intensities at our sites remained within ecological carrying capacity (Briske *et al.* 2020). Extensive grazing may therefore enhance SOC sequestration at scales meaningful for climate change mitigation, given the global extent of grazing land (Rumpel *et al.* 2020, Stevens *et al.* 2022, Pillar and Winck 2026). The potential for additional C storage above-ground on the other hand, is tightly limited in sub-arctic grassland and heathland. Our study showed that after 20-30 years without grazing, above-ground C stocks accumulated up to 5 Mg ha^{-1}, but without further increases with exclosure age (Figure 5-6). Thus, it is unlikely that plant biomass gains of ungrazed heathland or woodland offset lower SOC sequestration in our context (Ylänne *et al.* 2018, Snorrason *et al.* 2019, Sanchez *et al.* 2025).

Moreover, we hypothesise that negative impacts of grazing cessation on SOC may be reversible, given that the differences were confined to the top 10 cm of soil even after decades without grazing. Reintroducing grazing animals could restore N inputs and fine root growth, promoting a shift back from heathland to grassland and enhanced SOC sequestration (Te Beest *et al.* 2016, Stark *et al.* 2019, Fischer *et al.* 2022, Geremia *et al.* 2025). However, mycorrhizal associations at these sites have likely shifted from arbuscular to ericoid or ectomycorrhizal forms, altering nutrient and C cycling in ways that may sustain heathland (Clemmensen *et al.* 2015, Frey 2019, Castaño *et al.* 2023). Integrating mycorrhizal fungi into models of herbivore–plant–soil interactions will help to decipher soil C dynamics, particularly where vegetation composition shifts with changing grazing (Castaño *et al.* 2023, Zhou *et al.* 2026).

5.5 Conclusion

Our findings demonstrate that long-term grazed grassland stores more topsoil C than ungrazed grassland, heathland or birch woodland that formed under low or none grazing pressure. Enhanced soil N availability and greater production of fine roots under continued grazing likely underpin these higher SOC stocks (Kristensen *et al.* 2022). Given the limited protection of grasslands globally despite their large SOC stocks, our extensive spatial replication and paired grazed-vs.-exclosure comparison provide compelling evidence that extensive grazing represents an effective nature-based solution for maintaining existing SOC stocks and potentially increasing them in sub-arctic grassland, outperforming both cessation of grazing and heath and birch encroachment (Briske *et al.* 2024, Kristensen *et al.* 2024, Aslaksen *et al.* 2025, Ylänne and Stark 2025, Zhou *et al.* 2026).

6 Chapter VI: Cessation of Grazing in Iceland: Unearthing the Long-term Consequences for Root Biomass and Community-level Root Functional Traits

Abstract: In northern grassland and heathland, plants allocate biomass predominantly in roots. Roots play a central role in mediating the transfer of photosynthetically fixed carbon from plants into soil. These northern ecosystems have been maintained historically by traditional grazing which is increasingly abandoned today. Previous research has shown that grazing exerts strong control over root biomass allocation, via species turnover, favouring grasses with fine, fibrous roots, and root-soil interactions, via stimulated root exudation and root turnover. However, less is known about how root systems of different vegetation types adjust structurally and functionally in the long-term when grazing is ceased. Here we show that after > 20 years after cessation of grazing fine root biomass was strongly reduced in grassland but not in heathland, based on community-level root distribution and functional traits data compiled from adjacent grazed and long-term ungrazed (> 20 years) land at 34 sites in Iceland. Fine root biomass of our sites in 0-60 cm soil was on average 16.1 Mg ha^{-1} in grazed and 12.7 Mg ha^{-1} in ungrazed land, with 72 % of all roots distributed in 0-10 cm. Despite these large differences in root biomass, community-level root functional traits were largely unrelated to cessation of grazing, suggesting that rooting strategy is more controlled by climate or soil properties than grazing or vegetation composition in sub-arctic ecosystems in Iceland. Our findings support the perspective that grazing cessation decreases overall rhizosphere activity and thus carbon inputs from roots into soil, but not root resource acquisition strategy. [4]

6.1 Introduction

Roots play a central role in ecosystem processes, including nutrient and water uptake, anchoring plants, and driving the transfer of photosynthetically fixed carbon (C) into the soil (Bardgett *et al.* 2014, Barry *et al.* 2025). In northern ecosystems, the largest portion of the photosynthetically fixed C is allocated below-ground as an adaptation to short growing seasons and low average temperatures, where root-derived C dominates inputs to the stable soil C pool (Iversen *et al.* 2015, Jackson *et al.* 2017). Therefore, recognition of root dynamics has intensified, as soil C sequestration is increasingly viewed as a key nature-based solution for climate-change mitigation in northern ecosystems (Rasse *et al.* 2005, Sokol and Bradford 2019, Buckley *et al.* 2024, Chari *et al.* 2024).

[4] A version of this chapter is accepted for publication:
Klopsch, C., Thorhallsdottir, A.G., Thorsteinsson, B., Bardgett, R., Van Der Wal, R., Geirsdóttir, A.: Grazing abandonment in Iceland: unearthing the consequences for root biomass and community-level root functional traits, Plant and Soil, *in review*.

In northern ecosystems, mosaics of grassland and heathland are widely shaped by grazing of large mammalian herbivores (Maliniemi *et al.* 2018, Ylänne *et al.* 2018, Stark *et al.* 2023). Herbivore-mediated vegetation composition and nutrient dynamics also shape distribution and functioning of roots (Cai *et al.* 2024). Grazing influences plant C allocation by altering the balance between shoot regrowth and root investment: for example, defoliation can reduce root biomass but stimulate fine-root turnover and exudation, thereby sustaining C fluxes to soil microorganisms (Bardgett and Wardle 2003, Hamilton III *et al.* 2008, Sarquis *et al.* 2019). However, abandonment of traditional grazing practices is altering grazing regimes across northern ecosystems, such as in Scandinavia and Iceland (Stoessel *et al.* 2022, Defourneaux *et al.* 2024). As a consequence, cessation of grazing often triggers striking above-ground successional shifts from grazed grassland into heathland or birch woodland, potentially shifting interactions between fine roots and soil (Christie *et al.* 2015, Yu *et al.* 2017, Parker *et al.* 2021).

Under grazing, shallow, fibrous fine-root systems are typically promoted that maintain high labile soil C inputs to the soil microbial food web; conversely, grazing cessation and species turnover may lead to deeper and more conservative root systems with lower rhizosphere activity favouring longer retention of C in deeper soil (Franzluebbers 2022, Sierra *et al.* 2024). Previous studies have shown that fine root growth in graminoids is more continuous over the growing season, while shrub root growth is more concentrated in the early growing season in the Arctic (Radville *et al.* 2016, Wang, *et al.* 2016b). Other studies found high inter-specific plasticity in fine-root morphology and phenology which maintained root-soil interactions despite species turnover above-ground (Ylänne *et al.* 2018, Wang *et al.* 2023, Yang and Russo 2024). Thus, understanding how community root systems reorganise structurally and functionally in the long-term in response to ceased grazing is crucial as alterations in the rhizosphere can have cascading effects for the ecosystem C storage function (Poirier *et al.* 2018, Wang, B. *et al.* 2024; Wang *et al.* 2025).

Root functional traits are increasingly used to link functional variation in roots to ecosystem processes and to study how roots respond to above-ground disturbances such as changing grazing pressure (Weigelt *et al.* 2021, Matthus *et al.* 2025). In recent years, a two-dimensional root economics space has been conceptualised along a resource conservation trade-off and a collaboration trade-off across a broad range of plant species (Bergmann *et al.* 2020). This concept has been widely applied to study root responses to global change factors (Matthus *et al.* 2025). Recent advances in root functional ecology have emphasised to extent functional traits from the species-level to the community-level to better understand interactions with ecosystem processes, including soil C storage (Wang *et al.* 2023, Barry *et al.* 2025). This is particularly relevant in northern ecosystems, where roots dominate plant biomass allocation and which are rapidly changing on the whole community-level in response to changing grazing pressure and a warming climate (Bråthen *et al.* 2017, Myers-Smith and Hik 2018).

This study focuses on sub-arctic grassland, heathland and successional transitions from grassland into heathland or birch woodland that represent major vegetation types across northern ecosystems. Using contrasts between grazed land and adjacent long-term fenced exclosures in Iceland, we assess how root system characteristics at the vegetation-community level respond to long-term changes in herbivory pressure and how these responses relate to soil C storage. Specifically, we address three research questions:

(i) How are roots distributed in contrasting sub-arctic ecosystems, and how does their distribution respond to grazing cessation in the long-term?
(ii) How do fine-root morphological traits respond to grazing cessation at the community-level?
(iii) How are root traits linked to soil C concentration in grazed and ungrazed land?

By analysing community-level root trait data between grazed and long-term ungrazed land, this research advances our understanding of how grazing management shapes root systems and their role in C dynamics in sub-arctic ecosystems. This knowledge is vital not only for predicting ecosystem responses to changing land use but also for informing strategies that harness grazing systems as effective tools for sustaining soil C and ecosystem resilience.

6.2 Materials and Methods

6.2.1 Sampling Sites

Responses of roots to grazing cessation were studied, using 34 fenced exclosures across Iceland. The exclosures were located within long-term grazed land (centuries) and hence constituted a fence contrast of adjacent grazed and ungrazed land with other environmental factors as equal as possible in a natural system. At each site, three sub-plots were defined for root sampling in the exclosure and mirrored in the same topography in the grazed part (Supplemental Figure 8-16). As the aim of the study was to analyse roots systems, developed under grazing and without grazing, only long-term exclosures (> 20 years) were used to ensure that the measured effects were not recovery effects of previous grazing. Each of the 34 sampling sites was classified according to dominant above-ground vegetation types either as 'grassland', when both the grazed and ungrazed land was dominated by grasses (104 root profiles from 18 sites), 'heathland', when both the grazed and ungrazed land were dominated by heath or shrubs (45 root profiles from 8 sites), 'heath succession', when the grazed part was dominated by grasses and the ungrazed part by heath or shrubs that developed after grazing cessation (40 root profiles from 7 sites), or 'birch succession', when the grazed part was dominated by grasses and the ungrazed part by birch woodland, that developed after grazing cessation (12 root profiles from 2 sites; Appendix 5: Supplemental Table 8-10). At one site, vegetation was inconsistent between sub-plots, and one sub-plot was classified as grassland while the two others were classified as heath succession. All sites were in the Icelandic lowlands below 200 m a.s.l. and had a sub-arctic climate with mean annual temperature ranging between 2 - 4.5 ℃ (summer 7.4 - 10.3 ℃) and mean annual precipitation ranging between 470 - 1234 mm (summer 95 - 274 mm) at the nearest meteorological station of each site (< 30 km).

6.2.2 Root Sample Collection

The sampling site selection and sampling design were described in more detail in Chapter 5. Briefly, land use history was confirmed by landowners, including the year when grazing was ceased in the exclosures. One soil profile was excavated per sub-plot to a soil depth of 60 cm in August and September 2022 and 2023 (three soil profiles had a shallower soil depth than 60 cm until bedrock started). All soil profiles were in freely drained mineral soils. Above each soil profile, all above-ground biomass was collected, including standing living

and dead plant material and litter on the soil surface using a 10 cm×10 cm metal frame. Then, root samples were collected from each soil profile in four predetermined depth intervals. Complete soil samples were collected with a defined soil volume of 5 cm×5 cm surface area and the respective soil depth: 0-10 cm, 10-20 cm, 20-40 cm, 40-60 cm. After field sampling, root samples were stored in plastic bags at 4 °C. Above-ground biomass samples were air-dried, followed by and dry biomass determination to the nearest 0.01 g. In the same soil profiles, soil samples were collected for soil carbon and nitrogen analysis, which was described in more detail and analysed in Chapter 5. For this study, we used the soil organic carbon (SOC) concentration data of the soil profiles, summarised for the same soil depth intervals as the root samples.

6.2.3 Root Processing

No later than 14 days after sampling (typically within 7 days), root samples were washed from bulk soil. First, root samples were submerged for several hours in soap water to loosen soil particles. Then, all soil was washed off from the roots in multiple washing cycles, using stacked soil sieves with mesh sizes of 2 mm and 0.5 mm. The cleaned root samples were then stored in 30 % ethanol solution until further processing. Wet biomass of the fresh root samples was determined to the nearest 0.01 g after carefully drying all excess liquid from the roots. For the analysis of morphological root traits, the fresh roots samples were scanned using an Epson Expression 10000XL or Epson Expression 11000XL flatbed scanner. Each sample was submerged in water in a clear acrylic glass tray with 2 cm height and carefully spread to minimise root overlap, using plastic tweezers. For most of the 0-10 cm depth root samples, a subsample was used for scanning, due to the large sample sizes. The subsample was generated by taking a random portion of approximately 25 % of the total wet biomass from the whole sample. The wet biomass of the subsample was determined and the proportion of the subsample to the whole sample calculated. After scanning, the fresh root samples were oven-dried at 40 °C for 48 hours, until no further weight loss was detected. Dry root biomass was then determined to the nearest 0.01 g, separately for roots < 2 mm and roots > 2 mm diameter.

6.2.4 Root Trait Analysis

The scanned root images were analysed using RhizoVision Explorer version 2.0.3 (Seethepalli *et al.* 2021) with analysis mode set to broken roots, conversion of pixels into physical units and filtering of non-root (debris) objects up to 0.02 mm size. Root pruning was set to 10. Due to variable root sample sizes and variable quantity of debris left in the samples, image thresholding levels between 120-170 were applied to improve recognition of roots against non-root objects. In the feature extraction, five root diameter ranges were defined as 0-0.2, 0.2-0.5, 0.5-2, 2-5 and >5 mm. Root diameter classes < 2 mm were defined as fine roots and root diameter classes > 2 mm were defined as coarse roots. From RhizoVision Explorer, root length (mm), root volume (mm^3) and root surface area (mm^2) per diameter class and mean root diameter (mm) were extracted. For the 0-10 cm subsamples, root length, surface area and volume per diameter class were extrapolated from the subsample to the whole sample by dividing the trait value by the proportion of the subsample.

Table 6-1: Root functional traits used in the study. Calculation of the traits is based on fine root properties, following Freschet et al. (2021a). The functional expression of each trait (last column) is based on the cited literature.

Root trait	Explanation	Unit	Calculation†	Relatively higher values indicate:
RLD	Root length density	$m\,cm^{-3}$	Fine root length / soil volume	Greater ability to compete for resources[c], greater structural stability of soil[b], larger microbial activity[d]
RD	Mean fine root diameter	mm	-	More collaboration with arbuscular mycorrhizal fungi[a], greater root life span[b]
SRL	Specific root length	$cm\ g^{-1}$	Fine root length / dry fine root mass	Faster growth rate, more fibrous root system[c], more self-reliant roots[a]
SRA	Specific root area	$m^2\ g^{-1}$	Fine root surface area / dry fine root mass	Greater resource acquisition efficiency[b]
RTD	Root tissue density	$g\ cm^{-3}$	Dry fine root mass / fine root volume	More conservative root growth, greater root life span[b]

†Fine root = roots in diameter classes < 2 mm
[a]Weigelt *et al.* (2021), [b]Freschet *et al*. (2021b), [c]Poirier *et al.* (2018), [d]Lange *et al.* (2015)

With the data from the root image analysis, root biomass and soil volume, five functional root traits were calculated, summarised in Table 6-1—all root traits were calculated for fine roots only, following recommendations in Freschet *et al.* (2021a). Root traits were calculated for each of the four depth intervals separately and summarised for the whole soil column 0-60 by weighting the respective trait by the proportional dry root biomass of the soil layer ($biomass_{soil\ layer}$ / $biomass_{0\text{-}60\ cm}$). Additionally, root mass fraction was calculated as total root biomass / (total root biomass + above-ground biomass). For the root traits in Table 6-1, we did not find significant differences between the 10-20, 20-40 and 40-60 cm soil layers and pooled these layers together to a mean trait value for the deeper soil of 10-60 cm.

6.2.5 Data Analysis

Linear mixed effect models (LMM) were used to test how grazing cessation affected root distribution, fine and coarse root biomass and functional root traits in different vegetation types. Within the model structure, 'sub-plot' nested in 'sampling site' were specified as random effects for all models and 'Scanner' additionally for layer-wise models of root functional traits. As fixed effects, 'grazing cessation', 'vegetation type' and if applicable 'soil depth' were specified. Significance of differences between predictors was tested with least-squares means post-hoc tests (for significance of model predictors, see Appendix 5: Supplemental Table 8-11). Relationships between fine root biomass, root functional traits and SOC concentration were tested with Pearson correlation tests. If necessary, factors were

log-transformed to meet normality. Linear and non-linear regression was further used to analyse bivariate relationships between root functional traits, fine root biomass and SOC concentration. To visualise trade-offs in rooting strategies and to explore the multivariate nature of the root functional traits a principal component analysis (PCA) was used, including functional traits listed in Table 1.

All data processing and statistical analyses were performed using R statistical software, version 4.3.3 (R Core Team 2024) with the additional packages , lme4 (Bates *et al.* 2015), lmerTest (Kuznetsova *et al.* 2017), emmeans (Lenth 2023), multicomp (Hothorn *et al.* 2008) and vegan (Oksanen *et al.* 2025).

6.3 Results

6.3.1 Root Biomass Distribution in Grazed and Ungrazed Vegetation

Across all sites, the cessation of grazing was associated with 16.5% and 21.1% lower total and fine root biomass, respectively ($p < 0.05$). In grazed plots, total and fine root biomass amounted 18.8 ± 1.2 Mg ha^{-1} and 16.1 ± 1.0 Mg ha^{-1}, respectively, while in exclosures it amounted 15.7 ± 1.0 Mg ha^{-1} and 12.7 ± 0.8 Mg ha^{-1}, respectively (Table 6-2). In all four vegetation types, total root biomass was lower in the exclosures, although the difference was only significant in grassland (-27%, $p < 0.001$, Table 6-2). Total root biomass was larger in heathland than in grassland, but fine root biomass was larger in grazed grassland than in heathland (Table 6-2).

Overall, 72% of all root biomass was found in the top 10 cm of soil (Table 6-2). Across all sites and in all vegetation types except birch succession, grazing cessation was associated with a lower proportion of root biomass in the top 10 cm ($p < 0.05$). In birch succession, no differences were found between grazed and ungrazed land ($p > 0.05$). On average, fine root biomass with root diameter < 2 mm represented 85 % of the total root biomass. The fine root proportion was larger in grazed plots than in paired exclosures in all sites combined and all vegetation types, except heathland ($p < 0.05$; Table 6-2). In heathland, the fine root proportion was lower in grazed relative to ungrazed plots ($p = 0.007$).

The cessation of grazing had the largest impact on fine and course root biomass in the top 10 cm of soil, where the majority roots was found. With cessation of grazing, fine root biomass in 0-10 cm was 45% lower in grassland (11.4 vs. 6.3 Mg ha^{-1}; $p < 0.001$), 40% lower in birch succession (13.4 vs. 8.0 Mg ha^{-1}; $p = 0.087$), 30% lower in heath succession (13.5 vs. 9.5 Mg ha^{-1}; $p = 0.049$) but without differences in heathland, averaging at 9.5 Mg ha^{-1} ($p = 0.92$; Figure 6-1a). Coarse root biomass (root diameter > 2mm) in the top 10 cm was virtually absent in grazed and ungrazed grassland (on average 0.09 Mg ha^{-1}, $p = 0.13$) and grazed plots of birch and heath succession (Figure 6-1b). With cessation of grazing, coarse root biomass was larger in birch (0.3 vs. 2.0 Mg ha^{-1}) and heath succession (0.3 vs. 0.7 Mg ha^{-1}; $p < 0.05$). In heathland, coarse root biomass was overall higher than in other vegetation types and marginally higher in grazed than ungrazed plots (3.2 vs. 1.8 Mg ha^{-1}; $p = 0.087$). In the deeper soil layers (10-20, 20-40,40-60 cm), we found only weak and occasional differences in fine or coarse root biomass between grazed and ungrazed plots (Figure 6-1c-h). In general, fine root biomass decreased with every depth layer ($p < 0.001$), with < 4 % of

total fine root biomass found in the 40-60 cm soil layer. Notably, fine root biomass was slightly larger with cessation of grazing in 20-40 and 40-60 cm soil of the grassland sites ($p < 0.05$; Figure 6-1c,e). Coarse root biomass was overall low below 10 cm and did not differ between soil layers ($p > 0.05$). In heath succession, larger coarse root biomass was found in exclosures in the 10-20 cm soil layer (Figure 6-1d). In the birch succession, we found noticeably high coarse root biomass in the deeper soil layers (> 20 cm), compared to other vegetation types due to deep birch roots, but the total amount was still small (< 0.5 Mg ha^{-1}; Figure 6-1f,h).

Table 6-2: Root distribution of the whole root profile (0-60 cm). Total and fine root biomass, proportion of fine roots and proportion of roots in 0-10 cm soil for grazed land (G) and grazer exclosures (E) of all sites combined and the four vegetation types separately. The number of soil profiles per category is indicated by n. Different letters indicate significant differences with cessation of grazing ($p < 0.05$), retrieved from least squares mean post-hoc tests following linear mixed effect models.

Vegetation type		n	Total root biomass (Mg ha^{-1})	Fine root biomass (Mg ha^{-1})	%fine roots of total roots	% of total roots in 0-10 cm
Grassland	G	52	**15.7 ± 1.0^{a}**	**15.1 ± 0.9^{a}**	**96.2 ± 1.5^{a}**	**75.6 ± 1.6^{a}**
	E	52	**11.4 ± 0.7^{b}**	**10.3 ± 0.6^{b}**	**91.4 ± 1.5^{b}**	**60.2 ± 1.6^{b}**
Heath succession	G	20	19.4 ± 2.2^{a}	17.8 ± 2.0^{a}	92.1 ± 2.8^{a}	**74.9 ± 2.8^{a}**
	E	20	17.5 ± 2.0^{a}	15.0 ± 1.7^{a}	86.5 ± 2.8^{a}	**67.2 ± 2.9^{b}**
Birch succession	G	6	19.4 ± 3.7^{a}	17.6 ± 3.3^{a}	**91.1 ± 4.6^{a}**	73.1 ± 4.8^{a}
	E	6	16.3 ± 3.1^{a}	11.6 ± 2.2^{a}	**73.2 ± 4.6^{b}**	70.5 ± 4.8^{a}
Heathland	G	21	20.9 ± 2.1^{a}	14.1 ± 1.4^{a}	**69.9 ± 2.5^{b}**	**75.9 ± 2.8^{a}**
	E	24	18.6 ± 1.7^{a}	14.3 ± 1.3^{a}	**78.5 ± 2.3^{a}**	**69.9 ± 2.9^{b}**
All	G	99	**18.8 ± 1.2^{a}**	**16.1 ± 1.0^{a}**	**87.3 ± 1.5^{a}**	**74.9 ± 1.6^{a}**
	E	102	**15.7 ± 1.0^{b}**	**12.7 ± 0.8^{b}**	**82.4 ± 1.5^{b}**	**67.0 ± 1.6^{b}**

Different letters between G (Grazed) and E (Exclosure) mark significant ($p < 0.05$) differences in each vegetation type, derived from least-squares mean post-hoc tests

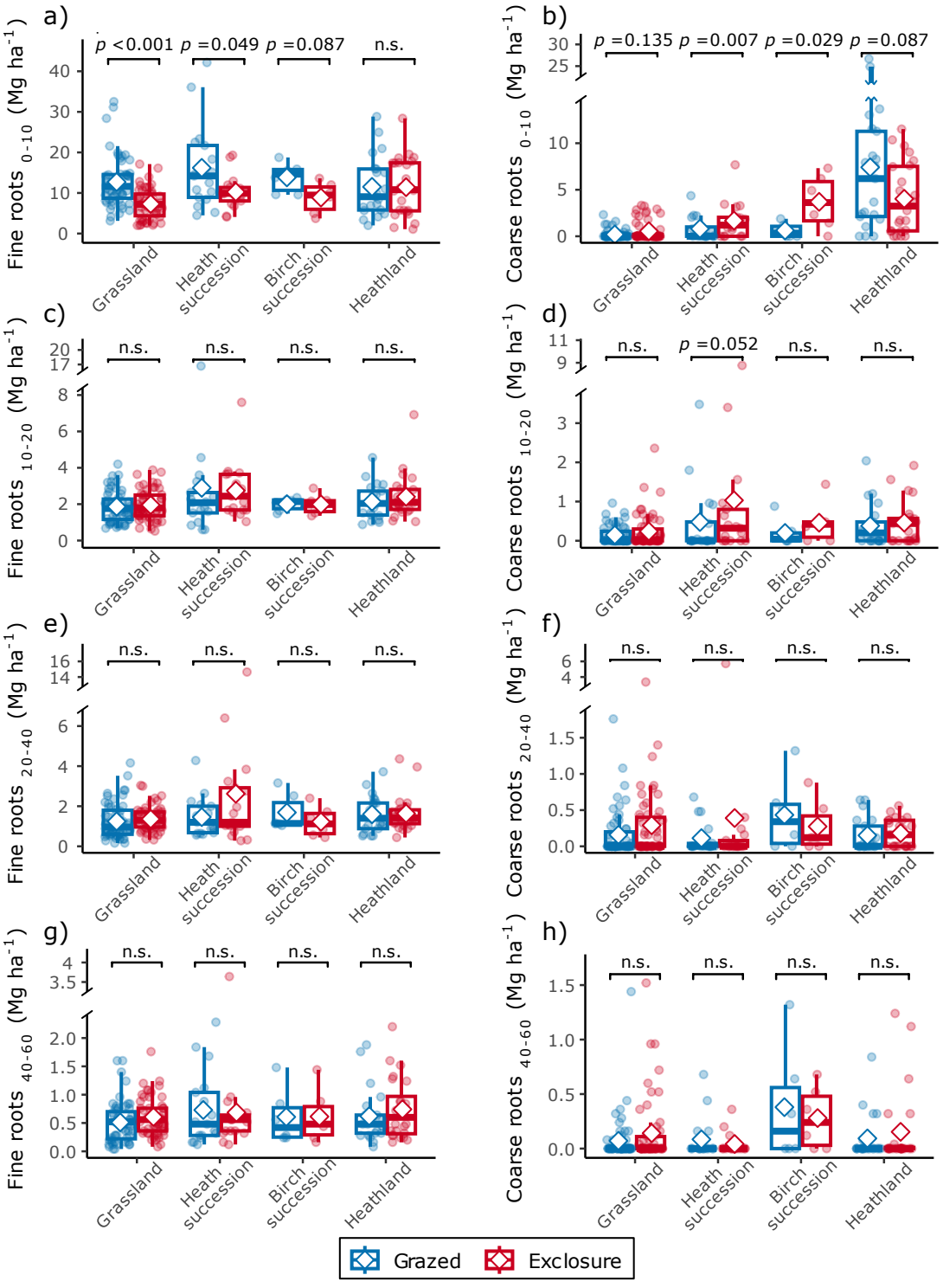

Figure 6-1: Root biomass through the soil profile. Distribution of fine root biomass (a,c,e,g) and coarse root biomass (b,d,f,h) in 0-10, 10-20, 20-40 and 40-60 cm soil depth in grazed and ungrazed land of four vegetation types. Significant effects of grazing cessation are indicated by p-values retrieved from least-squares post hoc tests following linear mixed effect models. The central bars in the box-plots mark median values, while the open diamonds mark mean values. Note the broken y-axis in b,c,d,e, f and g and the different scale of the y-axis in each graph.

6.3.2 Above-ground versus Below-ground Biomass

Living and dead above-ground plant biomass across all sites was higher in exclosures (21.5 Mg ha^{-1}) than in grazed plots (14.9 Mg ha^{-1}), albeit without quantifying offtake from grazing in grazed plots ($p < 0.001$; Table 6-3). Within the vegetation types, above-ground vegetation was higher in exclosures of grassland ($p < 0.001$), heath succession ($p < 0.001$) and heathland ($p = 0.05$). In birch succession differences were not significant, although tree biomass was not accounted for in the birch woodland. Total vegetation biomass, including living and dead above-ground biomass, above-ground litter and root biomass, ranged between 12.2 and 75.0 Mg ha^{-1} across our sampling sites. In contrast to above-ground vegetation alone, total vegetation biomass, averaged through all sites, did not differ between grazed (32.6 Mg ha^{-1}) and ungrazed land (35.7 Mg ha^{-1}), even though we did not account for above-ground offtake in grazed plots ($p = 0.114$; Table 6-3). Only in the heath succession with heathland in the exclosures and grassland in the grazed land, cessation of grazing was associated with larger total vegetation biomass ($p = 0.026$; Table 6-3). Overall, heathland vegetation (i.e. grazed and ungrazed heathland and ungrazed heathland succession) had consistently higher total vegetation biomass than grassland vegetation (i.e. grazed and ungrazed grassland and birch succession and grazed heath succession; $t = -5.6$, $p < 0.001$).

Table 6-3: Total biomass in vegetation types. Above-ground biomass, total vegetation biomass (above-ground + total root biomass) and root mass fraction for grazed land (G) and grazer exclosures (E) of all sites combined and the four vegetation types separately. The sample size per category is shown by n. Different letters indicate significant differences with cessation of grazing ($p < 0.05$), retrieved from least squares mean post-hoc tests following linear mixed effect models.

Vegetation type		n	Above-ground plant biomass (Mg ha^{-1}) †	Total vegetation biomass (Mg ha^{-1})	Root mass fraction (%)
Grassland	G	54	**12.8 ± 0.8^{a}**	29.1 ± 1.3^{a}	**54.5 ± 1.9^{a}**
	E	55	**20.0 ± 1.0^{b}**	31.5 ± 1.3^{a}	**37.0 ± 1.9^{b}**
Heath succession	G	17	**14.8 ± 1.6^{a}**	**35.1 ± 2.5^{b}**	**55.1 ± 3.4^{a}**
	E	17	**27.1 ± 2.2^{b}**	**43.4 ± 2.8^{a}**	**36.9 ± 3.4^{a}**
Birch succession	G	6	12.2 ± 2.5^{a}	30.4 ± 4.0^{a}	**58.9 ± 5.7^{a}**
	E	6	14.7 ± 2.7^{a}	27.3 ± 3.7^{a}	**44.9 ± 5.7^{a}**
Heathland	G	21	**20.6 ± 1.7^{a}**	36.2 ± 2.3^{a}	42.0 ± 3.1^{a}
	E	24	**25.4 ± 1.8^{b}**	32.6 ± 2.3^{a}	37.8 ± 2.9^{a}
All	G	98	**14.9 ± 0.9^{a}**	32.6 ± 1.4^{a}	**52.6 ± 1.9^{a}**
	E	102	**21.5 ± 1.1^{b}**	35.7 ± 1.4^{a}	**39.2 ± 1.9^{b}**

†Offtake in grazed plots not accounted for, tree biomass in birch succession not included
Different letters between G (Grazed) and E (Exclosure) indicate significant ($p < 0.05$) differences in each vegetation type, derived from least-squares mean post-hoc tests

In vegetation dominated by grassland in the grazed part (grassland, succession birch, succession heath), the cessation of grazing was associated with a lower root mass fraction, shifting the dominant plant biomass allocation above-ground ($p < 0.05$). When grazed, root mass fraction of these sites was on average > 50 %, i.e. more biomass in roots than above-

ground. In all ungrazed plots as well as the grazed heathland root mass fraction was < 50 % (Table 6-3).

6.3.3 Community-level Root Functional Traits

General Differences between Topsoil and Deeper Soil

As an overall pattern, the magnitudes of all community-level root functional traits (all based on fine roots) were significantly different in the topsoil (0-10 cm) than in deeper soil (10-60 cm; $p < 0.001$, Table 6-4). Root length density (RLD), as a metric for root-soil interaction, mirrored overall fine root biomass distribution and was of almost one magnitude larger in the topsoil (mean 1.15 m cm^{-3}) than the average of the deeper soil between 10-60 cm (mean 0.14 m cm^{-3}). Root diameter (RD), as a proxy for arbuscular mycorrhizal colonisation and root longevity, was overall larger in the top 10 cm (0.21 mm) compared to deeper roots (0.19 mm). Specific root length (SRL) and specific root area (SRA), as metrics for resource acquisition and rhizosphere activity, were 40% and 30.5% larger in 10-60 cm soil (mean SRL 179 cm g^{-1}; mean SRA 0.11 m^2 g^{-1}) compared to 0-10 cm soil (mean SRL 128 cm g^{-1}; mean SRA 0.08 m^2 g^{-1}), respectively. Root tissue density (RTD), as metric for resource conservation, was 13.3% larger in 0-10 cm roots (0.135 g cm^{-3}) than 10-60 cm roots (0.12 g cm^{-3}).

Table 6-4: Differences in functional root traits between roots in 0-10 cm depth and roots in 10-60 cm depth. F-statistics are derived from linear mixed effect models with 'Depth' as fixed effect. Percentage differences refer to the change in trait values in 10-60 cm in relation to 0-10, based on values derived from least-squares mean post-hoc tests together with t-ratio an p-value. Root trait abbreviations are explained in Table 6-1.

Root trait	**Depth**				**Comparison 0-10 vs. 10-60**		
	0-10 cm	**10-60 cm**	***F***	***p***	**Difference**	***t***	***p***
RLD (m cm^{-3})	1.15	0.14	1859.4	**<0.001**	-88.0%	43.1	**<0.001**
RD (mm)	0.21	0.19	53.8	**<0.001**	-7.6%	7.3	**<0.001**
SRL (cm g^{-1})	128	179	194.2	**<0.001**	+40.0%	-13.9	**<0.001**
SRA (m^2 g^{-1})	0.08	0.11	139.5	**<0.001**	+30.5%	-11.8	**<0.001**
RTD (g cm^{-3})	0.135	0.117	30.9	**<0.001**	-13.3%	5.6	**<0.001**

The Response of Community-level Root Functional Traits to Cessation of Grazing

Like overall fine root biomass, the cessation of grazing influenced root length density (RLD) in the top 10 cm of soil, but not in deeper soil (Figure 6-2). In grassland and in birch succession, RLD was 42% and 62% lower in exclosures, respectively ($p < 0.01$). In heathland and heath succession no differences were found with the cessation of grazing ($p > 0.05$, Figure 6-2a). Below 10 cm soil depth, cessation of grazing did not affect RLD in any of the vegetation types (Figure 6-2b).

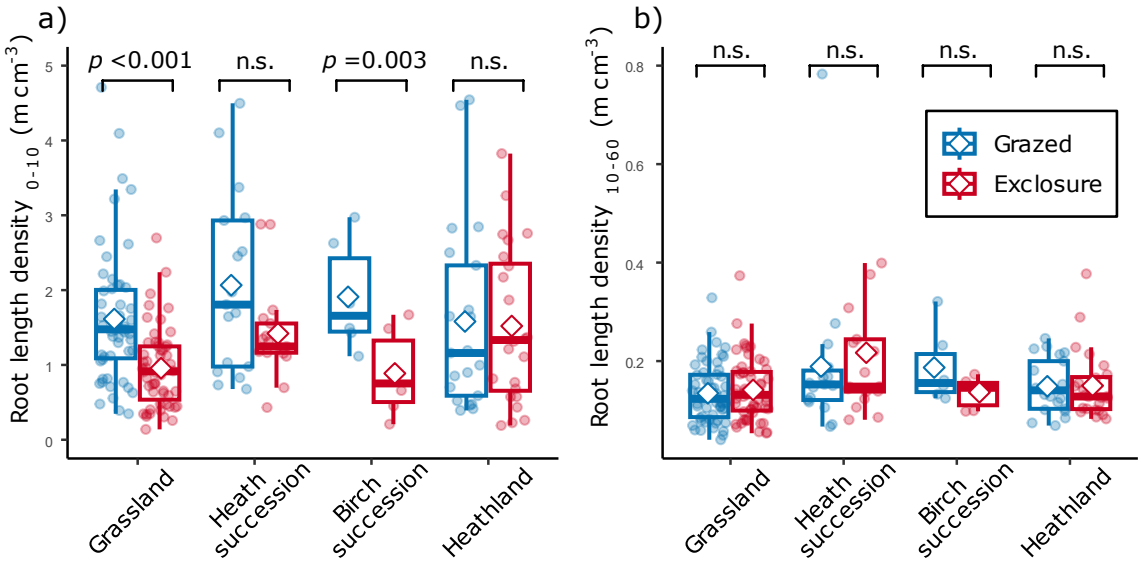

Figure 6-2: Root length density in grazed and ungrazed land. Root length density in 0-10 cm (a) and 10-60 cm (b) in grazed land and exclosures in four vegetation types. Significant effects of grazing cessation are indicated by p-values retrieved from least-squares post-hoc tests following linear mixed effect models. The central bars of the box-plots mark median values, while the open diamonds mark mean values. Note the different scale of the y-axis in a and b.

With the cessation of grazing root diameter was smaller in the top 10 cm relative to grazed plots (p = 0.009), although the difference was only significant for grassland (p < 0.001; Figure 6-3a). Below 10 cm, no significant differences in root diameter were found between grazed and ungrazed land (Figure 6-3b).

The cessation of grazing had no effect on specific root length (SRL) in 0-10 cm and SRL was similar across vegetation types; for the roots below 10 cm, SRL tended to be lower in exclosures than in grazed plots, although the difference was only significant in grassland (p = 0.015, Figure 6-3c,d). Specific root area (SRA) responded overall like SRL to the cessation of grazing in the different vegetation types (Figure 6-3e,f). In 0-10 cm, SRA was not different between exclosures and grazed land. In 10-60 cm, SRA had the strongest response of all traits to the cessation of grazing, with 8%, 12% and 11% lower SRA in exclosures compared to grazed land in grassland, heathland and heath succession, respectively (p < 0.05).

Root tissue density (RTD) in 0-10 cm soil was 10% larger in grassland exclosures compared to grazed grassland (p = 0.006), but did not differ with grazing cessation in other vegetation types (Figure 6-3g). For roots in 10-60 cm soil depth, RTD tended to be larger in exclosures than in grazed land across all vegetation types, with a significant difference only in heath succession (p = 0.035; Figure 6-3h).

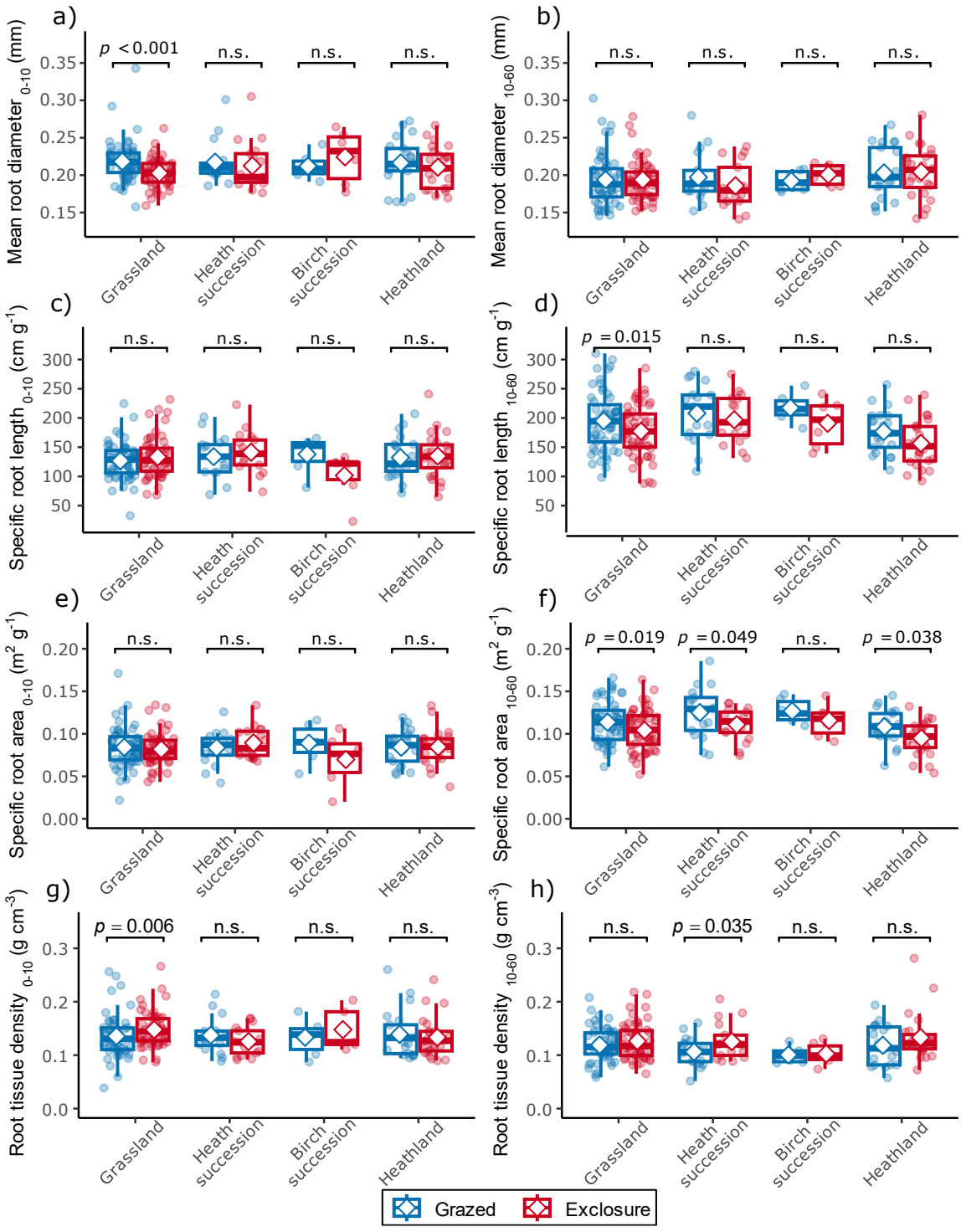

Figure 6-3: Root functional traits in grazed and ungrazed land. Mean root diameter (a, b), specific root length (c, d), specific root area (e, f) and root tissue density (g, h) in 0-10 cm and 10-60 cm in grazed land and exclosures in four vegetation types. Significant effects of grazing cessation are indicated by p-values retrieved from least-squares post-hoc tests following linear mixed effect models. The central bars of the box-plots mark median values, while the open diamonds mark mean values.

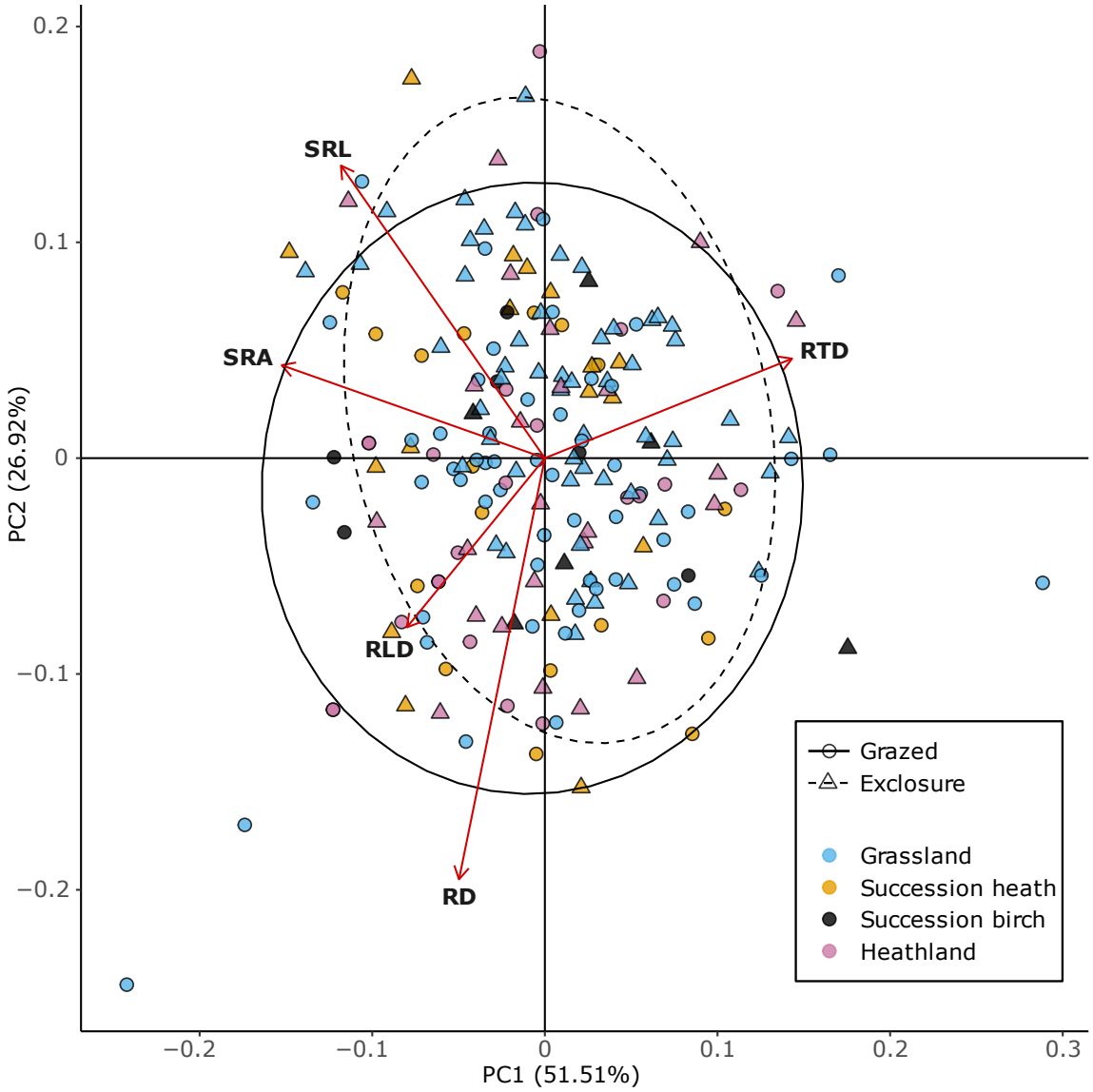

Figure 6-4: PCA biplot of root functional traits. Biplot of principal component analysis (PCA) for mean root functional trait values of 0-60 cm root depth along the first two principal component axes (PC1 and PC2). Each point represents one root profile of 0-60 cm and each arrow a root functional trait. The length of the arrows of functional traits corresponds to the effect size of the respective trait. Arrows pointing into the same direction indicate positive correlation and arrows pointing in opposing directions indicate negative correlation. For an explanation of the abbreviations of the traits, see Table 6-1.

6.3.4 PCA of Root Functional Traits

We used a PCA to explore how our community-level root functional traits relate to each other in a multivariate space to identify trade-off axes of rooting strategy. We included all root functional traits listed in Table 6-4 in the PCA as mean trait values per 0-60 cm root profile (Figure 6-4). Despite the community-level root trait differences between 0-10 cm and 10-60 cm revealed in Table 6-4, the assembly in the multivariate PCA space was similar in

0-10 and 10-60 cm, thus we only show the PCA for the whole root system (Appendix 5: Supplemental Figure 8-22).

The PCA biplot shows that the first two principal component axes, PC1 and PC2, explain 51.5% and 26.9% of the total variance, respectively, together 78.4%. PC1 mainly manifests as a trade-off axis between root tissue density (RTD) on the one side and specific root area (SRA) and root length density (RLD) on the other side, whereas PC2 displays a trade-off axis between specific root length (SRL) and mean root diameter (RD; Figure 6-4). Root profiles of grazed and ungrazed land were not strongly separated along any of the two PC axes, although grazed root systems tended to be more associated with higher SRA, RLD and RD (see circles in Figure 6-4). The four vegetation types were not separated along PC1 or PC2, meaning trade-offs in community-level rooting strategy were not associated with differences in vegetation types. Across vegetation types, we found the strongest trade-off axis along PC1 between SRA and RTD, following a negative power function without differences between grazed land and exclosures (R^2 = 0.68, p < 0.001, Appendix 5: Supplemental Figure 8-23a). The trade-off axis along PC2 between SRL and RD followed a linear equation, but was substantially weaker (R^2 = 0.12, p < 0.001, Appendix 5: Supplemental Figure 8-23b). Both trade-off axes were not influenced by the cessation of grazing.

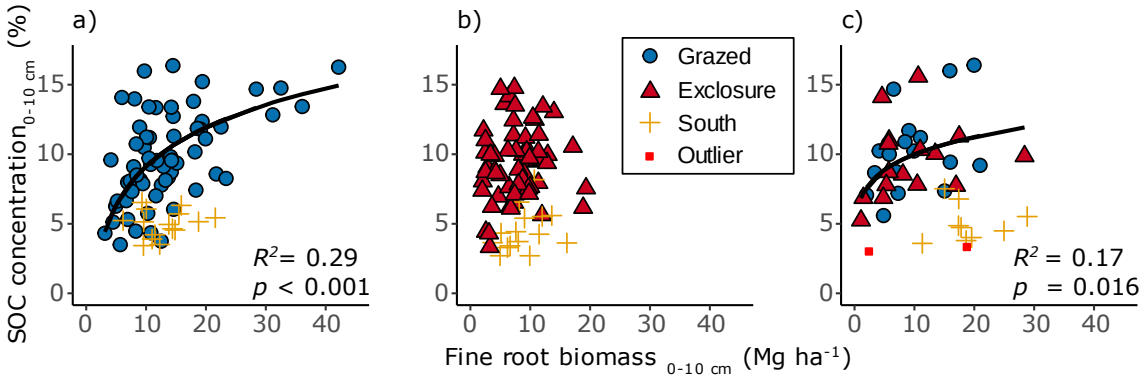

Figure 6-5: Association between fine root biomass and soil carbon (SOC) concentration in the top 0-10 cm of soil. In grazed grassland sites (a), SOC concentration was positively associated with fine root biomass, following a power regression, except for the sites in southern Iceland. In ungrazed grassland, including birch and heath succession (b), no relation was found. In grazed and ungrazed heathland (c), SOC concentration and fine root biomass had a positive relation with a power regression, when sites in southern Iceland and two outliers were excluded.

6.3.5 How are Roots and SOC related in Grazed and Ungrazed Land?

In grazed grassland (i.e. grassland, succession birch and succession heath), except for the sites in southern Iceland, fine root biomass in 0-10 cm was positively related to SOC concentration in 0-10 cm, following a power regression with a model fit of R^2 = 0.29 (p < 0.001; Figure 6-5a). In southern Iceland sites, fine root biomass and SOC concentration were not related and they were excluded from the regression analysis. In the exclosures of

grassland, heath succession and birch succession, fine root biomass was not related to SOC concentration (Figure 6-5b). In heathland, fine root biomass was positively related to SOC in 0-10 cm soil without differences between grazed land and exclosures, following a power regression with model fit of $R^2 = 0.17$ ($p = 0.016$; Figure 6-5c).

Again, heathland in southern Iceland were excluded from the analysis, as there was no relation found. In 0-10 cm, also root diameter had a weak positive ($r = 0.18$) and root tissue density a weak negative correlation ($r = -0.16$) with SOC concentration ($p < 0.05$, Appendix 5: Supplemental Table 8-12). Like in 0-10 cm, SOC concentration was positively related to fine root biomass in 10-60 cm soil depth without effects of grazing cessation, when soil profiles from southern Iceland were excluded, both in grassland ($R^2 = 0.21$, $p < 0.001$, Appendix 5: Supplemental Figure 8-24a) and in heathland ($R^2 = 0.22$, $p < 0.001$, Appendix 5: Supplemental Figure 8-24b). In contrast, above-ground biomass was not related to topsoil SOC concentration (Appendix 5: Supplemental Figure 8-25).

6.4 Discussion

Our study revealed that the cessation of grazing over multiple decades influenced vegetation structure below-ground in sub-arctic grassland and heathland that did not mirror above-ground responses (Ma *et al.* 2024). To our knowledge, this is the first study of whole-community root systems from natural grassland and heathland in Iceland. We showed that in grazed vegetation, the majority of biomass allocation was below-ground in fine roots (< 2 mm diameter), concentrated within the topsoil (0-10 cm) and positively associated with SOC concentration, which is similar to grasslands globally (McNaughton *et al.* 1998, Vaieretti *et al.* 2021, Liu, Yuzhen *et al.* 2023). Across sites with grassland on the grazed land, the ungrazed exclosures were consistently associated with lower fine root biomass, independent of whether the vegetation type remained grassland or shifted into heathland or birch woodland. Instead, plant biomass dominance shifted from below-ground to above-ground, accompanied by an increased proportion of coarse roots (> 2 mm diameter) and a collapsed association between fine roots and SOC concentration.

Although the cessation of grazing was associated with overall lower root biomass and root length density, morphological root functional traits were strikingly similar between grazed and long-term ungrazed land and between vegetation types. This indicates that resource acquisition and foraging strategies of fine roots are similar at the community-level between the vegetation types included in this study, regardless of the grazing pressure, as previously suggested by Wang *et al.* (2023). Community-level root functional traits differed mostly between roots in the topsoil and those located deeper than 10 cm, indicating that trait variation and rooting strategy are more driven by soil properties and climatic constraints than by vegetation type or grazing pressure (Bardgett *et al.* 2014, Cai *et al.* 2024).

6.4.1 Cessation of Grazing Alters the Distribution of Roots

Across our sampling sites, roots had predominantly a shallow distribution with > 90 % of all root biomass in the top 20 cm of soil and < 4 % of roots found below 40 cm, consistent with general distribution patterns of grassland globally (Jackson *et al.* 1996). Yet, the sharp decline of roots with increasing soil depth was more akin to tundra ecosystems than to temperate grassland (Radville *et al.* 2016, Wang, *et al.* 2016a). This likely reflects a general

adaptation to cold climate with short growing seasons and long periods of frozen soil and to a high coarse particle fraction in nutrient-poor subsoil (Chapter 5; Li *et al.* 2011; Iversen *et al.* 2015).

In grassland, > 95 % of root biomass were fine roots compared to < 80 % in heathland and fine root biomass was substantially higher in the topsoil of all grazed grassland compared to heathland or all ungrazed land (Figure 6-1). Graminoid root growth is typically continuous over the growing season and previous studies showed that grazing can stimulate fine root production in graminoid vegetation, which could explain the large fine root biomass in our grazed grassland soils in the late growing season (Garcia-Pausas *et al.* 2011, Wang, *et al.* 2016b, Liu, Yuzhen *et al.* 2023). Coarse roots were considerable only in heathland and ungrazed birch woodland and were largely confined to the topsoil. This distribution likely reflects shrub root-growth phenology which is initiated early in the season while deeper soil layers are still frozen, as suggested by evidence from tundra ecosystems (Radville *et al.* 2016, Wang, *et al.* 2016b). Interestingly, the coarse root biomass in heath succession, emerging after grazing ceased was still substantially lower compared to longer established heathland. This indicates that slow growth of woody heath roots is still lacking behind above-ground heath cover multiple decades after grazing was ceased and heathland started to develop (Rodríguez *et al.* 2007, Gallois *et al.* 2025, Klopsch *et al.* 2026b).

Total root biomass at our sites (mean 17.2 ± 1.1 Mg ha^{-1}) was substantially higher then reported from less productive tundra (mean 8.5 ± 0.9 Mg ha^{-1}; Wang *et al.* 2016a) or temperate grassland and heathland to comparable depths (3-10 Mg ha^{-1}; Fiala *et al.* 2009; Arndal *et al.* 2018; Poeplau *et al.* 2019; Yang *et al.* 2021; Yang and Russo 2024) but in the range of mountain grassland globally (Pucheta *et al.* 2004, Fiala *et al.* 2009, Garcia-Pausas *et al.* 2011, Liu, Yuzhen *et al.* 2023). In cold climates, such as in alpine or arctic ecosystems, plants allocate more resources below-ground, as indicated by generally high root:shoot ratios in arctic and alpine plants (Iversen *et al.* 2015, Qi *et al.* 2019). The root mass fraction applied in our study does not directly reflect root-to-shoot partitioning of vegetation; we did not account for offtake in the grazed plots and our biomass data included besides live green biomass and root biomass also woody biomass, standing litter and descended plant residuals above-ground that accumulated over years. Thus, we interpret our root mass fraction more as relative allocation trend. Following this interpretation, our results showed that whole plant biomass did not change in response to grazing cessation when no vegetation type change occurred but rather shifted from below-ground dominance in grazed plots (root mass fraction > 50 %) to above-ground dominance in ungrazed plots (root mass fraction < 50 %), consistent with previous research (Ylänne *et al.* 2018, Wu *et al.* 2021). This shows that the below-ground perspective is crucial when evaluating vegetation responses to changing grazing practices in northern ecosystems (Oñatibia *et al.* 2017, Ylänne *et al.* 2018, Träger *et al.* 2019).

In grassland, the topsoil of exclosures had markedly fewer fine roots compared to the paired grazed land. Without grazing for multiple decades, ungrazed grassland vegetation became dominated by few tall-growing grass species or the vegetation type shifted into heath or birch woodland. These above-ground changes were likely reflected below-ground with less vigorous growth of fibrous roots (Wang, *et al.* 2016b) and hampered fine root growth of low-statured and annual species (Frank *et al.* 2010, Wu *et al.* 2021). For example, in a large-scale grassland experiment, root production decreased over time in species-poor communities compared to more diverse communities (Ravenek *et al.* 2016, Eisenhauer *et al.* 2017), supporting our findings of lower root production in ungrazed grassland, which had,

on average, a lower small-scale plant diversity than grazed grassland (A.G. Þórhallsdóttir and B. Þorsteinsson, unpublished data). Over time, this may result in reduced inputs of C from plants into the soil (Jackson *et al.* 2017, Sokol, *et al.* 2019a).

6.4.2 Fine Root Biomass interacts with Soil Carbon Concentration

Numerous studies showed that the majority of SOC is derived from roots either via decaying roots or via C transferred from root exudates into mycorrhizal fungi or soil microorganisms (Jackson *et al.* 2017, Sokol, *et al.* 2019a, Chari *et al.* 2024). Indeed, we found that across most sites fine root biomass was positively related to SOC concentration under grazed conditions, both in the topsoil and the subsoil. This suggests that the high fine root biomass maintained under grazing contributes substantial C into soil that accumulates as SOC over time across our sites (Mikola *et al.* 2009, Fossum *et al.* 2022, Chavez *et al.* 2025). In the grassland exclosures, the relationship between fine root biomass and SOC concentration collapsed due to on average 45% lower fine root biomass, suggesting that markedly less root C is entering the SOC pool (Sokol, *et al.* 2019a). This is in line with a lower topsoil C sequestration rate after multiple decades of ceased grazing at our grassland sites (Chapter 5). In heathland, grazing pressure was generally low, thus grazing had less influence on root growth, as reflected by comparable fine root biomass in grazed and ungrazed heathland. Unlike grassland, heathland showed a consistently positive association between fine root biomass and SOC concentration, regardless of grazing. This may be because graminoids typically exhibit faster roots growth and turnover than shrubs, making graminoid roots more sensitive to grazing (Klumpp *et al.* 2009, Wang, *et al.* 2016b, Gallois *et al.* 2025).

Alternatively, in heath-dominated vegetation, much of the SOC accumulates in particulate organic matter derived from root litter, which could explain the positive relationship between roots and SOC concentration in our samples (Beier *et al.* 2009, Kopittke *et al.* 2013, Duddigan *et al.* 2024). We excluded the sites in southern Iceland sites from this analysis because SOC concentration there was largely unrelated to fine root biomass, especially in the topsoil (Figure 6-5). Unlike our other sites, these sites were located in the active volcanic zone of Iceland on prehistoric lavas, thus soils were younger and frequently replenished with fresh mineral material from volcanic eruptions or aeolian redistribution (Gunnarsson *et al.* 2015, Vilmundardóttir *et al.* 2018). Due to the young soil age, less C accumulated yet in these soils compared to the other regions (Chapter 5), despite vigorous root growth. This highlights that SOC accumulates slowly over time from the fraction of root and microbial C that is not rapidly respired back to the atmosphere (Bai and Cotrufo 2022, Bardgett 2025, Zhang *et al.* 2025). Accordingly, maintaining of large fine root biomass at these sites potentially drives continued SOC sequestration (Georgiou *et al.* 2025).

6.4.3 Morphological Fine Root Traits are largely unaffected by the Cessation of Grazing

Our analysis of community-level root functional traits revealed that morphological characteristics (RD, SRL, SRA, RTD) of fine roots were remarkable similar between grazed and ungrazed land and between different vegetation types, likely due to a high functional diversity in natural communities (Wang *et al.* 2023, Cai *et al.* 2024). As it was for root biomass, root functional traits varied mostly between the topsoil (0-10) and roots in deeper soil (10-60 cm). In the topsoil, roots occupied the soil more densely (higher RLD) and had

on average larger root diameter and root tissue density, but lower specific root length/area (Table 6-4), indicating more conservative root growth, longer root life span and higher collaboration with mycorrhizal fungi compared to deeper roots (Freschet, *et al.* 2021b, Matthus *et al.* 2025). This could be related to a high functional diversity in the topsoil at the community-level (Erktan *et al.* 2023, Barry *et al.* 2025). Both very thin short-lived roots for resource acquisition and larger, longer-lived roots collaborating with arbuscular mycorrhizal fungi (AMF) likely co-exist there, as indicated by the distribution of fine root diameter classes (Appendix 5: Supplemental Figure 8-26). The positive correlation between root diameter and topsoil SOC concentration, together with the negative correlation for root tissue density and topsoil SOC concentration, suggests that AMF association linked to thicker roots may enhance formation of SOC, whereas the lower turnover of dense, conservative roots contributes less to SOC formation (Guyonnet *et al.* 2018, Barceló *et al.* 2020, Sweeney *et al.* 2021). In the deeper soil thin, acquisitive roots (high SRL/SRA, low RTD) may prevail, likely serving mostly for exploration and nutrient and water uptake from deeper soil layers.

The community-level trait responding most to the cessation of grazing in our study was root length density (RLD), largely mirroring differences in fine root biomass. Except for long-established heathland, root length density was lower in exclosures compared to grazed land. A high root length density is often associated with fast growing, acquisitive roots with high root exudation, turnover rates and rhizosphere activity (Barry *et al.* 2025). This implies a large allocation of photosynthetic accumulated C below-ground in grazed land to sustain dense root systems with enhanced transfer of organic C from plants into the soil (Wilson *et al.* 2018, Williams *et al.* 2022, Xu *et al.* 2025). Data on CO_2 fluxes at our sites showed that particularly in grassland grazing cessation was associated with lower ecosystem respiration during the growing season, matching the lower root length density found in this study (Klopsch *et al.* 2026b). Grazing-mediated high root density probably also contributes to soil stability through increased binding of soil particles (Gould *et al.* 2016), effectively preventing soil and C losses due to wind of water erosion, which is particularly relevant in Iceland (Gunnarsson *et al.* 2015). In the roots below 10 cm, we also found a clear response in specific root area to the cessation of grazing across vegetation types: roots under grazing had higher SRA, indicating that deep roots of grazed vegetation are thinner, shorter-lived and more acquisitive than deep roots of ungrazed vegetation, possibly related to faster root turnover rates of grazed roots (Liu, Yan *et al.* 2023).

Community-level root functional traits are different from traits measured on individual plants or as community-weighted means which are used in most studies (Matthus *et al.* 2025). Our community-level traits represented average values of a natural community, likely including a high root functional diversity of co-existing roots. In contrast to species-specific traits, trait values in our samples were likely more controlled by environmental conditions rather than by individual plant resource acquisition strategies (Lachaise *et al.* 2022, Anderegg 2023). In natural communities, fine root morphology seems to be more controlled by climate and soil properties, indicated by the weak effects of cessation of grazing on functional traits, despite large effects on root biomass and above-ground vegetation (Bardgett *et al.* 2014, Iversen *et al.* 2015, Wang *et al.* 2023).

Our multivariate trait space revealed two major trade-off axes along our community-level root functional traits, broadly aligning to the major trade-off axes postulated for the root economics space (Bergmann *et al.* 2020). We identified a conservation trade-off along PC1 between communities with more fast growing, absorptive roots with short life-span, represented by high specific root area and low root tissue density and communities with

more slow-growing, conservative roots (high root tissue density, low specific root area, low root length density), aligning to previous studies based on community-level root traits (Wang *et al.* 2023, Cai *et al.* 2024, Yang and Russo 2024). The conservation trade-off is commonly defined between root tissue density and root N content (Weigelt *et al.* 2021). We did not measure root N in our samples. We, however, propose the strong relationship between specific root area and root tissue density in our samples as reasonable conservation gradient for root communities (Appendix 5: Supplemental Figure 8-23a). Notably, the conservation trade-off was both evident in the topsoil and the subsoil and unrelated to overall root density, supporting the generality of the relationship. Along the conservation trade-off, cessation of grazing did not select for a dominant rooting strategy, even with shifting dominant vegetation. This finding suggests that grazing was not a major driver of community-level resource use strategy in our samples (Weigelt *et al.* 2021, Wang *et al.* 2023, Yang and Russo 2024).

We identified a second trade-off axis along PC2 between root diameter (RD) and specific root length (SRL), although this trade-off was weaker than the conservation trade-off (Appendix 5: Supplemental Figure 8-23b). Previous studies associated this trade-off as a collaboration trade-off between roots collaborating with arbuscular mycorrhizal fungi (AMF), linked to relatively higher root diameter vs. self-reliant roots without collaboration, indicated by relatively higher specific root length (McCormack and Iversen 2019, Bergmann *et al.* 2020, Lachaise *et al.* 2022). In the grassland exclosures, we found that the topsoil roots were associated with a smaller community-level root diameter than in grazed grassland. This suggests a lower mycorrhizal cooperation and outsourcing of nutrient acquisition to AMF in ungrazed compared to grazed grassland (Matthus *et al.* 2025), potentially contributing to lower productivity and respiration that we measured at our ungrazed grassland plots (Klopsch *et al.* 2026b). However, as we did not directly measure AMF colonisation in our root samples, we are unable to ascertain whether root diameter serves as a reliable predictor of AMF collaboration at the community level, which has been recently questioned by Yang and Russo (2024). Future studies on community-level functional traits should directly measure AMF colonisation rates in response to grazing or shifts in vegetation to elucidate how such perturbations affect mycorrhizal collaboration in natural communities (Barto and Rillig 2010, Kytöviita and and Olofsson 2021). This is particularly relevant for shifts in vegetation composition leading to changing mycorrhizal associations, such as succession from grassland, primarily associated with AMF, to heathland or woodland, associated with ericoid or ectomycorrhiza (Parker *et al.* 2021, Castaño *et al.* 2023). The roots below 10 cm were generally associated with more self-reliant roots, particularly in grazed land, characterised by higher specific root length, indicating that in deeper soil short-lived and explorative roots dominated (Yang and Russo 2024).

6.5 Conclusion

In this study, we examined how root systems respond in the long-term to the cessation of grazing across a broad range of sub-arctic grassland and heathland in Iceland, providing new insights into below-ground vegetation dynamics in this region. Overall, grassland root systems showed stronger contrasts between grazed and ungrazed land than those in heathland. The lower fine root biomass in ungrazed grassland likely diminished rhizosphere activity and limit further SOC accumulation due to lower root-derived C inputs, highlighting fine roots as a central driver of SOC formation (Sokol, *et al.* 2019a). Despite large

differences in root density, community-level root functional traits were only weakly influenced by the cessation of grazing. This suggests that rooting strategies at the community level were shaped primarily by the sub-arctic climate and soil conditions (Yang and Russo 2024).

In northern ecosystems, plant activity occurs predominantly below-ground, and our findings showed that below-ground responses to changing grazing practices diverge from above-ground patterns, emphasising the importance to incorporate below-ground responses when studying ecosystem responses to the cessation of grazing (Bardgett and Wardle 2010, Iversen *et al.* 2015). Our study was limited to root biomass and morphological traits and we stress to include mycorrhizal associations and functional traits beyond morphology in future research to elucidate mechanisms driving community-level rooting strategies in relation to soil C dynamics.

7 Chapter VII: Conclusions

7.1 Grazing as a Long-term Regulator of Carbon Cycling in Sub-arctic Grassland and Heathland

In this dissertation, I aimed to evaluate how the long-term cessation of grazing affects carbon (C) cycling in sub-arctic grassland and heathland, using a unique network of multi-decadal (20-83 years) grazer exclosures with adjacent paired grazed land distributed across the Icelandic lowlands (below 200 m a.s.l.). By combining ecosystem CO_2 flux measurements, remote-sensed NDVI, soil organic carbon (SOC) stock assessments and root analyses, I jointly addressed in four chapters in this dissertation how grazing animals influence ecosystem C dynamics from direct atmospheric exchange to below-ground C accumulation (Chapter 3 - Chapter 6). The reported findings are in agreement with recent ecological theory emphasising the role of large herbivores in the C cycle (Schmitz *et al.* 2018, Malhi *et al.* 2022, Rizzuto *et al.* 2024). To my knowledge, the data compiled for the four papers in this thesis constitute the largest and most comprehensive assessment of CO_2 fluxes, SOC stocks and root traits in the context of grazing versus cessation of grazing in Icelandic grassland and heathland thus far. As livestock grazing is still the most important agricultural activity in Iceland, the results presented in this thesis have important implications for climate change mitigation within the land use sector in Iceland (Keller *et al.* 2026). Together, the four chapters show that sustained grazing is associated with large ecosystem C turnover between gross primary production and ecosystem respiration (acceleration effect; Ritchie *et al.* 1998; Bardgett 2025), while maintaining growing-season C sinks (negative net ecosystem exchange) and SOC storage, whereas the cessation of grazing weakens these processes in the long-term (deceleration effect). Multi-decadal cessation of grazing was also associated with an enhanced likelihood of successional shifts from grassland into heathland or birch woodland. These successional exclosures were associated with a lower C sink capacity, both in terms of net ecosystem exchange and topsoil SOC stocks. The cessation of grazing had consistently a larger effect on C cycling in grassland than in heathland, underscoring that grasses and grazers are mutual beneficial (McNaughton 1985, Olofsson and Post 2018, Frank and Fridley 2025, Ylänne and Stark 2025).

7.1.1 Grazing maintains Ecosystem Carbon Sink

Across all sites, both grazed and ungrazed grassland and heathland were net C sinks during the peak growing season, showing that treeless Icelandic ecosystems contribute to a net uptake of atmospheric CO_2 despite low above-ground biomass (Chapter 3). However, the magnitude of this sink was substantially lower under long-term cessation of grazing. Net ecosystem exchange, standardised to common light and temperature conditions (NEE_{600}), was on average 37 % lower in grazer exclosures compared to adjacent grazed land (Figure 3-2, Chapter 3). This difference was driven by lower gross primary productivity (GPP), while ecosystem respiration (ER) remained comparable, resulting in a markedly reduced CO_2 uptake efficiency under long-term cessation of grazing (Table 3-2, Chapter 3). These effects were strongest in grassland and particularly pronounced at ‘succession’ sites where grassland on the grazed part transitioned to heathland inside exclosures. At these sites,

NEE_{600} declined by more than 70%, indicating that these vegetation shifts, following cessation of grazing, amplify the negative effects of ceased grazing on the C sink strength (Te Beest *et al.* 2016, Sørensen *et al.* 2019). Importantly, these patterns persisted or even augmented across the full exclosure-age gradient of 20-83 years (Figure 3-6, Chapter 3), demonstrating that lower net C uptake is not a transient effect but a stable long-term outcome of cessation of grazing in sub-arctic grassland (Lara *et al.* 2017, Fischer *et al.* 2022, Thorhallsdottir and Gudmundsson 2023). These findings directly address objective (i) of my dissertation and support the emerging view that herbivores act as long-term regulators of ecosystem metabolism. Thereby they enhance C cycling through the ecosystem with a net strengthening of the C sink when kept within the ecological carrying capacity of the ecosystem (Briske *et al.* 2020, Rizzuto *et al.* 2024, Pillar and Winck 2026).

7.1.2 Linking CO_2 Fluxes to NDVI as a fast Indicator of the C Sink Strength

A key challenge in evaluating the climate change mitigation potential of land-use practices is scaling local measurements to landscape-relevant extents (Virkkala *et al.* 2021, 2024). Chapter 4 shows that ground-based NDVI provides a solid proxy for growing season gross primary production (GPP_{600}) and net ecosystem exchange (NEE_{600}) in Icelandic grassland, regardless of grazed or ungrazed (R^2 up to 0.80 for seasonal aggregated GPP_{600}; Figure 4-5, Chapter 4). Aggregation of NEE over July-August, including nighttime estimates, revealed that a 11% lower NDVI in ungrazed grassland compared to grazed grassland was associated with a fading of the net growing season C sink of grazed grassland (-0.44 ± 0.14 Mg C ha^{-1}) in ungrazed grassland (-0.07 ± 0.14 Mg C ha^{-1}; Table 4-3, Chapter 4). The calibration of ground-based NDVI with Sentinel-2 NDVI enabled upscaling of growing-season C sink estimates across Icelandic lowland grasslands (Figure 4-8; Chapter 4). Although satellite-based estimates carried substantial uncertainty, the approach successfully captured differences in NDVI between grazed and ungrazed grassland, a crucial perquisite for using this approach in land management monitoring (Beamish *et al.* 2020). These results address objective (ii) of my dissertation and demonstrate that NDVI can serve as a rapid, scalable indicator of grazing-mediated C uptake, especially when paired ground-based NDVI differences exceed the threshold of $NDVI_{exclosure} - NDVI_{grazed}$ ($\Delta NDVI$) > 0.1 (Juutinen *et al.* 2017). With further refinements of the calibration, such an indicator can be a powerful support for land-use policy aiming to evaluate the C sink strength of contrasting land use practices in sub-arctic grassland on spatial and temporal scales (Räsänen *et al.* 2019, Jespersen *et al.* 2023).

7.1.3 Grazing is linked to SOC Sequestration

While CO_2 flux measurements indicate how much photosynthetically assimilated C is taken up or released in ecosystems annually or during the growing season, long-term climate change mitigation depends on how effectively this C is stored (Pillar and Winck 2026). In grassland and heathland, most C is typically stored as SOC. Chapter 5 shows that grazer exclosures were associated with 8% lower SOC stocks in the top 10 cm of soil compared to continuously grazed land (Figure 5-2a, Chapter 5), with no detectable differences in deeper soil. Using a root-zone enrichment approach, I calculated that grazed grassland sequestered on average 0.15 Mg ha^{-1} $year^{-1}$ more SOC than ungrazed grassland (Table 5-2, Chapter 5). In heathland, the results were more variable and less associated with grazing, but relatively

more photosynthetically assimilated C was stored in roots and shoots than in SOC compared to grassland. In two sites where a mature birch woodland developed after more than 50 years following the cessation of grazing, SOC sequestration was 34% lower compared to the adjacent grazed grassland (Figure 5-3, Chapter 5), indicating that birch colonisation of previously grazed grassland – a common phenomenon across the arctic tundra – can diminish SOC sequestration (Mekonnen *et al.* 2021, Parker *et al.* 2021). These patterns align closely with changes in soil N availability and roots. The cessation of grazing was consistently linked to lower topsoil N and root C compared to grazed land (Table 5-2; Figure 5-5, Chapter 5), highlighting N as a key limiting factor for persistent SOC formation in grassland (Lavallee *et al.* 2020, Lehmann *et al.* 2020, Bai and Cotrufo 2022). Together, these results address objective (iii) of my dissertation and provide empirical support for theoretical models predicting herbivore-enhanced SOC sequestration through increased below-ground C flow and microbial processing (Kristensen *et al.* 2022, Rizzuto *et al.* 2024). Thus, when managed well, grazed ecosystems can be nature-based solutions for climate change mitigation by maintaining SOC stocks in grassland and additional SOC sequestration (Conant *et al.* 2017, Bai and Cotrufo 2022, Bardgett 2025, Pillar and Winck 2026).

7.1.4 Root Systems as the Link between Grazing and SOC

Chapter 6 provides a mechanistic underpinning for the observed SOC responses. Grazed grasslands maintained significantly higher fine root biomass in the top 10 cm of soil where over 70 % of total root biomass was concentrated (Figure 6-1; Table 6-2, Chapter 6). The cessation of grazing was associated with approximately 20-45 % lower fine root biomass in grassland and sites where heathland or birch woodland encroached previously grazed grassland. In long-established heathland, cessation of grazing had little effect on root biomass, consistent with the different growth strategies of graminoids and shrubs in northern ecosystems (Gallois *et al.* 2025). Fibrous root growth of graminoids is often stimulated by grazing, while shrub root systems grow mostly early in the growing season, often before grazing events (Wang, *et al.* 2016b). Despite large differences in root biomass, community-level root functional traits showed remarkable stability across grazed and ungrazed land (Figure 6-4, Chapter 6). Root traits varied mostly between topsoil roots (0-10 cm) and deeper roots (10-60 cm). Trade-off axes of rooting strategy (resource conservation trade-off and mycorrhizal collaboration trade-off) were conserved over soil depth, grazing contrasts and different vegetation types and likely more controlled by site conditions (Bardgett *et al.* 2014, Weigelt *et al.* 2021). Importantly, fine-root biomass, but not above-ground biomass, was positively related to SOC concentration in grazed grassland, whereas this relationship faded in grassland exclosures (Figure 6-5, Chapter 6; Malhotra *et al.* 2025). The largest potential for further SOC sequestration might be in grazed grassland within the volcanic active zone in southern Iceland. Soils there are frequently rejuvenated by fresh mineral material. SOC concentration was markedly lower than in other parts of the country, but fine root biomass in a comparable range. This indicates that the large availability of mineral surfaces in these soils can sequester relatively more root-derived C than in other parts of Iceland which requires further testing (Matus *et al.* 2024, Georgiou *et al.* 2025, Xu *et al.* 2025). These findings address objective (iv) of my dissertation and indicate that grazing influences SOC sequestration by regulating the quantity of root inputs, determined by fine root biomass, not by fundamentally altering rooting strategies (Sokol, *et al.* 2022b, George *et al.* 2024).

7.1.5 Integration across Studies and Implications for Land-use

Taken together, the four studies form a coherent narrative about the role of grazing for ecosystem C cycling in Icelandic lowland grassland and heathland, inferred from changes associated with the long-term cessation of grazing. In grassland, grazing stimulates efficient CO_2 uptake at the ecosystem level (Chapter 3) which can be monitored and upscaled using NDVI (Chapter 4). Sustained higher uptake over multiple decades (compared to 20-83 years old grazer exclosures) results in enhanced SOC stocks mediated by root biomass and N availability, indicating net SOC sequestration under grazing (Chapters 5 and 6). Cessation of grazing in grassland reverses this cascade in the long-term by reducing ecosystem metabolism, weakening root-mediated C inputs into soil and increasing the likelihood of vegetation shifts from grassland towards heathland or woodland with lower C-sink capacity for many decades (Parker *et al.* 2021, Kristensen *et al.* 2022, Lockwood *et al.* 2026). In heathland, grazing has an overall weaker effect on ecosystem C cycling with only slightly and temporary differences in the C sink strength between grazed and ungrazed heathland, without a strong link between NDVI and C uptake and without grazing-related differences in SOC stocks and fine root biomass. These weak responses to the cessation of grazing in heathland could be attributed to overall lower grazing intensity at these sites, driven by lower site productivity (indicated by low N) and slow growth of heath vegetation (Vowles and Björk 2019, Duddigan *et al.* 2024).

These findings challenge the assumption that grazing abandonment enhances C uptake in sub-arctic ecosystems, including Iceland (Metcalfe and Olofsson 2015, Ylänne and Stark 2019; Behrend *et al.* 2025; Sanchez *et al.* 2025). Instead, they show that low-input, extensive grazing can function as an effective nature-based solution for climate change mitigation, maintaining open grasslands that are both productive C sinks and maintain or even augment substantial soil C reservoirs (Borer and Risch 2024, Bardgett 2025, Pillar and Winck 2026). My dissertation supplies substantial data for the C balance of grazing land, thus far missing from the land-use-associated Icelandic carbon inventory reporting (Keller *et al.* 2026). Icelandic grassland, and to a smaller degree heathland, is a vital C sink and stores large SOC stocks. Based on the findings in this dissertation, grazing is the most efficient land use in these ecosystems to protect the stored SOC, by maintained soil stability through extensive fine root systems and even promote further SOC sequestration by stimulating soil C inputs, in agreement with Norderhaug *et al.* (2023). Contrary, cessation of grazing increases the risk of SOC losses in the long-term. This conclusion calls for an updating of the national accounting scheme of the C balance in grazing land within the National carbon inventory reporting.

Globally, wild herbivores continue to vanish on a large scale, putting them on top of extinction risk among all animal groups (Atwood *et al.* 2020, Davoli *et al.* 2024). Contrary, mounting evidence is showing the importance of large herbivores for ecosystem multifunctionality, including SOC sequestration, that could contribute to climate change mitigation (Forbes *et al.* 2019, Sandom *et al.* 2020, Malhi *et al.* 2022, Schmitz *et al.* 2023, Geremia *et al.* 2025). The link between herbivores and resilient ecosystems has sparked efforts to reintroduce large herbivores and trophic interactions to ecosystems (i.e. rewilding), aimed to improve resilience and adaptive capacity of ecosystems to a more uncertain future climate (Bakker and Svenning 2018, Svenning, *et al.* 2024a, Trepel *et al.* 2024). However, upscaling of rewilding efforts is often imperilled by land use conflicts and availability of animals (Svenning *et al.* 2016, De Jong *et al.* 2021). As an alternative, the findings of my dissertation, together with an increasing number of studies, are showing that extensive

livestock grazing in natural and semi-natural grassland and heathland can maintain C cycling through the plant-soil system at scale as livestock grazing is a major land use globally (Gordon *et al.* 2021, Kleppel and Frank 2022, Roy *et al.* 2023). Net SOC sequestration can thereby not only be an objective for land management in grazed systems but also a powerful indicator for ecosystem multifunctionality under grazing (Mutillod *et al.* 2024, Pillar and Winck 2026, Yang *et al.* 2026).

7.2 Limitations and Outlook

Several limitations should be acknowledged. First, CO_2 flux measurements were restricted to the peak growing season conditions (July-August) and daytime hours; although these represent the major fraction of annual C uptake in northern non-permafrost systems as daylengths are far longer than night length, winter and nighttime fluxes introduce uncertainty for full annual balances (See *et al.* 2024, Virkkala *et al.* 2024). For example, whole average daytime net C uptake (NEE_{600}, Chapter 3) suggests that both grazed and ungrazed grassland and heathland were net C sinks, refined estimates, including nighttime fluxes and daily average light conditions suggest that ungrazed grasslands were C neutral in July-August while grazed grasslands continued to be C sinks ($NEE_{July\text{-}August}$, Chapter 4). This potential depletion of the C sink strength with long-term cessation of grazing in Icelandic grassland, calls for more research and data to reduce uncertainties and improve C sink quantifications provided in this thesis.

Second, SOC sequestration was inferred from space-for-time substitution due to missing baseline data, an unavoidable constraint in long-term land-use studies (Chapter 5). Thus, additional studies experimentally testing our conclusions of larger SOC sequestration under grazing than cessation of grazing are inevitable to make our results more applicable for land users. Using methods such as stable isotope labelling could help to experimentally show C allocation and cycling in the plant-soil system (Klink *et al.* 2022, Xu *et al.* 2025). An alternative, unique to Iceland, to measure SOC sequestration rates over decades in grazed vs. ungrazed land, is to use recent tephra layers (ash deposits) in the topsoil as dating horizons. When assigned to the volcanic eruption they originate from, all SOC that accumulated above the tephra layer represents SOC sequestered since the eruption and could provide powerful comparisons for SOC sequestration under contrasting land uses (Leblans *et al.* 2017). Thus far, this approach has not been explored extensively but offers opportunities for future research.

Third, grazing intensity and livestock type varied among sites and likely also over time, given the large decline in sheep number over the last decades in Iceland (Table 1-2). Therefore, grazing was treated as a constant treatment across sites and time without more explicit parameterisation. A stricter standardisation and quantification of grazing would likely lead to stronger associations with the investigated parameters and defining limits for over-grazing, under-grazing and optimal grazing in terms of CO_2 exchange and SOC sequestration. For example, controlled re-introduction and modulation of grazing intensity, could provide powerful, experimental tests for conclusions drawn in this thesis for conditions under which measured effects of long-term cessation are reversible (Stanley *et al.* 2024).

Overall, future work should prioritise year-round flux measurements, explicit quantification of root turnover and microbial necromass formation as proposed key C input pathways for

persistent SOC formation (Buckeridge *et al.* 2022, Kou *et al.* 2023), and integration of mycorrhizal associations to better resolve below-ground mechanisms (Castaño *et al.* 2023, Hawkins *et al.* 2023, Zhou *et al.* 2026). Also, differentiation of SOC into MAOC and POC could inform more precise about formation pathways and persistence of SOC, particularly as the proportion of MAOC and POC in SOC has been proposed to differ in grassland (MAOC dominant) and heathland (POC dominant; (Lavallee *et al.* 2020, Angst *et al.* 2021). Likely grazing influences these components differently (Klumpp *et al.* 2009; Bai and Cotrufo 2022, Zhou *et al.* 2026). Improved high-resolution remote sensing (e.g. drone-based surveys) and more targeted calibration between ground measurements and airborne remote sensing indices could further refine landscape-scale estimates of grazing impacts (Siewert and Olofsson 2020, Jespersen *et al.* 2023, Zhao *et al.* 2024).

Currently, many grasslands globally are threatened by either poor grazing management, grazing abandonment and land use changes such as afforestation, jeopardising their C storage function (Feurdean *et al.* 2018, Bardgett *et al.* 2021, Briske *et al.* 2024, Kristensen *et al.* 2024). Therefore, it is timely to better recognise grazed grasslands as important sinks for atmospheric C, thereby contributing to climate change mitigation. This could improve conservation of grassland and associated herbivores, for example with the 'International year of rangelands and pastoralists 2026' (Bond 2019, Pillar and Overbeck 2025, Briske *et al.* 2026).

References

Abdalla, M., Hastings, A., Chadwick, D.R., Jones, D.L., Evans, C.D., Jones, M.B., Rees, R.M., Smith, P., 2018. Critical review of the impacts of grazing intensity on soil organic carbon storage and other soil quality indicators in extensively managed grasslands. Agric. Ecosyst. Environ. 253, 62–81. https://doi.org/10.1016/j.agee.2017.10.023

Alfreðsson, S.B., 2018. The effects of shrub encroachment on avian communities in lowland Iceland (Master thesis). University of Iceland, Reykjavik.

Allington, G.R.H., Valone, T.J., 2014. Islands of Fertility: A Byproduct of Grazing? Ecosystems 17, 127–141. https://doi.org/10.1007/s10021-013-9711-y

Alsos, I.G., Lammers, Y., Kjellman, S.E., Merkel, M.K.F., Bender, E.M., Rouillard, A., Erlendsson, E., Guðmundsdóttir, E.R., Benediktsson, Í.Ö., […], Schomacker, A., 2021. Ancient sedimentary DNA shows rapid post-glacial colonisation of Iceland followed by relatively stable vegetation until the Norse settlement (Landnám) AD 870. Quat. Sci. Rev. 259, 106903. https://doi.org/10.1016/j.quascirev.2021.106903

Anderegg, L.D.L., 2023. Why can't we predict traits from the environment? New Phytol. 237, 1998–2004. https://doi.org/10.1111/nph.18586

Andreatta, D., Gianelle, D., Scotton, M., Dalponte, M., 2022. Estimating grassland vegetation cover with remote sensing: A comparison between Landsat-8, Sentinel-2 and PlanetScope imagery. Ecol. Indic. 141, 109102. https://doi.org/10.1016/j.ecolind.2022.109102

Angst, G., Mueller, K.E., Nierop, K.G.J., Simpson, M.J., 2021. Plant- or microbial-derived? A review on the molecular composition of stabilized soil organic matter. Soil Biol. Biochem. 156, 108189. https://doi.org/10.1016/j.soilbio.2021.108189

Argenti, G., Chiesi, M., Fibbi, L., Maselli, F., 2022. Use of remote sensing and bio-geochemical models to estimate the net carbon fluxes of managed mountain grasslands. Ecol. Model. 474, 110152. https://doi.org/10.1016/j.ecolmodel.2022.110152

Arnalds, Ó., 2015. The soils of Iceland, World soils book series. Springer, Dordrecht Heidelberg.

Arndal, M.F., Tolver, A., Larsen, K.S., Beier, C., Schmidt, I.K., 2018. Fine Root Growth and Vertical Distribution in Response to Elevated CO_2, Warming and Drought in a Mixed Heathland–Grassland. Ecosystems 21, 15–30. https://doi.org/10.1007/s10021-017-0131-2

Aslaksen, I., Bryn, A., Clemmensen, K., De Wit, H., Emanuelsson, U., Garnåsjordet, P.A., Glomsrød, S., Graesse, M., Grimsrud, K., […], Thorhallsdottir, A.G., 2025. Afforestation on Nordic grasslands: Trade-offs and synergies for climate mitigation, biodiversity, and ecosystem services. Glob. Environ. Change Adv. 4, 100015. https://doi.org/10.1016/j.gecadv.2025.100015

Assmann, J.J., Kerby, J.T., Cunliffe, A.M., Myers-Smith, I.H., 2019. Vegetation monitoring using multispectral sensors — best practices and lessons learned from high latitudes. J. Unmanned Veh. Syst. 7, 54–75. https://doi.org/10.1139/juvs-2018-0018

Assmann, J.J., Myers-Smith, I.H., Kerby, J.T., Cunliffe, A.M., Daskalova, G.N., 2020. Drone data reveal heterogeneity in tundra greenness and phenology not captured by satellites. Environ. Res. Lett. 15, 125002. https://doi.org/10.1088/1748-9326/abbf7d

Atwood, T.B., Valentine, S.A., Hammill, E., McCauley, D.J., Madin, E.M.P., Beard, K.H., Pearse, W.D., 2020. Herbivores at the highest risk of extinction among mammals, birds, and reptiles. Sci. Adv. 6, eabb8458. https://doi.org/10.1126/sciadv.abb8458

Aune, S., Bryn, A., Hovstad, K.A., 2018. Loss of semi-natural grassland in a boreal landscape: impacts of agricultural intensification and abandonment. J. Land Use Sci. 13, 375–390. https://doi.org/10.1080/1747423X.2018.1539779

Azevedo, O., Parker, T.C., Siewert, M.B., Subke, J.-A., 2021. Predicting Soil Respiration from Plant Productivity (NDVI) in a Sub-Arctic Tundra Ecosystem. Remote Sens. 13, 2571. https://doi.org/10.3390/rs13132571

Badgley, G., Anderegg, L.D.L., Berry, J.A., Field, C.B., 2019. Terrestrial gross primary production: Using NIRV to scale from site to globe. Glob. Change Biol. 25, 3731–3740. https://doi.org/10.1111/gcb.14729

Bai, Y., Cotrufo, M.F., 2022. Grassland soil carbon sequestration: Current understanding, challenges, and solutions. Science 377, 603–608. https://doi.org/10.1126/science.abo2380

Bakker, E.S., Svenning, J.-C., 2018. Trophic rewilding: impact on ecosystems under global change. Philos. Trans. R. Soc. B Biol. Sci. 373, 20170432. https://doi.org/10.1098/rstb.2017.0432

Baldocchi, D., Chu, H., Reichstein, M., 2018. Inter-annual variability of net and gross ecosystem carbon fluxes: A review. Agric. For. Meteorol. 249, 520–533. https://doi.org/10.1016/j.agrformet.2017.05.015

Balzarolo, M., Vescovo, L., Hammerle, A., Gianelle, D., Papale, D., Tomelleri, E., Wohlfahrt, G., 2015. On the relationship between ecosystem-scale hyperspectral reflectance and CO_2 exchange in European mountain grasslands. Biogeosciences 12, 3089–3108. https://doi.org/10.5194/bg-12-3089-2015

Bannari, A., Morin, D., Bonn, F., Huete, A.R., 1995. A review of vegetation indices. Remote Sens. Rev. 13, 95–120. https://doi.org/10.1080/02757259509532298

Barbero-Palacios, L., Barrio, I.C., Criado, M.G., Kater, I., Bon, M.P., Kolari, T.H.M., Bjørkås, R., Trepel, J., Lundgren, E., […], Soininen, E.M., 2024. Herbivore diversity effects on Arctic tundra ecosystems: a systematic review. Environ. Evid. 13. https://doi.org/10.1186/s13750-024-00330-9

Barceló, M., Bodegom, P.M. van, Tedersoo, L., Haan, N. den, Veen, G.F. (Ciska), Ostonen, I., Trimbos, K., Soudzilovskaia, N.A., 2020. The abundance of arbuscular mycorrhiza in soils is linked to the total length of roots colonized at ecosystem level. PLOS ONE 15, e0237256. https://doi.org/10.1371/journal.pone.0237256

Bardgett, R.D., 2025. The Ecology of Soil: From communities to ecosystems. Oxford University Press. https://doi.org/10.1093/9780191858710.001.0001

Bardgett, R.D., Bullock, J.M., Lavorel, S., Manning, P., Schaffner, U., Ostle, N., Chomel, M., Durigan, G., L. Fry, E., […], Shi, H., 2021. Combatting global grassland degradation. Nat. Rev. Earth Environ. 2, 720–735. https://doi.org/10.1038/s43017-021-00207-2

Bardgett, R.D., Mommer, L., De Vries, F.T., 2014. Going underground: root traits as drivers of ecosystem processes. Trends Ecol. Evol. 29, 692–699. https://doi.org/10.1016/j.tree.2014.10.006

Bardgett, R.D., Wardle, D.A., 2003. Herbivore-mediated linkages between aboveground and belowground communities. Ecology 84, 2258–2268. https://doi.org/10.1890/02-0274

Bardgett, R.D., Wardle, D.A., 2010. Aboveground-Belowground Linkages: Biotic Interactions, Ecosystem Processes, and Global Change. Oxford University Press.

Barneze, A.S., Whitaker, J., McNamara, N.P., Ostle, N.J., 2024. Interactive effects of climate warming and management on grassland soil respiration partitioning. Eur. J. SOIL Sci. 75, e13491. https://doi.org/10.1111/ejss.13491

Barrio, I.C., Hik, D.S., Thórsson, J., Svavarsdóttir, K., Marteinsdóttir, B., Jónsdóttir, I.S., 2018. The sheep in wolf's clothing? Recognizing threats for land degradation in Iceland using state-and-transition models. Land Degrad. Dev. 29, 1714–1725. https://doi.org/10.1002/ldr.2978

Barry, K.E., Hennecke, J., Weigelt, A., Bergmann, J., Bruelheide, H., Freschet, G.T., Iversen, C.M., Kuyper, T.W., Laughlin, D.C., […], Mommer, L., 2025. Rooting for function: community-level fine-root traits relate to many ecosystem functions. New Phytol. 248, 3221–3239. https://doi.org/10.1111/nph.70606

Barthelemy, H., Stark, S., Michelsen, A., Olofsson, J., 2018. Urine is an important nitrogen source for plants irrespective of vegetation composition in an Arctic tundra: Insights from a 15N-enriched urea tracer experiment. J. Ecol. 106, 367–378. https://doi.org/10.1111/1365-2745.12820

Barthelemy, H., Stark, S., Olofsson, J., 2015. Strong Responses of Subarctic Plant Communities to Long-Term Reindeer Feces Manipulation. Ecosystems 18, 740–751. https://doi.org/10.1007/s10021-015-9856-y

Barto, E.K., Rillig, M.C., 2010. Does herbivory really suppress mycorrhiza? A meta-analysis. J. Ecol. 98, 745–753. https://doi.org/10.1111/j.1365-2745.2010.01658.x

Bates, D., Mächler, M., Bolker, B., Walker, S., 2015. Fitting linear mixed-effects models U-using lme4. J. Stat. Softw. 67, 1–48. https://doi.org/10.18637/jss.v067.i01

Batjes, N. h., 1996. Total carbon and nitrogen in the soils of the world. Eur. J. Soil Sci. 47, 151–163. https://doi.org/10.1111/j.1365-2389.1996.tb01386.x

Baty, F., Ritz, C., Charles, S., Brutsche, M., Flandrois, J.-P., Delignette-Muller, M.-L., 2015. A Toolbox for Nonlinear Regression in *R* : The Package nlstools. J. Stat. Softw. 66. https://doi.org/10.18637/jss.v066.i05

Bazzo, C.O.G., Kamali, B., Hütt, C., Bareth, G., Gaiser, T., 2023. A Review of Estimation Methods for Aboveground Biomass in Grasslands Using UAV. Remote Sens. 15, 639. https://doi.org/10.3390/rs15030639

Beamish, A., Raynolds, M.K., Epstein, H., Frost, G.V., Macander, M.J., Bergstedt, H., Bartsch, A., Kruse, S., Miles, V., […], Wagner, J., 2020. Recent trends and remaining challenges for optical remote sensing of Arctic tundra vegetation: A review and outlook. Remote Sens. Environ. 246, 111872. https://doi.org/10.1016/j.rse.2020.111872

Beer, C., Reichstein, M., Tomelleri, E., Ciais, P., Jung, M., Carvalhais, N., Rödenbeck, C., Arain, M.A., Baldocchi, D., […], Papale, D., 2010. Terrestrial Gross Carbon Dioxide Uptake: Global Distribution and Covariation with Climate. Science 329, 834–838. https://doi.org/10.1126/science.1184984

Behrend, A.M., Aradóttir, Á.L., Svavarsdóttir, K., Thórhallsdóttir, T.E., Pommerening, A., 2025a. Natural colonization as a means to upscale restoration of subarctic woodlands in Iceland. Restor. Ecol. 33, e14332. https://doi.org/10.1111/rec.14332

Behrend, A.M., Óskarsson, H., Raulund-Rasmussen, K., 2025b. Successional patterns of Icelandic subarctic mountain birch woodlands after decades of grazing exclusion. Restor. Ecol. e70244. https://doi.org/10.1111/rec.70244

Beier, C., Emmett, B.A., Tietema, A., Schmidt, I.K., Peñuelas, J., Láng, E.K., Duce, P., De Angelis, P., Gorissen, A., […], Spano, D., 2009. Carbon and nitrogen balances for six shrublands across Europe. Glob. Biogeochem. Cycles 23. https://doi.org/10.1029/2008GB003381

Beillouin, D., Cardinael, R., Berre, D., Boyer, A., Corbeels, M., Fallot, A., Feder, F., Demenois, J., 2022. A global overview of studies about land management, land-use

change, and climate change effects on soil organic carbon. Glob. Change Biol. 28, 1690–1702. https://doi.org/10.1111/gcb.15998
Bengtsson, J., Bullock, J.M., Egoh, B., Everson, C., Everson, T., O'Connor, T., O'Farrell, P.J., Smith, H.G., Lindborg, R., 2019. Grasslands—more important for ecosystem services than you might think. Ecosphere 10, e02582. https://doi.org/10.1002/ecs2.2582
Bergmann, J., Weigelt, A., van der Plas, F., Laughlin, D.C., Kuyper, T.W., Guerrero-Ramirez, N., Valverde-Barrantes, O.J., Bruelheide, H., Freschet, G.T., […], Mommer, L., 2020. The fungal collaboration gradient dominates the root economics space in plants. Sci. Adv. 6, eaba3756. https://doi.org/10.1126/sciadv.aba3756
Blair, J., Nippert, J., Briggs, J., 2014. Grassland Ecology, in: Monson, R.K. (Ed.), Ecology and the Environment. Springer New York, New York, NY, pp. 389–423. https://doi.org/10.1007/978-1-4614-7501-9_14
Blinnikov, M.S., Gaglioti, B.V., Walker, D.A., Wooller, M.J., Zazula, G.D., 2011. Pleistocene graminoid-dominated ecosystems in the Arctic. Quat. Sci. Rev. 30, 2906–2929. https://doi.org/10.1016/j.quascirev.2011.07.002
Blume-Werry, G., Wilson, S.D., Kreyling, J., Milbau, A., 2016. The hidden season: growing season is 50% longer below than above ground along an arctic elevation gradient. New Phytol. 209, 978–986. https://doi.org/10.1111/nph.13655
Bocherens, H., 2018. The rise of the anthroposphere since 50,000 years: An ecological replacement of megaherbivores by humans in terrestrial ecosystems? Front. Ecol. Evol. 6, 3. https://doi.org/10.3389/fevo.2018.00003
Bond, W.J., 2019. Open Ecosystems: ecology and evolution beyond the forest edge. Oxford University Press.
Borer, E.T., Risch, A.C., 2024. Planning for the future: Grasslands, herbivores, and nature-based solutions. J. Ecol. 112, 2442–2450. https://doi.org/10.1111/1365-2745.14323
Borer, E.T., Seabloom, E.W., Gruner, D.S., Harpole, W.S., Hillebrand, H., Lind, E.M., Adler, P.B., Alberti, J., Anderson, T.M., […], Yang, L.H., 2014. Herbivores and nutrients control grassland plant diversity via light limitation. Nature 508, 517–520. https://doi.org/10.1038/nature13144
Bork, E., Hewins, D., Lamb, E., Carlyle, C., Lyseng, M., Chang, S., Alexander, M., Willms, W., Iravani, M., 2023. Light to moderate long-term grazing enhances ecosystem carbon across a broad climatic gradient in northern temperate grasslands. Sci. Total Environ. 894, 164978. https://doi.org/10.1016/j.scitotenv.2023.164978
Bork, E.W., Raatz, L.L., Carlyle, C.N., Hewins, D.B., Thompson, K.A., 2020. Soil carbon increases with long-term cattle stocking in northern temperate grasslands. Soil Use Manag. 36, 387–399. https://doi.org/10.1111/sum.12580
Bossio, D.A., Cook-Patton, S.C., Ellis, P.W., Fargione, J., Sanderman, J., Smith, P., Wood, S., Zomer, R.J., von Unger, M., Emmer, I.M., Griscom, B.W., 2020. The role of soil carbon in natural climate solutions. Nat. Sustain. 3, 391–398. https://doi.org/10.1038/s41893-020-0491-z
Boulanger-Lapointe, N., Ágústsdóttir, K., Barrio, I.C., Defourneaux, M., Finnsdóttir, R., Jónsdóttir, I.S., Marteinsdóttir, B., Mitchell, C., Möller, M., […], Huettmann, F., 2022. Herbivore species coexistence in changing rangeland ecosystems: First high resolution national open-source and open-access ensemble models for Iceland. Sci. Total Environ. 845, 157140. https://doi.org/10.1016/j.scitotenv.2022.157140
Bråthen, K.A., Pugnaire, F.I., Bardgett, R.D., 2021. The paradox of forbs in grasslands and the legacy of the mammoth steppe. Front. Ecol. Environ. n/a. https://doi.org/10.1002/fee.2405

Bråthen, K.A., Ravolainen, V.T., Stien, A., Tveraa, T., Ims, R.A., 2017. Rangifer management controls a climate-sensitive tundra state transition. Ecol. Appl. 27, 2416–2427. https://doi.org/10.1002/eap.1618

Briske, D., 1991. Developmental morphology and physiology of grasses, in: Grazing Management: An Ecological Perspective. Timber Press, Portland, OR, USA.

Briske, D.D., 1996. Strategies of plant survival in grazed systems: A functional interpretation, in: Hodgson, J., Illius, A.W. (Eds.), The Ecology and Management of Grazing Systems. CAB International.

Briske, D.D., Coppock, D.L., Illius, A.W., Fuhlendorf, S.D., 2020. Strategies for global rangeland stewardship: Assessment through the lens of the equilibrium–non-equilibrium debate. J. Appl. Ecol. 57, 1056–1067. https://doi.org/10.1111/1365-2664.13610

Briske, D.D., Niamir-Fuller, M., Davies, J., Waters-Bayer, A., Hutchinson, B.S., Samuels, I., 2026. United Nations declares 2026 international year of rangelands and pastoralists. Camb. Prisms Drylands 3, e2. https://doi.org/10.1017/dry.2025.10016

Briske, D.D., Vetter, S., Coetsee, C., Turner, M.D., 2024. Rangeland afforestation is not a natural climate solution. Front. Ecol. Environ. 22, e2727. https://doi.org/10.1002/fee.2727

Buckeridge, K.M., Creamer, C., Whitaker, J., 2022. Deconstructing the microbial necromass continuum to inform soil carbon sequestration. Funct. Ecol. 36, 1396–1410. https://doi.org/10.1111/1365-2435.14014

Buckley, Y.M., Austin, A., Bardgett, R., Catford, J.A., Hector, A., Iler, A., Mariotte, P., 2024. The plant ecology of nature-based solutions for people, biodiversity and climate. J. Ecol. 112, 2424–2431. https://doi.org/10.1111/1365-2745.14441

Buisson, E., Archibald, S., Fidelis, A., Suding, K.N., 2022. Ancient grasslands guide ambitious goals in grassland restoration. Science 377, 594–598. https://doi.org/10.1126/science.abo4605

Bunn, R.A., Corrêa, A., Joshi, J., Kaiser, C., Lekberg, Y., Prescott, C.E., Sala, A., Karst, J., 2024. What determines transfer of carbon from plants to mycorrhizal fungi? New Phytol. 244, 1199–1215. https://doi.org/10.1111/nph.20145

Bürgi, M., Östlund, L., Mladenoff, D.J., 2017. Legacy Effects of Human Land Use: Ecosystems as Time-Lagged Systems. Ecosystems 20, 94–103. https://doi.org/10.1007/s10021-016-0051-6

Byrnes, R.C., Eastburn, D.J., Tate, K.W., Roche, L.M., 2018. A Global Meta-Analysis of Grazing Impacts on Soil Health Indicators. J. Environ. Qual. 47, 758–765. https://doi.org/10.2134/jeq2017.08.0313

Cahoon, S.M.P., Sullivan, P.F., Post, E., 2016. Greater Abundance of Betula nana and Early Onset of the Growing Season Increase Ecosystem CO_2 Uptake in West Greenland. Ecosystems 19, 1149–1163. https://doi.org/10.1007/s10021-016-9997-7

Cahoon, S.M.P., Sullivan, P.F., Post, E., Welker, J.M., 2012. Large herbivores limit CO_2 uptake and suppress carbon cycle responses to warming in West Greenland. Glob. Change Biol. 18, 469–479. https://doi.org/10.1111/j.1365-2486.2011.02528.x

Cai, J., Pan, X., Xiao, Y., Wang, Yue, Li, G., Wang, Yao, Zhang, M., Wang, L., 2024. Below-ground root nutrient-acquisition strategies are more sensitive to long-term grazing than above-ground leaf traits across a soil nutrient gradient. Funct. Ecol. 38, 1475–1485. https://doi.org/10.1111/1365-2435.14565

Castaño, C., Hallin, S., Egelkraut, D., Lindahl, B.D., Olofsson, J., Clemmensen, K.E., 2023. Contrasting plant–soil–microbial feedbacks stabilize vegetation types and uncouple

topsoil C and N stocks across a subarctic–alpine landscape. New Phytol. 238, 2621–2633. https://doi.org/10.1111/nph.18679

Chang, J., Ciais, P., Gasser, T., Smith, P., Herrero, M., Havlík, P., Obersteiner, M., Guenet, B., Goll, D.S., […], Zhu, D., 2021. Climate warming from managed grasslands cancels the cooling effect of carbon sinks in sparsely grazed and natural grasslands. Nat. Commun. 12, 118. https://doi.org/10.1038/s41467-020-20406-7

Chari, N.R., Tumber-Dávila, S.J., Phillips, R.P., Bauerle, T.L., Brunn, M., Hafner, B.D., Klein, T., Obersteiner, S., Reay, M.K., Ullah, S., Taylor, B.N., 2024. Estimating the global root exudate carbon flux. Biogeochemistry 167, 895–908. https://doi.org/10.1007/s10533-024-01161-z

Chavez, E.A., Adkins, J., Waring, B.G., Beard, K.H., Choi, R.T., Miller, L., Saunders, T., Atwood, T.B., 2025. Herbivory in a low Arctic wetland alters intraspecific plant root traits with consequences for carbon and nitrogen cycling. J. Ecol. 113, 1225–1238. https://doi.org/10.1111/1365-2745.70028

Chen, A., Mao, J., Ricciuto, D., Lu, D., Xiao, J., Li, X., Thornton, P.E., Knapp, A.K., 2021. Seasonal changes in GPP/SIF ratios and their climatic determinants across the Northern Hemisphere. Glob. Change Biol. 27, 5186–5197. https://doi.org/10.1111/gcb.15775

Chen, J., Shi, W., Cao, J., 2015. Effects of Grazing on Ecosystem CO_2 Exchange in a Meadow Grassland on the Tibetan Plateau During the Growing Season. Environ. Manage. 55, 347–359. https://doi.org/10.1007/s00267-014-0390-z

Christie, K.S., Bryant, J.P., Gough, L., Ravolainen, V.T., Ruess, R.W., Tape, K.D., 2015. The Role of Vertebrate Herbivores in Regulating Shrub Expansion in the Arctic: A Synthesis. BioScience 65, 1123–1133. https://doi.org/10.1093/biosci/biv137

Cicuéndez, V., Inclán, R., Sánchez-Cañete, E.P., Román-Cascón, C., Sáenz, C., Yagüe, C., 2024. Modeling Gross Primary Production (GPP) of a Mediterranean Grassland in Central Spain Using Sentinel-2 NDVI and Meteorological Field Information. Agronomy 14, 1243. https://doi.org/10.3390/agronomy14061243

Clemmensen, K.E., Finlay, R.D., Dahlberg, A., Stenlid, J., Wardle, D.A., Lindahl, B.D., 2015. Carbon sequestration is related to mycorrhizal fungal community shifts during long-term succession in boreal forests. New Phytol. 205, 1525–1536. https://doi.org/10.1111/nph.13208

Conant, R.T., Cerri, C.E.P., Osborne, B.B., Paustian, K., 2017. Grassland management impacts on soil carbon stocks: a new synthesis. Ecol. Appl. 27, 662–668. https://doi.org/10.1002/eap.1473

Cotrufo, M.F., Lavallee, J.M., 2022. Soil organic matter formation, persistence, and functioning: A synthesis of current understanding to inform its conservation and regeneration, in: Advances in Agronomy. Elsevier, pp. 1–66. https://doi.org/10.1016/bs.agron.2021.11.002

Cousins, S.A.O., Auffret, A.G., Lindgren, J., Tränk, L., 2015. Regional-scale land-cover change during the 20th century and its consequences for biodiversity. AMBIO 44, 17–27. https://doi.org/10.1007/s13280-014-0585-9

Cromsigt, J.P.G.M., te Beest, M., Kerley, G.I.H., Landman, M., le Roux, E., Smith, F.A., 2018. Trophic rewilding as a climate change mitigation strategy? Philos. Trans. R. Soc. B Biol. Sci. 373, 20170440. https://doi.org/10.1098/rstb.2017.0440

Da Silveira Pontes, L., Maire, V., Schellberg, J., Louault, F., 2015. Grass strategies and grassland community responses to environmental drivers: a review. Agron. Sustain. Dev. 35, 1297–1318. https://doi.org/10.1007/s13593-015-0314-1

Dahlgren, R.A., Saigusa, M., Ugolini, F.C., 2004. The Nature, Properties and Management of Volcanic Soils, in: Advances in Agronomy. Academic Press, pp. 113–182. https://doi.org/10.1016/S0065-2113(03)82003-5

Dangal, S.R.S., Tian, H., Pan, S., Zhang, L., Xu, R., 2020. Greenhouse gas balance in global pasturelands and rangelands. Environ. Res. Lett. 15, 104006. https://doi.org/10.1088/1748-9326/abaa79

Davoli, M., Monsarrat, S., Pedersen, R.Ø., Scussolini, P., Karger, D.N., Normand, S., Svenning, J.-C., 2024. Megafauna diversity and functional declines in Europe from the Last Interglacial to the present. Glob. Ecol. Biogeogr. 33, 34–47. https://doi.org/10.1111/geb.13778

De Jong, L., De Bruin, S., Knoop, J., Van Vliet, J., 2021. Understanding land-use change conflict: a systematic review of case studies. J. Land Use Sci. 16, 223–239. https://doi.org/10.1080/1747423X.2021.1933226

Dec, D., Dörner, J., Balocchi, O., López, I., 2012. Temporal dynamics of hydraulic and mechanical properties of an Andosol under grazing. Soil Tillage Res., Development of soil structure and functions: How can mechanical and hydraulic approaches contribute to quantify soil structure dynamics? 125, 44–51. https://doi.org/10.1016/j.still.2012.05.018

Defourneaux, M., Barrio, I.C., Boulanger-Lapointe, N., Speed, J.D.M., 2024. Long-term changes in herbivore community and vegetation impact of wild and domestic herbivores across Iceland. Ambio 53, 1124–1135. https://doi.org/10.1007/s13280-024-01998-6

Del Grosso, S.J., Parton, W.J., Derner, J.D., Chen, M., Tucker, C.J., 2018. Simple models to predict grassland ecosystem C exchange and actual evapotranspiration using NDVI and environmental variables. Agric. For. Meteorol. 249, 1–10. https://doi.org/10.1016/j.agrformet.2017.11.007

Dengler, J., Birge, T., Bruun, H.H., Rašomavičius, V., Rūsiņa, S., Sickel, H., 2020. Grasslands of Northern Europe and the Baltic States, in: Goldstein, M., DellaSala, D. (Eds.), Encyclopedia of the World's Biomes. Elsevier, Oxford, pp. 689–702.

Dengler, J., Janišová, M., Török, P., Wellstein, C., 2014. Biodiversity of Palaearctic grasslands: a synthesis. Agric. Ecosyst. Environ., Biodiversity of Palaearctic grasslands: processes, patterns and conservation 182, 1–14. https://doi.org/10.1016/j.agee.2013.12.015

Derner, J.D., Augustine, D.J., Frank, D.A., 2019. Does grazing matter for soil organic carbon sequestration in the Western North American Great Plains? Ecosystems 22, 1088–1094. https://doi.org/10.1007/s10021-018-0324-3

Deslippe, J.R., Simard, S.W., 2011. Below-ground carbon transfer among Betula nana may increase with warming in Arctic tundra. New Phytol. 192, 689–698. https://doi.org/10.1111/j.1469-8137.2011.03835.x

Don, A., Seidel, F., Leifeld, J., Kätterer, T., Martin, M., Pellerin, S., Emde, D., Seitz, D., Chenu, C., 2024. Carbon sequestration in soils and climate change mitigation—Definitions and pitfalls. Glob. Change Biol. 30, e16983. https://doi.org/10.1111/gcb.16983

Doughty, C.E., Roman, J., Faurby, S., Wolf, A., Haque, A., Bakker, E.S., Malhi, Y., Dunning, J.B., Svenning, J.-C., 2016. Global nutrient transport in a world of giants. Proc. Natl. Acad. Sci. 113, 868–873. https://doi.org/10.1073/pnas.1502549112

Du, E., De Vries, W., 2025. Links Between Nitrogen Limitation and Saturation in Terrestrial Ecosystems. Glob. Change Biol. 31. https://doi.org/10.1111/gcb.70271

Duddigan, S., Hales-Henao, A., Bruce, M., Diaz, A., Tibbett, M., 2024. Restored lowland heathlands store substantially less carbon than undisturbed lowland heath. Commun. Earth Environ. 5, 15. https://doi.org/10.1038/s43247-023-01176-8

Edwards, K.J., Erlendsson, E., Schofield, J.E., 2021. *Landnám* and the North Atlantic Flora, in: Panagiotakopulu, E., Sadler, J.P. (Eds.), Biogeography in the Sub-Arctic. Wiley, pp. 185–214. https://doi.org/10.1002/9781118561461.ch9

Egelkraut, D., Aronsson, K.-Å., Allard, A., Åkerholm, M., Stark, S., Olofsson, J., 2018a. Multiple feedbacks contribute to a centennial legacy of reindeer on tundra vegetation. Ecosystems 21, 1545–1563. https://doi.org/10.1007/s10021-018-0239-z

Egelkraut, D., Barthelemy, H., Olofsson, J., 2020. Reindeer trampling promotes vegetation changes in tundra heathlands: Results from a simulation experiment. J. Veg. Sci. 31, 476–486. https://doi.org/10.1111/jvs.12871

Egelkraut, D., Kardol, P., De Long, J.R., Olofsson, J., 2018b. The role of plant–soil feedbacks in stabilizing a reindeer-induced vegetation shift in subarctic tundra. Funct. Ecol. 32, 1959–1971. https://doi.org/10.1111/1365-2435.13113

Eisenhauer, N., Lanoue, A., Strecker, T., Scheu, S., Steinauer, K., Thakur, M.P., Mommer, L., 2017. Root biomass and exudates link plant diversity with soil bacterial and fungal biomass. Sci. Rep. 7, 44641. https://doi.org/10.1038/srep44641

Encarnation, D., Ashworth, D., Bardgett, R., Edwards, M., Hambler, C., Kristensen, J., Hector, A., 2025. Seasonal Sheep Grazing Does Not Enhance Stable or Total Soil Carbon Stocks in a Long-Term Calcareous Grassland Experiment. Ecol. Evol. 15, e71582. https://doi.org/10.1002/ece3.71582

Erktan, A., Roumet, C., Munoz, F., 2023. Dissecting fine root diameter distribution at the community level captures root morphological diversity. Oikos 2023. https://doi.org/10.1111/oik.08907

Eskelinen, A., Harpole, W.S., Jessen, M.-T., Virtanen, R., Hautier, Y., 2022. Light competition drives herbivore and nutrient effects on plant diversity. Nature 611, 301–305. https://doi.org/10.1038/s41586-022-05383-9

Eze, S., Palmer, S.M., Chapman, P.J., 2018. Upland grasslands in Northern England were atmospheric carbon sinks regardless of management regimes. Agric. For. Meteorol. 256–257, 231–241. https://doi.org/10.1016/j.agrformet.2018.03.016

Fagúndez, J., Pontevedra-Pombal, X., 2022. Soil properties of North Iberian wet heathlands in relation to climate, management and plant community. Plant Soil. https://doi.org/10.1007/s11104-022-05393-6

Falk, J.M., Schmidt, N.M., Christensen, T.R., Ström, L., 2015. Large herbivore grazing affects the vegetation structure and greenhouse gas balance in a high arctic mire. Environ. Res. Lett. 10, 045001. https://doi.org/10.1088/1748-9326/10/4/045001

FAO, 2020. A protocol for measurement, monitoring, reporting and verification of soil organic carbon in agricultural landscapes. FAO. https://doi.org/10.4060/cb0509en

February, E., Pausch, J., Higgins, S.I., 2020. Major contribution of grass roots to soil carbon pools and CO_2 fluxes in a mesic savanna. Plant Soil 454, 207–215. https://doi.org/10.1007/s11104-020-04649-3

Ferraro, K.M., Albrecht, D., Hendrix, J.G., Wal, E.V., Schmitz, O.J., Webber, Q.M.R., Bradford, M.A., 2024. The biogeochemical boomerang: Site fidelity creates nutritional hotspots that may promote recurrent calving site reuse. Ecol. Lett. 27, e14491. https://doi.org/10.1111/ele.14491

Ferraro, K.M., Schmitz, O.J., McCary, M.A., 2022. Effects of ungulate density and sociality on landscape heterogeneity: a mechanistic modeling approach. Ecography 2022. https://doi.org/10.1111/ecog.06039

Feurdean, A., Ruprecht, E., Molnár, Z., Hutchinson, S.M., Hickler, T., 2018. Biodiversity-rich European grasslands: Ancient, forgotten ecosystems. Biol. Conserv. 228, 224–232. https://doi.org/10.1016/j.biocon.2018.09.022

Fiala, K., Tůma, I., Holub, P., 2009. Effect of Manipulated Rainfall on Root Production and Plant Belowground Dry Mass of Different Grassland Ecosystems. Ecosystems 12, 906–914. https://doi.org/10.1007/s10021-009-9264-2

Fischer, W., Thomas, C.K., Zimov, N., Göckede, M., 2022. Grazing enhances carbon cycling but reduces methane emission during peak growing season in the Siberian Pleistocene Park tundra site. Biogeosciences 19, 1611–1633. https://doi.org/10.5194/bg-19-1611-2022

Forbes, E.S., Cushman, J.H., Burkepile, D.E., Young, T.P., Klope, M., Young, H.S., 2019. Synthesizing the effects of large, wild herbivore exclusion on ecosystem function. Funct. Ecol. 33, 1597–1610. https://doi.org/10.1111/1365-2435.13376

Fossum, C., Estera-Molina, K.Y., Yuan, M., Herman, D.J., Chu-Jacoby, I., Nico, P.S., Morrison, K.D., Pett-Ridge, J., Firestone, M.K., 2022. Belowground allocation and dynamics of recently fixed plant carbon in a California annual grassland. Soil Biol. Biochem. 165, 108519. https://doi.org/10.1016/j.soilbio.2021.108519

Foster, D., Swanson, F., Aber, J., Burke, I., Brokaw, N., Tilman, D., Knapp, A., 2003. The Importance of Land-Use Legacies to Ecology and Conservation. BioScience 53, 77–88. https://doi.org/10.1641/0006-3568(2003)053%5B0077:TIOLUL%5D2.0.CO;2

Francini, G., Liiri, M., Männistö, M., Stark, S., Kytöviita, M.-M., 2014. Response to reindeer grazing removal depends on soil characteristics in low Arctic meadows. Appl. Soil Ecol. 76, 14–25. https://doi.org/10.1016/j.apsoil.2013.12.003

Frank, D.A., Fridley, J.D., 2025. Herbivores override climate control of grassland production in Yellowstone National Park. Ecology 106, e70159. https://doi.org/10.1002/ecy.70159

Frank, D.A., McNaughton, S.J., Tracy, B.F., 1998. The ecology of the Earth's grazing ecosystems. BioScience 48, 513–521. https://doi.org/10.2307/1313313

Frank, D.A., Pontes, A.W., Maine, E.M., Caruana, J., Raina, R., Raina, S., Fridley, J.D., 2010. Grassland root communities: species distributions and how they are linked to aboveground abundance. Ecology 91, 3201–3209. https://doi.org/10.1890/09-1831.1

Frank, D.A., Wallen, R.L., Hamilton III, E.W., White, P.J., Fridley, J.D., 2018. Manipulating the system: How large herbivores control bottom-up regulation of grasslands. J. Ecol. 106, 434–443. https://doi.org/10.1111/1365-2745.12884

Franzluebbers, A.J., 2021. Soil organic carbon sequestration calculated from depth distribution. Soil Sci. Soc. Am. J. 85, 158–171. https://doi.org/10.1002/saj2.20176

Franzluebbers, A.J., 2022. Root-zone soil organic carbon enrichment is sensitive to land management across soil types and regions. Soil Sci. Soc. Am. J. 86, 79–90. https://doi.org/10.1002/saj2.20346

Franzluebbers, A.J., van Vliet, S., Young, S., Poore, M.H., 2023. Soil health and root-zone enrichment characteristics between paired grassland and cropland fields in the southeastern United States. Grassl. Res. 2, 299–308. https://doi.org/10.1002/glr2.12066

Freschet, G.T., Östlund, L., Kichenin, E., Wardle, D.A., 2014. Aboveground and belowground legacies of native Sami land use on boreal forest in northern Sweden 100 years after abandonment. Ecology 95, 963–977. https://doi.org/10.1890/13-0824.1

Freschet, G.T., Pagès, L., Iversen, C.M., Comas, L.H., Rewald, B., Roumet, C., Klimešová, J., Zadworny, M., Poorter, H., […], McCormack, M.L., 2021a. A starting guide to

root ecology: strengthening ecological concepts and standardising root classification, sampling, processing and trait measurements. New Phytol. 232, 973–1122. https://doi.org/10.1111/nph.17572
Freschet, G.T., Roumet, C., Comas, L.H., Weemstra, M., Bengough, A.G., Rewald, B., Bardgett, R.D., De Deyn, G.B., Johnson, D., […], Stokes, A., 2021b. Root traits as drivers of plant and ecosystem functioning: current understanding, pitfalls and future research needs. New Phytol. 232, 1123–1158. https://doi.org/10.1111/nph.17072
Frey, S.D., 2019. Mycorrhizal Fungi as Mediators of Soil Organic Matter Dynamics. Annu. Rev. Ecol. Evol. Syst. 50, 237–259. https://doi.org/10.1146/annurev-ecolsys-110617-062331
Fricke, E.C., Hsieh, C., Middleton, O., Gorczynski, D., Cappello, C.D., Sanisidro, O., Rowan, J., Svenning, J.-C., Beaudrot, L., 2022. Collapse of terrestrial mammal food webs since the Late Pleistocene. Science 377, 1008–1011. https://doi.org/10.1126/science.abn4012
Friggens, N.L., Hester, A.J., Mitchell, R.J., Parker, T.C., Subke, J.-A., Wookey, P.A., 2020. Tree planting in organic soils does not result in net carbon sequestration on decadal timescales. Glob. Change Biol. 26, 5178–5188. https://doi.org/10.1111/gcb.15229
Frigo, D., Eggertsson, Ó., Prendin, A.L., Dibona, R., Unterholzner, L., Carrer, M., 2023. Growth form and leaf habit drive contrasting effects of Arctic amplification in long-lived woody species. Glob. Change Biol. 29, 5896–5907. https://doi.org/10.1111/gcb.16895
Gallois, E.C., Myers-Smith, I.H., Iversen, C.M., Salmon, V.G., Turner, L.L., An, R., Elmendorf, S.C., Collins, C.G., Anderson, M.J.R., […], Hollister, R.D., 2025. Tundra Vegetation Community Type, Not Microclimate, Controls Asynchrony of Above- and Below-Ground Phenology. Glob. Change Biol. 31, e70153. https://doi.org/10.1111/gcb.70153
García Criado, M., Barrio, I.C., Speed, J.D.M., Bjorkman, A.D., Elmendorf, S.C., Myers-Smith, I.H., Aerts, R., Alatalo, J.M., Betway-May, K.R., […], Vowles, T., 2025. Borealisation of Plant Communities in the Arctic Is Driven by Boreal-Tundra Species. Ecol. Lett. 28, e70209. https://doi.org/10.1111/ele.70209
Garcia-Pausas, J., Casals, P., Romanyà, J., Vallecillo, S., Sebastià, M.-T., 2011. Seasonal patterns of belowground biomass and productivity in mountain grasslands in the Pyrenees. Plant Soil 340, 315–326. https://doi.org/10.1007/s11104-010-0601-1
Gargiulo, J.I., Lyons, N.A., Masia, F., Beale, P., Insua, J.R., Correa-Luna, M., Garcia, S.C., 2023. Comparison of Ground-Based, Unmanned Aerial Vehicles and Satellite Remote Sensing Technologies for Monitoring Pasture Biomass on Dairy Farms. Remote Sens. 15, 2752. https://doi.org/10.3390/rs15112752
Gavrichkova, O., Pretto, G., Brugnoli, E., Chiti, T., Ivashchenko, K.V., Mattioni, M., Moscatelli, M.C., Scartazza, A., Calfapietra, C., 2022. Consequences of Grazing Cessation for Soil Environment and Vegetation in a Subalpine Grassland Ecosystem. Plants 11, 2121. https://doi.org/10.3390/plants11162121
Ge, L., Lafleur ,P. M., and Humphreys, E.R., 2017. Respiration from Soil and Ground Cover Vegetation Under Tundra Shrubs. Arct. Antarct. Alp. Res. 49, 537–550. https://doi.org/10.1657/AAAR0016-064
Geirsdóttir, Á., Harning, D.J., Miller, G.H., Andrews, J.T., Zhong, Y., Caseldine, C., 2020. Holocene history of landscape instability in Iceland: Can we deconvolve the impacts of climate, volcanism and human activity? Quat. Sci. Rev. 249, 106633. https://doi.org/10.1016/j.quascirev.2020.106633

George, T.S., Bulgarelli, D., Carminati, A., Chen, Y., Jones, D., Kuzyakov, Y., Schnepf, A., Wissuwa, M., Roose, T., 2024. Bottom-up perspective – The role of roots and rhizosphere in climate change adaptation and mitigation in agroecosystems. Plant Soil. https://doi.org/10.1007/s11104-024-06626-6

Georgiou, K., Angers, D., Champiny, R.E., Cotrufo, M.F., Craig, M.E., Doetterl, S., Grandy, A.S., Lavallee, J.M., Lin, Y., […], Wieder, W.R., 2025. Soil Carbon Saturation: What Do We Really Know? Glob. Change Biol. 31, e70197. https://doi.org/10.1111/gcb.70197

Geremia, C., Hamilton III, E.W., Merkle, J.A., 2025. Yellowstone's free-moving large bison herds provide a glimpse of their past ecosystem function. Science 389, 904–908. https://doi.org/10.1126/science.adu0703

Gilmanov, T.G., Johnson, D.A., Saliendra, N.Z., Akshalov, K., Wylie, B.K., 2004. Gross Primary Productivity of the True Steppe in Central Asia in Relation to NDVI: Scaling up CO_2 Fluxes. Environ. Manage. 33, S492–S508. https://doi.org/10.1007/s00267-003-9157-7

Gilmanov, T.G., Soussana, J.F., Aires, L., Allard, V., Ammann, C., Balzarolo, M., Barcza, Z., Bernhofer, C., Campbell, C.L., […], Wohlfahrt, G., 2007. Partitioning European grassland net ecosystem CO_2 exchange into gross primary productivity and ecosystem respiration using light response function analysis. Agric. Ecosyst. Environ. 121, 93–120. https://doi.org/10.1016/j.agee.2006.12.008

Gong, Y.M., Mohammat, A., Liu, X.J., Li, K.H., Christie, P., Fang, F., Song, W., Chang, Y.H., Han, W.X., Lü, X.T., Liu, Y.Y., Hu, Y.K., 2014. Response of carbon dioxide emissions to sheep grazing and N application in an alpine grassland - Part 1: Effect of sheep grazing. Biogeosciences 11, 1743–1750. https://doi.org/10.5194/bg-11-1743-2014

Gordon, I.J., Pérez-Barbería, F.J., Manning, A.D., 2021. Rewilding Lite: Using Traditional Domestic Livestock to Achieve Rewilding Outcomes. Sustainability 13, 3347. https://doi.org/10.3390/su13063347

Gorelick, N., Hancher, M., Dixon, M., Ilyushchenko, S., Thau, D., Moore, R., 2017. Google Earth Engine: Planetary-scale geospatial analysis for everyone. Remote Sens. Environ., Big Remotely Sensed Data: tools, applications and experiences 202, 18–27. https://doi.org/10.1016/j.rse.2017.06.031

Gough, L., Moore, J.C., Shaver, G.R., Simpson, R.T., Johnson, D.R., 2012. Above- and belowground responses of arctic tundra ecosystems to altered soil nutrients and mammalian herbivory. Ecology 93, 1683–1694. https://doi.org/10.1890/11-1631.1

Gould, I.J., Quinton, J.N., Weigelt, A., De Deyn, G.B., Bardgett, R.D., 2016. Plant diversity and root traits benefit physical properties key to soil function in grasslands. Ecol. Lett. 19, 1140–1149. https://doi.org/10.1111/ele.12652

Griscom, B.W., Adams, J., Ellis, P.W., Houghton, R.A., Lomax, G., Miteva, D.A., Schlesinger, W.H., Shoch, D., Siikamäki, J.V., […], Fargione, J., 2017. Natural climate solutions. Proc. Natl. Acad. Sci. 114, 11645–11650. https://doi.org/10.1073/pnas.1710465114

Guðmundsson, J., Óskarsson, H., Pagneux, E.P., Þórðarson, H.N., 2026. Regional Estimates of CO_2 Fluxes and Stock Losses from Drained Uncultivated Peatlands in West Iceland. Environ. Model. Assess. https://doi.org/10.1007/s10666-026-10105-w

Gunnarsson, T.G., Arnalds, Ó., Appleton, G., Méndez, V., Gill, J.A., 2015. Ecosystem recharge by volcanic dust drives broad-scale variation in bird abundance. Ecol. Evol. 5, 2386–2396. https://doi.org/10.1002/ece3.1523

Guyonnet, J.P., Cantarel, A.A.M., Simon, L., Haichar, F. el Z., 2018. Root exudation rate as functional trait involved in plant nutrient-use strategy classification. Ecol. Evol. 8, 8573–8581. https://doi.org/10.1002/ece3.4383

Hamilton III, E.W., Frank, D.A., 2001. Can Plants Stimulate Soil Microbes and Their Own Nutrient Supply? Evidence from a Grazing Tolerant Grass. Ecology 82, 2397–2402. https://doi.org/10.1890/0012-9658(2001)082%5B2397:CPSSMA%5D2.0.CO;2

Hamilton III, E.W., Frank, D.A., Hinchey, P.M., Murray, T.R., 2008. Defoliation induces root exudation and triggers positive rhizospheric feedbacks in a temperate grassland. Soil Biol. Biochem. 40, 2865–2873. https://doi.org/10.1016/j.soilbio.2008.08.007

Harning, D.J., Florian, C.R., Geirsdóttir, Á., Thordarson, T., Miller, G.H., Axford, Y., Ólafsdóttir, S., 2025. High-resolution Holocene record based on detailed tephrochronology from Torfdalsvatn, north Iceland, reveals natural and anthropogenic impacts on terrestrial and aquatic environments. Clim. Past 21, 795–815. https://doi.org/10.5194/cp-21-795-2025

Hawkins, H.-J., Cargill, R.I.M., Van Nuland, M.E., Hagen, S.C., Field, K.J., Sheldrake, M., Soudzilovskaia, N.A., Kiers, E.T., 2023. Mycorrhizal mycelium as a global carbon pool. Curr. Biol. 33, r560–r573. https://doi.org/10.1016/j.cub.2023.02.027

He, M., Zhou, G., Yuan, T., van Groenigen, K.J., Shao, J., Zhou, X., 2020. Grazing intensity significantly changes the C : N : P stoichiometry in grassland ecosystems. Glob. Ecol. Biogeogr. 29, 355–369. https://doi.org/10.1111/geb.13028

Heggenes, J., Odland, A., Chevalier, T., Ahlberg, J., Berg, A., Larsson, H., Bjerketvedt, D.K., 2017. Herbivore grazing—or trampling? Trampling effects by a large ungulate in cold high-latitude ecosystems. Ecol. Evol. 7, 6423–6431. https://doi.org/10.1002/ece3.3130

Hejcman, M., Hejcmanová, P., Pavlů, V., Beneš, J., 2013. Origin and history of grasslands in Central Europe – a review. Grass Forage Sci. 68, 345–363. https://doi.org/10.1111/gfs.12066

Helgadóttir, A., Frankow-Lindberg, B.E., Seppänen, M.M., Søegaard, K., Østrem, L., 2014. European grasslands overview: Nordic region, in: The Future of European Grasslands, Grassland Science in Europe. Aberystwyth, pp. 15–29.

Herzon, I., Raatikainen, K.J., Wehn, S., Rusina, S., Helm, A., Cousins, S.A.O., Rasomavicius, V., 2021. Semi-natural habitats in boreal Europe: a rise of a social-ecological research agenda. Ecol. Soc. 26, 13. https://doi.org/10.5751/ES-12313-260213

Hewins, D.B., Lyseng, M.P., Schoderbek, D.F., Alexander, M., Willms, W.D., Carlyle, C.N., Chang, S.X., Bork, E.W., 2018. Grazing and climate effects on soil organic carbon concentration and particle-size association in northern grasslands. Sci. Rep. 8, 1336. https://doi.org/10.1038/s41598-018-19785-1

Hothorn, T., Bretz, F., Westfall, P., 2008. Simultaneous inference in general parametric models. Biom. J. 50, 346–363. https://doi.org/https://doi.org/10.1002/bimj.200810425

Housego, N.C., Parker, T.C., Street, L.E., Vanguelova, E.I., Mitchell, R.J., 2025. Natural tree colonisation of organo-mineral soils does not provide a net carbon capture benefit at decadal timescales. J. Appl. Ecol. n/a, 1–10. https://doi.org/10.1111/1365-2664.14861

Howison, R.A., Olff, H., Koppel, J. van de, Smit, C., 2017. Biotically driven vegetation mosaics in grazing ecosystems: the battle between bioturbation and biocompaction. Ecol. Monogr. 87, 363–378. https://doi.org/10.1002/ecm.1259

Hu, Z., Li, S., Guo, Q., Niu, S., He, N., Li, L., Yu, G., 2016. A synthesis of the effect of grazing exclusion on carbon dynamics in grasslands in China. Glob. Change Biol. 22, 1385–1393. https://doi.org/10.1111/gcb.13133

Huang, S., Tang, L., Hupy, J.P., Wang, Y., Shao, G., 2021. A commentary review on the use of normalized difference vegetation index (NDVI) in the era of popular remote sensing. J. For. Res. 32, 1–6. https://doi.org/10.1007/s11676-020-01155-1

Huang, X., Xiao, J., Mingguo, M., 2019. Evaluating the Performance of Satellite-Derived Vegetation Indices for Estimating Gross Primary Productivity Using FLUXNET Observations across the Globe. Remote Sens. 11, 1823. https://doi.org/10.3390/rs11151823

Hunziker, M., Arnalds, O., Kuhn, N.J., 2019. Evaluating the carbon sequestration potential of volcanic soils in southern Iceland after birch afforestation. SOIL 5, 223–238. https://doi.org/10.5194/soil-5-223-2019

Hyvarinen, O., Te Beest, M., le Roux, E., Kerley, G., de Groot, E., Vinita, R., Cromsigt, J.P.G.M., 2021. Megaherbivore impacts on ecosystem and Earth system functioning: the current state of the science. Ecography 44, 1579–1594. https://doi.org/10.1111/ecog.05703

Hyvarinen, O., te Beest, M., le Roux, E., Kerley, G.I.H., Findlay, N., Schenkeveld, W.D.C., Trouw, V., Cromsigt, J.P.G.M., 2023. Grazing in a megagrazer-dominated savanna does not reduce soil carbon stocks, even at high intensities. Oikos 2023, e09809. https://doi.org/10.1111/oik.09809

IPCC, 2021. Climate Change 2021: The Physical Science Basis. Contribution of Working Group I to the Sixth Assessment Report of the Intergovernmental Panel on Climate Change, in: Masson-Delmotte, Zhai, P., Pirani, A., Connors, S.L., Péan, C., Berger, S., Caud, N., Chen, Y., Goldfarb, L., Gomis, M.I., Huang, M., Leitzell, K., Lonnoy, E., Matthews, J.B.R., Maycock, T.K., Waterfield, T., Yelekçi, O., Yu, R., Zhou, B. (Eds.), IPCC 6th Assessment Report. Cambridge University Press, Cambridge, United Kingdom and New York, NY, USA, p. 2391. https://doi.org/doi:10.1017/9781009157896

IPCC, 2023. Climate Change 2023: Synthesis Report. Contribution of Working Groups I, II and III to the Sixth Assessment Report of the Intergovernmental Panel on Climate Change. IPCC, Geneva, Switzerland. https://doi.org/doi:%2010.59327/IPCC/AR6-9789291691647

Irving, L.J., 2015. Carbon assimilation, biomass partitioning and productivity in grasses. Agriculture 5, 1116–1134. https://doi.org/10.3390/agriculture5041116

IUSS Working Group WRB, 2022. World Reference Base for Soil Resources. International soil classification system for naming soils and creating legends for soil maps, 4th ed. International Union of Soil Sciences (IUSS), Vienna, Austria.

Iversen, C.M., Sloan, V.L., Sullivan, P.F., Euskirchen, E.S., McGuire, A.D., Norby, R.J., Walker, A.P., Warren, J.M., Wullschleger, S.D., 2015. The unseen iceberg: plant roots in arctic tundra. New Phytol. 205, 34–58. https://doi.org/10.1111/nph.13003

Jackson, R.B., Canadell, J., Ehleringer, J.R., Mooney, H.A., Sala, O.E., Schulze, E.D., 1996. A global analysis of root distributions for terrestrial biomes. Oecologia 108, 389–411. https://doi.org/10.1007/BF00333714

Jackson, R.B., Lajtha, K., Crow, S.E., Hugelius, G., Kramer, M.G., Piñeiro, G., 2017. The Ecology of Soil Carbon: Pools, Vulnerabilities, and Biotic and Abiotic Controls. Annu. Rev. Ecol. Evol. Syst. 48, 419–445. https://doi.org/10.1146/annurev-ecolsys-112414-054234

Janišová, M., Bojko, I., Ivașcu, C.M., Iuga, A., Biro, A.-S., Magnes, M., 2023. Grazing hay meadows: History, distribution, and ecological context. Appl. Veg. Sci. 26, e12723. https://doi.org/10.1111/avsc.12723

Janišová, M., Škodová, I., Magnes, M., Iuga, A., Biro, A.-S., Ivașcu, C.M., Ďuricová, V., Buzhdygan, O.Y., 2025. Role of livestock and traditional management practices in maintaining high nature value grasslands. Biol. Conserv. 309, 111301. https://doi.org/10.1016/j.biocon.2025.111301

Jespersen, R.G., Anderson-Smith, M., Sullivan, P.F., Dial, R.J., Welker, J.M., 2023. NDVI changes in the Arctic: Functional significance in the moist acidic tundra of Northern Alaska. PLOS ONE 18, e0285030. https://doi.org/10.1371/journal.pone.0285030

Jessen, M.-T., Auge, H., Harpole, W.S., Eskelinen, A., 2023. Litter accumulation, not light limitation, drives early plant recruitment. J. Ecol. 111, 1174–1187. https://doi.org/10.1111/1365-2745.14099

Jia, R., Sun, Q., Tang, B., Sun, W., Zhang, E., Lu, X., Wang, Y., Bai, Y., 2026. Enclosure duration modulates the coordination of plant functional traits and soil organic carbon sequestration in semi-arid grasslands. Agric. Ecosyst. Environ. 396, 109985. https://doi.org/10.1016/j.agee.2025.109985

Jian, J., Frissell, M., Hao, D., Tang, X., Berryman, E., Bond-Lamberty, B., 2022. The global contribution of roots to total soil respiration. Glob. Ecol. Biogeogr. 31, 685–699. https://doi.org/10.1111/geb.13454

Jiang, A., Mipam, T.D., Jing, L., Li, Z., Li, T., Liu, J., Tian, L., 2024. Large herbivore grazing accelerates litter decomposition in terrestrial ecosystems. Sci. Total Environ. 922, 171288. https://doi.org/10.1016/j.scitotenv.2024.171288

Jin, C., Jian, J., Bourque, C.P.-A., Zha, T., Dai, L., Yang, Y., Fu, R., Chen, Q., Liu, P., Li, X., Guo, Z., Hu, Z., 2024. Soil autotrophic-to-heterotrophic-respiration ratio and its controlling factors across several terrestrial biomes: A global synthesis. CATENA 242, 108118. https://doi.org/10.1016/j.catena.2024.108118

Jobbágy, E.G., Jackson, R.B., 2000. The vertical distribution of soil organic carbon and its relation to climate and vegetation. Ecol. Appl. 10, 423–436. https://doi.org/10.1890/1051-0761(2000)010%5B0423:TVDOSO%5D2.0.CO;2

Johannesson, T., 2025. Agriculture in Iceland. Conditions, Trends and Characteristics. Rit LbhÍ 179.

Johnson, D.R., Lara, M.J., Shaver, G.R., Batzli, G.O., Shaw, J.D., Tweedie, C.E., 2011. Exclusion of brown lemmings reduces vascular plant cover and biomass in Arctic coastal tundra: resampling of a 50 + year herbivore exclosure experiment near Barrow, Alaska. Environ. Res. Lett. 6, 045507. https://doi.org/10.1088/1748-9326/6/4/045507

Joly, F.-X., Cotrufo, M.F., Garnett, M.H., Johnson, D., Lavallee, J.M., Mueller, C.W., Perks, M.P., Subke, J.-A., 2025. Temperate grassland conversion to conifer forest destabilises mineral soil carbon stocks. J. Environ. Manage. 374, 124149. https://doi.org/10.1016/j.jenvman.2025.124149

Juutinen, S., Aurela, M., Tuovinen, J.-P., Ivakhov, V., Linkosalmi, M., Räsänen, A., Virtanen, T., Mikola, J., Nyman, J.[…], A., Laurila, T., 2022. Variation in CO_2 and CH_4 fluxes among land cover types in heterogeneous Arctic tundra in northeastern Siberia. Biogeosciences 19, 3151–3167. https://doi.org/10.5194/bg-19-3151-2022

Juutinen, S., Virtanen, T., Kondratyev, V., Laurila, T., Linkosalmi, M., Mikola, J., Nyman, J., Räsänen, A., Tuovinen, J.-P., Aurela, M., 2017. Spatial variation and seasonal dynamics of leaf-area index in the arctic tundra-implications for linking ground

observations and satellite images. Environ. Res. Lett. 12, 095002. https://doi.org/10.1088/1748-9326/aa7f85

Kantola, N., Väisänen, M., Leffler, A.J., Welker, J.M., 2024. Contrasting impacts of short- and long-term large herbivore exclusion on understory net CO_2 exchange in a boreal forest. Ecography 2024, e06724. https://doi.org/10.1111/ecog.06724

Karlsen, S.R., Anderson, H.B., Van Der Wal, R., Hansen, B.B., 2018. A new NDVI measure that overcomes data sparsity in cloud-covered regions predicts annual variation in ground-based estimates of high arctic plant productivity. Environ. Res. Lett. 13, 025011. https://doi.org/10.1088/1748-9326/aa9f75

Keller, N., Ásgeirsson, B.U., Jónsdóttir Thianthong, C., Höller, P., Helgadóttir, Á.K., Helgadóttir, D., Helgadóttir, I.R., Einarsdóttir, S.R., Thorlacius, S.L., […], Brink, S.H., 2026. National Inventory Document: Emissions of Greenhouse Gases in Iceland from 1990 to 2024 (UOS-2026:04). Icelandic Environment and Energy Agency, Akureyri.

Kindler, R., Siemens, J., Kaiser, K., Walmsley, D.C., Bernhofer, C., Buchmann, N., Cellier, P., Eugster, W., Gleixner, G., […], Kaupenjohann, M., 2011. Dissolved carbon leaching from soil is a crucial component of the net ecosystem carbon balance. Glob. Change Biol. 17, 1167–1185. https://doi.org/10.1111/j.1365-2486.2010.02282.x

Kitti, H., Forbes, B.C., Oksanen, J., 2009. Long- and short-term effects of reindeer grazing on tundra wetland vegetation. Polar Biol. 32, 253–261. https://doi.org/10.1007/s00300-008-0526-9

Kjær, K.H., Ruter, A.H., Menendez-Serra, M., Vogel, N.A., Ramsøe, A.D., Farnsworth, W.R., Siggaard-Andersen, M.-L., Huang, Z., Korneliussen, T.S., […], Willerslev, E., 2025. Environmental DNA Reveals Reykjavík's Human and Ecological History. https://doi.org/10.1101/2025.10.08.681091

Kleppel, G.S., Frank, D.A., 2022. Structure and functioning of wild and agricultural grazing ecosystems: A comparative review. Front. Sustain. Food Syst. 6, 945514. https://doi.org/10.3389/fsufs.2022.945514

Klink, S., Keller, A.B., Wild, A.J., Baumert, V.L., Gube, M., Lehndorff, E., Meyer, N., Mueller, C.W., Phillips, R.P., Pausch, J., 2022. Stable isotopes reveal that fungal residues contribute more to mineral-associated organic matter pools than plant residues. Soil Biol. Biochem. 168, 108634. https://doi.org/10.1016/j.soilbio.2022.108634

Klopsch, C., Thorhallsdottir, A.G., Thorsteinsson, B., Bardgett, R., Van Der Wal, R., Geirsdóttir, A., 2026a. Research data from PhD thesis Christian Klopsch: The effects of long-term cessation of grazing on carbon dynamics in Icelandic grassland and heathland. https://doi.org/10.5281/zenodo.18793200

Klopsch, C., Thorhallsdottir, A.G., van der Wal, R., Bardgett, R.D., Thorsteinsson, B., Geirsdottir, A., 2026b. Long-term cessation of grazing reduces net carbon uptake in northern grassland and heathland. Agriculture, Ecosystems & Environment 407, 110441. https://doi.org/10.1016/j.agee.2026.110441

Klumpp, K., Fontaine, S., Attard, E., Le Roux, X., Gleixner, G., Soussana, J.-F., 2009. Grazing triggers soil carbon loss by altering plant roots and their control on soil microbial community. J. Ecol. 97, 876–885. https://doi.org/10.1111/j.1365-2745.2009.01549.x

Kodl, G., Streeter, R., Cutler, N., Bolch, T., 2024. Arctic tundra shrubification can obscure increasing levels of soil erosion in NDVI assessments of land cover derived from satellite imagery. Remote Sens. Environ. 301, 113935. https://doi.org/10.1016/j.rse.2023.113935

Kögel-Knabner, I., Amelung, W., 2021. Soil organic matter in major pedogenic soil groups. Geoderma 384, 114785. https://doi.org/10.1016/j.geoderma.2020.114785
Koltz, A.M., Gough, L., McLaren, J.R., 2022. Herbivores in Arctic ecosystems: Effects of climate change and implications for carbon and nutrient cycling. Ann. N. Y. Acad. Sci. 1516, 28–47. https://doi.org/10.1111/nyas.14863
Kopittke, G.R., Tietema, A., van Loon, E.E., Kalbitz, K., 2013. The age of managed heathland communities: implications for carbon storage? Plant Soil 369, 219–230. https://doi.org/10.1007/s11104-012-1558-z
Kou, X., Morriën, E., Tian, Y., Zhang, X., Lu, C., Xie, H., Liang, W., Li, Q., Liang, C., 2023. Exogenous carbon turnover within the soil food web strengthens soil carbon sequestration through microbial necromass accumulation. Glob. Change Biol. 29, 4069–4080. https://doi.org/10.1111/gcb.16749
Kristensen, J.Å., Barbero-Palacios, L., Barrio, I.C., Jacobsen, I.B.D., Kerby, J.T., López-Blanco, E., Malhi, Y., Le Moullec, M., Mueller, C.W., Post, E., Raundrup, K., Macias-Fauria, M., 2024. Tree planting is no climate solution at northern high latitudes. Nat. Geosci. 17, 1087–1092. https://doi.org/10.1038/s41561-024-01573-4
Kristensen, J.Å., Svenning, J.-C., Georgiou, K., Malhi, Y., 2022. Can large herbivores enhance ecosystem carbon persistence? Trends Ecol. Evol. 37, 117–128. https://doi.org/10.1016/j.tree.2021.09.006
Krzic, M., Lamagna, S.F., Newman, R.F., Bradfield, G., Wallace, B.M., 2014. Long-term grazing effects on rough fescue grassland soils in southern British Columbia. Can. J. Soil Sci. 94, 337–345. https://doi.org/10.4141/cjss2013-019
Kutsch, W.L., Bahn, M., Heinemeyer, A., 2009. Soil Carbon Dynamics: An Integrated Methodology. Cambridge University Press.
Kuznetsova, A., Brockhoff, P.B., Christensen, R.H.B., 2017. lmerTest package: Tests in linear mixed effects models. J. Stat. Softw. 82, 1–26. https://doi.org/10.18637/jss.v082.i13
Kytöviita, M.-M., and Olofsson, J., 2021. Idiosyncratic responses to simulated herbivory by root fungal symbionts in a subarctic meadow. Arct. Antarct. Alp. Res. 53, 80–92. https://doi.org/10.1080/15230430.2021.1878738
Lachaise, T., Bergmann, J., Hölzel, N., Klaus, V.H., Kleinebecker, T., Rillig, M.C., van Kleunen, M., 2022. Soil conditions drive below-ground trait space in temperate agricultural grasslands. J. Ecol. 110, 1189–1200. https://doi.org/10.1111/1365-2745.13862
Lai, L., Kumar, S., 2020. A global meta-analysis of livestock grazing impacts on soil properties. PLOS ONE 15, e0236638. https://doi.org/10.1371/journal.pone.0236638
Lal, R., 2018. Digging deeper: A holistic perspective of factors affecting soil organic carbon sequestration in agroecosystems. Glob. Change Biol. 24, 3285–3301. https://doi.org/10.1111/gcb.14054
Lal, R., Monger, C., Nave, L., Smith, P., 2021. The role of soil in regulation of climate. Philos. Trans. R. Soc. B-Biol. Sci. 376, 20210084. https://doi.org/10.1098/rstb.2021.0084
Lange, M., Eisenhauer, N., Sierra, C.A., Bessler, H., Engels, C., Griffiths, R.I., Mellado-Vázquez, P.G., Malik, A.A., Roy, J., […], Gleixner, G., 2015. Plant diversity increases soil microbial activity and soil carbon storage. Nat. Commun. 6, 6707. https://doi.org/10.1038/ncomms7707
Lara, M.J., Johnson, D.R., Andresen, C., Hollister, R.D., Tweedie, C.E., 2017. Peak season carbon exchange shifts from a sink to a source following 50+ years of herbivore

exclusion in an Arctic tundra ecosystem. J. Ecol. 105, 122–131. https://doi.org/10.1111/1365-2745.12654
Lavallee, J.M., Soong, J.L., Cotrufo, M.F., 2020. Conceptualizing soil organic matter into particulate and mineral-associated forms to address global change in the 21st century. Glob. Change Biol. 26, 261–273. https://doi.org/10.1111/gcb.14859
Leblans, N.I.W., Sigurdsson, B.D., Aerts, R., Vicca, S., Magnússon, B., Janssens, I.A., 2017. Icelandic grasslands as long-term C sinks under elevated organic N inputs. Biogeochemistry 134, 279–299. https://doi.org/10.1007/s10533-017-0362-5
Lehmann, J., Hansel, C.M., Kaiser, C., Kleber, M., Maher, K., Manzoni, S., Nunan, N., Reichstein, M., Schimel, J.P., Torn, M.S., Wieder, W.R., Kögel-Knabner, I., 2020. Persistence of soil organic carbon caused by functional complexity. Nat. Geosci. 13, 529–534. https://doi.org/10.1038/s41561-020-0612-3
Lenth, R.V., 2023. emmeans: Estimated marginal means, aka least-squares means.
Li, Q., Larsen, K.S., Kopittke, G., Van Loon, E., Tietema, A., 2023. Long-term temporal patterns in ecosystem carbon flux components and overall balance in a heathland ecosystem. Sci. Total Environ. 875, 162658. https://doi.org/10.1016/j.scitotenv.2023.162658
Li, S., Xing, T., Sa, R., Zhang, Y., Chen, H., Jin, K., Shao, Q., Tang, S., Wang, C., 2024. Effects of grazing on soil respiration in global grassland ecosystems. Soil Tillage Res. 238, 106033. https://doi.org/10.1016/j.still.2024.106033
Li, X., Zhang, X., Wu, J., Shen, Z., Zhang, Y., Xu, X., Fan, Y., Zhao, Y., Yan, W., 2011. Root biomass distribution in alpine ecosystems of the northern Tibetan Plateau. Environ. Earth Sci. 64, 1911–1919. https://doi.org/10.1007/s12665-011-1004-1
Liang, C., Amelung, W., Lehmann, J., Kästner, M., 2019. Quantitative assessment of microbial necromass contribution to soil organic matter. Glob. Change Biol. 25, 3578–3590. https://doi.org/10.1111/gcb.14781
Liang, C., Zhu, X., 2021. The soil Microbial Carbon Pump as a new concept for terrestrial carbon sequestration. Sci. China-Earth Sci. 64, 545–558. https://doi.org/10.1007/s11430-020-9705-9
Lindahl, B.D., Kyaschenko, J., Varenius, K., Clemmensen, K.E., Dahlberg, A., Karltun, E., Stendahl, J., 2021. A group of ectomycorrhizal fungi restricts organic matter accumulation in boreal forest. Ecol. Lett. 24, 1341–1351. https://doi.org/10.1111/ele.13746
Lindborg, R., Hartel, T., Helm, A., Prangel, E., Reitalu, T., Ripoll-Bosch, R., 2023. Ecosystem services provided by semi-natural and intensified grasslands: Synergies, trade-offs and linkages to plant traits and functional richness. Appl. Veg. Sci. 26, e12729. https://doi.org/10.1111/avsc.12729
Linder, H.P., Lehmann, C.E.R., Archibald, S., Osborne, C.P., Richardson, D.M., 2018. Global grass (Poaceae) success underpinned by traits facilitating colonization, persistence and habitat transformation: Grass success. Biol. Rev. 93, 1125–1144. https://doi.org/10.1111/brv.12388
Lisiecki, L.E., 2010. A benthic δ^{13} C-based proxy for atmospheric pCO_2 over the last 1.5 Myr. Geophys. Res. Lett. 37, 2010GL045109. https://doi.org/10.1029/2010GL045109
Liu, H., Zang, R., Chen, H.Y.H., 2016. Effects of grazing on photosynthetic features and soil respiration of rangelands in the Tianshan Mountains of Northwest China. Sci. Rep. 6, 30087. https://doi.org/10.1038/srep30087
Liu, X.-J.A., Finley, B.K., Mau, R.L., Schwartz, E., Dijkstra, P., Bowker, M.A., Hungate, B.A., 2020. The soil priming effect: Consistent across ecosystems, elusive

mechanisms. Soil Biol. Biochem. 140, 107617. https://doi.org/10.1016/j.soilbio.2019.107617
Liu, Yan, Cordero, I., Bardgett, R.D., 2023. Defoliation and fertilisation differentially moderate root trait effects on soil abiotic and biotic properties. J. Ecol. n/a. https://doi.org/10.1111/1365-2745.14215
Liu, Yuzhen, Zhao, X., Liu, W., Yang, X., Feng, B., Zhang, C., Yu, Y., Cao, Q., Sun, S., Degen, A.A., Shang, Z., Dong, Q., 2023. Herbivore assemblages affect soil microbial communities by altering root biomass and available nutrients in an alpine meadow. Front. Plant Sci. 14. https://doi.org/10.3389/fpls.2023.1117372
Lockwood, T., Elias, J.L., Stone, M., Kemp, H.R., Spiers, M., Davess, B., Izard, N., Mason, E., Hartill, J., Morecroft, M.D., 2026. Semi-natural grasslands as a nature-based solution for climate change mitigation: An assessment of carbon and plant communities across age gradients. Agric. Ecosyst. Environ. 395, 109887. https://doi.org/10.1016/j.agee.2025.109887
Løvschal, M., Damgaard, C.F., 2022. Mapping the ecological resilience of Atlantic postglacial heathlands. J. Appl. Ecol. 59, 2825–2838. https://doi.org/10.1111/1365-2664.14278
Ma, F., Zhang, R., Svenning, J.-C., Zhang, F., He, Y., Wang, J., Tian, D., Zhou, Q., Niu, S., 2024. Decoupled responses of the stability of above- and belowground productivity to drought and clipping in an alpine meadow. J. Ecol. 112, 2585–2597. https://doi.org/10.1111/1365-2745.14389
Ma, S., He, F., Tian, D., Zou, D., Yan, Z., Yang, Y., Zhou, T., Huang, K., Shen, H., Fang, J., 2018. Variations and determinants of carbon content in plants: a global synthesis. Biogeosciences 15, 693–702. https://doi.org/10.5194/bg-15-693-2018
Maes, S.L., Dietrich, J., Midolo, G., Schwieger, S., Kummu, M., Vandvik, V., Aerts, R., Althuizen, I.H.J., Biasi, C., […], Dorrepaal, E., 2024. Environmental drivers of increased ecosystem respiration in a warming tundra. Nature 629, 105–113. https://doi.org/10.1038/s41586-024-07274-7
Malek, Ž., Schulze, K., Bartl, H., Keja, W., Petersen, J.-E., Tieskens, K., Jones, G., Verburg, P.H., 2024. Mapping livestock grazing in semi-natural areas in the European Union and United Kingdom. Landsc. Ecol. 39, 31. https://doi.org/10.1007/s10980-024-01810-6
Malhi, Y., Lander, T., le Roux, E., Stevens, N., Macias-Fauria, M., Wedding, L., Girardin, C., Kristensen, J.Å., Sandom, C.J., Evans, T.D., Svenning, J.-C., Canney, S., 2022. The role of large wild animals in climate change mitigation and adaptation. Curr. Biol. 32, R181–R196. https://doi.org/10.1016/j.cub.2022.01.041
Malhotra, A., Moore, J.A.M., Weintraub-Leff, S., Georgiou, K., Berhe, A.A., Billings, S.A., de Graaff, M.-A., Fraterrigo, J.M., Grandy, A.S., […], Jackson, R.B., 2025. Fine root and soil carbon stocks are positively related in grasslands but not in forests. Commun. Earth Environ. 6, 497. https://doi.org/10.1038/s43247-025-02486-9
Maliniemi, T., Kapfer, J., Saccone, P., Skog, A., Virtanen, R., 2018. Long-term vegetation changes of treeless heath communities in northern Fennoscandia: Links to climate change trends and reindeer grazing. J. Veg. Sci. 29, 469–479. https://doi.org/10.1111/jvs.12630
Marshall, F., Reid, R.E.B., Goldstein, S., Storozum, M., Wreschnig, A., Hu, L., Kiura, P., Shahack-Gross, R., Ambrose, S.H., 2018. Ancient herders enriched and restructured African grasslands. Nature 561, 387–390. https://doi.org/10.1038/s41586-018-0456-9

Marteinsdóttir, B., Barrio, I.C., Jónsdóttir, I.S., 2017. Assessing the ecological impacts of extensive sheep grazing in Iceland. Icel. Agric. Sci. 30, 55–72. https://doi.org/10.16886/IAS.2017.07

Matthus, E., Zwetsloot, M., Delory, B.M., Hennecke, J., Andraczek, K., Henning, T., Mommer, L., Weigelt, A., Bergmann, J., 2025. Revisiting the root economics space—its applications, extensions and nuances advance our understanding of fine-root functioning. Plant Soil 514, 1–27. https://doi.org/10.1007/s11104-025-07379-6

Matus, F., Rumpel, C., Neculman, R., Panichini, M., Mora, M.L., 2014. Soil carbon storage and stabilisation in andic soils: A review. CATENA 120, 102–110. https://doi.org/10.1016/j.catena.2014.04.008

Matus, F.J., Paz-Pellat, F., Covaleda, S., Etchevers, J.D., Hidalgo, C., Báez, A., 2024. Upper limit of mineral-associated organic carbon in temperate and sub-tropical soils: How far is it? Geoderma Reg. 37, e00811. https://doi.org/10.1016/j.geodrs.2024.e00811

McCormack, M.L., Iversen, C.M., 2019. Physical and Functional Constraints on Viable Belowground Acquisition Strategies. Front. Plant Sci. 10. https://doi.org/10.3389/fpls.2019.01215

McKenzie, N., Coughlan, K., Cresswell, H., 2002. Soil physical measurement and interpretation for land evaluation. Csiro Publishing.

McNaughton, S.J., 1979. Grazing as an optimization process: Grass-ungulate relationships in the Serengeti. Am. Nat. 113, 691–703.

McNaughton, S.J., 1983. Compensatory plant growth as a response to herbivory. Oikos 40, 329–336. https://doi.org/10.2307/3544305

McNaughton, S.J., 1985. Ecology of a grazing ecosystem: The Serengeti. Ecol. Monogr. 55, 260–294. https://doi.org/10.2307/1942578

McNaughton, S.J., Banyikwa, F.F., McNaughton, M.M., 1998. Root Biomass and Productivity in a Grazing Ecosystem: The Serengeti. Ecology 79, 587–592. https://doi.org/10.1890/0012-9658(1998)079%5B0587:RBAPIA%5D2.0.CO;2

McSherry, M.E., Ritchie, M.E., 2013. Effects of grazing on grassland soil carbon: a global review. Glob. Change Biol. 19, 1347–1357. https://doi.org/10.1111/gcb.12144

Medina-Roldán, E., Paz-Ferreiro, J., Bardgett, R.D., 2012. Grazing exclusion affects soil and plant communities, but has no impact on soil carbon storage in an upland grassland. Agric. Ecosyst. Environ. 149, 118–123. https://doi.org/10.1016/j.agee.2011.12.012

Mekonnen, Z.A., Riley, W.J., Berner, L.T., Bouskill, N.J., Torn, M.S., Iwahana, G., Breen, A.L., Myers-Smith, I.H., Criado, M.G., […], Grant, R.F., 2021. Arctic tundra shrubification: a review of mechanisms and impacts on ecosystem carbon balance. Environ. Res. Lett. 16, 053001. https://doi.org/10.1088/1748-9326/abf28b

Metcalfe, D.B., Olofsson, J., 2015. Distinct impacts of different mammalian herbivore assemblages on arctic tundra CO_2 exchange during the peak of the growing season. Oikos 124, 1632–1638. https://doi.org/10.1111/oik.02085

Meyer, G.A., Leroux, S.J., 2024. A theory for context-dependent effects of mammalian trampling on ecosystem nitrogen cycling. J. Anim. Ecol. 93, 583–598. https://doi.org/10.1111/1365-2656.14066

Meyer, N., Welp, G., Amelung, W., 2018. The Temperature Sensitivity (Q10) of Soil Respiration: Controlling Factors and Spatial Prediction at Regional Scale Based on Environmental Soil Classes. Glob. Biogeochem. Cycles 32, 306–323. https://doi.org/10.1002/2017GB005644

Miao, L., Sun, Z., Ren, Y., Schierhorn, F., Müller, D., 2021. Grassland greening on the Mongolian Plateau despite higher grazing intensity. Land Degrad. Dev. 32, 792–802. https://doi.org/10.1002/ldr.3767

Mikola, J., Setälä, H., Virkajärvi, P., Saarijärvi, K., Ilmarinen, K., Voigt, W., Vestberg, M., 2009. Defoliation and patchy nutrient return drive grazing effects on plant and soil properties in a dairy cow pasture. Ecol. Monogr. 79, 221–244. https://doi.org/10.1890/08-1846.1

Milchunas, D.G., Lauenroth, W.K., 1993. Quantitative Effects of Grazing on Vegetation and Soils Over a Global Range of Environments. Ecol. Monogr. 63, 327–366. https://doi.org/10.2307/2937150

Min, E., Wilcots, M.E., Naeem, S., Gough, L., McLaren, J.R., Rowe, R.J., Rastetter, E.B., Boelman, N.T., Griffin, K.L., 2021. Herbivore absence can shift dry heath tundra from carbon source to sink during peak growing season. Environ. Res. Lett. 16, 024027. https://doi.org/10.1088/1748-9326/abd3d0

Mipam, T.-D., Zhong, L.-L., Liu, J.-Q., Miehe, G., Tian, L.-M., 2019. Productive Overcompensation of Alpine Meadows in Response to Yak Grazing in the Eastern Qinghai-Tibet Plateau. Front. Plant Sci. 10. https://doi.org/https://doi.org/10.3389/fpls.2019.00925

Mutillod, C., Buisson, E., Tatin, L., Mahy, G., Dufrêne, M., Mesléard, F., Dutoit, T., 2024. Managed as wild, horses influence grassland vegetation differently than domestic herds. Biol. Conserv. 290, 110469. https://doi.org/10.1016/j.biocon.2024.110469

Myers-Smith, I.H., Forbes, B.C., Wilmking, M., Hallinger, M., Lantz, T., Blok, D., Tape, K.D., Macias-Fauria, M., Sass-Klaassen, U., […], Hik, D.S., 2011. Shrub expansion in tundra ecosystems: dynamics, impacts and research priorities. Environ. Res. Lett. 6, 045509. https://doi.org/10.1088/1748-9326/6/4/045509

Myers-Smith, I.H., Hik, D.S., 2018. Climate warming as a driver of tundra shrubline advance. J. Ecol. 106, 547–560. https://doi.org/10.1111/1365-2745.12817

Myrsky, E., Mikola, J., Kaarlejärvi, E., Olofsson, J., Sjögersten, S., Tupek, B., Männistö, M.K., Stark, S., 2024. Higher vascular plant abundance associated with decreased ecosystem respiration after 20 years of warming in the forest–tundra ecotone. Funct. Ecol. 38, 219–232. https://doi.org/10.1111/1365-2435.14466

Nakhavali, M., Lauerwald, R., Regnier, P., Guenet, B., Chadburn, S., Friedlingstein, P., 2021. Leaching of dissolved organic carbon from mineral soils plays a significant role in the terrestrial carbon balance. Glob. Change Biol. 27, 1083–1096. https://doi.org/10.1111/gcb.15460

Nestola, E., Calfapietra, C., Emmerton, C.A., Wong, C.Y.S., Thayer, D.R., Gamon, J.A., 2016. Monitoring Grassland Seasonal Carbon Dynamics, by Integrating MODIS NDVI, Proximal Optical Sampling, and Eddy Covariance Measurements. Remote Sens. 8, 260. https://doi.org/10.3390/rs8030260

Nevalainen, O., Niemitalo, O., Fer, I., Juntunen, A., Mattila, T., Koskela, O., Kukkamäki, J., Höckerstedt, L., Mäkelä, L., […], Liski, J., 2022. Towards agricultural soil carbon monitoring, reporting, and verification through the Field Observatory Network (FiON). Geosci. Instrum. Methods Data Syst. 11, 93–109. https://doi.org/10.5194/gi-11-93-2022

Newton, A.C., Stewart, G.B., Myers, G., Diaz, A., Lake, S., Bullock, J.M., Pullin, A.S., 2009. Impacts of grazing on lowland heathland in north-west Europe. Biol. Conserv. 142, 935–947. https://doi.org/10.1016/j.biocon.2008.10.018

Niu, W., Ding, J., Fu, B., Zhao, W., Eldridge, D., 2025. Global effects of livestock grazing on ecosystem functions vary with grazing management and environment. Agric. Ecosyst. Environ. 378, 109296. https://doi.org/10.1016/j.agee.2024.109296

Norderhaug, A., Clemmensen, K.E., Kardol, P., Thorhallsdottir, A.G., Aslaksen, I., 2023. Carbon sequestration potential and the multiple functions of Nordic grasslands. Clim. Change 176, 55. https://doi.org/10.1007/s10584-023-03537-w

Normand, S., Høye, T.T., Forbes, B.C., Bowden, J.J., Davies, A.L., Odgaard, B.V., Riede, F., Svenning, J.-C., Treier, U.A., Willerslev, R., Wischnewski, J., 2017. Legacies of Historical Human Activities in Arctic Woody Plant Dynamics. Annu. Rev. Environ. Resour. 42, 541–567. https://doi.org/10.1146/annurev-environ-110615-085454

Oksanen, J., Simpson, G.L., Blanchet, F.G., Kindt, R., Legendre, P., Minchin, P.R., O'Hara, R.B., Solymos, P., Stevens, M.H.H., […], Weedon, J., 2025. vegan: Community ecology package (manual).

Olofsson, J., Post, E., 2018. Effects of large herbivores on tundra vegetation in a changing climate, and implications for rewilding. Philos. Trans. R. Soc. Lond. B. Biol. Sci. 373, 20170437. https://doi.org/10.1098/rstb.2017.0437

Oñatibia, G.R., Reyes, M.F., Aguiar, M.R., 2017. Fine-scale root community structure and below-ground responses to grazing show independence from above-ground patterns. J. Veg. Sci. 28, 1097–1106. https://doi.org/10.1111/jvs.12571

Óskarsson, B.V., Riishuus, M.S., Arnalds, Ó., 2012. Climate-dependent chemical weathering of volcanic soils in Iceland. Geoderma 189–190, 635–651. https://doi.org/10.1016/j.geoderma.2012.05.030

Óskarsson, H., Arnalds, Ó., Gudmundsson, J., Gudbergsson, G., 2004. Organic carbon in Icelandic andosols: geographical variation and impact of erosion. CATENA, Volcanic Soil Resources: Occurrence, Development and Properties 56, 225–238. https://doi.org/10.1016/j.catena.2003.10.013

Ottaviani, G., Molina-Venegas, R., Charles-Dominique, T., Chelli, S., Campetella, G., Canullo, R., Klimešová, J., 2020. The neglected belowground dimension of plant dominance. Trends Ecol. Evol. 35, 763–766. https://doi.org/10.1016/j.tree.2020.06.006

Ottoson, J.G., Sveinsdottir, A., Hardardottir, M., 2016. Vistgerðir á Íslandi (No. 54), Fjölrit Náttúrufræðistofnunar. Náttúrufræðistofnun Íslands, Garðabær.

Owen-Smith, N., 1987. Pleistocene extinctions: the pivotal role of megaherbivores. Paleobiology 13, 351–362. https://doi.org/10.1017/S0094837300008927

Parada, J., Neaman, A., Zamorano, D., Nájera, F., Matus, F., 2024. Management and liming-induced changes in organo-Al/Fe complexes and amorphous mineral-associated organic carbon: Implications for carbon sequestration in volcanic soils. Soil Tillage Res. 242, 106133. https://doi.org/10.1016/j.still.2024.106133

Parker, T.C., Subke, J.-A., Wookey, P.A., 2015. Rapid carbon turnover beneath shrub and tree vegetation is associated with low soil carbon stocks at a subarctic treeline. Glob. Change Biol. 21, 2070–2081. https://doi.org/10.1111/gcb.12793

Parker, T.C., Thurston, A.M., Raundrup, K., Subke, J.-A., Wookey, P.A., Hartley, I.P., 2021. Shrub expansion in the Arctic may induce large-scale carbon losses due to changes in plant-soil interactions. Plant Soil 463, 643–651. https://doi.org/10.1007/s11104-021-04919-8

Pärtel, M., Bruun, H.H., Sammul, M., 2005. Biodiversity in temperate European grasslands: origin and conservation. Grassl. Sci. Eur. 10, 1–14.

Peco, B., Navarro, E., Carmona, C.P., Medina, N.G., Marques, M.J., 2017. Effects of grazing abandonment on soil multifunctionality: The role of plant functional traits. Agric. Ecosyst. Environ. 249, 215–225. https://doi.org/10.1016/j.agee.2017.08.013

Penner, J.F., Frank, D.A., 2021. Density-dependent plant growth drives grazer stimulation of aboveground net primary production in Yellowstone grasslands. Oecologia 196, 851–861. https://doi.org/10.1007/s00442-021-04960-5

Petit Bon, M., Beard, K.H., Bråthen, K.A., Lee, H., Jónsdóttir, I.S., 2025. Goose grubbing and warming suppress summer net ecosystem CO_2 uptake differentially across high-Arctic tundra habitats. Ecology 106, e4498. https://doi.org/10.1002/ecy.4498

Petit Bon, M., Gunnarsdotter Inga, K., Jónsdóttir, I.S., Utsi, T.A., Soininen, E.M., Bråthen, K.A., 2020. Interactions between winter and summer herbivory affect spatial and temporal plant nutrient dynamics in tundra grassland communities. Oikos 129, 1229–1242. https://doi.org/10.1111/oik.07074

Petit Bon, M., Hansen, B.B., Loonen, M.J.J.E., Petraglia, A., Bråthen, K.A., Böhner, H., Layton-Matthews, K., Beard, K.H., Le Moullec, M., Jónsdóttir, I.S., van der Wal, R., 2023. Long-term herbivore removal experiments reveal how geese and reindeer shape vegetation and ecosystem CO-fluxes in high-Arctic tundra. J. Ecol. 111, 2627–2642. https://doi.org/10.1111/1365-2745.14200

Pettorelli, N., 2013. The Normalized Difference Vegetation Index. OUP Oxford.

Pillar, V.D., Overbeck, G.E., 2025. Nature conservation policies are biased toward forests and neglect grassy ecosystems worldwide. Science 388, eadx7441. https://doi.org/10.1126/science.adx7441

Pillar, V.D., Winck, B.R., 2026. Natural grasslands used for grazing livestock can mitigate climate change. Science 391, eaea8344. https://doi.org/10.1126/science.aea8344

Piñeiro, G., Paruelo, J.M., Oesterheld, M., Jobbágy, E.G., 2010. Pathways of grazing effects on soil organic carbon and nitrogen. Rangel. Ecol. Manag. 63, 109–119. https://doi.org/10.2111/08-255.1

Plieninger, T., Draux, H., Fagerholm, N., Bieling, C., Bürgi, M., Kizos, T., Kuemmerle, T., Primdahl, J., Verburg, P.H., 2016. The driving forces of landscape change in Europe: A systematic review of the evidence. Land Use Policy 57, 204–214. https://doi.org/10.1016/j.landusepol.2016.04.040

Poeplau, C., Don, A., Vesterdal, L., Leifeld, J., Van Wesemael, B., Schumacher, J., Gensior, A., 2011. Temporal dynamics of soil organic carbon after land-use change in the temperate zone – carbon response functions as a model approach. Glob. Change Biol. 17, 2415–2427. https://doi.org/10.1111/j.1365-2486.2011.02408.x

Poeplau, C., Germer, K., Schwarz, K.-U., 2019. Seasonal dynamics and depth distribution of belowground biomass carbon and nitrogen of extensive grassland and a Miscanthus plantation. Plant Soil 440, 119–133. https://doi.org/10.1007/s11104-019-04074-1

Poirier, V., Roumet, C., Munson, A.D., 2018. The root of the matter: Linking root traits and soil organic matter stabilization processes. Soil Biol. Biochem. 120, 246–259. https://doi.org/10.1016/j.soilbio.2018.02.016

Porensky, L.M., McGee, R., Pellatz, D.W., 2020. Long-term grazing removal increased invasion and reduced native plant abundance and diversity in a sagebrush grassland. Glob. Ecol. Conserv. 24, e01267. https://doi.org/10.1016/j.gecco.2020.e01267

Price, J.N., Sitters, J., Ohlert, T., Tognetti, P.M., Brown, C.S., Seabloom, E.W., Borer, E.T., Prober, S.M., Bakker, E.S., […], Wardle, G.M., 2022. Evolutionary history of grazing and resources determine herbivore exclusion effects on plant diversity. Nat. Ecol. Evol. 6, 1290–1298. https://doi.org/10.1038/s41559-022-01809-9

Pucheta, E., Bonamici, I., Cabido, M., Díaz, S., 2004. Below-ground biomass and productivity of a grazed site and a neighbouring ungrazed exclosure in a grassland in

central Argentina. Austral Ecol. 29, 201–208. https://doi.org/10.1111/j.1442-9993.2004.01337.x

Pumpanen, J., Kolari, P., Ilvesniemi, H., Minkkinen, K., Vesala, T., Niinistö, S., Lohila, A., Larmola, T., Morero, M., […], Hari, P., 2004. Comparison of different chamber techniques for measuring soil CO_2 efflux. Agric. For. Meteorol. 123, 159–176. https://doi.org/10.1016/j.agrformet.2003.12.001

Pumpanen, J., Longdoz, B., L. Kutsch, W., 2010. Field measurements of soil respiration: principles and constraints, potentials and limitations of different methods, in: Heinemeyer, A., Bahn, M., Kutsch, W.L. (Eds.), Soil Carbon Dynamics: An Integrated Methodology. Cambridge University Press, Cambridge, pp. 16–33. https://doi.org/10.1017/CBO9780511711794.003

QGIS Development Team, 2025. QGIS Geographic Information System (Version 3.3434). Available from https://www.qgis.org.

Qi, M., Gadd, M., De Martini, D., Davis, K.J., Xiong, B., Rosen, A., Krishna Moorthy, S.M., Hawes, N., Salguero-Gómez, R., 2025. Biodiversity research requires more motors in air, water and on land. Methods Ecol. Evol. n/a. https://doi.org/10.1111/2041-210x.70217

Qi, Y., Wei, W., Chen, C., Chen, L., 2019. Plant root-shoot biomass allocation over diverse biomes: A global synthesis. Glob. Ecol. Conserv. 18, e00606. https://doi.org/10.1016/j.gecco.2019.e00606

Qu, Q., Deng, L., Shangguan, Z., Sun, J., He, J., Wang, K., Zhou, Z., Li, J., Peñuelas, J., 2024. Belowground C sequestrations response to grazing exclusion in global grasslands: Dynamics and mechanisms. Agric. Ecosyst. Environ. 360, 108771. https://doi.org/10.1016/j.agee.2023.108771

Quin, S.L.O., Artz, R.R.E., Coupar, A.M., Woodin, S.J., 2015. *Calluna vulgaris*-dominated upland heathland sequesters more CO_2 annually than grass-dominated upland heathland. Sci. Total Environ. 505, 740–747. https://doi.org/10.1016/j.scitotenv.2014.10.037

R Core Team, 2024. R: A language and environment for statistical computing (Version 4.3.3). Available from https://www.r-project.org.

Radville, L., Post, E., Eissenstat, D.M., 2016. Root phenology in an Arctic shrub-graminoid community: the effects of long-term warming and herbivore exclusion. Clim. Change Responses 3, 4. https://doi.org/10.1186/s40665-016-0017-0

Rae, J.W.B., Zhang, Y.G., Liu, X., Foster, G.L., Stoll, H.M., Whiteford, R.D.M., 2021. Atmospheric CO_2 over the past 66 million years from marine archives. Annu. Rev. Earth Planet. Sci. 49, 609–641. https://doi.org/10.1146/annurev-earth-082420-063026

Räsänen, A., Juutinen ,S., Aurela ,M., and Virtanen, T., 2019. Predicting aboveground biomass in Arctic landscapes using very high spatial resolution satellite imagery and field sampling. Int. J. Remote Sens. 40, 1175–1199. https://doi.org/10.1080/01431161.2018.1524176

Rasse, D.P., Rumpel, C., Dignac, M.-F., 2005. Is soil carbon mostly root carbon? Mechanisms for a specific stabilisation. Plant Soil 269, 341–356. https://doi.org/10.1007/s11104-004-0907-y

Ravenek, J.M., Mommer, L., Visser, E.J.W., van Ruijven, J., van der Paauw, J.W., Smit-Tiekstra, A., de Caluwe, H., de Kroon, H., 2016. Linking root traits and competitive success in grassland species. Plant Soil 407, 39–53. https://doi.org/10.1007/s11104-016-2843-z

Raynolds, M., Magnússon, B., Metúsalemsson, S., Magnússon, S., 2015. Warming, Sheep and Volcanoes: Land Cover Changes in Iceland Evident in Satellite NDVI Trends. Remote Sens. 7, 9492–9506. https://doi.org/10.3390/rs70809492

Ren, Z., Zhao, W., Bang, S., Zhou, X., Liang, D., Yao, W., 2024. The role of nutrients, light, and litter in species loss in an alpine meadow community. Acta Oecologica 122, 103984. https://doi.org/10.1016/j.actao.2024.103984

Ricca, M.A., Miles, A.K., Van Vuren, D.H., Eviner, V.T., 2016. Impacts of introduced Rangifer on ecosystem processes of maritime tundra on subarctic islands. Ecosphere 7, e01219. https://doi.org/10.1002/ecs2.1219

Ritchie, M.E., Penner, J.F., 2020. Episodic herbivory, plant density dependence, and stimulation of aboveground plant production. Ecol. Evol. 10, 5302–5314. https://doi.org/10.1002/ece3.6274

Ritchie, M.E., Tilman, D., Knops, J.M.H., 1998. Herbivore Effects on Plant and Nitrogen Dynamics in Oak Savanna. Ecology 79, 165–177. https://doi.org/10.1890/0012-9658(1998)079%5B0165:HEOPAN%5D2.0.CO;2

Rittl, T.F., Farsund, P.G., Pommeresche, R., Sørheim, K.M., Wibe, A., Hellekås, J., Velle, L.G., 2025. Traditional Norwegian farming practices drive biodiversity – A case study from coastal heathlands. Agric. Ecosyst. Environ. 388, 109662. https://doi.org/10.1016/j.agee.2025.109662

Rizzuto, M., Leroux, S.J., Schmitz, O.J., 2024. Rewiring the Carbon Cycle: A Theoretical Framework for Animal-Driven Ecosystem Carbon Sequestration. J. Geophys. Res. Biogeosciences 129, e2024JG008026. https://doi.org/10.1029/2024JG008026

Rockström, J., Beringer, T., Hole, D., Griscom, B., Mascia, M.B., Folke, C., Creutzig, F., 2021. Opinion: We need biosphere stewardship that protects carbon sinks and builds resilience. Proc. Natl. Acad. Sci. 118. https://doi.org/10.1073/pnas.2115218118

Rockström, J., Donges, J.F., Fetzer, I., Martin, M.A., Wang-Erlandsson, L., Richardson, K., 2024. Planetary Boundaries guide humanity's future on Earth. Nat. Rev. Earth Environ. 5, 773–788. https://doi.org/10.1038/s43017-024-00597-z

Rodeghiero, M., Heinemeyer, A., Schrumpf, M., Bellamy, P., 2010. Determination of soil carbon stocks and changes, in: Heinemeyer, A., Bahn, M., Kutsch, W.L. (Eds.), Soil Carbon Dynamics: An Integrated Methodology. Cambridge University Press, Cambridge, pp. 49–75. https://doi.org/10.1017/CBO9780511711794.005

Rodríguez, M.V., Bertiller, M.B., Sain, C.L., 2007. Spatial patterns and chemical characteristics of root biomass in ecosystems of the Patagonian Monte disturbed by grazing. J. Arid Environ. 70, 137–151. https://doi.org/10.1016/j.jaridenv.2006.12.010

Roe, S., Streck, C., Beach, R., Busch, J., Chapman, M., Daioglou, V., Deppermann, A., Doelman, J., Emmet-Booth, J., […], Lawrence, D., 2021. Land-based measures to mitigate climate change: Potential and feasibility by country. Glob. Change Biol. 27, 6025–6058. https://doi.org/10.1111/gcb.15873

Rosa García, R., Fraser, M.D., Celaya, R., Ferreira, L.M.M., García, U., Osoro, K., 2013. Grazing land management and biodiversity in the Atlantic European heathlands: a review. Agrofor. Syst. 87, 19–43. https://doi.org/10.1007/s10457-012-9519-3

Ross, L.C., Austrheim, G., Asheim, L.-J., Bjarnason, G., Feilberg, J., Fosaa, A.M., Hester, A.J., Holand, Ø., Jónsdóttir, I.S., […], Thórhallsdóttir, A.G., 2016. Sheep grazing in the North Atlantic region: A long-term perspective on environmental sustainability. Ambio 45, 551–566. https://doi.org/10.1007/s13280-016-0771-z

Roy, S., Bagchi, S., 2022. Large mammalian herbivores and the paradox of soil carbon in grazing ecosystems: Role of microbial decomposers and their enzymes. Ecosystems 25, 976–988. https://doi.org/10.1007/s10021-021-00696-8

Roy, S., Naidu, D.G.T., Bagchi, S., 2023. Functional substitutability of native herbivores by livestock for soil carbon stock is mediated by microbial decomposers. Glob. Change Biol. 29, 2141–2155. https://doi.org/10.1111/gcb.16600

Ruimy, A., Jarvis, P.G., Baldocchi, D.D., Saugier, B., 1995. CO_2 fluxes over plant canopies and solar radiation: A review, in: Advances in Ecological Research. Elsevier, pp. 1–68. https://doi.org/10.1016/S0065-2504(08)60063-X

Rumpel, C., Amiraslani, F., Chenu, C., Garcia Cardenas, M., Kaonga, M., Koutika, L.-S., Ladha, J., Madari, B., Shirato, Y., […], Wollenberg, E., 2020. The 4p1000 initiative: Opportunities, limitations and challenges for implementing soil organic carbon sequestration as a sustainable development strategy. Ambio 49, 350–360. https://doi.org/10.1007/s13280-019-01165-2

Rupprecht, D., Gilhaus, K., Hölzel, N., 2016. Effects of year-round grazing on the vegetation of nutrient-poor grass- and heathlands—Evidence from a large-scale survey. Agric. Ecosyst. Environ., Grazing in European open landscapes: how to reconcile sustainable land management and biodiversity conservation? 234, 16–22. https://doi.org/10.1016/j.agee.2016.02.015

Ryde, I., Kristinsdóttir, J.F., Halmová, M., Baussay, A., Anne Bråthen, K., Neilson, E.H.J., Jónsdóttir, I.S., 2025. Volcanic soils alleviate the allelopathic capacity of Empetrum nigrum in degraded tundra ecosystems. Oikos 2025, e11336. https://doi.org/10.1002/oik.11336

Saccone, P., Virtanen, R., 2016. Extrapolating multi-decadal plant community changes based on medium-term experiments can be risky: evidence from high-latitude tundra. Oikos 125, 76–85. https://doi.org/10.1111/oik.02399

Salisbury, J., Hu, X., Speed, J.D.M., Iordan, C.M., Austrheim, G., Cherubini, F., 2023. Net climate effects of moose browsing in early successional boreal forests by integrating carbon and albedo dynamics. J. Geophys. Res. Biogeosciences 128, e2022JG007279. https://doi.org/10.1029/2022JG007279

Sanchez, S., Arnalds, Ó., Thorsson, J., Dahlgren, R., Aradóttir, Á.L., 2025. Soil carbon stocks of regenerating Icelandic native birch woodlands: Effects of space and time. Sci. Total Environ. 958, 178063. https://doi.org/https://doi.org/10.1016/j.scitotenv.2024.178063

Sanderman, J., Hengl, T., Fiske, G.J., 2017. Soil carbon debt of 12,000 years of human land use. Proc. Natl. Acad. Sci. 114, 9575–9580. https://doi.org/10.1073/pnas.1706103114

Sandom, C., Faurby, S., Sandel, B., Svenning, J.-C., 2014. Global late Quaternary megafauna extinctions linked to humans, not climate change. Proc. R. Soc. B Biol. Sci. 20133254. https://doi.org/http://dx.doi.org/10.1098/rspb.2013.3254

Sandom, C.J., Middleton, O., Lundgren, E., Rowan, J., Schowanek, S.D., Svenning, J.-C., Faurby, S., 2020. Trophic rewilding presents regionally specific opportunities for mitigating climate change. Philos. Trans. R. Soc. B Biol. Sci. 375, 20190125. https://doi.org/10.1098/rstb.2019.0125

Sarquis, A., Pestoni, S., Cingolani, A.M., Pérez Harguindeguy, N., 2019. Physiognomic changes in response to herbivory increase carbon allocation to roots in a temperate grassland of central Argentina. Plant Ecol. 220, 699–709. https://doi.org/10.1007/s11258-019-00945-w

Scharlemann, J.P., Tanner, E.V., Hiederer, R., Kapos, V., 2014. Global soil carbon: understanding and managing the largest terrestrial carbon pool. Carbon Manag. 5, 81–91. https://doi.org/10.4155/cmt.13.77

Schellenberg, J., Bergmeier, E., 2022. The Calluna life cycle concept revisited: implications for heathland management. Biodivers. Conserv. 31, 119–141. https://doi.org/10.1007/s10531-021-02325-1

Schils, R.L.M., Bufe, C., Rhymer, C.M., Francksen, R.M., Klaus, V.H., Abdalla, M., Milazzo, F., Lellei-Kovács, E., Berge, H. ten, […], Price, J.P.N., 2022. Permanent grasslands in Europe: Land use change and intensification decrease their multifunctionality. Agric. Ecosyst. Environ. 330, 107891. https://doi.org/10.1016/j.agee.2022.107891

Schmitt, M., Bahn, M., Wohlfahrt, G., Tappeiner, U., Cernusca, A., 2010. Land use affects the net ecosystem CO_2 exchange and its components in mountain grasslands. Biogeosciences 7, 2297–2309. https://doi.org/10.5194/bg-7-2297-2010

Schmitz, O.J., Raymond, P.A., Estes, J.A., Kurz, W.A., Holtgrieve, G.W., Ritchie, M.E., Schindler, D.E., Spivak, A.C., Wilson, R.W., […], Wilmers, C.C., 2014. Animating the carbon cycle. Ecosystems 17, 344–359. https://doi.org/10.1007/s10021-013-9715-7

Schmitz, O.J., Sylvén, M., Atwood, T.B., Bakker, E.S., Berzaghi, F., Brodie, J.F., Cromsigt, J.P.G.M., Davies, A.B., Leroux, S.J., […], Ylänne, H., 2023. Trophic rewilding can expand natural climate solutions. Nat. Clim. Change 1–10. https://doi.org/10.1038/s41558-023-01631-6

Schmitz, O.J., Wilmers, C.C., Leroux, S.J., Doughty, C.E., Atwood, T.B., Galetti, M., Davies, A.B., Goetz, S.J., 2018. Animals and the zoogeochemistry of the carbon cycle. Science 362, eaar3213. https://doi.org/10.1126/science.aar3213

Schoenecker, K.A., Zeigenfuss, L.C., Augustine, D.J., 2022. Can grazing by elk and bison stimulate herbaceous plant productivity in semiarid ecosystems? Ecosphere 13. https://doi.org/10.1002/ecs2.4025

Schrama, M., Heijning, P., Bakker, J.P., van Wijnen, H.J., Berg, M.P., Olff, H., 2013a. Herbivore trampling as an alternative pathway for explaining differences in nitrogen mineralization in moist grasslands. Oecologia 172, 231–243. https://doi.org/10.1007/s00442-012-2484-8

Schrama, M., Quist, C.W., Arjen de Groot, G., Cieraad, E., Ashworth, D., Laros, I., Hansen, L.H., Leff, J., Fierer, N., Bardgett, R.D., 2023. Cessation of grazing causes biodiversity loss and homogenization of soil food webs. Proc. R. Soc. B Biol. Sci. 290, 20231345. https://doi.org/10.1098/rspb.2023.1345

Schrama, M., Veen, G.F. (Ciska), Bakker, E.S. (Liesbeth), Ruifrok, J.L., Bakker, J.P., Olff, H., 2013b. An integrated perspective to explain nitrogen mineralization in grazed ecosystems. Perspect. Plant Ecol. Evol. Syst. 15, 32–44. https://doi.org/10.1016/j.ppees.2012.12.001

See, C.R., Virkkala, A.-M., Natali, S.M., Rogers, B.M., Mauritz, M., Biasi, C., Bokhorst, S., Boike, J., Bret-Harte, M.S., […], Schuur, E.A.G., 2024. Decadal increases in carbon uptake offset by respiratory losses across northern permafrost ecosystems. Nat. Clim. Change 14, 853–862. https://doi.org/10.1038/s41558-024-02057-4

Seethepalli, A., Dhakal, K., Griffiths, M., Guo, H., Freschet, G.T., York, L.M., 2021. RhizoVision Explorer: Open-source software for root image analysis and measurement standardization. AoB PLANTS 13, plab056. https://doi.org/https://doi.org/10.1093/aobpla/plab056

Shaver, G.R., Rastetter, E.B., Salmon, V., Street, L.E., van de Weg, M.J., Rocha, A., van Wijk, M.T., Williams, M., 2013. Pan-Arctic modelling of net ecosystem exchange of CO_2. Philos. Trans. R. Soc. B Biol. Sci. 368, 20120485. https://doi.org/10.1098/rstb.2012.0485

Shaver, G.R., Street, L.E., Rastetter, E.B., Van Wijk, M.T., Williams, M., 2007. Functional convergence in regulation of net CO_2 flux in heterogeneous tundra landscapes in Alaska and Sweden. J. Ecol. 95, 802–817. https://doi.org/10.1111/j.1365-2745.2007.01259.x

Shu, X., Ye, Q., Huang, H., Xia, L., Tang, H., Liu, X., Wu, J., Li, Y., Zhang, Y., Deng, L., Liu, W., 2024. Effects of grazing exclusion on soil microbial diversity and its functionality in grasslands: a meta-analysis. Front. Plant Sci. 15. https://doi.org/10.3389/fpls.2024.1366821

Sierra, C.A., Ahrens, B., Bolinder, M.A., Braakhekke, M.C., von Fromm, S., Kätterer, T., Luo, Z., Parvin, N., Wang, G., 2024. Carbon sequestration in the subsoil and the time required to stabilize carbon for climate change mitigation. Glob. Change Biol. 30, e17153. https://doi.org/10.1111/gcb.17153

Siewert, M.B., Olofsson, J., 2020. Scale-dependency of Arctic ecosystem properties revealed by UAV. Environ. Res. Lett. 15, 094030. https://doi.org/10.1088/1748-9326/aba20b

Silveira, M.L., Rodrigues da Cruz, P.J., Vendramini, J.M.B., Boughton, E., Bracho, R., da Silva Cardoso, A., 2024. Opportunities to increase soil carbon sequestration in grazing lands in the southeastern United States. Grassl. Res. 3, 69–78. https://doi.org/10.1002/glr2.12074

Sitters, J., Bakker, E.S., Veldhuis, M.P., Veen, G.F., Olde Venterink, H., Vanni, M.J., 2017. The Stoichiometry of Nutrient Release by Terrestrial Herbivores and Its Ecosystem Consequences. Front. Earth Sci. 5. https://doi.org/https://doi.org/10.3389/feart.2017.00032

Sitters, J., Wubs, E.R.J., Bakker, E.S., Crowther, T.W., Adler, P.B., Bagchi, S., Bakker, J.D., Biederman, L., Borer, E.T., […], Veen, G.F. (Ciska), 2020. Nutrient availability controls the impact of mammalian herbivores on soil carbon and nitrogen pools in grasslands. Glob. Change Biol. 26, 2060–2071. https://doi.org/10.1111/gcb.15023

Sjögersten, S., Llurba, R., Ribas, À., Yanez-Serrano, A., Sebastià, M.-T., 2012. Temperature and Moisture Controls of C Fluxes in Grazed Subalpine Grasslands. Arct. Antarct. Alp. Res. 44, 239–246. https://doi.org/10.1657/1938-4246-44.2.239

Smit, C., Ruifrok, J.L., van Klink, R., Olff, H., 2015. Rewilding with large herbivores: The importance of grazing refuges for sapling establishment and wood-pasture formation. Biol. Conserv. 182, 134–142. https://doi.org/10.1016/j.biocon.2014.11.047

Smith, P., Singh, P.K., Ballal, V.P., Cherubini, F., Díaz-José, J., Duchková, H., Gupta, H., Hori, M., Ito, A., […], McElwee, P.D., 2025. Impacts of Climate Change Interventions on Biodiversity, Water, the Food System and Human Health and Well-Being. Glob. Change Biol. 31, e70444. https://doi.org/10.1111/gcb.70444

Smith, P., Soussana, J., Angers, D., Schipper, L., Chenu, C., Rasse, D.P., Batjes, N.H., Egmond, F., McNeill, S., […], Klumpp, K., 2020. How to measure, report and verify soil carbon change to realize the potential of soil carbon sequestration for atmospheric greenhouse gas removal. Glob. Change Biol. 26, 219–241. https://doi.org/10.1111/gcb.14815

Snorrason, A., Jónsson, T.H., Eggertsson, Ó., 2019. Aboveground woody biomass of natural birch woodland in Iceland – Comparison of two inventories 1987-1988 and 2005-2011. Icel. Agric. Sci. 32, 21–29. https://doi.org/10.16886/IAS.2019.03

Sokol, N.W., Bradford, M.A., 2019. Microbial formation of stable soil carbon is more efficient from belowground than aboveground input. Nat. Geosci. 12, 46–53. https://doi.org/10.1038/s41561-018-0258-6

Sokol, N.W., Kuebbing, Sara.E., Karlsen-Ayala, E., Bradford, M.A., 2019a. Evidence for the primacy of living root inputs, not root or shoot litter, in forming soil organic carbon. New Phytol. 221, 233–246. https://doi.org/10.1111/nph.15361

Sokol, N.W., Sanderman, J., Bradford, M.A., 2019b. Pathways of mineral-associated soil organic matter formation: Integrating the role of plant carbon source, chemistry, and point of entry. Glob. Change Biol. 25, 12–24. https://doi.org/10.1111/gcb.14482

Sokol, N.W., Slessarev, E., Marschmann, G.L., Nicolas, A., Blazewicz, S.J., Brodie, E.L., Firestone, M.K., Foley, M.M., Hestrin, R., […], Pett-Ridge, J., 2022a. Life and death in the soil microbiome: how ecological processes influence biogeochemistry. Nat. Rev. Microbiol. 1–16. https://doi.org/10.1038/s41579-022-00695-z

Sokol, N.W., Whalen, E.D., Jilling, A., Kallenbach, C., Pett-Ridge, J., Georgiou, K., 2022b. Global distribution, formation and fate of mineral-associated soil organic matter under a changing climate: A trait-based perspective. Funct. Ecol. 36, 1411–1429. https://doi.org/10.1111/1365-2435.14040

Søndergaard, S.A., Ejrnæs, R., Svenning, J.-C., Fløjgaard, C., 2025. From Grasslands to Forblands: Year-round grazing as a driver of plant diversity. J. Appl. Ecol. 62, 1104–1113. https://doi.org/10.1111/1365-2664.70047

Sørensen, M.V., Graae, B.J., Classen, A., Enquist, B.J., Strimbeck, R., 2019. Drivers of C cycling in three arctic-alpine plant communities. Arct. Antarct. Alp. Res. 51, 128–147. https://doi.org/10.1080/15230430.2019.1592649

Sørensen, M.V., Graae, B.J., Hagen, D., Enquist, B.J., Nystuen, K.O., Strimbeck, R., 2018a. Experimental herbivore exclusion, shrub introduction, and carbon sequestration in alpine plant communities. BMC Ecol. 18, 29. https://doi.org/10.1186/s12898-018-0185-9

Sørensen, M.V., Strimbeck, R., Nystuen, K.O., Kapas, R.E., Enquist, B.J., Graae, B.J., 2018b. Draining the pool? Carbon storage and fluxes in three alpine plant communities. Ecosystems 21, 316–330. https://doi.org/10.1007/s10021-017-0158-4

Soussana, J.-F., Lemaire, G., 2014. Coupling carbon and nitrogen cycles for environmentally sustainable intensification of grasslands and crop-livestock systems. Agric. Ecosyst. Environ., Integrated Crop-Livestock System Impacts on Environmental Processes 190, 9–17. https://doi.org/10.1016/j.agee.2013.10.012

Soussana, J.F., Tallec, T., Blanfort, V., 2010. Mitigating the greenhouse gas balance of ruminant production systems through carbon sequestration in grasslands. Animal 4, 334–350. https://doi.org/10.1017/S1751731109990784

Stanley, P.L., Roche, L., Bowles, T., 2025. Amping up soil carbon: soil carbon stocks in California rangelands under adaptive multi-paddock and conventional grazing management. Int. J. Agric. Sustain. 23, 2461826. https://doi.org/10.1080/14735903.2025.2461826

Stanley, P.L., Spertus, J., Chiartas, J., Stark, P.B., Bowles, T., 2023. Valid inferences about soil carbon in heterogeneous landscapes. Geoderma 430, 116323. https://doi.org/10.1016/j.geoderma.2022.116323

Stanley, P.L., Wilson, C., Patterson, E., Machmuller, M.B., Cotrufo, M.F., 2024. Ruminating on soil carbon: Applying current understanding to inform grazing management. Glob. Change Biol. 30, e17223. https://doi.org/10.1111/gcb.17223

Stark, S., Egelkraut, D., Aronsson, K.-Å., Olofsson, J., 2019. Contrasting vegetation states do not diverge in soil organic matter storage: evidence from historical sites in tundra. Ecology 100, e02731. https://doi.org/10.1002/ecy.2731

Stark, S., Horstkotte, T., Kumpula, J., Olofsson, J., Tømmervik, H., Turunen, M., 2023. The ecosystem effects of reindeer (*Rangifer tarandus*) in northern Fennoscandia: Past, present and future. Perspect. Plant Ecol. Evol. Syst. 58, 125716. https://doi.org/10.1016/j.ppees.2022.125716

Stark, S., Männistö, M.K., Eskelinen, A., 2015. When do grazers accelerate or decelerate soil carbon and nitrogen cycling in tundra? A test of theory on grazing effects in fertile and infertile habitats. Oikos 124, 593–602. https://doi.org/10.1111/oik.01355

StatIce, 2026. Livestock by region from 1980. [WWW Document]. Stat. Icel. URL https://px.hagstofa.is/pxen/pxweb/en/Atvinnuvegir/Atvinnuvegir__landbunadur__landbufe/LAN10102.px/table/tableViewLayout2/ (accessed 17.5.26).

Steinthorsdottir, M., Coxall, H.K., de Boer, A.M., Huber, M., Barbolini, N., Bradshaw, C.D., Burls, N.J., Feakins, S.J., Gasson, E., […], Strömberg, C. a. E., 2021. The Miocene: The Future of the Past. Paleoceanogr. Paleoclimatology 36, e2020PA004037. https://doi.org/10.1029/2020PA004037

Stevens, N., Bond, W., Feurdean, A., Lehmann, C.E.R., 2022. Grassy ecosystems in the Anthropocene. Annu. Rev. Environ. Resour. 47, 261–289. https://doi.org/10.1146/annurev-environ-112420-015211

Stewart, K. e. j., Bourn, N. a. d., Thomas, J. a., 2002. An evaluation of three quick methods commonly used to assess sward height in ecology. J. Appl. Ecol. 38, 1148–1154. https://doi.org/10.1046/j.1365-2664.2001.00658.x

Stockmann, U., Adams, M.A., Crawford, J.W., Field, D.J., Henakaarchchi, N., Jenkins, M., Minasny, B., McBratney, A.B., Courcelles, V. de R. de, […], D., Zimmermann, M., 2013. The knowns, known unknowns and unknowns of sequestration of soil organic carbon. Agric. Ecosyst. Environ. 164, 80–99. https://doi.org/10.1016/j.agee.2012.10.001

Stoessel, M., Moen, J., Lindborg, R., 2022. Mapping cumulative pressures on the grazing lands of northern Fennoscandia. Sci. Rep. 12, 16044. https://doi.org/10.1038/s41598-022-20095-w

Street, L.E., Shaver, G.R., Williams, M., Van Wijk, M.T., 2007. What is the relationship between changes in canopy leaf area and changes in photosynthetic CO_2 flux in arctic ecosystems? J. Ecol. 95, 139–150. https://doi.org/10.1111/j.1365-2745.2006.01187.x

Street, L.E., Subke, J.A., Sommerkorn, M., Heinemeyer, A., Williams, M., 2011. Turnover of recently assimilated carbon in arctic bryophytes. Oecologia 167, 325–337. https://doi.org/10.1007/s00442-011-1988-y

Strimbeck, G.R., Graae, B.J., Lang, S., Sørensen, M.V., 2019. Functional group contributions to carbon fluxes in arctic-alpine ecosystems. Arct. Antarct. Alp. Res. 51, 58–68. https://doi.org/10.1080/15230430.2019.1578163

Strömberg, C.A.E., 2011. Evolution of Grasses and Grassland Ecosystems. Annu. Rev. Earth Planet. Sci. 39, 517–544. https://doi.org/10.1146/annurev-earth-040809-152402

Su, J., Xu, F., 2021. Root, not aboveground litter, controls soil carbon storage under grazing exclusion across grasslands worldwide. Land Degrad. Dev. 32, 3326–3337. https://doi.org/10.1002/ldr.4008

Sun, Y., Frankenberg, C., Wood, J.D., Schimel, D.S., Jung, M., Guanter, L., Drewry, D.T., Verma, M., Porcar-Castell, A., […], Yuen, K., 2017. OCO-2 advances

photosynthesis observation from space via solar-induced chlorophyll fluorescence. Science 358, eaam5747. https://doi.org/10.1126/science.aam5747
Sundqvist, M.K., Moen, J., Björk, R.G., Vowles, T., Kytöviita, M.-M., Parsons, M.A., Olofsson, J., 2019. Experimental evidence of the long-term effects of reindeer on Arctic vegetation greenness and species richness at a larger landscape scale. J. Ecol. 107, 2724–2736. https://doi.org/10.1111/1365-2745.13201
Sundqvist, M.K., Sanders, N.J., Dorrepaal, E., Lindén, E., Metcalfe, D.B., Newman, G.S., Olofsson, J., Wardle, D.A., Classen, A.T., 2020. Responses of tundra plant community carbon flux to experimental warming, dominant species removal and elevation. Funct. Ecol. 34, 1497–1506. https://doi.org/10.1111/1365-2435.13567
Susiluoto, S., Rasilo, T., Pumpanen, J., Berninger, F., 2008. Effects of grazing on the vegetation structure and carbon dioxide exchange of a Fennoscandian fell ecosystem. Arct. Antarct. Alp. Res. 40, 422–431. https://doi.org/10.1657/1523-0430(07-035)%5BSUSILUOTO%5D2.0.CO;2
Svenning, J.-C., Buitenwerf, R., Roux, E.L., 2024a. Trophic rewilding as a restoration approach under emerging novel biosphere conditions. Curr. Biol. 34, R435–R451. https://doi.org/10.1016/j.cub.2024.02.044
Svenning, J.-C., Lemoine, R.T., Bergman, J., Buitenwerf, R., Roux, E.L., Lundgren, E., Mungi, N., Pedersen, R.Ø., 2024b. The late-Quaternary megafauna extinctions: Patterns, causes, ecological consequences and implications for ecosystem management in the Anthropocene. Camb. Prisms Extinction 2, e5. https://doi.org/10.1017/ext.2024.4
Svenning, J.-C., Pedersen, P.B.M., Donlan, C.J., Ejrnæs, R., Faurby, S., Galetti, M., Hansen, D.M., Sandel, B., Sandom, C.J., Terborgh, J.W., Vera, F.W.M., 2016. Science for a wilder Anthropocene: Synthesis and future directions for trophic rewilding research. Proc. Natl. Acad. Sci. 113, 898–906. https://doi.org/10.1073/pnas.1502556112
Sweeney, C.J., de Vries, F.T., van Dongen, B.E., Bardgett, R.D., 2021. Root traits explain rhizosphere fungal community composition among temperate grassland plant species. New Phytol. 229, 1492–1507. https://doi.org/10.1111/nph.16976
Tau Strand, L., Fjellstad, W., Jackson-Blake, L., De Wit, H.A., 2021. Afforestation of a pasture in Norway did not result in higher soil carbon, 50 years after planting. Landsc. Urban Plan. 207, 104007. https://doi.org/10.1016/j.landurbplan.2020.104007
Te Beest, M., Sitters, J., Ménard, C.B., Olofsson, J., 2016. Reindeer grazing increases summer albedo by reducing shrub abundance in Arctic tundra. Environ. Res. Lett. 11, 125013. https://doi.org/10.1088/1748-9326/aa5128
Thorhallsdottir, A.G., Gudmundsson, J., 2023. Carbon dioxide fluxes and soil carbon storage in relation to long-term grazing and no grazing in Icelandic semi-natural grasslands. Appl. Veg. Sci. 26, e12757. https://doi.org/10.1111/avsc.12757
Thorhallsdottir, A.G., Júlíusson, A.D., Ögmundardottir, H., 2013. The sheep, the market and the soil: Environmental destruction in Icelandic highlands 1880-1910, in: Jørgensen, D., Sørlin, S. (Eds.), Northscapes: History, Technology and the Making of Northern Environments. University of British Columbia Press, Vancouver, Vancouver, pp. 155–174.
Thorhallsdottir, T.E., 2021. The Vascular Floras of High-Latitude Islands with Special Reference to Iceland, in: Biogeography in the Sub-Arctic. John Wiley & Sons, Ltd, pp. 113–146. https://doi.org/10.1002/9781118561461.ch6

Tjoelker, M.G., Oleksyn, J., Reich, P.B., 2001. Modelling respiration of vegetation: evidence for a general temperature-dependent Q10. Glob. Change Biol. 7, 223–230. https://doi.org/10.1046/j.1365-2486.2001.00397.x

Träger, S., Öpik, M., Vasar, M., Wilson, S.D., 2019. Belowground plant parts are crucial for comprehensively estimating total plant richness in herbaceous and woody habitats. Ecology 100, e02575. https://doi.org/10.1002/ecy.2575

Trepel, J., le Roux, E., Abraham, A.J., Buitenwerf, R., Kamp, J., Kristensen, J.A., Tietje, M., Lundgren, E.J., Svenning, J.-C., 2024. Meta-analysis shows that wild large herbivores shape ecosystem properties and promote spatial heterogeneity. Nat. Ecol. Evol. 1–12. https://doi.org/10.1038/s41559-024-02327-6

Tuomi, M., Väisänen, M., Ylänne, H., Brearley, F.Q., Barrio, I.C., Anne Bråthen, K., Eischeid, I., Forbes, B.C., Jónsdóttir, I.S., […], Bueno, C.G., 2021. Stomping in silence: Conceptualizing trampling effects on soils in polar tundra. Funct. Ecol. 35, 306–317. https://doi.org/10.1111/1365-2435.13719

Vaieretti, M.V., Conti, G., Poca, M., Kowaljow, E., Gorné, L., Bertone, G., Cingolani, A.M., Pérez-Harguindeguy, N., 2021. Plant and soil carbon stocks in grassland patches maintained by extensive grazing in the highlands of central Argentina. Austral Ecol. 46, 374–386. https://doi.org/10.1111/aec.12992

Väisänen, M., Ylänne, H., Kaarlejärvi, E., Sjögersten, S., Olofsson, J., Crout, N., Stark, S., 2014. Consequences of warming on tundra carbon balance determined by reindeer grazing history. Nat. Clim. Change 4, 384–388. https://doi.org/10.1038/nclimate2147

Valkó, O., Venn, S., Żmihorski, M., Biurrun, I., Labadessa, R., Loos, J., 2018. The challenge of abandonment for the sustainable management of Palaearctic natural and semi-natural grasslands. Hacquetia 17, 5–16. https://doi.org/10.1515/hacq-2017-0018

Valls Fox, H., Bonnet, O., Cromsigt, J.P.G.M., Fritz, H., Shrader, A.M., 2015. Legacy Effects of Different Land-Use Histories Interact with Current Grazing Patterns to Determine Grazing Lawn Soil Properties. Ecosystems 18, 720–733. https://doi.org/10.1007/s10021-015-9857-x

Van der Wal, R., 2006. Do herbivores cause habitat degradation or vegetation state transition? Evidence from the tundra. Oikos 114, 177–186. https://doi.org/10.1111/j.2006.0030-1299.14264.x

Van der Wal, R., Bardgett, R.D., Harrison, K.A., Stien, A., 2004. Vertebrate herbivores and ecosystem control: cascading effects of faeces on tundra ecosystems. Ecography 27, 242–252. https://doi.org/10.1111/j.0906-7590.2004.03688.x

Van der Wal, R., Brooker, R.W., 2004. Mosses mediate grazer impacts on grass abundance in arctic ecosystems. Funct. Ecol. 18, 77–86. https://doi.org/10.1111/j.1365-2435.2004.00820.x

Vera, F.W.M. (Ed.), 2000. Grazing ecology and forest history, 1st ed. CABI Publishing, UK. https://doi.org/10.1079/9780851994420.0000

Vidaller, C., Malik, C., Dutoit, T., 2022. Grazing intensity gradient inherited from traditional herding still explains Mediterranean grassland characteristics despite current land-use changes. Agric. Ecosyst. Environ. 338, 108085. https://doi.org/10.1016/j.agee.2022.108085

Viglizzo, E.F., Ricard, M.F., Taboada, M.A., Vázquez-Amábile, G., 2019. Reassessing the role of grazing lands in carbon-balance estimations: Meta-analysis and review. Sci. Total Environ. 661, 531–542. https://doi.org/10.1016/j.scitotenv.2019.01.130

Villarino, S.H., Pinto, P., Jackson, R.B., Piñeiro, G., 2021. Plant rhizodeposition: A key factor for soil organic matter formation in stable fractions. Sci. Adv. 7, eabd3176. https://doi.org/10.1126/sciadv.abd3176

Vilmundardóttir, O.K., Sigurmundsson, F.S., Møller Pedersen, G.B., Belart, J.M.-C., Kizel, F., Falco, N., Benediktsson, J.A., Gísladóttir, G., 2018. Of mosses and men: Plant succession, soil development and soil carbon accretion in the sub-Arctic volcanic landscape of Hekla, Iceland. Prog. Phys. Geogr. 42, 765–791. https://doi.org/10.1177/0309133318798754

Virkkala, A.-M., Aalto, J., Rogers, B.M., Tagesson, T., Treat, C.C., Natali, S.M., Watts, J.D., Potter, S., Lehtonen, A., […], Luoto, M., 2021. Statistical upscaling of ecosystem CO_2 fluxes across the terrestrial tundra and boreal domain: Regional patterns and uncertainties. Glob. Change Biol. 27, 4040–4059. https://doi.org/10.1111/gcb.15659

Virkkala, A.-M., Niittynen, P., Kemppinen, J., Marushchak, M.E., Voigt, C., Hensgens, G., Kerttula, J., Happonen, K., Tyystjärvi, V., […], Luoto, M., 2024. High-resolution spatial patterns and drivers of terrestrial ecosystem carbon dioxide, methane, and nitrous oxide fluxes in the tundra. Biogeosciences 21, 335–355. https://doi.org/10.5194/bg-21-335-2024

Virkkala, A.-M., Rogers, B.M., Watts, J.D., Arndt, K.A., Potter, S., Wargowsky, I., Schuur, E.A.G., See, C.R., Mauritz, M., […], Natali, S.M., 2025a. Wildfires offset the increasing but spatially heterogeneous Arctic–boreal CO_2 uptake. Nat. Clim. Change. https://doi.org/10.1038/s41558-024-02234-5

Virkkala, A.-M., Virtanen, T., Lehtonen, A., Rinne, J., Luoto, M., 2018. The current state of CO_2 flux chamber studies in the Arctic tundra: A review. Prog. Phys. Geogr. Earth Environ. 42, 162–184. https://doi.org/10.1177/0309133317745784

Virkkala, A.-M., Wargowsky, I., Vogt, J., Kuhn, M.A., Madaan, S., O'Keefe, R., Windholz, T., Arndt, K.A., Rogers, B.M., […], Natali, S.M., 2025b. ABCFlux v2: Arctic-boreal CO_2 and CH_4 monthly flux observations and ancillary information across terrestrial and freshwater ecosystems. Earth Syst. Sci. Data Discuss. 1–86. https://doi.org/10.5194/essd-2025-585

Vowles, T., Björk, R.G., 2019. Implications of evergreen shrub expansion in the Arctic. J. Ecol. 107, 650–655. https://doi.org/10.1111/1365-2745.13081

Vowles, T., Gunnarsson, B., Molau, U., Hickler, T., Klemedtsson, L., Björk, R.G., 2017a. Expansion of deciduous tall shrubs but not evergreen dwarf shrubs inhibited by reindeer in Scandes mountain range. J. Ecol. 105, 1547–1561. https://doi.org/10.1111/1365-2745.12753

Vowles, T., Lovehav, C., Molau, U., Björk, R.G., 2017b. Contrasting impacts of reindeer grazing in two tundra grasslands. Environ. Res. Lett. 12, 034018. https://doi.org/10.1088/1748-9326/aa62af

Vuorinen, K.E.M., Austrheim, G., Mysterud, A., Gya, R., Vandvik, V., Grytnes, J.-A., Speed, J.D.M., 2021. Functional traits of alpine plant communities show long-term resistance to changing herbivore densities. Ecosphere 12, e03887. https://doi.org/10.1002/ecs2.3887

Walker, L.R., del Moral, R., 2003. Primary succession and ecosystem rehabilitation. Cambridge University Press. https://doi.org/10.1017/CBO9780511615078

Walker, L.R., Wardle, D.A., Bardgett, R.D., Clarkson, B.D., 2010. The use of chronosequences in studies of ecological succession and soil development. J. Ecol. 98, 725–736. https://doi.org/10.1111/j.1365-2745.2010.01664.x

Wang, B., Dou, Y., Liang, C., Liu, C., Ao, D., Yao, H., Yang, E., An, S., Wen, Z., 2024. Microbial necromass in soil profiles increases less efficiently than root biomass in long-term fenced grassland: Effects of microbial nitrogen limitation and soil depth. Sci. Total Environ. 956, 177058. https://doi.org/10.1016/j.scitotenv.2024.177058

Wang, C., Li, X., Lu, X., Wang, Y., Bai, Y., 2023. Intraspecific trait variation governs grazing-induced shifts in plant community above- and below-ground functional trait composition. Agric. Ecosyst. Environ. 346, 108357. https://doi.org/10.1016/j.agee.2023.108357

Wang, H., Liu, H., Wang, Y., Xu, W., Liu, A., Ma, Z., Mi, Z., Zhang, Z., Wang, S., He, J.-S., 2017. Warm- and cold- season grazing affect soil respiration differently in alpine grasslands. Agric. Ecosyst. Environ. 248, 136–143. https://doi.org/10.1016/j.agee.2017.07.041

Wang, J., Liu, Y., Cao, W., Li, W., Wang, X., Zhang, D., Shi, S., Pan, D., Liu, W., 2020. Effects of grazing exclusion on soil respiration components in an alpine meadow on the north-eastern Qinghai-Tibet Plateau. CATENA 194, 104750. https://doi.org/10.1016/j.catena.2020.104750

Wang, J., Liu, Y., Wang, S., Ma, P., Li, Y., Wang, R., Liu, W., Jia, Z., Li, W., Niu, Y., Cao, W., 2024. Enhanced ecosystem carbon sink in shrub-grassland ecotone under grazing exclusion on Tibetan plateau. Ecol. Indic. 160, 111854. https://doi.org/10.1016/j.ecolind.2024.111854

Wang, J., Zhang, A., Zheng, Y., Song, J., Ru, J., Zheng, M., Hui, D., Wan, S., 2021. Long-term litter removal rather than litter addition enhances ecosystem carbon sequestration in a temperate steppe. Funct. Ecol. 35, 2799–2807. https://doi.org/10.1111/1365-2435.13920

Wang, P., Heijmans, M.M.P.D., Mommer, L., van Ruijven, J., Maximov, T.C., Berendse, F., 2016a. Belowground plant biomass allocation in tundra ecosystems and its relationship with temperature. Environ. Res. Lett. 11, 055003. https://doi.org/10.1088/1748-9326/11/5/055003

Wang, P., Mommer, L., van Ruijven, J., Berendse, F., Maximov, T.C., Heijmans, M.M.P.D., 2016b. Seasonal changes and vertical distribution of root standing biomass of graminoids and shrubs at a Siberian tundra site. Plant Soil 407, 55–65. https://doi.org/10.1007/s11104-016-2858-5

Wang, Q., Ding, J., Zhang, Z., Liang, C., Lambers, H., Zhu, B., Wang, D., Wang, J., Zhang, [...], Yin, H., 2025. Rhizosphere as a hotspot for microbial necromass deposition into the soil carbon pool. J. Ecol. 113, 168–179. https://doi.org/10.1111/1365-2745.14448

Wang, Z., Ma, Y., Zhang, Y., Shang, J., 2022. Review of Remote Sensing Applications in Grassland Monitoring. Remote Sens. 14, 2903. https://doi.org/10.3390/rs14122903

Ward, A., Dargusch, P., Thomas, S., Liu, Y., Fulton, E.A., 2014. A global estimate of carbon stored in the world's mountain grasslands and shrublands, and the implications for climate policy. Glob. Environ. Change 28, 14–24. https://doi.org/10.1016/j.gloenvcha.2014.05.008

Ward, S.E., Bardgett, R.D., McNamara, N.P., Adamson, J.K., Ostle, N.J., 2007. Long-Term Consequences of Grazing and Burning on Northern Peatland Carbon Dynamics. Ecosystems 10, 1069–1083. https://doi.org/10.1007/s10021-007-9080-5

Wąsowicz, P., 2020. Annotated checklist of vascular plants of Iceland (No. 57), Fjölrit Náttúrufræðistofnunar. Náttúrufræðistofnun Íslands. https://doi.org/10.33112/1027-832X.57

Weigelt, A., Mommer, L., Andraczek, K., Iversen, C.M., Bergmann, J., Bruelheide, H., Fan, Y., Freschet, G.T., Guerrero-Ramírez, N.R., […], McCormack, M.L., 2021. An integrated framework of plant form and function: the belowground perspective. New Phytol. 232, 42–59. https://doi.org/10.1111/nph.17590

Weintraub, M.N., Schimel, J.P., 2005. Nitrogen Cycling and the Spread of Shrubs Control Changes in the Carbon Balance of Arctic Tundra Ecosystems. BioScience 55, 408–415. https://doi.org/10.1641/0006-3568(2005)055%5B0408:NCATSO%5D2.0.CO;2

Welker, J.M., Fahnestock, J.T., Povirk, K.L., Bilbrough, C.J., Piper, R.E., 2004. Alpine Grassland CO_2 Exchange and Nitrogen Cycling: Grazing History Effects, Medicine Bow Range, Wyoming, U.S.A. Arct. Antarct. Alp. Res. 36, 11–20. https://doi.org/10.1657/1523-0430(2004)036%5B0011:AGCEAN%5D2.0.CO;2

Widmer, S., Riedel, S., Babbi, M., Herzog, F., Wohlgemuth, T., Kessler, M., Dengler, J., 2026. A century of change: Many losers vs. few winners among Swiss grassland plants. Biol. Conserv. 315, 111679. https://doi.org/10.1016/j.biocon.2025.111679

Willerslev, E., Davison, J., Moora, M., Zobel, M., Coissac, E., Edwards, M.E., Lorenzen, E.D., Vestergård, M., Gussarova, G., […], Taberlet, P., 2014. Fifty thousand years of Arctic vegetation and megafaunal diet. Nature 506, 47–51. https://doi.org/10.1038/nature12921

Williams, A., Langridge, H., Straathof, A.L., Muhamadali, H., Hollywood, K.A., Goodacre, R., de Vries, F.T., 2022. Root functional traits explain root exudation rate and composition across a range of grassland species. J. Ecol. 110, 21–33. https://doi.org/10.1111/1365-2745.13630

Williams, M., Bell, R., Spadavecchia, L., Street, L.E., Van Wijk, M.T., 2008. Upscaling leaf area index in an Arctic landscape through multiscale observations. Glob. Change Biol. 14, 1517–1530. https://doi.org/10.1111/j.1365-2486.2008.01590.x

Williams, M., Street, L.E., van Wijk, M.T., Shaver, G.R., 2006. Identifying differences in carbon exchange among Arctic ecosystem types. Ecosystems 9, 288–304. https://doi.org/10.1007/s10021-005-0146-y

Wilson, C.H., Strickland, M.S., Hutchings, J.A., Bianchi, T.S., Flory, S.L., 2018. Grazing enhances belowground carbon allocation, microbial biomass, and soil carbon in a subtropical grassland. Glob. Change Biol. 24, 2997–3009. https://doi.org/10.1111/gcb.14070

Windirsch, T., Grosse, G., Ulrich, M., Forbes, B.C., Göckede, M., Wolter, J., Macias-Fauria, M., Olofsson, J., Zimov, N., Strauss, J., 2022. Large herbivores on permafrost— a pilot study of grazing impacts on permafrost soil carbon storage in northeastern Siberia. Front. Environ. Sci. 10. https://doi.org/10.3389/fenvs.2022.893478

Wu, J., Xi, N., Yang, G., Delgado-Baquerizo, M., Wang, D., 2025. Soil legacy of grazing shapes current ecosystem multifunctionality in a temperate grassland. J. Environ. Manage. 395, 127922. https://doi.org/10.1016/j.jenvman.2025.127922

Wu, X., Wang, Y., Sun, S., 2021. Long-term fencing decreases plant diversity and soil organic carbon concentration of the Zoige alpine meadows on the eastern Tibetan plateau. Plant Soil 458, 191–200. https://doi.org/10.1007/s11104-019-04373-7

Xiang, M., Luo, R., Wu, J., Niu, B., Pan, Y., Zhang, X., Duo, L., Ma, T., Han, C., 2025. Grazing intensity modifies alpine grassland fine root traits on the Qinghai-Tibetan Plateau. Plant Ecol. 226, 363–374. https://doi.org/10.1007/s11258-025-01499-w

Xu, T., Johnson, D., Bardgett, R.D., 2025. Defoliation modifies the impact of drought on the transfer of recent plant-assimilated carbon to soil and arbuscular mycorrhizal fungi. Plant Soil 507, 693–711. https://doi.org/10.1007/s11104-024-06762-z

Yan, K., Gao, Si, Yan, G., Ma, X., Chen, X., Zhu, P., Li, J., Gao, Sicong, Gastellu-Etchegorry, J.-P., Myneni, R.B., Wang, Q., 2025. A global systematic review of the remote sensing vegetation indices. Int. J. Appl. Earth Obs. Geoinformation 139, 104560. https://doi.org/10.1016/j.jag.2025.104560

Yang, J., Yang, Z., Wang, J., Wu, X., Song, Y., Hang, R., Xu, T., Zhao, X., Pan, D., Wang, D., Wu, D., Kooch, Y., 2026. Livestock grazing as a nature-based solution for restoring soil nematode communities and ecosystem multifunctionality. Agric. Ecosyst. Environ. 399, 110168. https://doi.org/10.1016/j.agee.2025.110168

Yang, X., Wang, B., An, S., 2021. Root derived C rather than root biomass contributes to the soil organic carbon sequestration in grassland soils with different fencing years. Plant Soil 469, 161–172. https://doi.org/10.1007/s11104-021-05144-z

Yang, Y., Russo, S.E., 2024. Trade-offs in rooting strategy dimensions along an edaphic gradient in a grassland ecosystem. Funct. Ecol. 38, 792–807. https://doi.org/10.1111/1365-2435.14514

Ylänne, H., Castaño, C., Clemmensen, K.E., 2025. Fungi in treeline ecotones – Halting or causing abrupt ecosystem change? Fungal Ecol. 74, 101409. https://doi.org/10.1016/j.funeco.2024.101409

Ylänne, H., Olofsson, J., Oksanen, L., Stark, S., 2018. Consequences of grazer-induced vegetation transitions on ecosystem carbon storage in the tundra. Funct. Ecol. 32, 1091–1102. https://doi.org/10.1111/1365-2435.13029

Ylänne, H., Stark, S., 2025. Can large animals direct the fate of the vast arctic soil carbon reserves – a review. Environ. Res. Commun. 7, 022004. https://doi.org/10.1088/2515-7620/adb7be

Ylänne, H., Stark, S., 2019. Distinguishing rapid and slow C cycling feedbacks to grazing in Sub-arctic tundra. Ecosystems 22, 1145–1159. https://doi.org/10.1007/s10021-018-0329-y

Yu, Q., Epstein, H., Engstrom, R., Walker, D., 2017. Circumpolar arctic tundra biomass and productivity dynamics in response to projected climate change and herbivory. Glob. Change Biol. 23, 3895–3907. https://doi.org/10.1111/gcb.13632

Zhang, R., Wei, Y., Dong, C., Wei, B., Rillig, M.C., Badgery, W.B., Yang, G., Liu, N., Zhang, Y., 2025. Quantifying the Positive Effect of Ungulate Herbivory on Living Root-Derived Soil Organic Carbon Formation: Evidence From an Eight-Year Simulated Grazing Field Experiment With 13C Pulse Labeling. Glob. Change Biol. 31, e70336. https://doi.org/10.1111/gcb.70336

Zhao, W., Rong, Y., Zhou, Y., Zhang, Y., Li, S., Liu, L., 2024. The Relationship of Gross Primary Productivity with NDVI Rather than Solar-Induced Chlorophyll Fluorescence Is Weakened under the Stress of Drought. Remote Sens. 16, 555. https://doi.org/10.3390/rs16030555

Zhou, L., Liu, S., Schrama, M., Ashworth, D., Bardgett, R.D., 2026. Grazer exclusion is associated with higher fast-cycling carbon pools but lower slow-cycling mineral-associated carbon across grasslands. Proc. Natl. Acad. Sci. 123, e2512048123. https://doi.org/10.1073/pnas.2512048123

Zhou, Y., Xu, M., Ren, S., Du, Y., Yue, Y., Yu, H., Zhang, Y., Jiang, S., Xu, T., Wang, L., 2025. More Than a Decade of Moderate Grazing: No Impact on Soil Organic Carbon Stocks and Enhancement of Mineral-Associated Organic Carbon via Livestock Diversification. Glob. Change Biol. 31, e70466. https://doi.org/10.1111/gcb.70466

Zhu, D., Ciais, P., Chang, J., Krinner, G., Peng, S., Viovy, N., Peñuelas, J., Zimov, S., 2018. The large mean body size of mammalian herbivores explains the productivity

paradox during the Last Glacial Maximum. Nat. Ecol. Evol. 2, 640–649. https://doi.org/10.1038/s41559-018-0481-y
Zimov, S.A., Zimov, N.S., Tikhonov, A.N., Chapin, F.S., 2012. Mammoth steppe: a high-productivity phenomenon. Quat. Sci. Rev. 57, 26–45. https://doi.org/10.1016/j.quascirev.2012.10.005

8 Appendix

Appendix 1: Supplemental Information for Chapter II

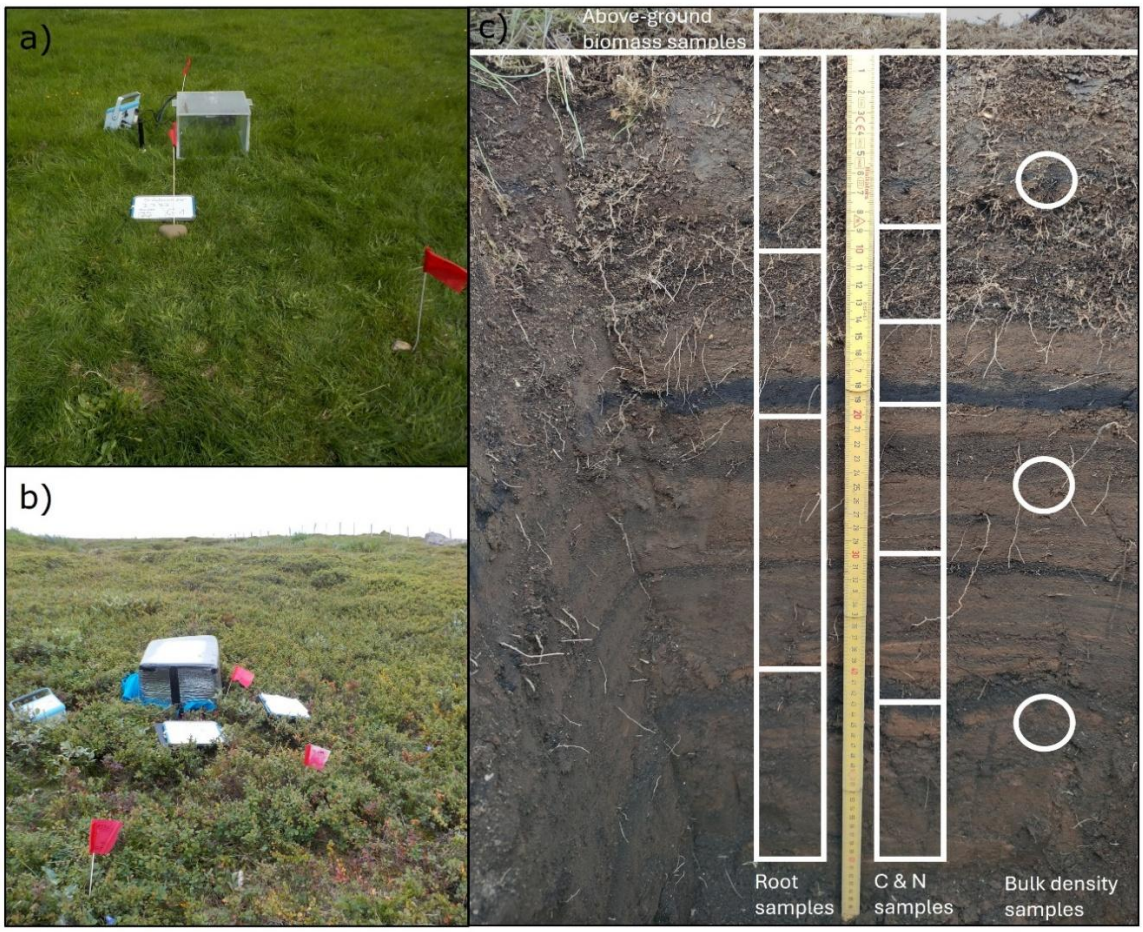

Supplemental Figure 8-1: Exemplary setup for flux measurements and soil sampling. CO_2 fluxes were measured in ambient light with a transparent chamber pressed on the soil surface (a) and in dark conditions with all light excluded by an opaque hood (b), connected to an infrared gas analyser. Red flags mark permanent measurement points. Soil profiles were excavated to 60 cm depth (c). Above each soil profile, an above-ground biomass sample was collected. Root samples and C & N samples (carbon and nitrogen analysis) were collected as complete blocks in the respective soil depth. Root samples were collected in four consistent depth intervals, while number of samples and depth intervals for C & N varied according to soil horizons. Bulk density samples were collected from at least three depths in the upper, middle and deeper soil using cylinders pushed horizontally into the soil. With more variability in the soil, bulk density samples were increased accordingly. Photographs taken by Christian Klopsch.

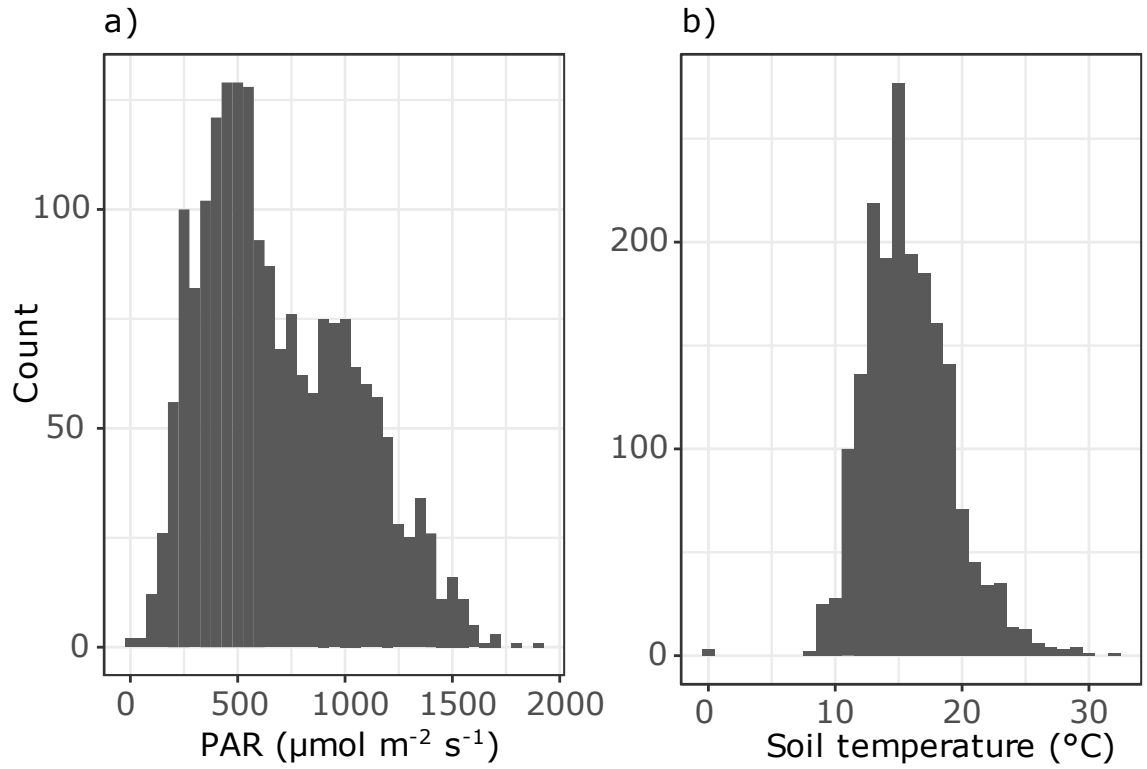

Supplemental Figure 8-2: Histogram of PAR and Tsoil. Data distribution of PAR (Photosynthetic active radiation) and soil temperature over the two measurement periods in all sites with four or more measurement days (n = 18)

Supplemental Table 8-1: Vascular plant species lists recorded during measurement days at each study site in 5 m radius around sub-plots. Abbreviated plant species are: Ach_mil = Achillea millefolium, Agr_cap = Agrostis capillaris, Agr_sto = Agrostis stolonifera, Agr_vin = Agrostis vinealis, Agr_sp = Agrostis sp., Alc_alp = Alchemilla alpina, Alc_vul = Alchemilla vulgaris, Alo_pra = Alopecurus pratensis, Ant_odo = Anthoxanthum odoratum, Ara_pet = Arabidopsis_petrea, Arc_uva = Arctostaphylos uva-ursi, Arm_mar = Armeria maritima, Are_nor = Areneraria norvegica, Arg_ans = Argentina anserina, Ave_fle = Avenella flexuosa, Bar_alp = Bartsia alpina, Bet_nan = Betula nana, Bet_pub = Betula pubescens, Bis_viv = Bistorta vivipara, Bot_lun = Botrychium lunaria, Cal_str = Calamagrostis stricta, Cal_vul = Calluna vulgaris, Cam_rot = Campanula rotundifolia, Cap_bur = Capsella bursa-pastoris, Car_pra = Cardamine pratensis subsp. angustifolia, Car_big = Carex bigelowii, Car_cps = Carex capillaris, Car_cpa = Carex capitata, Car_dio = Carex dioica, Car_mar = Carex maritima, Car_nig = Carex nigra, Car_pan = Carex panicea, Car_sax = Carex saxatalis, Car_vag = Carex vaginata, Cer_alp = Cerastium alpinum Cer_fon = Cerastium fontanum, Coe_vir = Coeloglossum viride, Cor_tri = Corallorhiza trifida, Dac_mac = Dactylorhiza maculata, Des_ces = Deschampsia cespitosa, Dra_inc = Draba incana, Dry_oct = Dryas octopetala, Emp_nig = Empetrum nigrum, Epi_pal = Epilobium palustre, Equ_arv = Equisetum arvense, Equ_flu = Equisetum fluviatile, Equ_hye = Equisetum hyemale, Equ_pal = Equisetum palustre, Equ_pra = Equisetum pratense, Equ_var = Equisetum variegatum, Eri_bor = Erigeron borealis, Eri_ang = Eriophorum angustifolium, Eup_fri = Euphrasia frigida, Fes_rub = Festuca rubra, Fes_viv = Festuca vivipara, Fil_ulm = Filipendula ulmaria, Gal_bor = Galium boreale, Gal_nor = Galium normanii, Gal_ver = Galium verum, Gen_niv = Gentiana nivalis, Gen_ama = Gentianella amarella, Gen_cam = Gentianella campestris, Ger_syl = Geranium sylvaticum, Geu_riv = Geum rivale, Hie_alp = Hieracium alpina, Hie_tha = Hieracium thaectolepium, Hie_sp = Hieracium sp., Hie_odo = Hierochloe odorata, Jun_arc = Juncus arctica, Jun_buf = Juncus bufonius, Jun_trif = Juncus trifidus, Jun_trig = Juncus triglumis, Jun_com = Juniperus communis, Kob_myo = Kobresia myosuroides, Koe_isl = Koenigia islandica, Leo_aut = Leontodon autumnalis, Lep_sua = Lepidotheca suaveolens, Luz_mul = Luzula multiflora, Luz_spi = Luzula spicata, Lyn_alp = Lynchis alpina, Myo_arv = Myosotis arvensis, Nar_str = Nardus stricta, Par_pal = Parnassia palustris, Phl_alp = Phleum alpinum, Pil_isl = Pilosella islandica, Pin_vul = Pinguicula vulgaris, Pla_mar = Plantago maritima, Pla_hyp = Platanthera hyperborea, Poa_alp = Poa alpina, Poa_ann = Poa annua, Poa_glau = Poa glauca, Poa_nem = Poa nemoralis, Poa_pra = Poa pratensis, Pol_avi = Polygonum aviculare, Pop_tre = Populus tremula, Pot_cra = Potentilla crantzii, Pru_vul = Prunella vulgaris, Pse_str_Pseudorchis stramia, Pyr_min = Pyrola minor, Ran_acr = Ranunculus acris, Rhi_min = Rhinanthus minor, Rub_sax = Rubus saxatilis, Rum_osa = Rumex acetosa, Rum_ella = Rumex acetosella, Sag_pro = Sagina procumbens, Sal_arc = Salix arctica, sal_her = Salix herbaceae, Sal_lan = salix lanata, Sal_phy = Salix phylicifolia, Sal_sp = Salix sp., San_off = Sanguisorba officinalis, Sax_ces = Saxifraga cespitosa, Sax_hir = Saxifraga hirculus, Sed_vil = Sedum villosum, Sel_sel = Selaginella_selaginoides, Sil_aca = Silene acaulis, Sor_auc = Sorbus aucuparia, Spe_arc = Spergula arvensis, Ste_gra = Stellaria graminea, Ste_med = Stellaria media, Tar_sp = Taraxacum sp., Tha_alp = Thalictrum alpinum, Thy_pra = Thymus praecox subsp. Arcticus, Tof_pus = Tofieldia pusilla, Tri_ces = Trichophorum cespitosum, Tri_rep = Trifolium repens, Tri_pal = Triglochin palustre, Tri_spi = Trisetum spicatum, Vac_myr = Vaccinium myrtillus, Vac_uli = Vaccinium uliginosum, Ver_ser = Veronica serphyllifolia, Vic_cra = Vicia cracca, Vio_can = Viola canina, Vio_pal = Viola palustris. Species names follow Wąsowicz (2020).

Eastern	Gun		Hja		Holt		Lei		Pho		Phv		Reyk		Skb		Vid	
Iceland	G	E	G	E	G	E	G	E	G	E	G	E	G	E	G	E	G	E
Ach_mil	0	0	0	0	0	0	1	1	1	1	1	1	1	0	0	0	0	0
Agr_cap	1	1	1	1	0	0	1	1	1	1	1	0	1	1	0	0	0	0
Agr_sto	0	0	0	0	0	0	0	0	1	1	0	0	0	0	0	0	0	0
Agr_vin	1	0	0	0	0	0	0	0	0	0	0	0	0	0	0	0	1	1
Agr_sp	0	0	0	0	1	1	0	0	0	0	0	1	0	0	1	0	0	0
Alc_alp	1	0	0	0	1	0	1	1	1	1	1	1	1	1	1	1	0	0
Alc_vul	1	1	1	1	1	1	0	0	1	1	1	0	0	0	0	0	0	0
Alo_pra	0	0	0	0	0	0	0	0	0	0	0	0	0	0	0	0	0	0
Ant_odo	1	1	1	0	1	1	1	1	1	1	1	1	1	1	1	0	1	1
Ara_pet	0	0	0	0	0	0	0	0	0	0	0	0	0	0	0	0	0	0
Arc_uva	0	0	0	0	0	0	0	0	0	0	1	1	0	0	1	0	1	1
Arm_mar	1	1	0	0	1	1	0	0	0	0	0	0	0	0	0	1	1	1
Are_nor	0	0	0	0	0	0	0	0	0	0	0	0	0	0	0	0	0	0
Arg_ans	0	0	0	0	0	0	0	0	0	0	0	0	0	0	0	0	0	0
Bar_alp	1	1	1	1	1	1	0	1	0	0	0	0	1	1	1	1	1	1
Bet_nan	0	1	1	1	1	1	1	1	0	0	1	1	1	1	1	1	1	1
Bet_pub	0	0	1	1	0	0	0	1	0	0	1	1	0	1	0	0	0	0
Bis_viv	1	1	1	1	1	1	1	1	1	1	1	1	1	1	1	1	1	1
Bot_lun	1	0	0	0	1	0	1	1	1	1	1	0	1	1	0	0	0	0
Cal_str	0	0	0	0	0	0	0	0	0	0	0	0	0	0	0	0	0	0
Cal_vul	0	0	1	1	0	0	1	1	1	0	1	1	1	1	1	1	1	1
Cam_rot	1	1	1	1	1	1	0	0	0	0	0	0	0	0	0	0	1	1
Cap_bur	0	0	0	0	0	0	0	0	0	0	0	0	0	0	0	0	0	0
Car_pra	1	1	0	0	0	0	0	0	0	0	0	0	1	1	0	0	0	0
Car_big	1	1	0	0	1	1	1	1	1	0	1	0	0	0	0	0	0	0
Car_cps	0	1	1	1	0	0	0	0	0	0	1	0	1	0	0	0	0	0
Car_cpa	0	0	0	0	1	1	0	0	0	0	0	0	0	1	0	0	0	0
Car_dio	0	0	0	0	0	0	0	0	0	0	0	0	0	0	0	0	0	0
Car_mar	0	0	0	0	0	0	0	0	0	0	0	0	0	0	0	0	0	0
Car_nig	1	1	0	0	1	0	0	0	0	1	0	0	1	0	0	0	0	0
Car_pan	0	0	0	0	0	0	0	0	0	0	0	1	0	0	0	0	0	0
Car_sax	0	0	0	0	0	0	0	0	0	0	0	0	0	0	0	0	0	0
Car_vag	0	1	1	1	1	1	1	1	0	1	0	1	1	1	1	0	1	1
Cer_alp	1	1	0	0	1	1	1	0	1	1	0	0	0	0	0	0	0	0
Cer_fon	1	1	0	0	1	0	1	0	1	0	0	0	0	0	0	0	0	0
Coe_vir	1	1	0	0	1	1	1	0	1	0	1	1	1	1	0	0	1	1
Cor_tri	0	0	0	0	0	0	1	0	0	0	0	0	0	0	0	0	0	0
Dac_mac	0	0	0	0	0	0	0	0	0	0	0	1	0	0	0	0	0	0
Des_ces	1	1	1	1	0	0	0	0	0	1	1	1	1	0	0	0	0	0
Des_fle	0	0	0	1	0	0	0	0	0	0	0	1	0	0	1	1	0	1

(continued)

Dra_inc	1	0	0	0	0	0	0	0	1	0	0	0	0	0	0	0	0	0
Dry_oct	1	0	0	0	1	1	1	1	0	0	1	0	0	1	0	1	1	1
Emp_nig	1	1	1	1	1	1	1	1	1	1	1	1	1	1	1	1	1	1
Epi_pal	0	0	0	0	0	0	0	0	0	0	0	0	0	0	0	0	0	0
Equ_arv	1	1	0	0	1	1	0	0	1	1	0	0	0	0	0	1	0	0
Equ_flu	0	0	0	0	0	0	0	0	0	0	0	0	0	0	0	0	0	0
Equ_hye	0	0	0	0	0	0	0	0	0	0	0	0	0	0	0	0	0	0
Equ_pal	1	0	0	1	0	0	0	0	0	0	0	0	0	0	0	0	0	0
Equ_pra	1	0	0	1	1	1	0	1	1	1	1	0	1	1	1	1	1	1
Equ_var	1	1	0	0	1	1	0	0	1	1	1	0	1	1	1	1	1	1
Eri_bor	1	0	0	0	0	0	1	1	1	0	0	0	0	0	0	0	1	0
Eri_ang	0	0	0	0	0	0	0	0	0	0	0	0	0	0	0	0	0	0
Eup_fri	1	0	0	0	1	0	1	0	1	0	1	0	0	0	0	0	0	0
Fes_rub	1	1	1	1	1	1	1	1	1	1	1	1	1	1	1	1	1	1
Fes_viv	1	1	1	1	1	0	1	1	1	1	1	0	1	1	1	1	1	1
Fil_ulm	0	0	0	0	0	0	0	0	0	0	0	0	0	0	0	0	0	0
Gal_bor	0	0	0	0	0	0	0	0	0	0	0	0	0	0	0	0	0	0
Gal_nor	1	1	1	1	1	0	1	1	1	1	1	1	1	1	1	0	0	0
Gal_ver	0	0	1	1	0	0	1	1	1	1	1	1	1	1	1	0	1	1
Gen_niv	0	0	0	0	0	0	0	0	0	0	0	0	0	0	0	0	0	0
Gen_ama	0	0	0	0	0	0	0	0	0	0	0	0	0	0	0	0	0	0
Gen_cam	1	0	0	0	0	0	1	0	1	0	1	0	0	0	0	0	0	0
Ger_syl	0	0	1	1	0	0	0	0	0	0	0	0	0	1	0	0	0	0
Geu_riv	0	1	1	1	0	0	0	0	0	0	0	0	0	0	0	0	0	0
Hie_alp	0	0	0	0	0	0	0	0	0	0	0	0	0	0	0	0	0	0
Hie_tha	0	0	0	0	0	0	0	0	0	0	0	0	0	0	0	0	0	0
Hie_sp	0	0	1	1	1	1	1	1	0	0	0	1	1	1	1	1	1	1
Hie_odo	0	1	1	1	0	0	0	0	0	0	0	0	0	0	0	0	1	1
Jun_arc	0	0	0	1	1	0	0	0	0	0	0	0	0	0	0	0	0	0
Jun_buf	0	0	0	0	0	0	0	0	0	0	0	0	0	0	0	0	0	0
Jun_trif	1	1	0	1	1	0	1	1	0	0	0	0	1	1	1	1	1	1
Jun_trig	0	0	0	0	0	0	0	0	0	0	0	0	0	0	0	0	0	0
Jun_com	0	0	0	1	0	0	0	0	0	0	0	0	0	0	1	1	0	0
Kob_myo	1	0	0	0	1	0	1	1	1	0	1	0	0	0	1	1	1	0
Koe_isl	0	0	0	0	0	0	0	0	0	0	0	0	0	0	0	0	0	0
Leo_aut	1	1	1	0	1	0	1	1	1	1	1	0	0	0	0	0	0	0
Lep_sua	0	0	0	0	0	0	0	0	0	0	0	0	0	0	0	0	0	0
Luz_mul	1	1	1	1	1	1	1	1	1	0	1	1	1	0	1	1	1	1
Luz_spi	1	1	0	0	1	0	1	1	0	0	0	0	0	0	1	0	0	0
Lyn_alp	0	0	0	0	0	0	0	0	0	0	0	0	0	0	0	0	0	0
Myo_arv	0	0	0	0	0	0	0	0	0	0	1	0	0	0	0	0	0	0
Nar_str	0	0	0	0	0	0	0	0	0	0	0	1	0	0	0	0	0	0
Par_pal	1	1	1	1	1	1	1	1	0	0	1	0	0	0	0	1	1	0

(continued)

Phl_alp	1	1	1	0	0	0	0	0	0	0	0	0	0	0	0	0	0	0
Pil_isl	0	0	0	0	0	0	0	0	0	0	0	0	0	0	0	0	0	0
Pin_vul	1	1	0	0	1	1	1	1	0	0	0	0	0	0	1	0	1	0
Pla_mar	0	0	0	0	1	1	0	0	0	0	0	0	0	0	0	0	0	0
Pla_hyp	1	1	0	1	1	1	1	0	0	0	1	0	1	0	0	0	1	0
Poa_alp	1	0	0	0	1	0	0	0	0	0	0	0	0	0	0	0	0	0
Poa_ann	0	0	0	0	0	0	0	0	0	0	0	0	0	0	0	0	1	0
Poa_glau	1	0	0	0	1	0	0	0	0	0	0	0	0	0	0	0	0	0
Poa_nem	0	0	0	0	0	0	0	0	0	0	0	0	0	0	0	0	0	0
Poa_pra	1	1	1	0	1	0	1	0	1	1	1	0	1	0	0	0	0	0
Pol_avi	0	0	0	0	0	0	0	0	0	0	0	0	0	0	0	0	0	0
Pop_tre	0	0	0	0	0	0	0	0	0	0	0	0	0	0	0	0	0	0
Pop_tre	1	1	1	0	1	1	0	1	1	1	0	0	1	1	0	0	0	0
Pru_vul	0	0	0	0	0	0	0	0	0	0	1	0	0	0	0	0	0	0
Pse_str	0	0	0	0	0	1	0	0	0	0	0	0	0	0	0	0	0	0
Pyr_min	0	1	1	0	0	0	0	1	0	0	1	0	1	0	0	0	0	0
Ran_acr	0	1	1	1	0	0	0	1	1	1	1	1	1	1	1	1	1	1
Rhi_min	1	0	1	1	0	0	1	1	1	0	1	0	0	0	0	0	1	0
Rub_sax	0	0	0	0	0	0	0	0	0	0	0	0	1	0	0	0	0	0
Rum_osa	1	1	1	1	0	1	0	0	1	1	0	0	0	0	0	0	0	0
Rum_ella	0	0	0	0	0	0	0	0	0	0	0	0	0	0	0	0	0	0
Sag_pro	0	0	0	0	0	0	0	0	0	0	0	0	0	0	0	0	1	0
Sal_arc	0	0	0	0	0	0	0	0	0	0	0	0	0	0	0	0	1	1
Sal_her	1	1	0	0	1	1	1	1	0	0	0	0	0	0	1	1	0	0
Sal_lan	0	1	1	1	0	1	0	0	0	0	0	0	1	1	1	1	1	1
Sal_phy	0	0	1	1	0	0	0	0	0	0	1	0	0	0	1	1	1	1
Sal_sp	0	1	1	1	1	1	0	1	0	0	0	0	0	1	0	1	0	0
San_off	0	0	0	0	0	0	0	0	0	0	0	0	0	0	0	0	0	0
Sax_ces	0	0	0	0	0	0	0	0	0	0	0	0	0	0	0	0	0	0
Sax_hir	0	0	0	0	0	0	0	0	0	0	0	0	0	0	0	0	0	0
Sed_vil	1	1	0	0	0	0	0	0	0	0	0	0	0	0	0	0	0	0
Sel_sel	1	1	0	1	0	0	1	1	0	0	1	0	1	0	0	0	1	0
Sil_aca	1	0	0	0	0	1	1	0	0	0	0	0	0	0	0	0	0	0
Sor_auc	0	0	0	0	0	0	0	0	0	0	0	1	0	0	0	0	0	0
Spe_arc	0	0	0	0	0	0	0	0	0	0	0	0	0	0	0	0	0	0
Ste_gra	0	0	0	0	0	0	0	0	0	0	0	0	0	0	0	0	0	0
Ste_med	0	0	0	0	0	0	0	0	0	0	0	0	0	0	0	0	0	0
Tar_sp	1	1	1	1	1	1	1	1	1	1	1	1	1	1	0	1	1	1
Tha_alp	1	1	1	1	1	0	1	1	0	1	1	0	1	1	1	1	1	1
Thy_pra	1	1	0	0	1	0	1	1	1	0	1	0	1	0	1	1	1	1
Tof_pus	0	1	0	0	1	1	1	1	0	0	0	0	0	0	0	0	1	1
Tri_ces	0	0	0	0	0	0	0	0	0	0	0	0	0	0	1	0	0	0
Tri_rep	0	0	0	0	0	0	0	0	1	0	1	1	0	0	0	0	0	0

(continued)

Tri_pal	0	0	0	0	0	0	0	0	0	0	0	0	0	0	0	0	0	0
Tri_spi	1	0	0	0	1	0	1	0	0	0	0	0	0	0	0	0	0	0
Vac_myr	0	0	0	0	0	0	0	0	0	0	1	1	1	1	0	0	0	0
Vac_uli	1	1	1	1	1	1	1	1	0	0	1	1	1	1	1	1	1	1
Ver_ser	0	0	0	0	0	0	0	0	0	0	0	0	0	0	0	0	0	0
Vic_cra	0	0	0	0	0	0	0	0	0	0	1	1	0	0	0	0	0	0
Vio_can	0	1	0	0	0	0	0	0	1	1	1	0	0	0	0	0	1	0
Vio_pal	1	0	0	0	0	0	0	0	0	0	0	0	0	0	0	0	0	0
SUM	**55**	**49**	**37**	**40**	**49**	**35**	**43**	**41**	**37**	**28**	**46**	**29**	**38**	**32**	**32**	**29**	**41**	**32**

G = Grazed, E = Exclosure

Northern	**Alf**		**Ber**		**Gsk**		**LL**		**Mh**		**Orl**		**Rod**		**SB**		**Skr**	
Iceland	**G**	**E**	**G**	**E**	**G**	**E**	**G**	**E**	**G**	**E**	**G**	**E**	**G**	**E**	**G**	**E**	**G**	**E**
Ach_mil	1	0	1	0	1	1	0	0	0	0	1	1	0	0	1	1	1	0
Agr_cap	1	1	1	1	1	1	1	0	1	1	1	1	1	0	1	0	1	0
Agr_sto	0	0	0	0	0	0	0	0	0	0	0	0	0	0	1	0	0	0
Agr_vin	1	1	1	0	0	0	0	0	0	0	1	0	1	0	0	0	1	0
Agr_sp	0	0	0	0	0	0	0	1	0	0	0	0	0	0	0	1	0	1
Alc_alp	1	1	1	1	1	1	1	1	1	1	0	0	1	0	1	0	0	0
Alc_vul	1	0	1	0	1	1	0	1	1	1	0	0	0	0	1	0	0	0
Alo_pra	0	0	0	0	0	0	0	0	0	1	0	1	0	0	0	0	0	0
Ant_odo	1	1	1	0	1	1	1	0	1	1	1	1	1	1	1	1	1	1
Ara_pet	0	0	0	0	0	0	0	0	0	0	0	0	0	0	0	0	0	0
Arc_uva	0	1	0	0	0	0	0	0	0	0	0	0	1	1	0	0	0	0
Arm_mar	0	1	0	0	0	0	1	0	1	1	0	0	1	1	0	0	0	0
Are_nor	0	0	0	0	0	0	0	0	0	0	0	0	0	0	0	0	0	0
Arg_ans	0	0	0	0	0	0	0	0	0	0	0	0	0	0	0	0	0	0
Bar_alp	0	1	0	0	0	0	0	0	0	0	1	1	0	1	0	0	1	0
Bet_nan	0	0	0	0	0	0	1	0	0	1	0	0	1	1	1	1	0	1
Bet_pub	0	1	0	0	0	1	1	1	0	1	1	1	1	1	1	1	1	1
Bis_viv	1	1	1	1	1	1	1	1	1	1	1	1	1	1	1	1	1	1
Bot_lun	0	0	0	0	1	0	1	0	0	0	1	0	0	0	1	1	0	1
Cal_str	0	0	0	0	0	0	0	0	0	0	0	0	0	0	0	0	0	0
Cal_vul	0	0	0	0	0	0	0	0	0	0	0	0	0	0	0	0	0	0
Cam_rot	0	0	0	0	0	0	0	0	0	0	0	0	0	0	0	0	0	0
Cap_bur	1	0	0	0	0	0	0	0	0	0	0	0	0	0	0	0	0	0
Car_pra	0	0	0	1	0	0	1	1	0	0	0	0	1	1	0	0	0	0
Car_big	0	1	1	1	1	0	1	1	1	1	1	1	1	1	0	0	0	0
Car_cps	1	0	0	0	1	0	1	0	1	0	1	0	0	0	0	0	0	0
Car_cpa	0	0	0	0	0	0	0	0	0	0	0	0	0	0	0	0	0	0
Car_dio	0	0	0	0	0	0	0	0	0	0	0	0	0	1	0	0	0	0
Car_mar	0	0	0	0	0	0	0	0	0	0	0	0	0	0	0	0	0	0
Car_nig	1	0	0	1	0	1	0	1	0	1	1	1	0	0	1	1	1	1

(continued)

Car_pan	0	0	0	0	0	0	0	0	1	0	0	1	0	0	0	1	1	1
Car_sax	0	0	0	1	0	0	0	0	0	0	0	0	0	0	0	0	0	0
Car_vag	0	1	1	1	1	1	1	1	0	1	1	1	1	1	1	1	1	1
Cer_alp	0	1	0	0	0	0	0	0	1	1	0	1	1	1	0	0	1	0
Cer_fon	1	0	1	1	1	1	1	0	1	1	1	1	1	1	1	0	1	0
Coe_vir	0	1	1	1	1	0	1	0	0	0	0	0	0	0	0	1	0	0
Cor_tri	0	0	0	0	0	0	0	0	0	0	0	0	1	0	0	0	0	0
Dac_mac	0	0	0	0	0	0	0	0	0	0	0	0	0	0	0	0	0	0
Des_ces	1	1	1	1	1	1	1	1	1	1	1	1	1	1	1	0	1	1
Des_fle	0	0	0	0	0	1	0	0	0	1	0	0	0	1	0	1	0	0
Dra_inc	1	1	1	0	0	0	1	0	0	0	1	1	1	1	0	0	1	0
Dry_oct	0	1	1	0	1	0	1	0	1	0	0	0	1	1	0	0	0	0
Emp_nig	0	1	0	0	0	0	1	1	0	1	0	0	1	1	0	1	0	1
Epi_pal	0	0	0	0	0	0	0	0	0	0	0	0	0	0	0	0	0	0
Equ_arv	0	0	1	1	1	1	1	0	1	1	1	1	0	1	1	0	1	0
Equ_flu	0	0	0	0	0	0	0	0	0	0	0	0	0	0	0	0	0	1
Equ_hye	0	0	0	0	0	0	0	0	0	0	0	0	0	0	0	0	0	0
Equ_pal	0	0	0	0	0	0	0	0	0	1	0	0	0	0	0	0	1	0
Equ_pra	0	1	1	1	1	1	1	1	1	1	1	1	0	1	1	1	0	1
Equ_var	0	1	1	1	0	1	1	0	1	1	1	1	0	1	0	1	0	0
Eri_bor	0	0	1	0	1	0	1	0	1	0	1	1	1	0	1	0	0	0
Eri_ang	0	0	0	0	0	0	0	0	0	0	0	0	0	0	0	0	0	0
Eup_fri	1	0	1	0	1	0	1	0	1	0	1	0	1	0	0	0	0	0
Fes_rub	1	1	1	1	0	1	1	1	1	1	1	1	1	1	1	1	1	0
Fes_viv	1	1	1	0	1	1	1	1	1	1	1	1	1	1	1	1	1	1
Fil_ulm	0	0	0	0	0	0	0	0	0	0	0	0	0	0	0	0	0	0
Gal_bor	0	0	0	0	0	0	0	0	0	0	0	0	0	0	0	0	0	0
Gal_nor	1	1	1	1	1	1	1	0	1	1	1	0	1	1	1	1	1	1
Gal_ver	1	1	1	1	1	1	1	1	1	1	1	1	1	1	1	1	1	1
Gen_niv	1	0	0	0	1	0	0	0	1	0	0	0	0	0	0	0	0	0
Gen_ama	0	0	0	0	1	0	0	0	0	0	0	0	0	0	0	0	0	0
Gen_cam	1	0	1	0	1	0	0	0	1	0	0	0	0	0	1	0	0	0
Ger_syl	0	0	0	0	0	1	0	0	0	0	0	0	0	0	0	0	0	0
Geu_riv	0	0	1	1	0	0	0	0	0	0	0	0	1	0	1	1	1	1
Hie_alp	0	0	0	0	0	0	0	0	0	0	0	0	0	0	0	0	0	0
Hie_tha	0	0	0	0	0	0	0	0	0	0	0	0	0	0	0	0	0	0
Hie_sp	1	0	1	1	1	1	1	0	1	0	1	1	1	1	1	1	0	0
Hie_odo	0	0	0	1	1	1	0	0	0	0	1	0	0	0	1	1	1	1
Jun_arc	0	0	0	0	0	0	0	0	0	0	0	1	0	0	0	0	0	0
Jun_buf	0	0	0	0	0	0	0	0	0	0	0	0	0	0	0	0	0	0
Jun_trif	0	1	1	0	1	0	1	1	1	1	0	0	1	0	0	1	0	0
Jun_trig	0	0	0	0	0	0	0	0	0	0	0	0	0	0	0	0	0	0
Jun_com	0	0	0	0	0	0	0	0	0	0	0	0	0	0	0	0	0	0

(continued)

Kob_myo	1	1	1	1	1	0	1	0	1	1	1	1	1	0	1	1	0	0
Koe_isl	0	0	0	0	0	0	0	0	0	0	0	0	0	0	0	0	0	0
Leo_aut	1	0	1	1	1	1	1	0	1	1	1	0	1	0	1	1	1	0
Lep_sua	0	0	0	0	1	0	0	0	0	0	0	0	0	0	0	0	0	0
Luz_mul	1	1	1	0	1	1	1	0	1	1	1	1	1	1	1	1	1	0
Luz_spi	0	1	1	0	0	0	1	0	0	0	0	0	1	0	1	0	0	0
Lyn_alp	0	0	0	0	0	0	0	0	0	0	0	0	1	0	0	0	0	0
Myo_arv	0	0	1	0	0	1	1	0	0	0	1	1	0	0	1	0	1	0
Nar_str	0	0	0	0	0	0	0	0	0	0	0	0	0	0	0	0	0	0
Par_pal	1	0	1	0	0	0	0	0	1	0	1	0	1	0	0	0	0	0
Phl_alp	0	0	0	0	0	0	0	0	0	0	0	1	0	0	1	0	0	0
Pil_isl	0	0	0	0	1	1	1	0	0	0	0	0	1	0	0	0	0	0
Pin_vul	0	0	0	0	0	0	1	0	1	0	0	0	1	1	0	0	0	0
Pla_mar	0	0	0	0	0	0	1	0	0	0	0	0	1	1	0	0	0	0
Pla_hyp	0	0	1	0	0	0	1	0	0	0	0	1	1	0	0	0	0	0
Poa_alp	1	0	1	0	0	0	1	0	0	0	0	0	0	0	0	0	0	0
Poa_ann	0	0	0	0	1	0	0	0	0	0	0	0	0	0	0	0	0	0
Poa_glau	1	0	0	0	0	0	0	0	1	0	1	0	1	0	0	0	0	0
Poa_nem	0	0	0	0	0	0	0	0	0	0	0	0	0	0	0	0	0	0
Poa_pra	1	1	1	0	0	1	0	1	1	1	1	1	1	1	1	1	1	0
Pol_avi	0	0	0	0	0	0	0	0	0	0	0	0	0	0	0	0	0	0
Pop_tre	0	0	0	0	0	0	0	0	0	0	0	1	0	0	0	0	0	0
pop_tre	1	1	1	0	0	1	1	0	1	1	0	1	1	1	1	0	1	0
Pru_vul	0	0	0	0	0	0	0	0	0	0	0	0	0	0	0	0	0	0
Pse_str	0	0	0	0	0	1	1	0	0	0	0	0	1	0	0	0	0	0
Pyr_min	0	0	0	0	0	0	0	0	0	0	0	0	0	0	0	0	0	0
Ran_acr	1	1	0	1	1	1	1	1	1	1	0	1	1	1	1	0	1	1
Rhi_min	1	0	1	0	1	1	1	0	1	0	1	1	1	0	1	1	1	0
Rub_sax	0	0	0	0	1	1	0	0	0	0	0	0	0	0	0	0	0	1
Rum_osa	1	1	1	1	1	1	1	1	0	1	1	1	1	1	1	0	1	1
Rum_ella	0	0	0	0	0	0	0	0	0	0	0	0	0	0	0	0	0	0
Sag_pro	0	0	0	0	0	0	0	0	0	0	0	0	0	0	0	0	0	0
Sal_arc	0	0	0	0	0	0	0	0	0	0	0	0	0	0	0	0	0	0
Sal_her	1	1	1	0	0	0	1	1	0	0	0	0	1	0	1	1	0	0
Sal_lan	0	0	0	0	0	0	0	0	0	0	0	0	1	1	0	0	0	0
Sal_phy	0	0	0	0	0	0	0	0	0	0	0	0	0	0	0	0	1	1
Sal_sp	0	1	0	0	0	1	1	1	0	1	0	1	1	1	0	0	1	1
San_off	0	0	0	0	0	0	0	0	0	0	0	0	0	0	0	0	0	0
Sax_ces	0	0	0	0	0	0	0	0	0	0	0	0	1	0	0	0	0	0
Sax_hir	0	0	0	0	0	0	0	0	0	0	0	0	0	0	0	0	0	0
Sed_vil	0	0	0	0	0	0	0	0	0	0	0	0	1	0	0	0	0	0
Sel_sel	0	0	1	0	0	0	1	0	1	1	0	0	1	0	0	0	0	0
Sil_aca	0	0	1	0	0	0	1	0	1	1	0	0	1	0	0	0	0	0

(continued)

Sor_auc	0	0	0	0	0	0	0	0	0	0	0	0	0	0	0	0	0	0
Spe_arc	0	0	0	0	0	0	0	0	0	0	0	0	0	0	0	0	0	0
Ste_gra	0	0	0	0	0	0	0	0	0	0	0	1	0	0	0	0	0	0
Ste_med	1	0	1	0	1	0	0	0	0	0	0	0	0	0	0	0	0	0
Tar_sp	1	1	1	1	1	1	1	0	1	1	1	1	1	1	1	1	1	1
Tha_alp	1	1	1	1	1	1	1	0	1	0	1	1	1	1	1	1	1	1
Thy_pra	1	1	1	0	1	1	1	1	1	1	1	1	1	1	1	0	0	0
Tof_pus	0	0	0	0	0	0	1	0	0	0	0	0	1	0	0	0	0	0
Tri_ces	0	0	0	0	0	0	0	0	0	0	0	0	0	0	0	0	0	0
Tri_rep	0	0	1	1	1	1	0	0	1	0	1	1	0	0	1	0	1	0
Tri_pal	0	0	0	0	0	0	0	0	0	0	0	0	0	0	0	0	0	0
Tri_spi	0	0	0	0	0	0	0	0	0	0	0	0	0	1	0	1	0	0
Vac_myr	0	0	0	0	0	0	0	0	0	0	0	0	0	0	0	0	0	0
Vac_uli	0	0	0	1	0	0	1	0	0	1	0	1	1	1	0	1	0	1
Ver_ser	0	0	0	0	0	0	0	0	0	0	0	0	0	0	0	0	0	0
Vic_cra	0	0	0	0	1	1	0	0	0	0	0	0	0	0	0	0	0	0
Vio_can	0	0	0	0	1	1	0	0	0	1	1	0	0	0	1	0	0	0
Vio_pal	0	0	0	0	0	0	0	0	0	0	0	0	0	0	0	0	0	0
SUM	**37**	**36**	**47**	**28**	**44**	**40**	**53**	**24**	**42**	**40**	**40**	**42**	**57**	**40**	**42**	**33**	**35**	**26**

G = Grazed, E = Exclosure

Southern	**H43**		**H60**		**Hau**		**Hva**		**Sk40**		**Sk90**		**Skl**	
Iceland	**G**	**E**	**G**	**E**	**G**	**E**	**G**	**E**	**G**	**E**	**G**	**E**	**G**	**E**
Ach_mil	0	0	0	0	0	0	0	0	0	0	0	0	0	0
Agr_cap	1	1	1	0	1	1	1	1	1	1	1	1	1	1
Agr_sto	0	0	0	0	0	0	0	0	0	0	0	0	0	0
Agr_vin	0	0	0	0	0	1	0	0	0	0	0	0	0	0
Agr_sp	0	0	0	0	0	0	0	0	0	0	0	0	0	0
Alc_alp	1	0	1	0	0	0	0	0	1	0	1	0	0	0
Alc_vul	0	0	0	0	0	0	0	0	0	0	0	0	0	0
Alo_pra	0	0	0	1	0	0	0	0	0	0	0	0	0	0
Ant_odo	0	0	0	0	0	0	0	0	0	0	0	0	0	0
Ara_pet	0	0	0	0	0	0	0	0	0	0	0	0	0	0
Arc_uva	0	0	0	0	0	0	0	0	0	0	0	0	0	0
Arm_mar	0	0	0	0	0	0	0	0	0	0	0	0	0	0
Are_nor	0	0	0	0	0	0	0	0	0	0	0	0	0	0
Arg_ans	0	0	0	0	0	0	0	0	1	0	1	0	1	1
Bar_alp	0	0	0	0	0	0	0	0	0	0	0	0	1	0
Bet_nan	0	0	0	0	0	0	0	0	1	1	1	1	0	0
Bet_pub	1	1	0	1	0	0	0	0	1	1	1	0	0	0
Bis_viv	1	1	1	0	0	0	0	0	1	1	1	1	0	0
Bot_lun	1	1	0	0	1	0	0	0	1	1	1	1	0	1

(continued)

Cal_str	0	0	0	0	0	1	0	0	0	0	0	0	0	0
Cal_vul	0	0	0	0	0	0	0	0	0	0	0	0	0	0
Cam_rot	0	0	0	0	0	0	0	0	0	0	0	0	0	0
Cap_bur	0	0	0	0	0	0	0	0	0	0	0	0	0	0
Car_pra	0	0	0	0	0	0	0	0	0	0	0	0	0	0
Car_big	0	0	0	0	0	0	0	0	0	0	0	0	0	0
Car_cps	0	0	0	0	0	0	0	0	0	0	0	0	0	0
Car_cpa	0	0	0	0	0	0	0	0	0	0	0	0	0	0
Car_dio	0	0	0	0	0	0	0	0	0	0	0	0	0	0
Car_mar	0	0	0	0	0	0	0	0	0	0	0	0	0	0
Car_nig	0	0	1	1	1	1	0	0	1	0	1	1	1	1
Car_pan	0	0	0	0	0	0	0	0	0	0	0	0	0	0
Car_sax	0	0	0	0	0	0	0	0	0	0	0	0	0	0
Car_vag	0	0	0	0	0	0	0	0	0	0	0	0	1	1
Cer_alp	0	0	0	0	0	1	0	0	0	0	0	0	0	0
Cer_fon	1	1	1	0	1	0	1	0	0	1	0	1	1	0
Coe_vir	0	0	0	0	0	0	0	0	0	0	0	0	0	0
Cor_tri	0	0	0	0	0	0	0	0	0	0	0	0	0	0
Dac_mac	0	0	0	0	0	0	0	0	0	0	0	0	0	0
Des_ces	0	0	0	0	0	0	0	0	0	0	0	0	0	0
Des_fle	0	1	1	1	0	0	0	0	1	0	1	0	0	0
Dra_inc	0	0	0	0	0	0	0	0	0	0	0	0	0	0
Dry_oct	0	0	0	0	0	0	0	0	0	0	0	0	0	0
Emp_nig	0	0	0	0	0	0	0	0	1	1	1	0	1	0
Epi_pal	0	0	1	0	0	0	0	0	0	0	0	0	0	0
Equ_arv	1	1	1	0	1	1	1	1	0	1	0	0	1	0
Equ_flu	0	0	0	0	0	0	0	0	0	0	0	0	0	0
Equ_hye	0	0	0	0	0	0	0	0	1	1	1	1	0	0
Equ_pal	0	0	0	0	0	0	0	0	0	0	0	0	0	0
Equ_pra	1	1	0	0	0	0	0	0	1	1	1	1	0	0
Equ_var	0	0	1	1	1	1	1	1	0	0	0	0	1	0
Eri_bor	0	0	1	0	0	0	0	0	0	0	0	0	0	0
Eri_ang	0	0	0	0	0	0	0	0	0	0	0	0	0	0
Eup_fri	0	0	0	0	0	0	0	0	0	0	0	0	0	0
Fes_rub	1	0	1	0	1	1	1	1	1	1	1	1	1	1
Fes_viv	1	0	1	1	1	1	1	1	0	0	0	1	1	1
Fil_ulm	0	0	0	0	0	0	0	0	0	0	0	0	0	0
Gal_bor	1	1	1	1	1	1	1	1	1	1	1	1	1	1
Gal_nor	1	0	1	0	0	0	0	0	1	1	1	1	0	0
Gal_ver	1	1	1	1	1	1	1	1	1	1	1	1	1	1
Gen_niv	0	0	0	0	0	0	0	0	0	0	0	0	0	0
Gen_ama	0	0	0	0	0	0	0	0	0	0	0	0	0	0
Gen_cam	0	0	0	0	0	0	0	0	0	0	0	0	0	0

(continued)

Ger_syl	0	0	0	0	0	0	0	0	0	0	0	0	0	0
Geu_riv	0	0	0	0	0	0	0	0	0	0	0	0	0	0
Hie_alp	0	0	0	0	0	0	0	0	0	0	0	0	0	0
Hie_tha	0	0	0	0	0	0	0	0	0	0	0	0	0	0
Hie_sp	0	0	0	0	0	0	0	0	0	0	0	0	0	0
Hie_odo	0	1	0	0	0	1	1	1	1	1	1	1	0	0
Jun_arc	0	0	0	0	0	1	0	0	0	0	0	0	1	1
Jun_buf	0	0	0	0	0	0	0	0	0	0	0	0	0	0
Jun_trif	0	0	0	0	0	0	0	0	0	0	0	0	0	0
Jun_trig	0	0	0	0	0	0	0	0	0	0	0	0	0	0
Jun_com	0	0	0	0	0	0	0	0	0	0	0	0	0	0
Kob_myo	1	0	1	0	1	1	1	1	1	1	1	1	0	0
Koe_isl	0	0	0	0	0	0	0	0	0	0	0	0	0	0
Leo_aut	1	1	0	0	0	1	0	0	1	1	1	1	0	0
Lep_sua	0	0	0	0	0	0	0	0	0	0	0	0	0	0
Luz_mul	1	0	1	0	1	1	1	1	1	1	1	1	1	1
Luz_spi	0	0	0	0	0	0	0	0	0	0	0	0	0	0
Lyn_alp	0	0	0	0	0	0	0	0	0	0	0	0	0	0
Myo_arv	0	0	1	0	0	0	0	0	0	0	0	0	0	0
Nar_str	0	0	0	0	0	0	0	0	0	0	0	0	0	0
Par_pal	1	0	0	0	0	0	0	0	0	0	0	0	0	0
Phl_alp	0	0	0	0	0	0	0	0	0	0	0	0	0	0
Pil_isl	0	0	0	0	0	0	0	0	0	0	0	0	0	1
Pin_vul	0	0	0	0	0	0	0	0	0	0	0	0	0	0
Pla_mar	0	0	0	0	0	0	0	0	0	0	0	0	0	0
Pla_hyp	0	0	0	0	0	0	0	0	0	0	0	0	0	0
Poa_alp	0	0	0	0	0	0	0	0	0	0	0	0	0	0
Poa_ann	0	0	0	0	0	0	0	0	0	0	0	0	0	0
Poa_glau	0	0	0	0	0	0	0	0	0	0	0	0	0	0
Poa_nem	0	1	0	1	0	0	0	0	0	0	0	0	0	0
Poa_pra	1	1	1	1	1	1	1	1	1	1	1	0	1	1
Pol_avi	0	0	0	0	0	0	0	0	0	0	0	0	0	0
Pop_tre	0	0	0	0	0	0	0	0	0	0	0	0	0	0
pop_tre	0	0	0	0	1	1	0	0	1	0	1	0	0	0
Pru_vul	0	0	0	0	0	0	0	0	0	0	0	0	0	0
Pse_str	0	0	0	0	0	0	0	0	0	0	0	0	0	0
Pyr_min	0	0	0	0	0	0	0	0	0	0	0	0	0	0
Ran_acr	1	1	0	0	0	1	0	0	0	0	0	0	0	0
Rhi_min	1	1	1	0	0	0	0	0	1	0	1	0	0	0
Rub_sax	0	1	0	1	0	0	0	0	1	0	1	0	0	0
Rum_osa	1	1	0	0	0	0	0	0	0	0	0	0	0	0
Rum_ella	0	0	0	0	0	0	0	0	0	0	0	0	0	0
Sag_pro	0	0	0	0	0	0	0	0	0	0	0	0	0	0

(continued)

Sal_arc	0	0	0	1	0	0	0	0	1	1	1	1	0	0
Sal_her	0	0	0	0	0	0	0	0	1	0	1	0	0	0
Sal_lan	0	0	0	0	0	0	0	0	1	1	1	1	0	0
Sal_phy	0	1	0	1	0	0	0	0	1	1	1	1	0	0
Sal_sp	0	0	0	0	0	0	0	0	0	0	0	0	0	0
San_off	0	0	0	0	0	0	0	0	0	0	0	0	0	0
Sax_ces	0	0	0	0	0	0	0	0	0	0	0	0	0	0
Sax_hir	0	0	0	0	0	0	0	0	0	0	0	0	0	0
Sed_vil	0	0	0	0	0	0	0	0	0	0	0	0	0	0
Sel_sel	1	0	0	0	0	0	0	0	0	0	0	0	0	0
Sil_aca	0	0	0	0	0	0	0	0	0	0	0	0	0	0
Sor_auc	0	0	0	0	0	0	0	0	0	0	0	0	0	0
Spe_arc	0	0	0	0	0	0	0	0	0	0	0	0	0	0
Ste_gra	0	0	0	0	0	0	0	0	0	0	0	0	0	0
Ste_med	0	0	0	0	0	0	0	0	0	0	0	0	0	0
Tar_sp	1	1	0	0	0	1	1	0	0	0	0	1	1	1
Tha_alp	0	1	0	0	1	1	0	0	1	1	1	1	1	0
Thy_pra	1	0	1	0	1	0	1	0	1	1	1	1	0	0
Tof_pus	0	0	0	0	0	0	0	0	0	0	0	0	0	0
Tri_ces	0	0	0	0	0	0	0	0	0	0	0	0	0	0
Tri_rep	0	0	0	0	0	0	0	0	0	0	0	0	0	0
Tri_pal	0	0	0	0	0	0	0	0	0	0	0	0	0	0
Tri_spi	0	0	0	0	0	0	0	0	1	1	1	0	0	0
Vac_myr	0	0	0	0	0	0	0	0	0	0	0	0	0	0
Vac_uli	0	0	0	0	0	0	0	0	1	1	1	0	0	0
Ver_ser	0	0	0	0	0	0	0	0	0	0	0	0	0	0
Vic_cra	0	0	0	0	0	0	0	0	0	0	0	0	0	0
Vio_can	0	0	0	0	0	0	0	0	0	0	0	0	0	0
Vio_pal	0	0	0	0	0	0	0	0	0	0	0	0	1	1
SUM	**24**	**21**	**21**	**13**	**16**	**21**	**14**	**11**	**32**	**26**	**32**	**23**	**19**	**15**

G = Grazed, E = Exclosure

Western	**Gil**		**Holl**		**Lun**		**Mel**		**Odd**		**SA**		**Stein**		**Thor**		**Vatn**	
Iceland	**G**	**E**	**G**	**E**	**G**	**E**	**G**	**E**	**G**	**E**	**G**	**E**	**G**	**E**	**G**	**E**	**G**	**E**
Ach_mil	0	0	0	0	0	0	1	0	0	0	0	0	0	0	0	0	0	0
Agr_cap	1	1	1	1	1	1	1	1	1	1	1	1	1	1	1	1	1	1
Agr_sto	0	0	0	0	0	0	0	0	0	0	0	0	0	0	0	0	0	0
Agr_vin	1	0	0	1	0	0	0	1	0	0	0	0	1	1	1	1	1	0
Agr_sp	0	0	0	0	0	0	0	0	0	0	0	0	0	0	0	0	0	0
Alc_alp	1	0	0	0	0	0	0	0	1	1	1	0	0	1	1	0	0	0
Alc_vul	1	0	1	1	1	0	1	1	1	1	1	0	0	1	1	1	0	0
Alo_pra	0	0	0	0	0	0	1	1	0	0	0	0	0	0	0	0	0	0

(continued)

Ant_odo	1	1	1	1	1	1	1	1	1	1	1	0	0	1	1	1	1	0
Ara_pet	0	1	0	0	0	0	0	0	0	0	0	0	0	0	0	0	0	0
Arc_uva	0	0	0	0	0	0	0	0	0	0	0	0	0	0	0	0	0	0
Arm_mar	1	0	0	1	0	0	0	0	0	0	1	1	0	1	0	0	0	0
Are_nor	0	0	0	0	0	0	0	0	0	0	0	1	0	0	0	0	0	0
Arg_ans	0	0	0	0	0	1	0	0	1	0	0	0	0	0	0	0	0	0
Bar_alp	0	0	0	0	0	0	0	0	0	0	0	0	0	0	0	0	0	0
Bet_nan	0	0	0	0	0	0	0	0	0	0	1	1	0	0	0	0	0	0
Bet_pub	1	1	0	1	0	0	0	1	0	0	1	1	1	1	0	0	0	1
Bis_viv	1	1	1	1	1	0	1	0	1	1	1	1	1	1	1	0	0	0
Bot_lun	1	1	1	0	1	0	0	0	1	1	1	0	0	0	0	0	0	0
Cal_str	0	0	0	1	0	0	0	0	0	1	0	0	0	0	1	0	0	0
Cal_vul	0	0	0	1	0	0	0	0	0	1	1	1	0	0	0	0	0	0
Cam_rot	0	0	0	0	0	0	0	0	0	0	0	0	0	0	0	0	0	0
Cap_bur	0	0	0	0	0	0	0	0	0	0	0	0	1	0	0	0	0	0
Car_pra	0	0	0	0	0	0	1	1	0	0	0	0	0	0	0	0	1	1
Car_big	1	1	1	1	1	1	0	0	1	1	1	1	0	0	1	1	0	1
Car_cps	1	0	1	0	0	0	0	0	1	0	1	0	0	0	0	0	0	0
Car_cpa	0	0	0	0	0	0	0	0	0	0	0	0	0	0	0	0	0	0
Car_dio	0	0	0	0	0	0	0	0	0	0	0	0	0	0	0	0	0	0
Car_mar	0	0	0	0	0	0	0	0	0	0	1	0	0	0	0	0	0	0
Car_nig	0	0	0	0	0	0	1	1	0	1	0	0	1	1	1	0	1	0
Car_pan	0	0	1	1	0	0	0	0	1	1	0	0	0	0	1	1	0	0
Car_sax	0	0	0	0	0	0	0	0	0	0	0	0	0	0	0	0	0	0
Car_vag	1	1	0	0	1	1	0	0	1	1	0	1	0	1	0	0	0	0
Cer_alp	1	1	0	1	0	0	0	0	0	0	1	1	1	0	0	0	0	0
Cer_fon	1	1	1	0	1	0	1	0	1	0	1	0	1	0	1	0	1	0
Coe_vir	1	1	0	0	0	0	0	0	0	0	0	0	0	0	0	0	0	0
Cor_tri	0	0	0	0	0	0	0	0	0	0	0	0	0	0	0	0	0	0
Dac_mac	0	0	0	0	0	0	0	0	0	0	0	0	0	0	0	0	0	0
Des_ces	1	0	1	1	1	1	1	1	1	1	1	1	1	1	1	1	1	1
Des_fle	0	1	1	1	0	0	0	0	1	0	1	1	0	0	1	0	0	0
Dra_inc	0	0	0	0	0	0	0	0	0	0	0	0	0	0	0	0	0	0
Dry_oct	0	0	0	1	0	0	0	0	0	0	1	1	0	0	0	0	0	0
Emp_nig	1	1	0	1	0	0	0	0	0	0	1	1	0	0	0	0	0	0
Epi_pal	0	0	0	0	0	0	0	0	1	0	0	0	0	0	1	0	0	0
Equ_arv	1	0	1	1	0	1	1	1	1	1	1	1	0	0	0	0	0	0
Equ_flu	0	0	0	0	0	0	0	0	0	0	0	0	0	0	0	0	0	0
Equ_hye	0	0	0	0	0	0	0	0	0	0	0	0	0	0	0	0	0	0
Equ_pal	0	0	0	0	0	0	0	0	0	0	0	0	0	0	0	0	0	0
Equ_pra	1	1	1	1	1	1	0	1	1	1	1	1	0	0	1	1	1	1
Equ_var	0	0	1	1	0	0	0	0	0	0	1	0	0	0	0	0	0	0
Eri_bor	1	1	1	0	0	0	0	0	0	1	1	1	0	0	1	0	0	0

(continued)

Eri_ang	0	0	0	0	0	0	0	0	0	0	0	0	0	0	1	0	0	0
Eup_fri	1	0	1	0	0	0	0	0	0	0	1	0	1	0	1	0	0	0
Fes_rub	1	1	1	1	1	0	0	0	1	1	1	1	1	1	1	1	1	1
Fes_viv	1	1	1	1	1	1	1	1	1	1	1	1	1	1	1	1	1	1
Fil_ulm	0	0	0	0	0	0	1	1	1	1	0	0	0	0	0	0	0	0
Gal_bor	1	1	1	1	1	1	1	1	1	1	1	0	1	1	1	1	1	1
Gal_nor	1	1	1	1	1	0	0	0	0	0	1	1	1	1	0	1	1	0
Gal_ver	1	0	1	1	1	1	1	1	1	1	1	1	1	1	1	1	1	1
Gen_niv	1	0	0	0	0	0	0	0	0	0	0	0	0	0	0	0	0	0
Gen_ama	0	0	0	0	0	0	0	0	0	0	1	0	0	0	0	0	0	0
Gen_cam	1	0	0	0	0	0	0	0	0	0	1	0	1	0	0	0	0	0
Ger_syl	0	0	0	0	0	0	0	0	0	0	0	0	0	0	1	0	0	0
Geu_riv	0	0	0	0	0	0	0	0	1	1	0	0	0	0	0	0	0	0
Hie_alp	0	1	0	0	0	0	0	0	1	0	0	0	0	0	0	0	0	0
Hie_tha	0	0	0	0	0	0	0	0	0	0	1	0	0	0	0	0	0	0
Hie_sp	0	0	0	0	0	0	0	0	0	0	0	0	0	0	0	0	0	0
Hie_odo	0	0	0	0	0	0	0	0	0	0	0	0	0	0	0	0	0	0
Jun_arc	0	0	1	1	0	0	0	0	0	1	1	0	0	0	0	0	0	0
Jun_buf	0	0	0	0	0	0	0	0	0	0	0	0	0	0	1	0	0	0
Jun_trif	0	1	0	1	0	0	0	0	1	0	1	1	0	0	0	1	0	0
Jun_trig	0	0	1	0	0	0	0	0	0	0	0	0	0	0	1	0	0	0
Jun_com	0	0	0	0	0	0	0	0	0	0	0	0	0	0	0	0	0	0
Kob_myo	1	1	1	1	0	0	0	0	1	0	1	1	0	0	0	0	0	0
Koe_isl	0	0	1	0	0	0	0	0	0	0	0	0	0	0	1	0	0	0
Leo_aut	0	0	1	0	0	0	1	0	1	0	1	0	1	1	1	0	1	0
Lep_sua	0	0	0	0	0	0	0	0	0	0	0	0	0	0	0	0	0	0
Luz_mul	1	1	1	1	1	1	1	0	1	1	1	1	1	1	1	1	1	0
Luz_spi	1	0	1	1	0	0	0	0	0	0	1	1	1	0	1	0	0	0
Lyn_alp	0	0	0	0	0	0	0	0	0	0	0	0	0	0	0	0	0	0
Myo_arv	0	0	0	0	1	0	0	0	1	0	0	0	0	0	1	0	0	0
Nar_str	0	0	0	0	0	0	0	0	0	0	0	0	0	0	0	0	0	0
Par_pal	0	0	0	0	0	0	0	0	0	0	1	0	0	0	0	0	0	0
Phl_alp	0	0	0	0	0	0	0	0	1	0	0	0	0	0	0	0	0	0
Pil_isl	0	0	0	0	0	0	0	0	1	0	1	1	0	0	1	0	0	0
Pin_vul	1	0	1	0	0	0	0	0	0	0	1	1	1	0	0	0	0	0
Pla_mar	0	0	1	1	0	0	0	0	0	1	1	1	1	0	0	0	0	0
Pla_hyp	1	0	0	1	0	0	0	0	0	0	1	1	0	0	1	0	0	0
Poa_alp	0	0	0	0	0	0	0	0	0	0	0	0	0	0	0	0	0	0
Poa_ann	0	0	0	0	0	0	1	0	0	0	0	0	0	0	0	0	0	0
Poa_glau	0	0	0	0	0	0	0	0	0	0	0	1	0	0	0	1	0	0
Poa_nem	0	0	0	0	0	0	0	0	0	0	0	0	0	0	0	0	0	0
Poa_pra	1	0	1	1	1	1	1	1	1	1	1	1	1	1	1	1	1	1
Pol_avi	0	0	0	0	0	0	0	0	0	0	0	0	1	0	0	0	0	0

(continued)

Pop_tre	0	0	0	0	0	0	0	0	0	0	0	1	0	0	0	0	0	0
pop_tre	0	1	1	1	0	0	0	0	1	0	1	1	1	0	0	0	0	0
Pru_vul	0	0	0	0	0	0	0	0	0	0	0	0	0	0	0	0	0	0
Pse_str	1	1	0	0	0	0	0	0	0	0	0	1	0	0	0	0	0	0
Pyr_min	0	0	0	0	0	0	0	0	0	0	0	0	0	0	0	0	0	0
Ran_acr	1	0	1	1	1	1	1	1	1	1	0	0	1	1	1	1	0	0
Rhi_min	1	0	1	0	0	0	0	0	1	0	1	0	1	0	1	0	0	0
Rub_sax	0	0	0	0	0	0	0	0	0	0	0	0	0	0	0	0	0	0
Rum_osa	1	0	1	1	1	1	1	1	1	1	1	0	1	1	1	1	1	0
Rum_ella	0	0	0	0	0	0	0	0	0	0	0	1	0	0	0	0	0	0
Sag_pro	0	0	0	0	0	0	0	0	0	0	0	0	0	0	0	0	0	0
Sal_arc	0	0	1	1	0	0	0	0	0	1	1	1	0	0	1	1	0	0
Sal_her	1	1	1	1	0	0	0	0	0	1	1	1	0	0	0	0	0	0
Sal_lan	0	0	0	0	0	0	0	0	0	1	0	0	0	0	0	0	0	0
Sal_phy	1	0	0	0	0	0	0	0	0	0	0	0	0	0	0	0	0	0
Sal_sp	0	0	0	0	0	0	0	0	0	0	0	0	0	0	0	0	0	0
San_off	0	0	0	0	0	0	1	1	0	0	0	0	0	0	0	0	0	0
Sax_ces	0	0	0	0	0	0	0	0	0	0	0	0	0	0	0	0	0	0
Sax_hir	0	0	0	0	0	0	0	0	0	0	1	0	0	0	1	0	0	0
Sed_vil	0	0	0	0	0	0	0	0	0	0	1	0	0	0	1	0	0	0
Sel_sel	1	0	0	0	0	0	1	0	0	0	1	0	1	0	0	0	0	0
Sil_aca	1	1	1	0	0	0	0	0	0	0	1	1	0	0	1	0	0	0
Sor_auc	0	0	0	0	0	0	0	0	0	0	0	0	0	0	0	0	0	0
Spe_arc	0	0	0	0	0	0	0	0	0	0	0	0	0	0	1	0	0	0
Ste_gra	0	0	0	0	0	0	0	0	0	0	0	0	0	0	0	0	0	0
Ste_med	0	0	1	0	0	0	1	0	0	0	0	0	1	0	0	0	0	0
Tar_sp	1	0	1	0	1	1	1	1	1	1	1	1	1	1	1	1	1	1
Tha_alp	1	1	1	1	0	0	0	0	1	1	1	1	1	1	0	1	0	0
Thy_pra	1	1	1	1	0	0	1	0	1	1	1	1	1	0	1	0	0	0
Tof_pus	0	0	0	0	0	0	0	0	0	0	1	1	0	0	0	0	0	0
Tri_ces	0	0	0	0	0	0	0	0	0	0	0	0	0	0	0	0	0	0
Tri_rep	1	0	0	0	0	0	0	0	0	0	0	0	0	0	0	0	1	0
Tri_pal	0	0	0	0	0	0	0	0	0	0	1	0	0	0	1	0	0	0
Tri_spi	1	0	0	0	0	0	0	0	0	0	0	0	0	0	0	0	0	0
Vac_myr	0	0	0	0	0	0	0	0	0	0	0	0	0	0	0	0	0	0
Vac_uli	1	1	0	1	0	0	0	0	0	0	1	1	0	0	1	1	0	0
Ver_ser	0	0	0	0	1	0	1	0	0	0	0	0	0	0	0	0	0	0
Vic_cra	0	0	0	0	0	0	0	0	0	0	0	0	0	0	0	0	0	0
Vio_can	1	0	0	0	0	0	0	0	0	0	0	0	0	0	0	0	0	0
Vio_pal	0	0	1	0	1	1	0	0	0	0	0	0	0	0	0	0	0	0
SUM	**49**	**32**	**43**	**40**	**23**	**17**	**27**	**20**	**39**	**34**	**59**	**44**	**32**	**24**	**45**	**23**	**19**	**13**

G = Grazed, E = Exclosure

Appendix 2: Supplemental Information for Chapter III

Supplemental Table 8-2: Study site summary for Chapter 3. Climate data were gathered from the Icelandic Met Office (https://en.vedur.is/climatology/data/ [accessed 24.02.2026]) for the closest meteorological station with a > 20 years climate record to each site (< 30 km). LRC group refers to the classification into four groups used for light response curve (LRC) modelling (see Supplemental Figure 8-3). Mean sward height is the average over the measurement period. Exc = Exclosure, Gr = Grazed

Site ID	Region	Sampling days	Elevation	MAT	MST (JJA)	MAP
			m a.s.l.	°C	°C	mm
Alf	N	6	186	2.4	8.8	469.5
Ber	N	6	190	2.4	8.8	469.5
Gsk	N	6	67	3.1	9.1	476.5
Gil	W	7	183	3.2	9.3	733.5
Gun	E	2	5	3.1	8.7	561.5
Hau	S	3	102	4.5	10.3	1234.4
Hja	E	1	6	2.3	8.8	516.9
Holl	W	7	74	3.2	9.3	733.5
Holt	E	2	52	3.1	8.7	561.5
Hva	S	3	76	3.6	9.9	1105.8
LL	N	5	32	3.1	9.1	476.5
Lei	E	2	20	2	7.4	732.4
Lun	W	7	67	3.2	9.3	733.5
Mel	W	4	13	4.3	9.7	792
Mh	N	5	48	3.1	9.1	476.5
Odd	W	7	64	3.2	9.3	733.5
Orl	N	6	40	2.4	8.8	469.5
Pho	E	2	25	2.7	8.3	563.8
Phv	E	2	45	2.1	9	629.5
Reyk	E	1	198	2.1	9	629.5
Rod	N	5	118	3.1	9.1	476.5
Skb	E	2	52	3.4	9.6	721.8
Skl	S	3	144	3.6	9.9	1105.8
Sk40	S	2	165	4.5	10.3	1234.4
Sk90	S	2	165	4.5	10.3	1234.4
Skr	N	6	70	3.2	9.9	489.6
Stein	W	7	63	3.2	9.3	733.5
SA	W	7	98	3.2	9.3	733.5
SB	N	5	174	3.2	9.9	489.6
Thor	W	7	59	3.2	9.3	733.5
Vatn	W	6	122	3.3	9.6	904.6
Vid	E	1	41	2.3	8.8	516.9

MSP (JJA) mm	Ref. period	Dominant vegetation	Years	LRC group		Mean sward height (mm)	
				Exc	Gr	Gr	Exc
128.9	1961-1990	Grass - Succession	52	H2	G1	21.5	146.9
128.9	1961-1990	Grass	42	G1	G1	64.7	210.3
123.3	1982-2001	Grass	22	G1	G1	109.7	180.7
169.1	1957-1986	Grass - Succession	33	H2	G1	77.28	109.7
133.9	1984-2004	Grass	34	G1	G1	89.1	207.7
274.3	1961-1990	Grass	33	G2	G2	96.7	181.2
127.6	1966-1998	Grass - Succession	80	H1	G2	95.6	205.9
169.1	1957-1986	Grass - Succession	45	H1	G1	82.3	143.0
133.9	1984-2004	Shrub heath	30	H1	H1	120.6	238.6
274.2	1961-1990	Grass	23	G2	G2	87.9	184.6
123.3	1982-2001	Grass	52	G2	G2	47.8	206.1
145	1961-1990	Shrub heath	72	H2	H1	73.2	127.6
169.1	1957-1986	Grass	68	G1	G1	69	229.3
172.6	1965-1987	Grass	28	G1	G1	48.1	241.8
123.3	1982-2001	Grass	27	G1	G1	36.6	218.1
169.1	1957-1986	Grass	43	G1	G1	129.6	194.5
128.9	1961-1990	Grass	52	G2	G2	133.6	207.3
174.7	1961-1990	Grass	22	G2	G1	113.4	190.2
134	1962-1991	Grass - Succession	42	H1	G2	25.6	187.4
134	1962-1991	Shrub heath	42	H1	H1	123.2	188.6
123.3	1982-2001	Shrub heath	52	H1	H1	119	203.1
155.5	1961-1990	Shrub heath	42	H1	H1	133.7	121.5
274.2	1961-1990	Grass	33	G2	G2	64.6	140.2
274.3	1961-1990	Shrub heath	83	H1	H1	133.1	161.6
274.3	1961-1990	Shrub heath	33	H1	H1	133.1	189.1
95.4	1961-1990	Grass - Succession	66	H1	G1	160.8	240.2
169.1	1957-1986	Grass	23	G1	G1	78	166.5
169.1	1957-1986	Grass - Succession	23	H2	G2	125	133.9
95.4	1961-1990	Grass	60	G1	G1	132.3	150.4
169.1	1957-1986	Grass	43	G1	G1	98.6	198.9
173.1	1963-1994	Grass	71	G1	G1	130.6	223.1
127.6	1966-1998	Shrub heath	22	H1	H1	94.4	184.3

MAT = Mean annual temperature, MST = Mean summer temperature (June, July, August), MAP = Mean annual precipitation, MSP = Mean summer precipitation (June, July, August), Reference period = time period for climate data
E = East, N = North, S = South, W = West

(continued)

Supplemental Table 8-3*: Model diagnostics for PAR and T_{soil} over measurement period. Both PAR and T_{soil} (soil temperature) were higher in 2023 than in 2022 and higher in grazed than ungrazed land, but without interactive effects, indicating that there was no systematic bias towards brighter and warmer conditions during measurements in grazed or ungrazed plots.*

	Sampling year (Y)		**Grazing Cessation (G)**		**Y × G**	
Response	***df***	***F***	***df***	***F***	***df***	***F***
PAR	1, 63	**8.6****	1, 2044	**5.2***	1, 2044	0.3
T_{soil}	1, 64	**7.6****	1, 1893	**220.9*****	1, 1893	1.5

Significance levels: *** < 0.001; ** < 0.01; * < 0.05

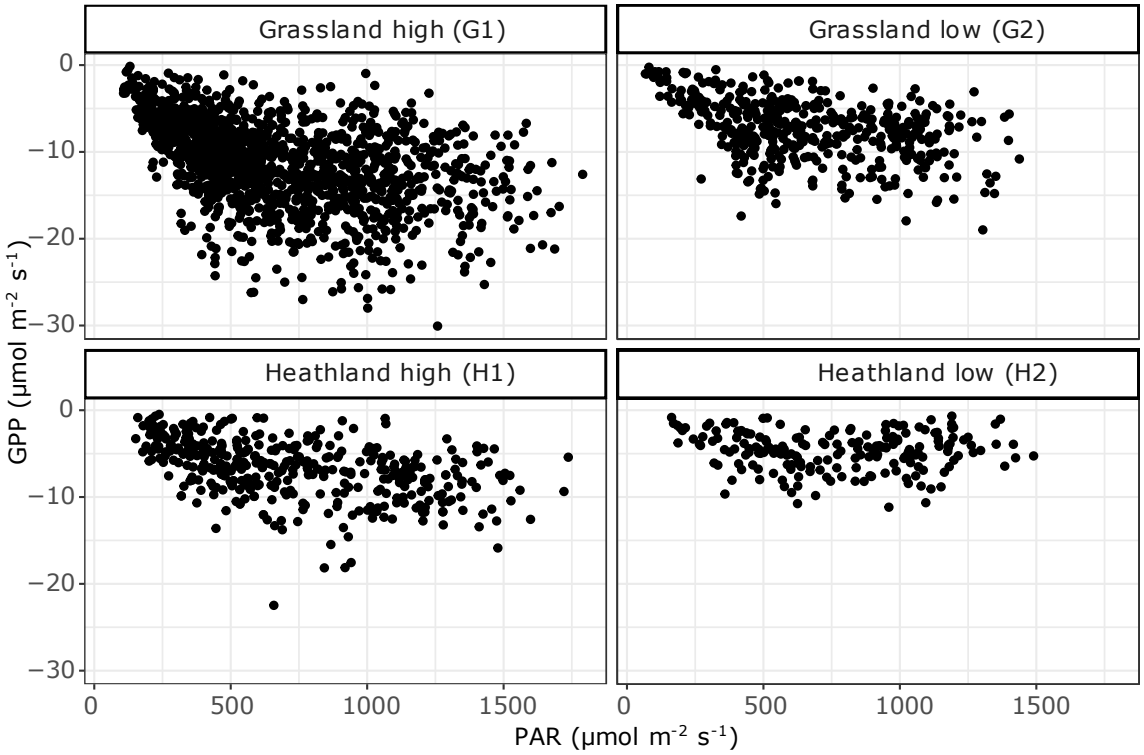

Supplemental Figure 8-3: Light use response groups used for modelling of standardised GPP (GPP_{600}). "Grassland high" includes 1396 measurements with maximum GPP > 20 µmol m^{-2} s^{-1} (G1), "Grassland low" includes 477 measurements with maximum GPP < 20 µmol m^{-2} s^{-1} (G2), "Heath high" includes 465 measurements with maximum GPP > 10 µmol m^{-2} s^{-1} (H1), and "Heath low" includes 198 measurements with maximum GPP < 10 µmol m^{-2} s^{-1} (H2).

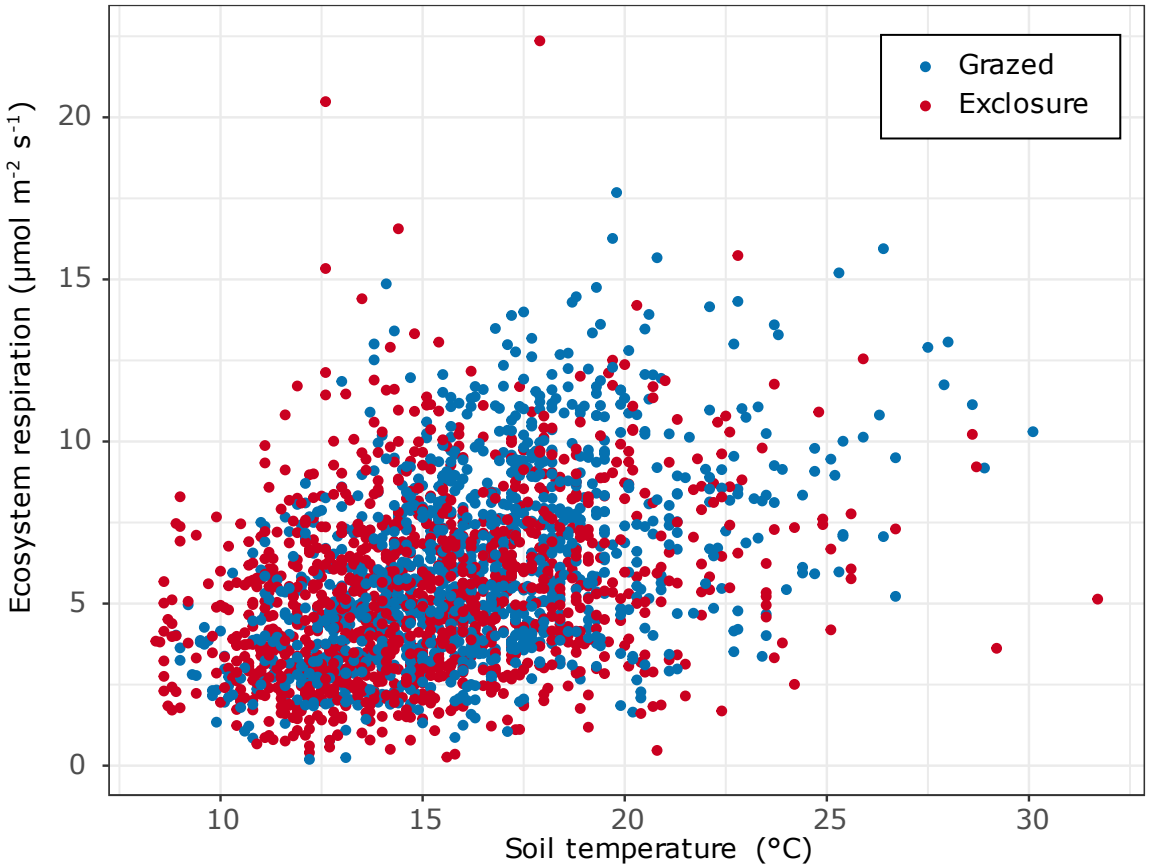

Supplemental Figure 8-4: Scatterplot of soil temperature and ecosystem respiration. Based on the correlation of both variables, soil temperature was used to standardise ecosystem respiration to a soil temperature of 15 °C.

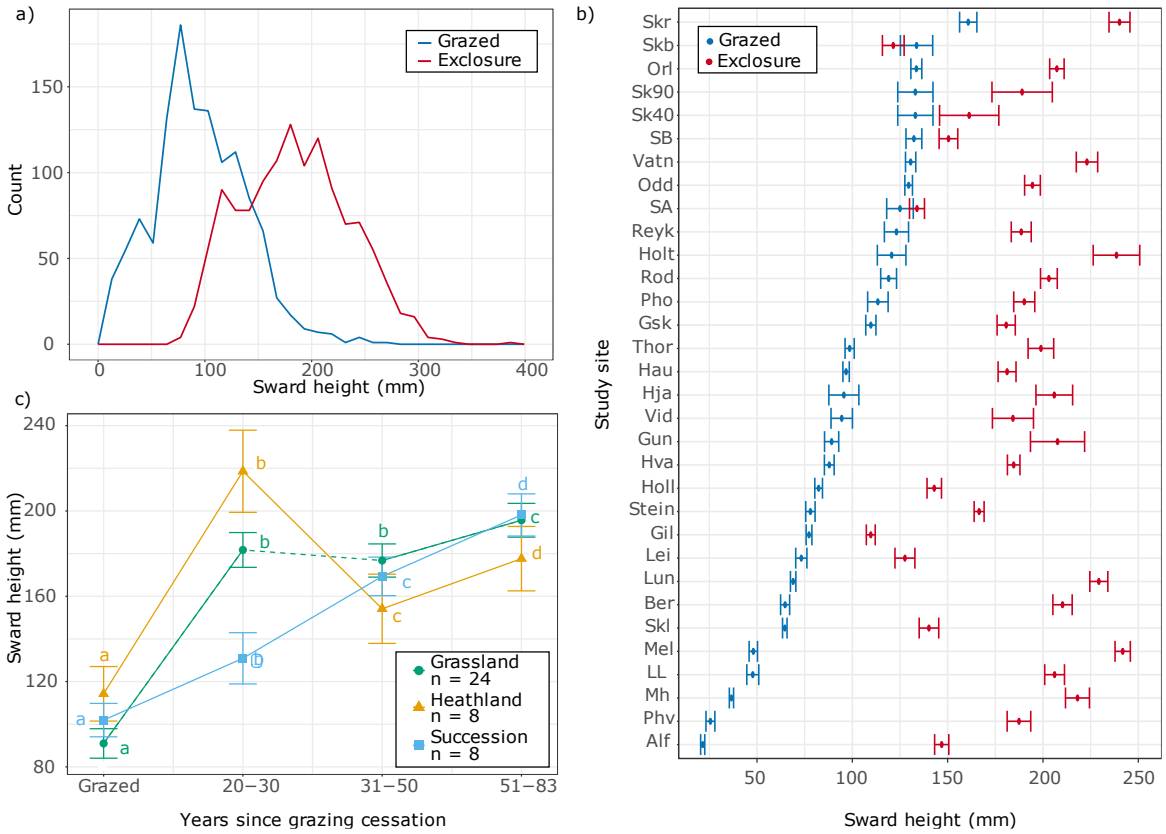

Supplemental Figure 8-5: Differences in sward height between grazed and ungrazed plots. Differences are shown as frequency distribution in grazed and ungrazed plots (a), mean seasonal sward height in every study site (n = 32) in grazed (blue) and ungrazed (red) plots in the order of decreasing sward height in grazed plots (b) and change of sward height with increasing duration of grazing cessation with different letters and solid lines indicating significant differences between categories of years since grazing cessation (c), derived from least-squares means post-hoc tests following linear mixed effects models.

Appendix 3: Supplemental Information for Chapter IV

Supplemental Table 8-4: Grassland sites included in this study. In five sites, heathland expanded into the grassland, either partly or completely following the cessation of grazing.

Site ID	Region	Elevation (m a.s.l.)	Exclosure age (years)	Sampling days	Vegetation type	
					Grazed	Exclosure
Alf	North	186	52	6	Grassland	Heath
Ber	North	192	42	6	Grassland	Grassland
Gsk	North	67	22	6	Grassland	Grassland
LL	North	32	23	5	Grassland	Grassland
Mh	North	48	27	5	Grassland	Grassland
Orl	North	41	52	6	Grassland	Grassland
SB	North	176	60	5	Grassland	Grassland
Skr	North	70	66	6	Grassland	Grassland/Heath
Gil	West	174	33	7	Grassland	Heath
Holl	West	72	45	7	Grassland	Heath
Lun	West	80	68	7	Grassland	Grassland
Mel	West	33	28	4	Grassland	Grassland
Odd	West	66	43	7	Grassland	Grassland
SA	West	93	23	7	Grassland	Heath/Grassland
Stein	West	49	23	7	Grassland	Grassland
Thor	West	74	43	7	Grassland	Grassland
Vatn	West	121	71	6	Grassland	Grassland

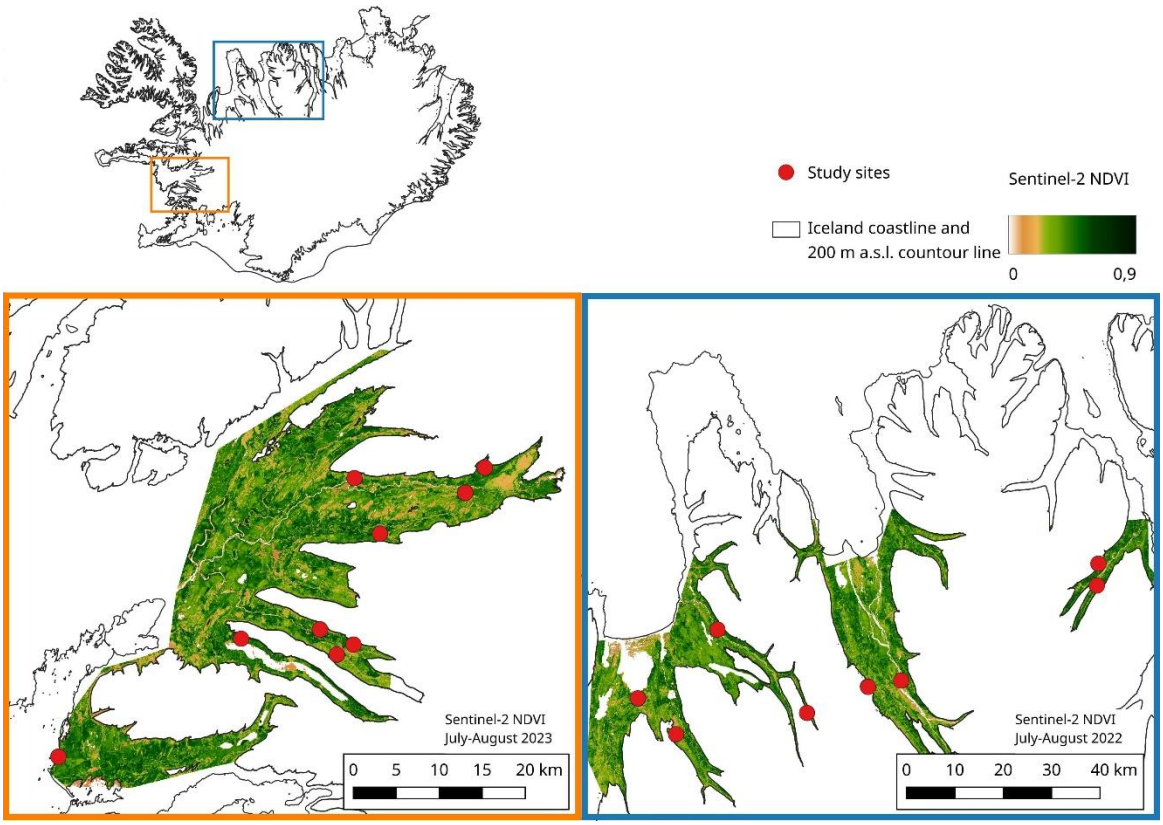

Supplemental Figure 8-6: Detailed map of the two study regions. The right close-up map (blue framed) outlines the study sites in northern Iceland, sampled in July-August 2022 and the left close-up map (orange framed) outlines the sites in western Iceland, sampled in July-August 2023.

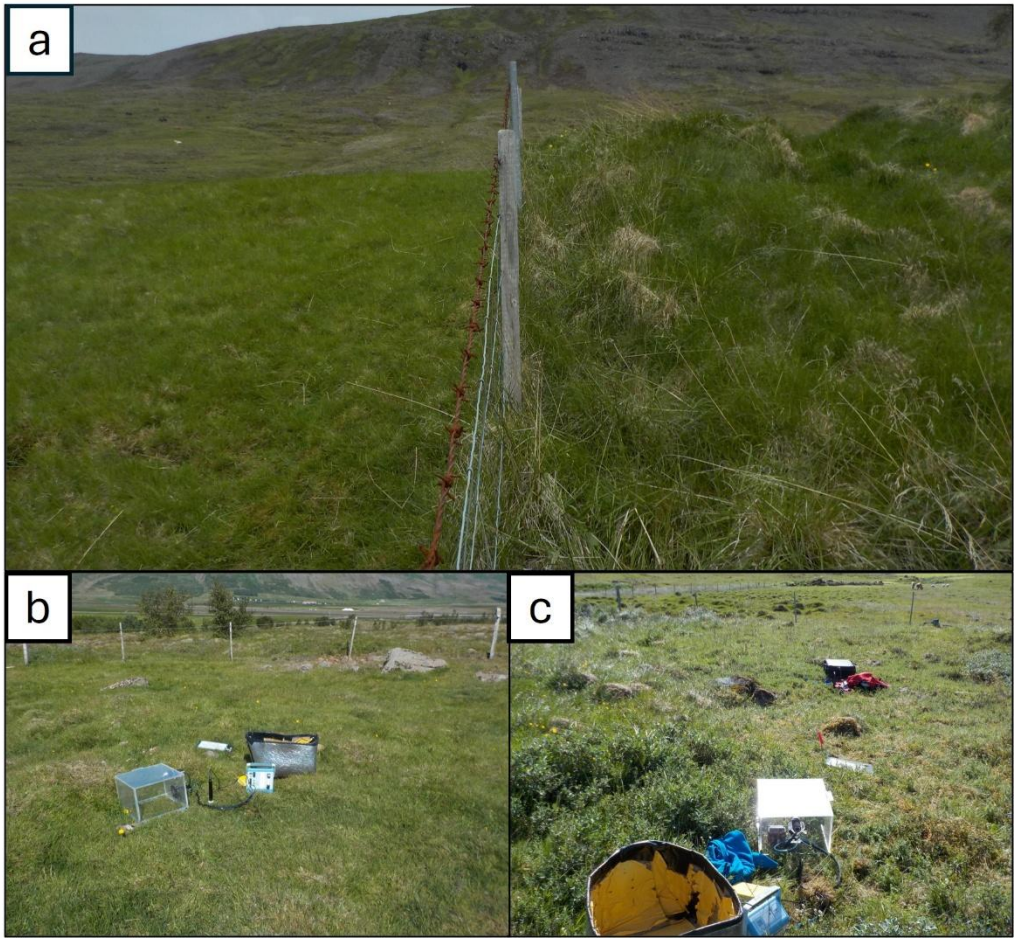

Supplemental Figure 8-7: Images of grazed and ungrazed grassland, divided by a fence (a), and an expansion of heath into the grassland following the cessation of grazing with grassland in the grazed part (b) and heathland in the exclosure (c). Both b and c show the same site (Holl); the perspective is from opposite directions towards the same fence dividing the grazed and ungrazed part, visible in the upper half of both photographs. Photographs were taken by Christian Klopsch.

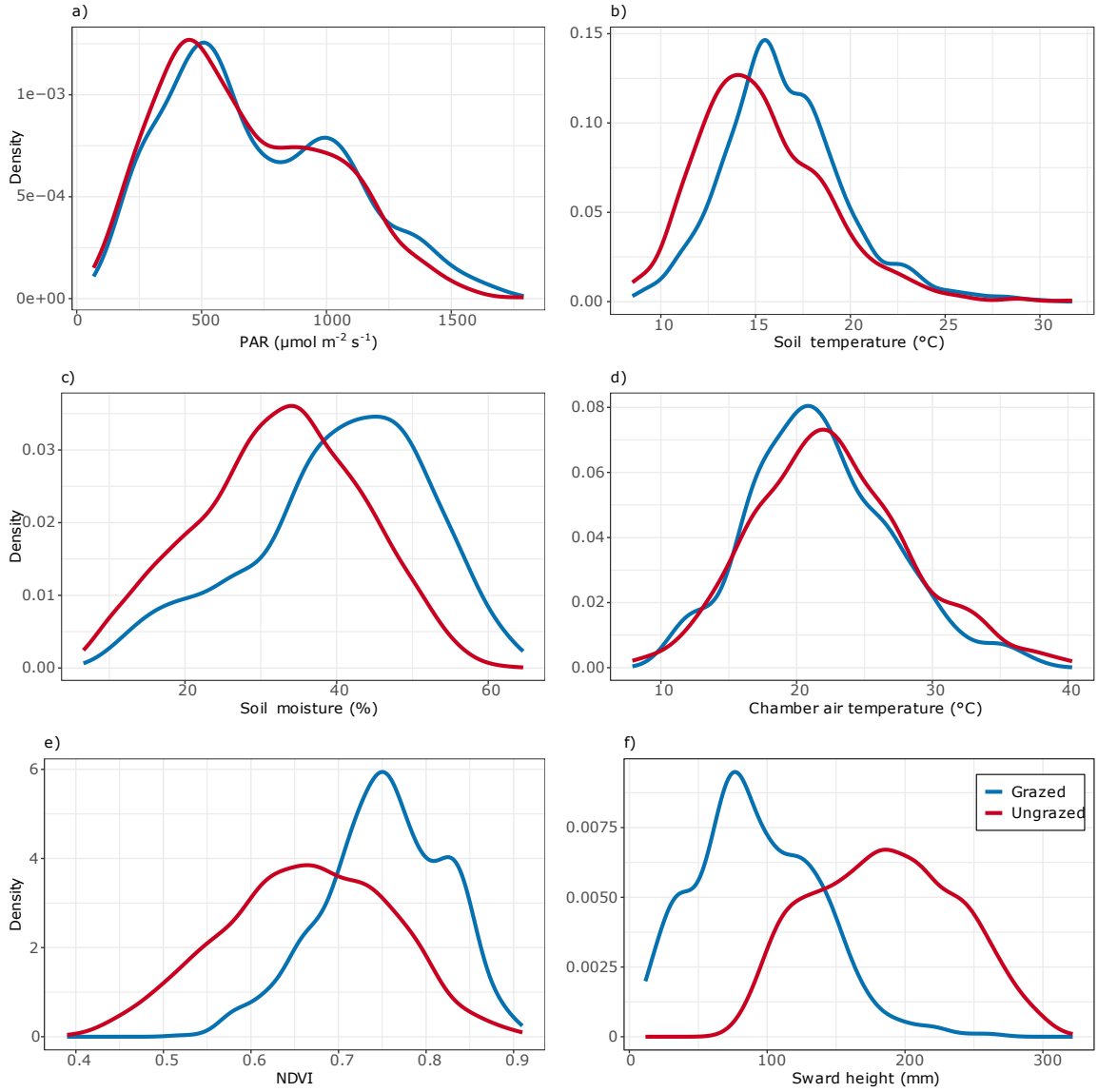

Supplemental Figure 8-8: Density line graphs of environmental data distribution: including PAR (a), soil temperature (b), soil moisture (c), chamber air temperature (d), NDVI (e), sward height (f) in grazed and ungrazed plots.

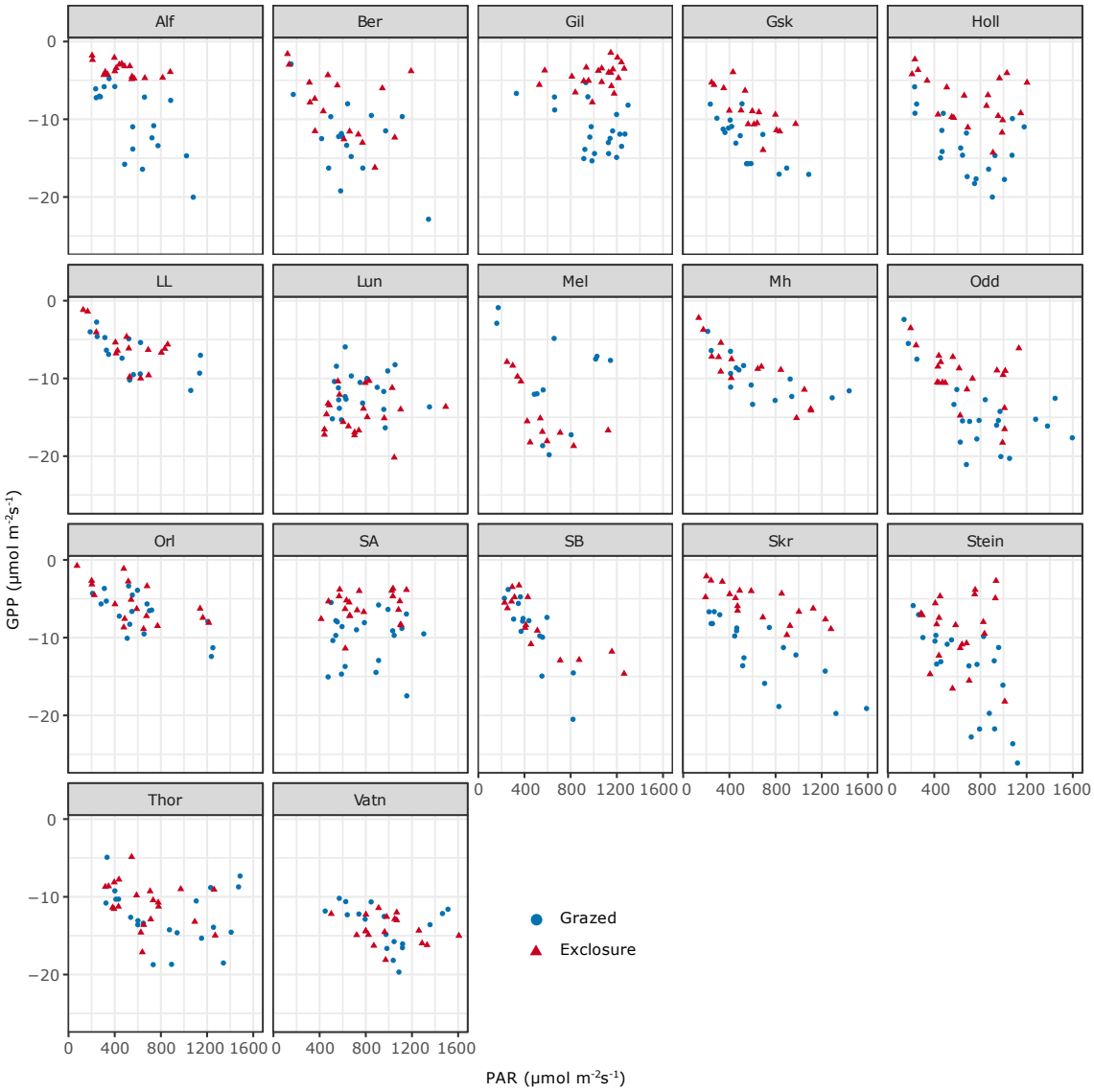

Supplemental Figure 8-9: Scatterplots showing relations between gross primary production (GPP) and PAR at all sampling sites. At most sites, GPP increasing linearly with increasing PAR at low PAR and levels off at higher PAR.

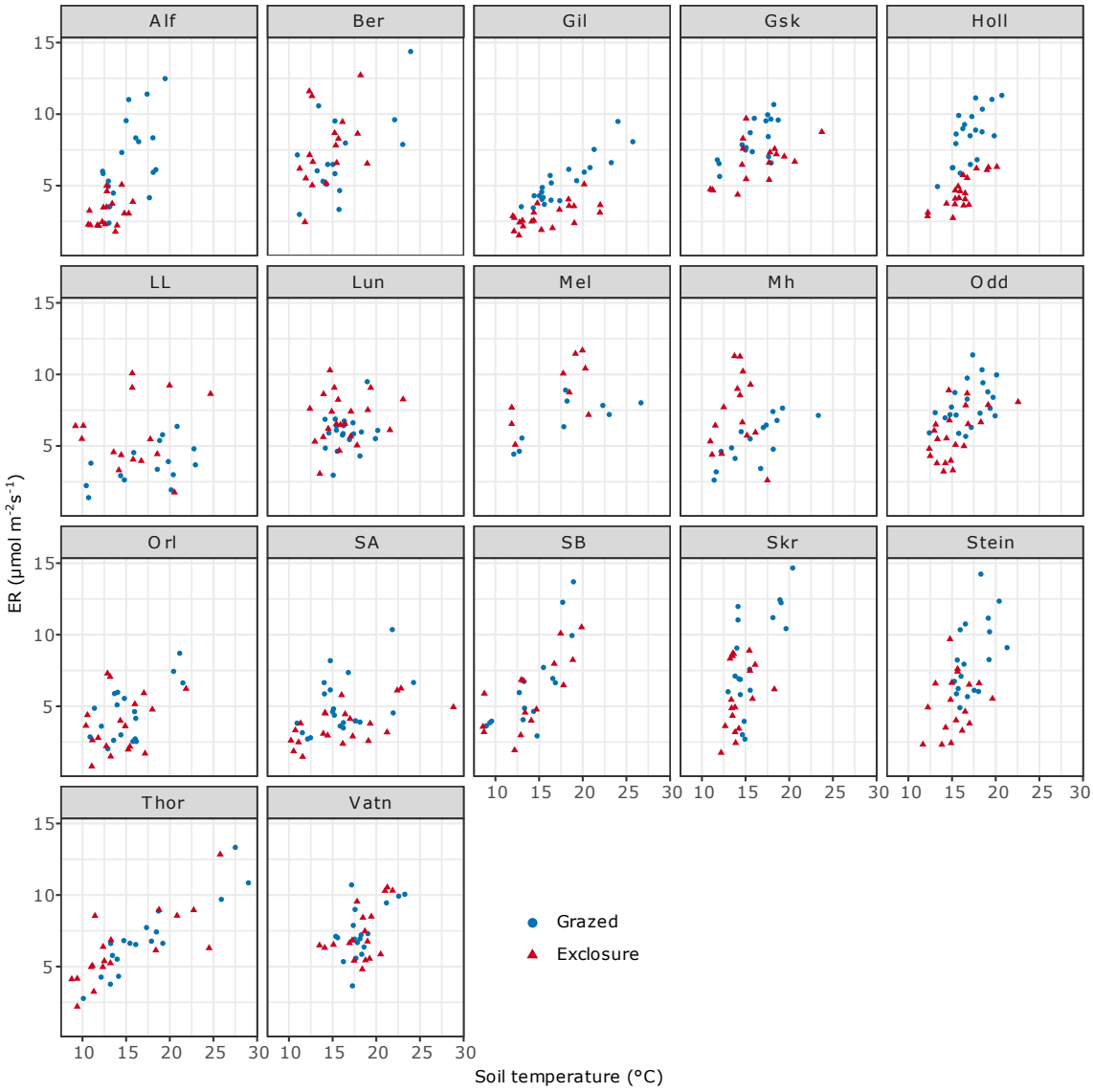

Supplemental Figure 8-10: Scatterplots showing relation between ecosystem respiration (ER) and soil temperature at all sampling sites. At most sites, ER increased linearly with increasing soil temperatures.

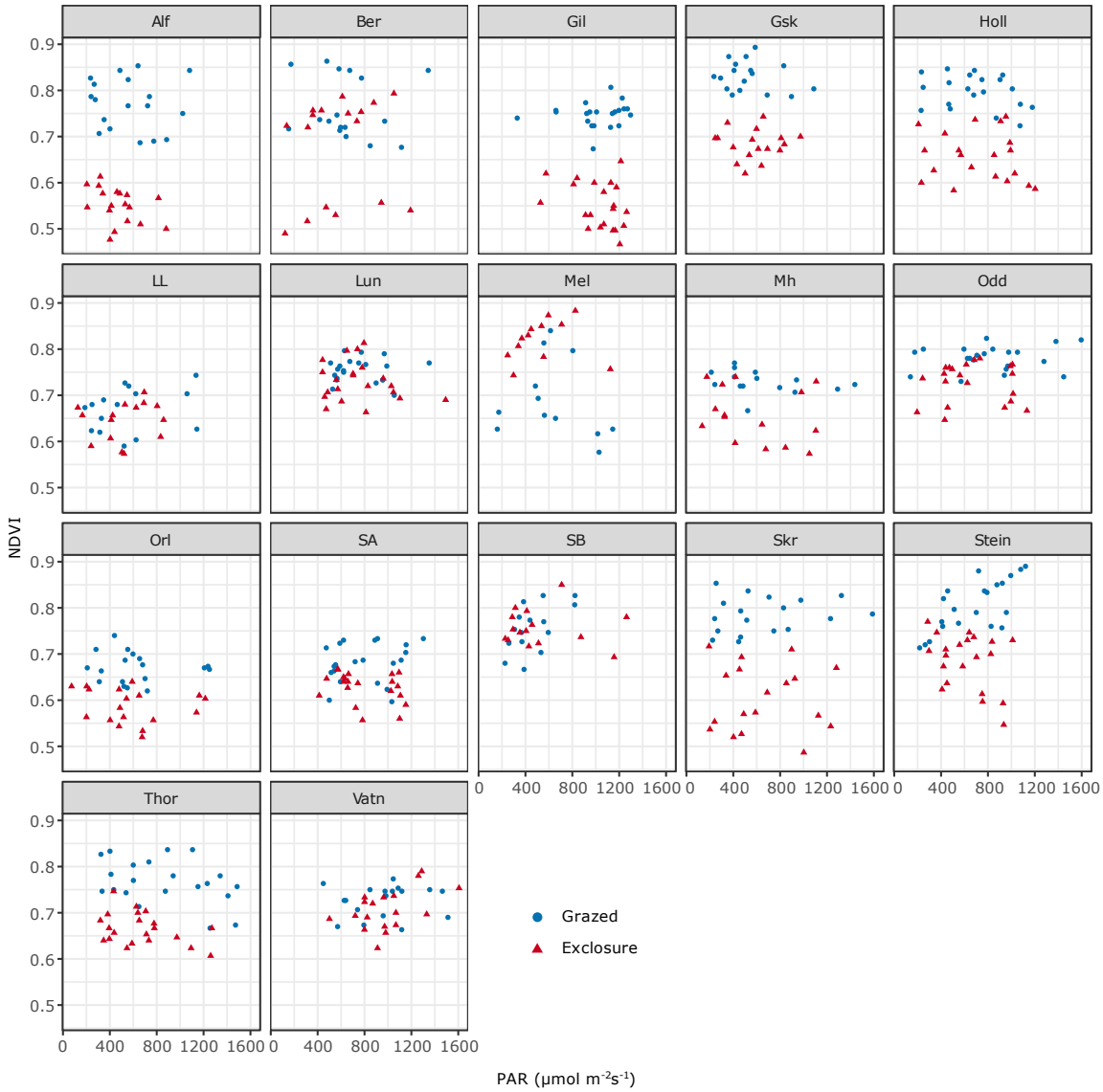

Supplemental Figure 8-11: Scatterplots showing that NDVI was not related to PAR at the sampling sites.

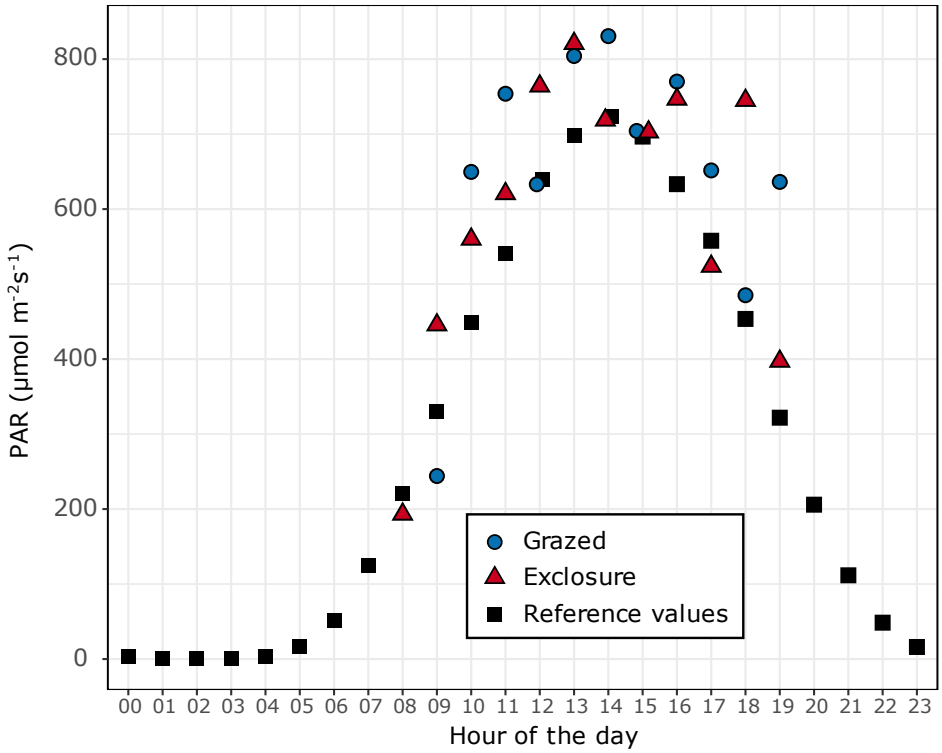

Supplemental Figure 8-12: Distribution of photosynthetic active radiation (PAR) over the course of a day as the average for July-August. Reference values (black squares) are based on complete 30-minute averages over two years from two sites in western Iceland (Guðmundsson et al. 2026), while grazed (blue dots) and exclosure (red triangles) average values are based on data from the 17 sites in this study.

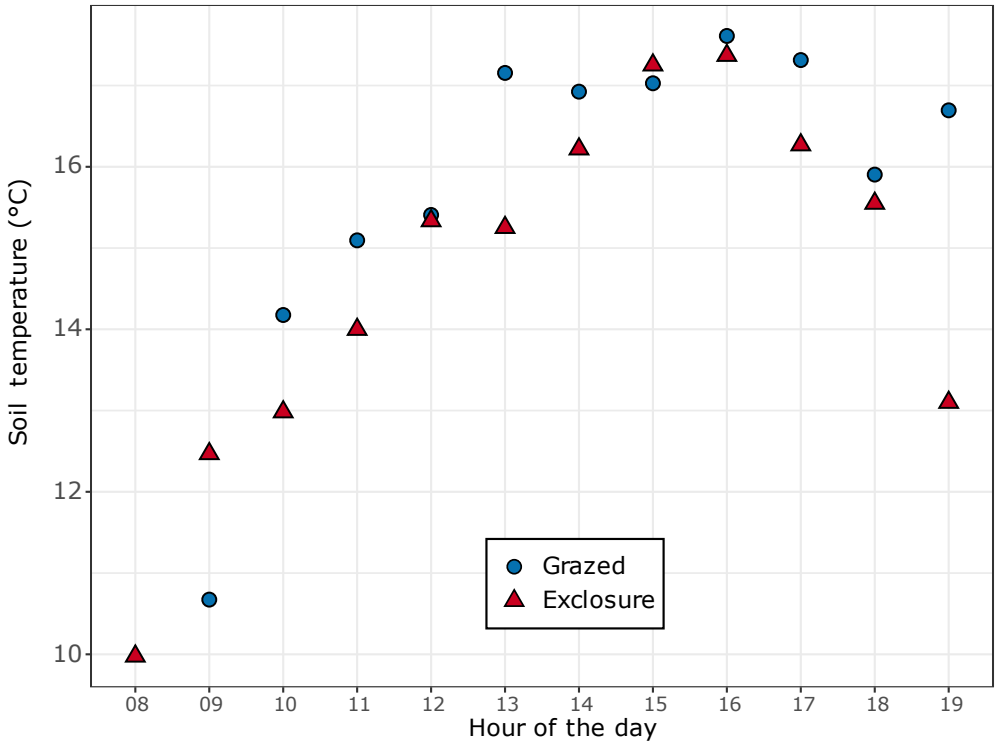

Supplemental Figure 8-13: Distribution of soil temperature between 8:00 and 19:00 as the average for July-August 2022 and 2023. The distribution is based on measurements from the 17 sites in this study.

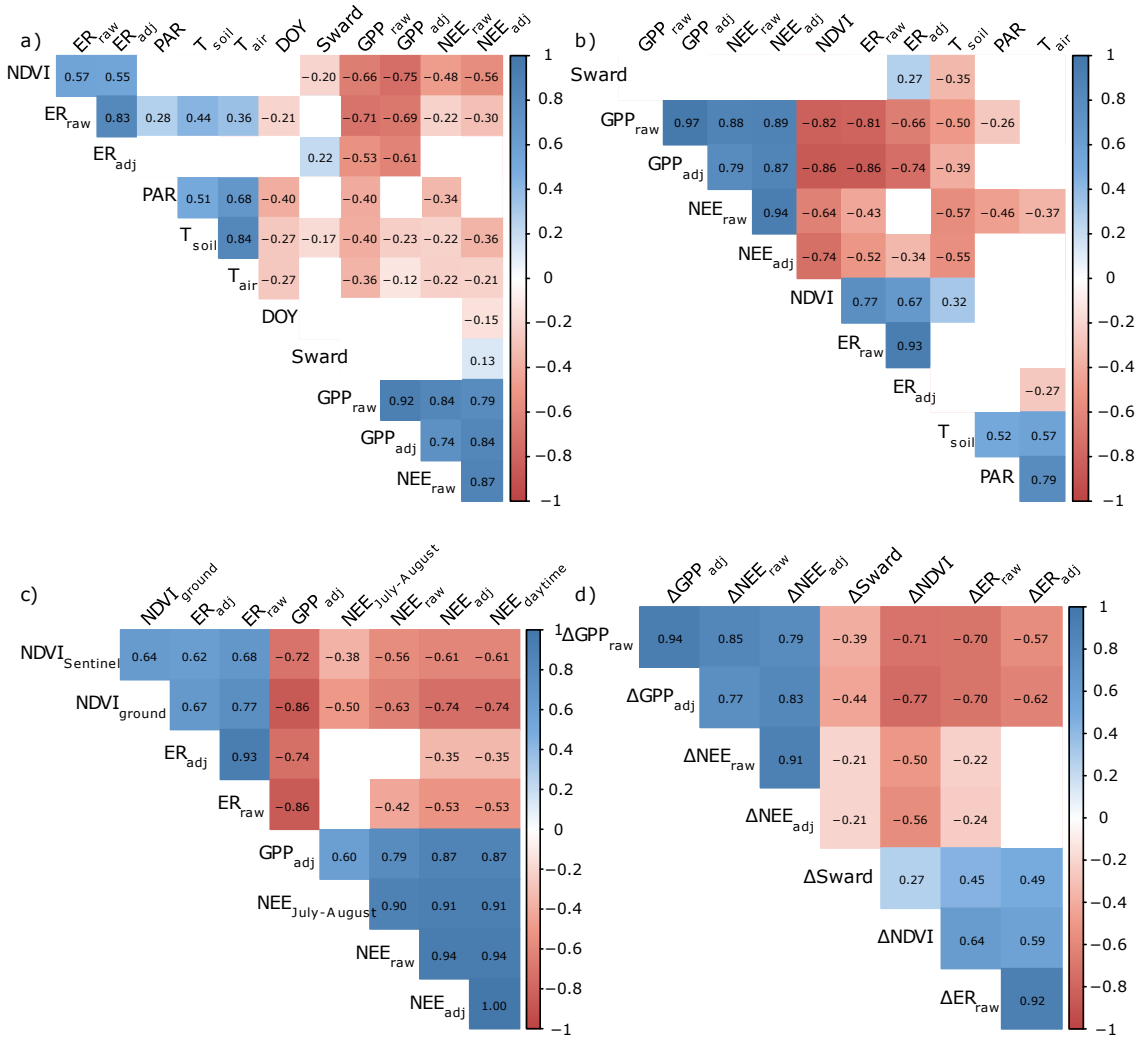

Supplemental Figure 8-14: Pearson correlation matrices of NDVI, CO_2 fluxes and environmental parameters. Correlations are presented per measurement day (a) and aggregated over the measurement period (b). In c) correlations are shown between ground-based and Sentinel-2-based NDVI with CO_2 fluxes and cumulated NEE over growing season. In d) correlations of rate of change (Δ) from grazed plots to ungrazed plots are shown for NDVI and CO_2 fluxes. Applied significance level < 0.01, non-significant associations are left blank, positive correlations are highlighted in red, negative correlations in blue. PAR = Photosynthetic active radiation, T_{soil} = Soil temperature, T_{air} = Chamber air temperature, DOY = Day of year, GPP = Gross primary production, NEE = Net ecosystem exchange, ER = Ecosystem respiration, $NDVI_{ground}$ = ground-based NDVI, $NDVI_{Sentinel}$ = satellite-derived NDVI, $NEE_{July\text{-}August}$ = Calculated NEE day + night for measurement period, NEE daytime = cumulated seasonal daytime NEE. If needed, variables were log-transformed to improve normal distributions.

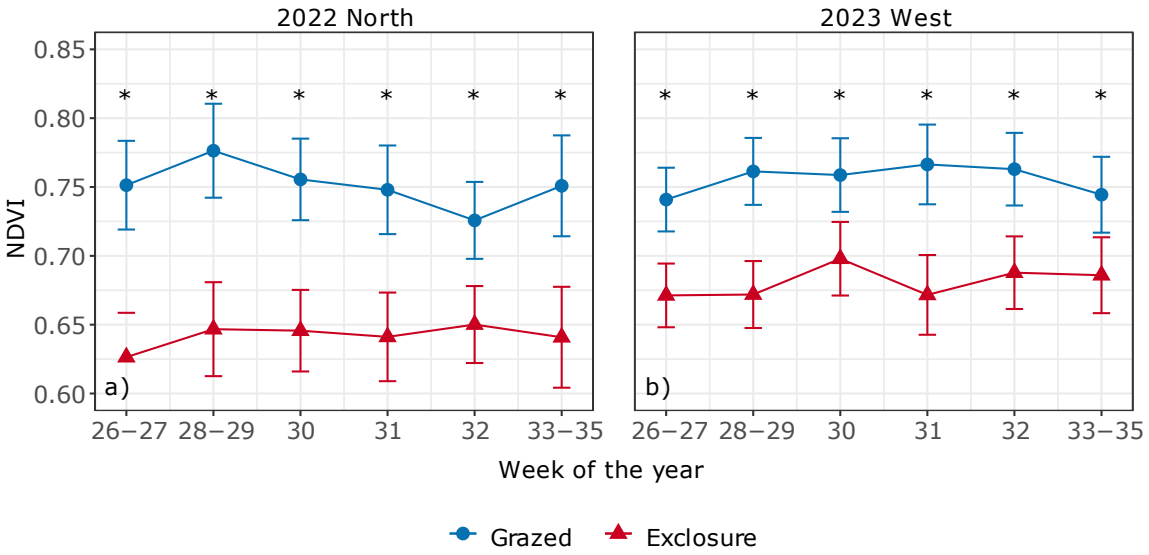

Supplemental Figure 8-15: Pooled average NDVI over the measurement period. In 2022, 8 sites were measured in northern Iceland (a) and in 2023, 9 sites were measured in western Iceland (b). Week 26 is the beginning of July and week 35 is the end of August. Significant differences between grazed land and grazer exclosures are indicated by asterisks ($p < 0.001$), derived from least squares means post-hoc tests.

Appendix 4: Supplemental Information for Chapter V

Supplemental Table 8-5: Sampling site information and mean soil properties. Bedrock age is in 10^6 years and retrieved from the Natural Science Institute of Iceland. Elev = Elevation in m a.s.l., MAT = Mean Annual Temperature, MAP = Mean annual Precipitation, Excl. years = Exclosure age years, SOC = Soil organic carbon, N = Nitrogen.

ID	Elev	MAT (°C)	MAP (mm)	Ref Period†	Excl. years	Bedrock age	Habitat
Alf	186	2.4	469.5	1961-1990	52	>3.3	Grassland
Ber	190	2.4	469.5	1961-1990	42	>3.3	Grassland
Gil	183	3.2	733.5	1957-1986	33	0.8-3.3	Succession
Gsk	67	3.1	476.5	1982-2001	22	>3.3	Grassland
Gun	5	3.1	561.5	1984-2004	34	>3.3	Succession
H43	110	4.5	1234.4	1961-1990	80	<0.8	Succession (Birch)
H60	95	4.5	1234.4	1961-1990	63	<0.8	Succession (Birch)
Hau	102	4.5	1234.4	1961-1990	33	<0.8	Grassland
Hja	6	2.3	516.9	1966-1998	80	>3.3	Succession
Holl	74	3.2	733.5	1957-1986	45	>3.3	Succession
Holt	52	3.1	561.5	1984-2004	30	>3.3	Heathland
Hva	76	3.6	1105.8	1961-1990	23	>871 AD	Grassland
LL	32	3.1	476.5	1982-2001	52	>3.3	Grassland
Lei	20	2	732.4	1961-1990	72	<0.8	Heathland
Lun	67	3.2	733.5	1957-1986	68	>3.3	Grassland
Mel	13	4.3	792	1965-1987	28	>3.3	Grassland
Mh	48	3.1	476.5	1982-2001	27	>3.3	Grassland
Odd	64	3.2	733.5	1957-1986	43	>3.3	Grassland
Orl	40	2.4	469.5	1961-1990	52	>3.3	Grassland
Pho	25	2.7	563.8	1961-1990	22	>871 AD	Grassland
Phv	45	2.1	629.5	1962-1991	42	<0.8	Succession
Reyk	198	2.1	629.5	1962-1991	42	0.8-3.3	Heathland
Rod	118	3.1	476.5	1982-2001	52	>3.3	Heathland
SA	98	3.2	733.5	1957-1986	23	<0.8	Succession/ Grassl.
SB	174	3.2	489.6	1961-1990	60	>3.3	Grassland
Sk40	165	4.5	1234.4	1961-1990	83	>871 AD	Heathland
Sk90	165	4.5	1234.4	1961-1990	33	>871 AD	Heathland
Skb	52	3.4	721.8	1961-1990	42	<0.8	Heathland
Skl	144	3.6	1105.8	1961-1990	33	>871 AD	Grassland
Skr	70	3.2	489.6	1961-1990	66	>3.3	Succession/ Grassl.
Stein	63	3.2	733.5	1957-1986	23	>3.3	Grassland
Thor	5	3.2	733.5	1957-1986	43	>3.3	Grassland
Vatn	122	3.3	904.6	1963-1994	71	>3.3	Grassland
Vid	41	2.3	516.9	1966-1998	22	>3.3	Heathland
All	**87.3**	**3.2**	**733.6**		**45.2**		

†Climate data from the closest meteorological station with sufficient long record, retrieved from https://en.vedur.is/climatology/data/.

SOC concentration (%)		N concentration (%)		SOC stock (Mg ha^{-1})	
grazed	**ungrazed**	**grazed**	**ungrazed**	**grazed**	**ungrazed**
3.84 ± 0.5	4.03 ± 0.28	0.27 ± 0.04	0.3 ± 0.02	113.86 ± 17.55	111.27 ± 7.07
5.29 ± 0.23	4.17 ± 0.11	0.41 ± 0.01	0.35 ± 0.01	171.9 ± 2.79	147.93 ± 17.39
3.12 ± 0.78	3.02 ± 0.67	0.22 ± 0.06	0.22 ± 0.05	127.1 ± 25.9	117.67 ± 26.53
3.25 ± 0.25	4.21 ± 1.57	0.25 ± 0.02	0.33 ± 0.13	98.91 ± 14.44	113.31 ± 25.67
7.91 ± 2.57	6.16 ± 1.13	0.56 ± 0.19	0.42 ± 0.1	255.91 ± 48.46	220.25 ± 27.56
2.68 ± 0.12	2.69 ± 0.03	0.2 ± 0.01	0.2 ± 0.01	128.22 ± 3.78	119.5 ± 0.17
1.54 ± 0.17	1.29 ± 0.07	0.1 ± 0.01	0.09 ± 0.01	76.75 ± 9.75	70.98 ± 6.1
2.53 ± 0.01	2.48 ± 0.29	0.21 ± 0.01	0.21 ± 0.02	92.56 ± 3.32	85.72 ± 5.95
4.67 ± 0.37	5.18 ± 0.76	0.34 ± 0.03	0.36 ± 0.07	162.64 ± 17.59	168.39 ± 23.43
4.28 ± 1.43	3.89 ± 1.03	0.31 ± 0.11	0.28 ± 0.07	112.33 ± 43.54	101.35 ± 33.25
5.52 ± 0.36	5.81 ± 0.34	0.37 ± 0.02	0.42 ± 0.04	164.12 ± 5.15	180.97 ± 2.48
2.34 ± 0.12	2.33 ± 0.13	0.18 ± 0.01	0.18 ± 0.01	109.35 ± 7.09	112.92 ± 5.72
1.79 ± 0.32	2.32 ± 0.19	0.12 ± 0.03	0.18 ± 0.02	107.78 ± 14.09	125.26 ± 7.36
5.1 ± 0.2	3.96 ± 0.61	0.33 ± 0.03	0.23 ± 0.03	173.32 ± 1.82	142.12 ± 16.36
4.72 ± 0.37	6.19 ± 0.72	0.39 ± 0.03	0.48 ± 0.05	138.05 ± 13.86	190.16 ± 32.99
6.94 ± 1.76	5.27 ± 0.78	0.56 ± 0.15	0.44 ± 0.06	218.46 ± 20.55	193.72 ± 26.94
5.18 ± 1.74	5.74 ± 0.85	0.44 ± 0.18	0.47 ± 0.07	160.99 ± 26.05	187.82 ± 27.36
5.33 ± 0.33	5.19 ± 0.95	0.45 ± 0.03	0.43 ± 0.09	166.03 ± 12.27	160.54 ± 31.19
4.44 ± 0.81	4.98 ± 0.4	0.35 ± 0.06	0.43 ± 0.05	142.33 ± 10.86	159.94 ± 11.85
6.25 ± 0.39	5.69 ± 0.99	0.42 ± 0.03	0.41 ± 0.06	199.65 ± 14.18	165.88 ± 42.2
3.51 ± 0.34	4.59 ± 0.26	0.23 ± 0.03	0.3 ± 0.02	118.8 ± 10.77	142.19 ± 6.67
4.48 ± 0.1	5 ± 0.28	0.26 ± 0.02	0.28 ± 0.03	119.93 ± 6.27	132.48 ± 8.95
4.09 ± 0.57	4.15 ± 0.36	0.3 ± 0.06	0.31 ± 0.03	128.57 ± 24.75	125.8 ± 22.31
3.52 ± 0.5	3.18 ± 0.83	0.27 ± 0.04	0.22 ± 0.06	134.35 ± 19.81	125.15 ± 26.89
3.13 ± 0.52	3.37 ± 0.21	0.23 ± 0.04	0.24 ± 0.02	88.66 ± 15.77	101.57 ± 3.73
2.17 ± 0.04	1.44 ± 0.05	0.14 ± 0	0.09 ± 0	106.25 ± 5.18	63.44 ± 2.92
2.17 ± 0.04	1.89 ± 0.11	0.14 ± 0	0.11 ± 0.01	106.25 ± 5.18	82.45 ± 0.81
5.79 ± 0.39	4.92 ± 0.55	0.29 ± 0.01	0.26 ± 0.02	120.36 ± 15.4	125.51 ± 5.24
2.3 ± 0.12	1.77 ± 0.1	0.19 ± 0.01	0.14 ± 0.01	95.55 ± 4.6	82.08 ± 2.64
5.89 ± 0.21	4.08 ± 0.35	0.5 ± 0.01	0.29 ± 0.03	129.88 ± 9.86	112.71 ± 18.05
2.98 ± 0.44	3.26 ± 0.65	0.22 ± 0.04	0.24 ± 0.06	102.81 ± 13.85	107.39 ± 18.21
5.14 ± 0.43	5.42 ± 1.49	0.47 ± 0.07	0.52 ± 0.14	142.92 ± 17.21	164.01 ± 53.22
6.88 ± 0.34	6.46 ± 0.5	0.56 ± 0.02	0.54 ± 0.04	174.48 ± 10.27	175.58 ± 16.04
3.25 ± 0.2	3.76 ± 0.3	0.2 ± 0.02	0.26 ± 0.01	107.95 ± 8.33	136.12 ± 1.76
4.11 ± 0.19	**3.97 ± 0.16**	**0.3 ± 0.02**	**0.29 ± 0.01**	**134.39 ± 4.55**	**132.26 ± 4.61**

(continued)

N stock (Mg ha^{-1})		Bulk density (g cm^{-3})		Coarse fraction	
grazed	**ungrazed**	**grazed**	**ungrazed**	**grazed**	**ungrazed**
7.86 ± 1.37	8.1 ± 0.5	0.75 ± 0.05	0.74 ± 0.02	0.32 ± 0.08	0.39 ± 0.03
13.03 ± 0.7	12.53 ± 1.3	0.55 ± 0.03	0.63 ± 0.05	0.03 ± 0	0.03 ± 0.01
8.44 ± 1.84	8.19 ± 1.92	0.81 ± 0.06	0.83 ± 0.02	0.2 ± 0.11	0.22 ± 0.11
7.57 ± 1.22	8.82 ± 2.3	0.69 ± 0.07	0.71 ± 0.15	0.26 ± 0.09	0.31 ± 0.01
17.8 ± 3.92	15.03 ± 2.53	0.61 ± 0.09	0.63 ± 0.06	0 ± 0	0 ± 0
9.34 ± 0.26	8.47 ± 0.18	0.81 ± 0.01	0.77 ± 0.01	0.03 ± 0.01	0.03 ± 0
4.78 ± 0.62	4.51 ± 0.51	0.88 ± 0.02	0.86 ± 0.02	0.01 ± 0	0.01 ± 0
7.56 ± 0.06	7 ± 0.39	0.67 ± 0.02	0.67 ± 0.06	0.23 ± 0.02	0.21 ± 0.03
11.83 ± 1.51	11.21 ± 1.99	0.6 ± 0.04	0.6 ± 0.07	0 ± 0	0 ± 0
7.9 ± 3.24	6.97 ± 2.36	0.74 ± 0.08	0.68 ± 0.04	0.28 ± 0.05	0.36 ± 0.08
10.5 ± 0.55	12.7 ± 0.33	0.5 ± 0.04	0.52 ± 0.05	0.02 ± 0.02	0 ± 0
8.23 ± 0.54	8.6 ± 0.44	0.8 ± 0.01	0.81 ± 0.01	0.01 ± 0.01	0 ± 0
7 ± 1.17	9.33 ± 0.77	1.02 ± 0.06	0.91 ± 0.03	0.06 ± 0.06	0 ± 0
11.1 ± 0.89	8.19 ± 0.82	0.54 ± 0.01	0.6 ± 0.07	0 ± 0	0.01 ± 0.01
11.43 ± 1.21	14.35 ± 1.77	0.67 ± 0.02	0.6 ± 0.04	0.21 ± 0.02	0.16 ± 0.06
17.61 ± 1.85	15.86 ± 2.24	0.63 ± 0.13	0.79 ± 0.05	0.07 ± 0.06	0.18 ± 0.05
13.24 ± 2.76	15.34 ± 2.17	0.82 ± 0.14	0.75 ± 0.04	0.09 ± 0.05	0.07 ± 0.03
14.03 ± 0.56	12.96 ± 2.82	0.55 ± 0.02	0.54 ± 0.02	0.05 ± 0.02	0.08 ± 0.08
11.22 ± 0.66	13.48 ± 1.37	0.6 ± 0.09	0.56 ± 0.04	0.04 ± 0.02	0.03 ± 0.02
13.41 ± 1.14	11.75 ± 2.83	0.54 ± 0.02	0.51 ± 0.02	0.1 ± 0.08	0.22 ± 0.21
7.87 ± 0.72	8.85 ± 0.49	0.55 ± 0.04	0.51 ± 0.02	0 ± 0	0.02 ± 0.02
6.78 ± 0.53	7.25 ± 0.87	0.45 ± 0.01	0.46 ± 0.02	0 ± 0	0 ± 0
9.42 ± 2.27	9.33 ± 1.69	0.84 ± 0.08	0.68 ± 0.04	0.23 ± 0.04	0.22 ± 0.04
10.23 ± 1.55	8.35 ± 1.87	0.86 ± 0.09	0.81 ± 0.07	0.23 ± 0.02	0.19 ± 0.04
6.43 ± 1.33	6.97 ± 0.28	0.62 ± 0.04	0.61 ± 0.01	0.41 ± 0.03	0.3 ± 0
6.29 ± 0.08	3.87 ± 0.21	0.8 ± 0.03	0.79 ± 0.03	0.02 ± 0.01	0.04 ± 0.01
6.29 ± 0.08	4.96 ± 0.24	0.8 ± 0.03	0.83 ± 0.01	0.02 ± 0.01	0.03 ± 0
6.64 ± 1.14	7.05 ± 0.29	0.46 ± 0.09	0.51 ± 0.02	0.01 ± 0.01	0 ± 0
7.57 ± 0.48	6.17 ± 0.25	0.72 ± 0.01	0.79 ± 0.02	0.01 ± 0	0.01 ± 0
11.01 ± 1.14	7.99 ± 1.5	0.55 ± 0.01	0.54 ± 0.02	0.38 ± 0.07	0.2 ± 0.06
7.5 ± 1.02	8.02 ± 1.83	0.83 ± 0.04	0.76 ± 0.09	0.37 ± 0.05	0.26 ± 0.11
12.15 ± 1.57	15.73 ± 5.18	0.68 ± 0.05	0.71 ± 0.13	0.33 ± 0.08	0.28 ± 0.08
14.1 ± 0.59	14.3 ± 1.36	0.61 ± 0.04	0.65 ± 0.01	0.28 ± 0.03	0.23 ± 0.04
6.63 ± 0.93	8.96 ± 0.27	0.56 ± 0.02	0.61 ± 0.02	0.02 ± 0.01	0.01 ± 0.01
9.7 ± 0.37	**9.52 ± 0.38**	**0.68 ± 0.02**	**0.68 ± 0.01**	**0.12 ± 0.01**	**0.12 ± 0.01**

(continued)

Supplemental Table 8-6: Indicative attributes of the samples and profiles that were excluded from analysis of the respective soil layer (sample) or the whole profile (Profile). The suspicious parameter in each profile is highlighted in bold and with coloured shading. In total, 4 out of 201 profiles and 16 out of 1208 soil layers were excluded or missing. Gr = Grazed, Ex = Exclosure, %C = soil carbon concentration, %CF = Percent course fraction.

Site	Plot	Profile	Depth	%CF	%C	Sample	Profile	Explanation
Holt	Ex	3	0-10	**50**	5.2	x	x	Large %CF and low %C in 0-30 cm, not in other profiles of the site - Avalanche deposit?
			10-20	**50**	3	x		
			20-30	**50**	2.6	x		
Holt - all other profiles			0-10	**0-1**	8.5-11.7			
			10-20	**0**	5.4-6.9			
			20-30	**0**	5.2-5.9			
Lun	Ex	3	20-30	8	**9.89**	x	x	Anomalous large %C in 20-40 cm, not in other soil profiles of the site, close to historical animal shelter - artifact?
			30-40	15	**10.4**	x		
Lun - all other profiles			20-30	5-30	**1.3-4.6**			
			30-40	5-50	**1.0-4.0**			
Gsk	Ex	1	0-10	**35**	**0.97**	x	x	Very low %C in 0-10 cm, high %CF, not in other profiles of the site - Avalanche deposit?
Gsk - all other profiles			0-10	**0-10**	**8.6-10.2**			
Pho	Ex	3	20-30	**80**	5.81	x	x	Solid lava rock below 22 cm - very shallow soil, other profiles of the site deeper
			30-40	**100**	NA	x		
			40-50	**100**	NA	x		
			50-60	**100**	NA	x		
Pho	Gr	2	40-50	**45**	4.52	x		Solid lava rock below 45 cm, generally rel. low %C in 40-60 cm depth, therefore not excluded from whole profile models
			50-60	**100**	NA	x		
Pho - all other profiles				**0-10**				
Mh	Gr	3	40-50	0	**8**	x		Anomalous large %C in 40-60 cm, only in sub-plot pair 3 of the site, both layers excluded from whole profile analyses - artifact?
			50-60	2	**1.4**	x		
Mh	Ex	3	40-50	2	**9.9**	x		
			50-60	0	**11.7**	x		
Mh - all other profiles			40-50	8-25	**0.3-2.8**			
			50-60	10-25	**0.2-1.3**			

Supplemental Table 8-7: Model diagnostics for linear mixed effects models (LMM) used in the study. Fixed effects were 'grazing cessation', 'vegetation type' and their interaction (if significant). Random effects in each LMM were 'sub-plot' nested in 'site' and 'region'. SOC = soil organic carbon stock, N = nitrogen stock, $C_{sequest}$ = sequestered SOC, C:N = carbon-to-nitrogen-ratio, $C_{above\text{-}ground}$ = C in above-ground plant biomass, C_{root} = C in roots of 0-10 cm soil depth, C_{total} = SOC + C_{root} + $C_{above\text{-}ground}$, ranges in subscripts refer to the soil layer included in the model.

	Grazing cessation G)			**Vegetation type (V)**			**G×V**		
Response	**df**	***F***	***p***	**df**	***F***	***p***	**df**	***F***	***p***
$SOC_{0\text{-}10}$	1, 99	**9.8**	**0.002**	2, 97	**6**	**<0.001**	-	-	-
$SOC_{10\text{-}20}$	1, 99	0	0.9	2, 97	**6.2**	**0.003**	-	-	-
$SOC_{20\text{-}30}$	1, 97	0.7	0.4	2, 96	**4.3**	**0.02**	-	-	-
$SOC_{30\text{-}40}$	1, 99	0.6	0.5	2, 96	0.8	0.5	-	-	-
$SOC_{40\text{-}50}$	1, 98	0.1	0.8	2, 92	0.4	0.7	-	-	-
$SOC_{50\text{-}60}$	1, 97	0	0.9	2, 93	0.1	0.9	-	-	-
$SOC_{30\text{-}60}$	1, 96	0.8	0.4	2, 98	0.7	0.5	-	-	-
$SOC_{0\text{-}60}$	1, 93	0.1	0.7	2, 98	**5.4**	**0.006**	-	-	-
$C_{sequest\ 0–10}$	1, 99	**5.6**	**0.019**	2, 96	**4.7**	**0.011**	-	-	-
$C_{sequest\ 10–20}$	1, 99	0	0.9	2, 98	**3.5**	**0.034**	-	-	-
$C_{sequest\ 0–20\ Birch}$	1, 5	**7.0**	**0.045**	-	-	-	-	-	-
$N_{0\text{-}10}$	1, 99	**9.9**	**0.002**	2, 97	**20.4**	**<0.001**	-	-	-
$N_{10\text{-}20}$	1, 97	0.2	0.6	2, 97	**8.6**	**<0.001**	2, 97	**3.7**	**0.029**
$N_{20\text{-}30}$	1, 96	0	0.9	2, 97	**5.6**	**0.005**	2, 96	2.4	0.097
$N_{30\text{-}60}$	1, 98	0.1	0.8	2, 70	0.1	0.9	-	-	-
$N_{0\text{-}60}$	1, 95	1.6	0.2	2, 98	**8.5**	**<0.001**	2, 96	2.4	0.096
$C{:}N_{0\text{-}10}$	1, 97	1.6	0.2	2, 96	**46.7**	**<0.001**	2, 96	**7.2**	**0.001**
$C{:}N_{10\text{-}30}$	1, 297	**15.0**	**<0.001**	2, 93	**16.2**	**<0.001**	2, 296	**7.5**	**<0.001**
$C{:}N_{30\text{-}60}$	1, 493	0	0.8	2, 89	0.6	0.6	-	-	-
$C_{above\text{-}ground}$	1, 97	**42.5**	**<0.001**	2, 77	**12.9**	**<0.001**	2, 97	1.3	0.3
$C_{above\text{-}ground}{:}C_{total}$	1, 99	**51.2**	**<0.001**	2, 70	**15.4**	**<0.001**	2, 99	1.3	0.3
C_{root}	1, 100	**20.7**	**<0.001**	2, 85	**11.3**	**<0.001**	2, 99	0.7	0.5
$C_{root}{:}C_{total}$	1, 95	**22.2**	**<0.001**	2, 97	**13.7**	**<0.001**	2, 94	2.1	0.13

Supplemental Table 8-8: Model diagnostics of linear mixed effect models for additional grazing cessation effects: including bulk density (BD) and general relationships of soil organic carbon concentration (%SOC), soil organic carbon stock (SOC), nitrogen (N) and BD, with soil depth and the environment. Subscript ranges refer to respective soil layer depths.

Response	**Fixed effect**	**df $_{num,den}$**	***F***
ln(%SOC)	ln(BD)	1, 1212	**377.6*****
	Soil layer	5, 1134	**89.1*****
	ln(BD):Soil layer	5, 1142	**4.5*****
$BD_{0\text{-}10}$	Grazing cessation	1, 97	2.9· *(p = 0.09)*
	Vegetation type	2, 97	**4.7***
$BD_{10\text{-}20}$	Grazing cessation	1, 98	**6.9****
	Vegetation type	2, 97	0.9
$BD_{20\text{-}60}$	Grazing cessation	1, 100	0.1
	Vegetation type	2, 97	1.6
$BD_{0\text{-}60}$	Grazing cessation	1, 1096	0.1
	Vegetation type	2, 98	2.1
	Soil layer	5, 1092	**60.1*****
$SOC_{30\text{-}60}$	Vegetation type	2, 34	0
$SOC_{10\text{-}30}$	Vegetation type	2, 34	**4.9***
$SOC_{0\text{-}60}$	ln(Elevation)	1,35	**34.6*****
sqrt(SOC)	Soil layer	5, 1094	**341.7*****
sqrt(N)	Soil layer	5, 1095	**224.8*****
sqrt($\%SO_{0\text{-}10}$)	Grazing cessation	1, 104	**5.6***
	Vegetation type	2, 36	1.9

Significance codes: '***' < 0.001; '**' < 0.01; '*'< 0.05; '·' < 0.1

Supplemental Table 8-9: Pearson correlation coefficients of soil parameters: including correlations between soil organic carbon (SOC) concentration and other soil parameters and between topsoil C sequestration ($C_{sequest\ 0\text{-}10\ cm}$) and above- and belowground biomass C in grassland. Variables were log- or square-root-transformed to meet assumptions on normality.

Variables	***r***	**df**	***p***
log(SOC concentration) ~ log(Bulk density)	-0.63	1201	<0.001
log(SOC concentration) ~ log(SOC stock)	0.90	1201	<0.001
log(SOC concentration) ~ log(N concentration)	0.97	1201	<0.001
sqrt($C_{sequest\ 0\text{-}10\ cm}$) ~ sqrt($C_{above\text{-}ground}$)†	-0.25	100	0.012
sqrt($C_{sequest\ 0\text{-}10\ cm}$) ~ log($C_{root\ 0\text{-}10}$)†	0.24	100	0.017

† Only sites with grassland in grazed and exclosure plot (n = 17)

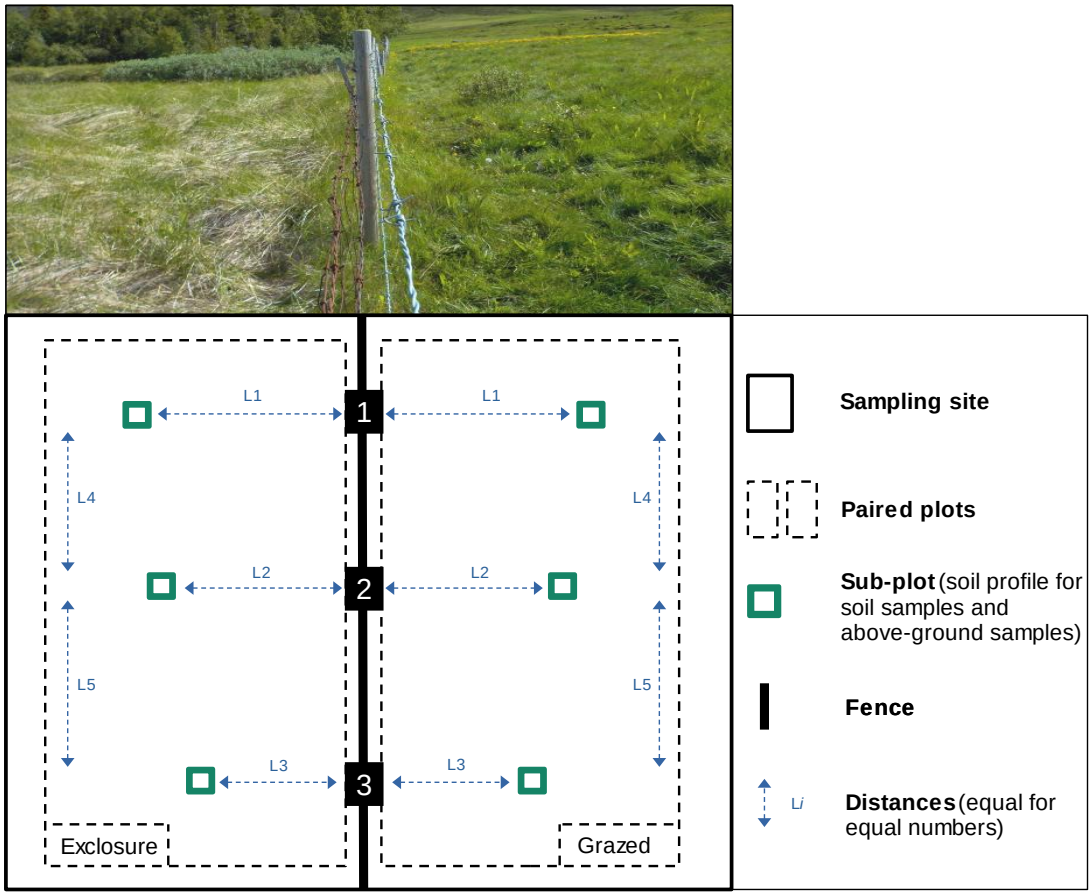

Supplemental Figure 8-16: Study design at each sampling site with one soil profile per sub-plot. Photograph was taken by Christian Klopsch.

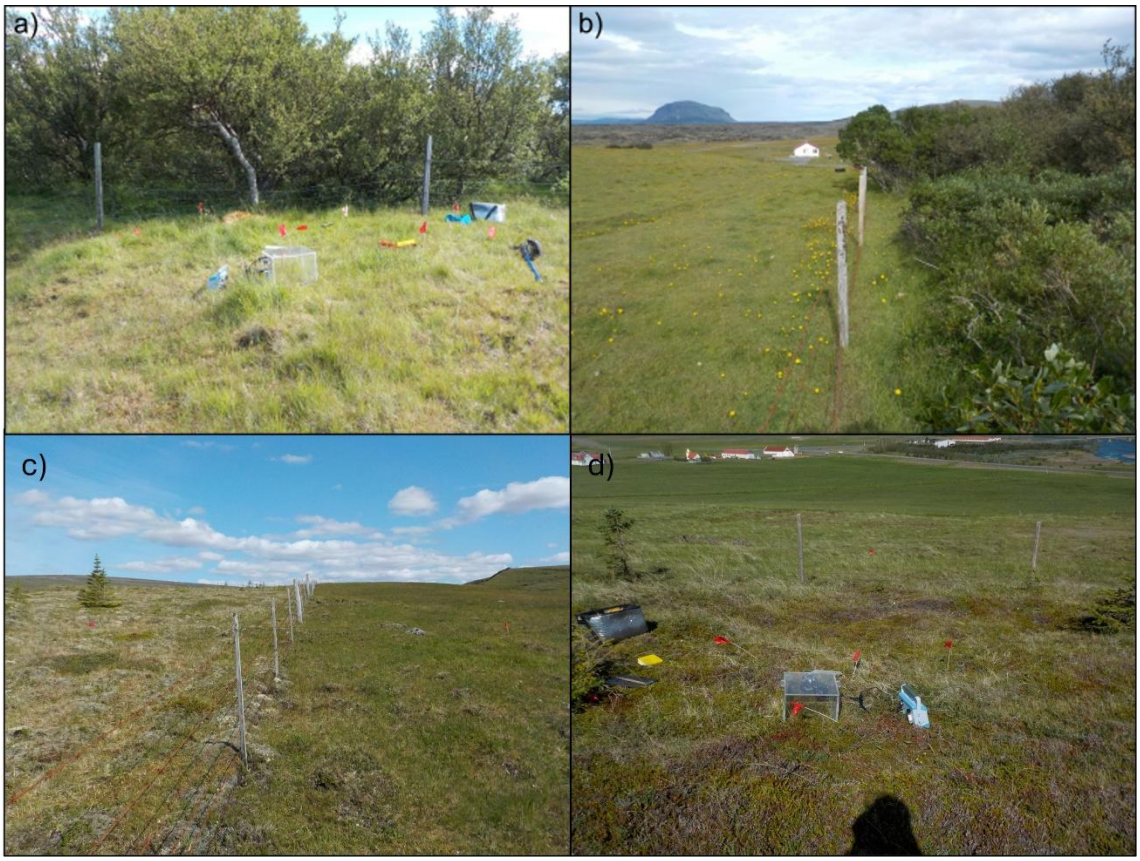

Supplemental Figure 8-17: Succession sites in this study. Birch woodland succession at two sites from grassland in the grazed plot to mature birch woodland in the ungrazed plot 63 (a) and 80 years (b) after grazing had ceased. In contrast to other succession sites, grassland developed into birch woodland and not into heathland at these sites because of mature birch woodland, serving as seed sources, in the proximity of these two sites in southern Iceland but no heathland. At other succession sites, birches were rare or absent in the vicinity and heath, dwarf shrubs and mosses were more abundant, facilitating development of heathland following > 20 years of grazing cessation (c, d). Photographs were taken by Christian Klopsch.

Supplemental Figure 8-18: Exemplary soil profile to recover soil samples with the depth profile down to 60 cm (a) and after sampling of the whole soil column (b). Note the black bands throughout the profile which are tephra deposits from past volcanic eruptions. Photographs were taken by Christian Klopsch.

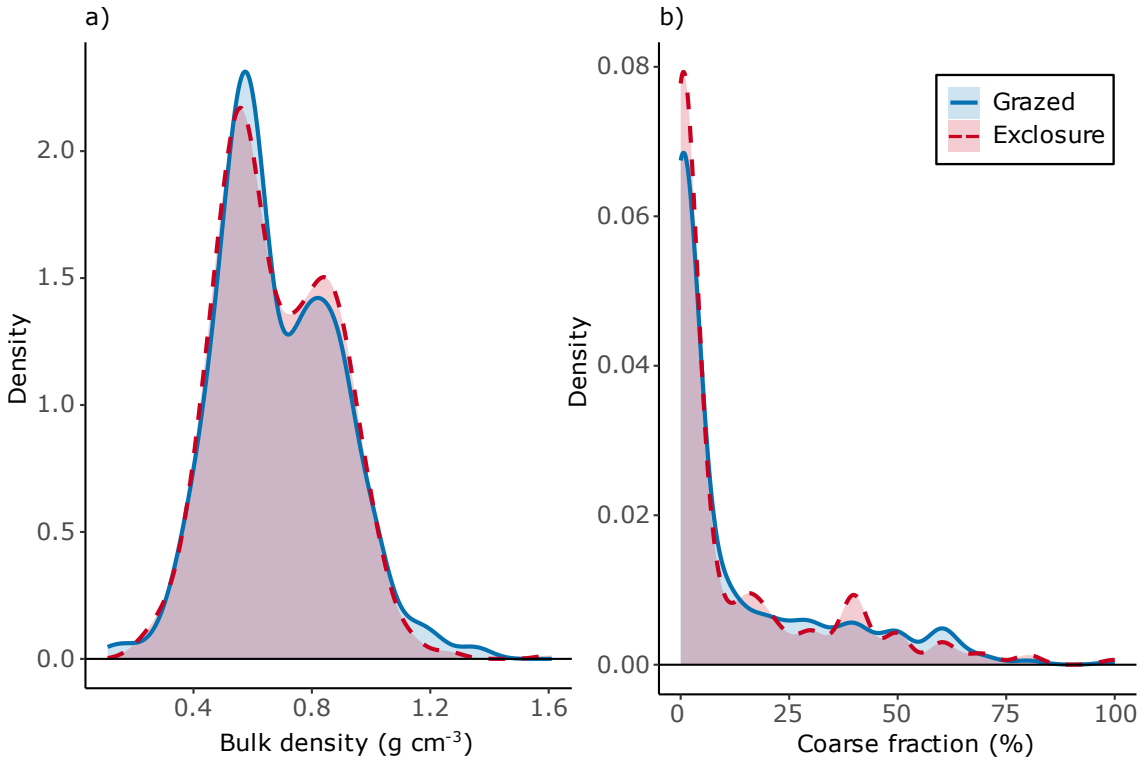

Supplemental Figure 8-19: Frequency distribution of bulk density (a) and coarse fraction (b) across soil samples.

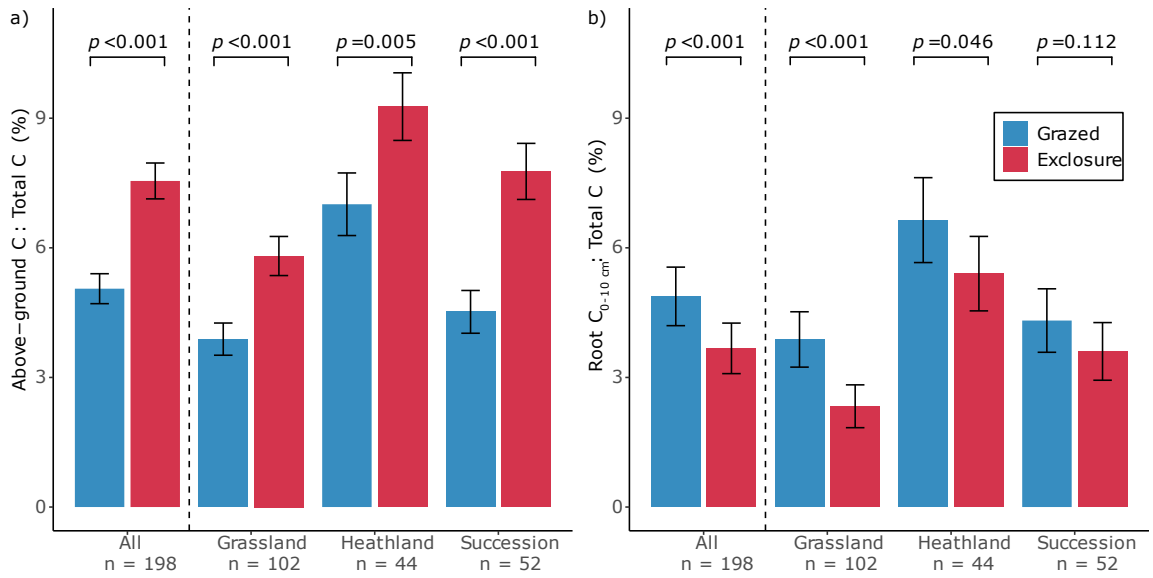

Supplemental Figure 8-20: Fraction of biomass C in total C. Mean fraction of above-ground carbon (C) in total carbon ($SOC_{0\text{-}60\ cm}$ + $C_{root\ 0\text{-}10\ cm}$ + $C_{above\text{-}ground}$) in % (a) and mean fraction of root C in total C in % (b) across all sites, and for each vegetation type (n = number of samples included per category). P-values indicate significant differences with grazing cessation as derived from least-squares mean post-hoc tests and error bars represent standard error.

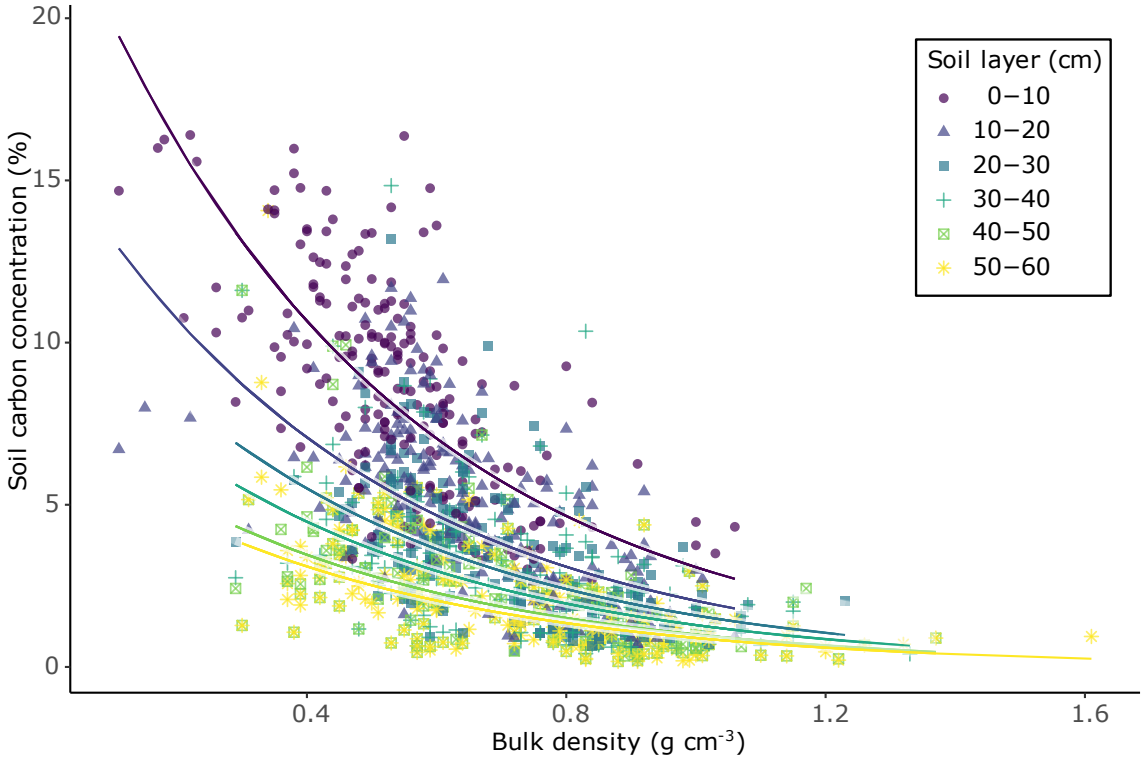

Supplemental Figure 8-21: Regression of bulk density and SOC concentration. For each 10 cm depth interval between 0-60 cm a separate non-linear regression curve was calculated with an exponential decay function between bulk density and SOC concentration. SOC concentration decreased with depth while bulk density increased with depth.

Appendix 5: Supplemental Information for Chapter VI

Supplemental Table 8-10: Summary table of sampling site information with vegetation classification for this study.

Site ID	Region	Elevation m a.s.l.	Exclosure years	Bedrock age (10^6 years)	Vegetation type
Alf	N	186	52	>3.3	Grassland
Ber	N	190	42	>3.3	Grassland
Gil	W	183	33	0.8 - 3.3	Heath succession
Gsk	N	67	22	>3.3	Grassland
Gun	E	5	34	>3.3	Heath succession
H43	S	110	80	<0.8	Birch succession
H60	S	95	63	<0.8	Birch succession
Hau	S	102	33	<0.8	Grassland
Hja	E	6	80	>3.3	Heath succession
Holl	W	74	45	>3.3	Heath succession
Holt	E	52	30	>3.3	Heathland
Hva	S	76	23	<871 AD	Grassland
LL	N	32	52	>3.3	Grassland
Lei	E	20	72	<0.8	Heathland
Lun	W	67	68	>3.3	Grassland
Mel	W	13	28	>3.3	Grassland
Mh	N	48	27	>3.3	Grassland
Odd	W	64	43	>3.3	Grassland
Orl	N	40	52	>3.3	Grassland
Pho	E	25	22	<871 AD	Grassland
Phv	E	45	42	<0.8	Heath succession
Reyk	E	198	42	0.8 - 3.3	Heathland
Rod	N	118	52	>3.3	Heathland
SA	W	98	23	<0.8	Heath succession / Grassland
SB	N	174	60	>3.3	Grassland
Sk40	S	165	83	<871 AD	Heathland
Sk90	S	165	33	<871 AD	Heathland
Skb	E	52	42	<0.8	Heathland
Skl	S	144	33	<871 AD	Grassland
Skr	N	70	66	>3.3	Heath succession / Grassland
Stein	W	63	23	>3.3	Grassland
Thor	W	59	43	>3.3	Grassland
Vatn	W	122	71	>3.3	Grassland
Vid	E	41	22	>3.3	Heathland

Supplemental Table 8-11: Summary table of model statistics for all linear mixed effects models used in the study. Random effects in the biomass models were 'sub-plot' nested in 'site' and 'region' and in the root trait models 'sub-plot' nested in 'site' and 'scanner'. For abbreviations of root traits, see Table 6-1. Prop. = Proportion, RMF = root mass fraction.

	Grazing cessation (G)		**Vegetation type (V)**		**G×V**	
Response	**df**	***F***	**df**	***F***	**df**	***F***
Total root$_{0\text{-}60}$	1, 97	**5.0***	3, 98	**8.5*****	3, 98	1.0
Fine root$_{0\text{-}60}$	1, 97	**8.9****	3, 98	**2.8***	3, 97	**2.6***
Fine root$_{0\text{-}10}$	1, 96	**13.6*****	3, 98	2.0	3, 97	**3.7***
Fine root$_{10\text{-}20}$	1, 192	1.9	3, 192	2.2· (p=0.08)	3, 192	0.8
Fine root$_{20\text{-}40}$	1, 94	0	3, 96	1.4	3, 95	1.3
Fine root$_{40\text{-}60}$	1, 93	0.9	3, 96	0.4	3, 94	0.7
Coarse root$_{0\text{-}60}$	1, 97	**10.0****	3, 99	**23.1*****	3, 98	**3.8***
Coarse root$_{0\text{-}10}$	1, 97	**7.8****	3, 99	**31.4*****	3, 98	**4.7****
Coarse root$_{10\text{-}20}$	1, 97	**6.3***	3, 99	**2.8***	3, 97	0.7
Coarse root$_{20\text{-}40}$	1, 95	0	3, 98	1.6	3, 96	1.6
Coarse root$_{40\text{-}60}$	1, 89	0.2	3, 90	2.5· (p=0.07)	3, 90	0.4
Fine root prop.	1, 97	**6.3***	3, 98	**28.5*****	3, 98	**7.2*****
Prop. 0-10 cm	1, 94	**17.6*****	3, 97	1.7	3, 95	**3.8***
Total plant biomass	1, 97	2.5	3, 98	**11.4*****	3, 98	1.2
Above-ground biomass	1, 94	**23.0*****	3, 95	**10.7*****	3, 94	2.0
RMF	1, 93	**32.1*****	3, 94	2.6· (p=0.058)	3, 94	**3.3***
RLD$_{0\text{-}10}$	1, 96	**19.7*****	3, 96	1.7	3, 96	**3.2***
RLD$_{10\text{-}60}$	1, 97	0	3, 99	**3.8***	3, 98	0.9
Mean root diameter$_{0\text{-}10}$	1, 97	**7.2****	3, 96	0.7	-	-
Mean root diameter$_{10\text{-}60}$	1, 95	0	3, 98	1.2	3, 95	1.3
SRL$_{0\text{-}10}$	1, 101	0.1	3, 101	0.4	3, 99	0.9
SRL$_{10\text{-}60}$	1, 100	**10.4****	3, 98	**4.2****	-	-
SRA$_{0\text{-}10}$	1, 96	1.8	3, 96	0.6	3, 95	1.1
SRA$_{10\text{-}60}$	1, 97	**9.2****	3, 99	**3.8***	3, 98	0.2
RTD$_{0\text{-}10}$	1, 96	1.5	2, 95	1.5	3, 94	2.3· (p=0.09)
RTD$_{10\text{-}60}$	1, 97	3.6· (p=0.06)	2, 99	1.4	3, 97	0.5

Significance codes: '***' < 0.001; '**' < 0.01; '*'< 0.05; '·' < 0.1

Supplemental Table 8-12: Pearson correlation matrix between vegetation parameters: including above-ground biomass (AGBM), below-ground biomass (BGBM), root functional traits (RLD = root length density, RD = mean root diameter, RTD = root tissue density, SRL = specific root length, SRA = specific root area) and soil carbon concentration (%C soil) in 0 – 10 and 10 – 60 cm soil. Factors were log-transformed if needed to meet normality assumption. Significant correlations are indicated by bold numbers and asterisks, positive correlations are highlighted in blue while negative correlations are highlighted in red.

0-10 cm	BGBM†	AGBM†	RLD†	RD†	RTD†	SRL	SRA	%C soil
BGBM†	-	*	***	***	*			**
AGBM†	**-0.17**	-	*					
RLD†	**0.9**	**-0.15**	-	*	***	***	***	**
RD†	**0.27**	-0.07	**0.14**	-	***		***	*
RTD†	**-0.14**	0.05	**-0.42**	**-0.47**	-	***	***	*
SRL	-0.1	0.04	**0.33**	**-0.25**	**-0.61**	-	***	
SRA	-0.03	-0.05	**0.4**	**0.17**	**-0.86**	**0.88**	-	
%C soil	**0.21**	-0.09	**0.19**	**0.18**	**-0.16**	-0.03	0.06	-

10-60 cm	BGBM†	AGBM†	RLD†	RD†	RTD†	SRL	SRA	%C soil†
BGBM†	-	*	***	**		***	***	**
AGBM†	**-0.16**	-				**	**	
RLD†	**0.82**	0.05	-		*	*	*	***
RD†	**0.23**	0.01	-0.03	-	***	***		
RTD†	-0.04	0.12	**-0.14**	**-0.61**	-	***	***	
SRL	**-0.37**	**-0.21**	**0.17**	**-0.5**	**-0.28**	-	***	
SRA	**-0.27**	**-0.23**	**0.18**	0.08	**-0.74**	**0.81**	-	
%C soil†	**0.18**	0.11	**0.24**	-0.1	0.05	0.07	0.03	-

Significance codes: '***' < 0.001; '**' < 0.01; '*'< 0.05; '·' < 0.1

† log-transformed

(continued)

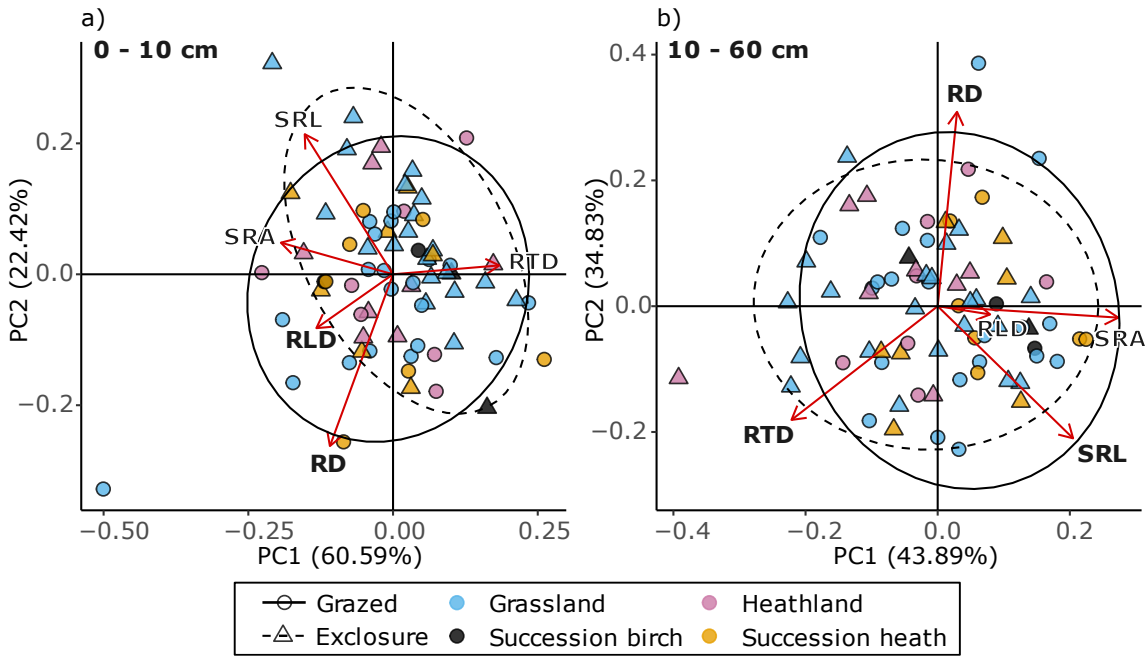

Supplemental Figure 8-22: PCA, based on five community-level root functional in 0-10 cm soil depth (a) and the average of 10-60 cm soil depth (b). The length of the arrows refers to the importance of the respective traits to explain variance in the data traits (see Table 6-1 for explanation of the traits). Percentage values of PC1 and PC2 refer to the variance explained by the respective principal component axis.

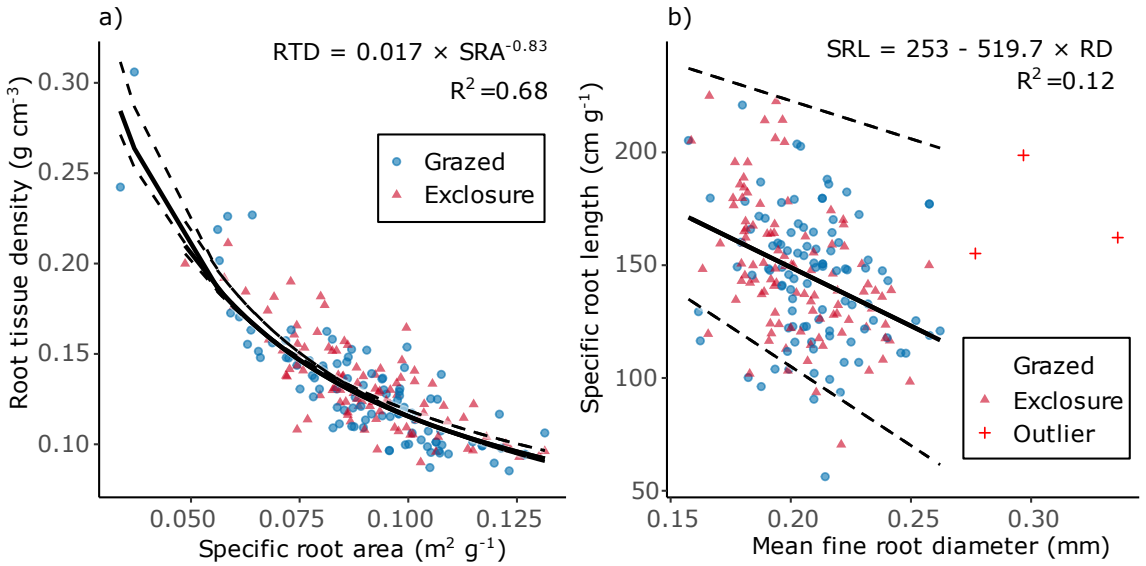

Supplemental Figure 8-23: Major trade-off axes in root functional traits. Specific root area (SRA) and root tissue density (RTD) had a negative relation, following a power equation for complete root profiles in 0-60 cm (a). Mean fine root diameter (RD) and specific root length (SRL) had a negative relation, following a linear regression, when three outliers were removed (red crosses) (b). Grazing cessation had no effect on both relations.

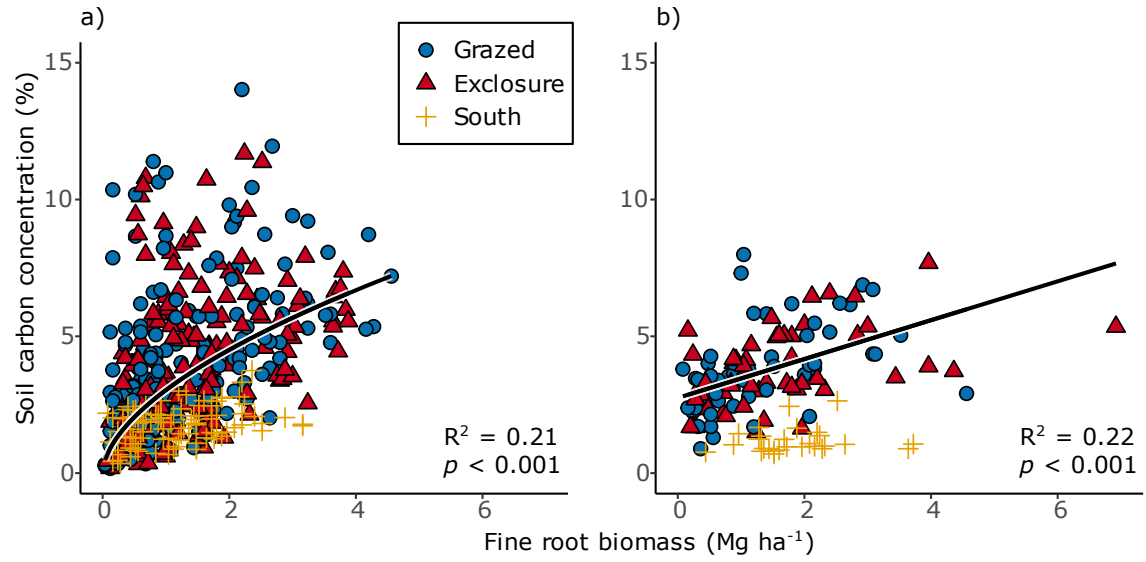

Supplemental Figure 8-24: Association between soil carbon concentration and fine root biomass in 10-60 cm soil in grassland, including birch and heath succession (a) and heathland (b). In grassland the relation follows a positive log-linear regression and in heathland a positive linear regression. Samples from sites in southern Iceland (yellow crosses) were excluded due to a poor relation between fine root biomass and soil carbon concentration. The cessation of grazing had no influence on the relationships.

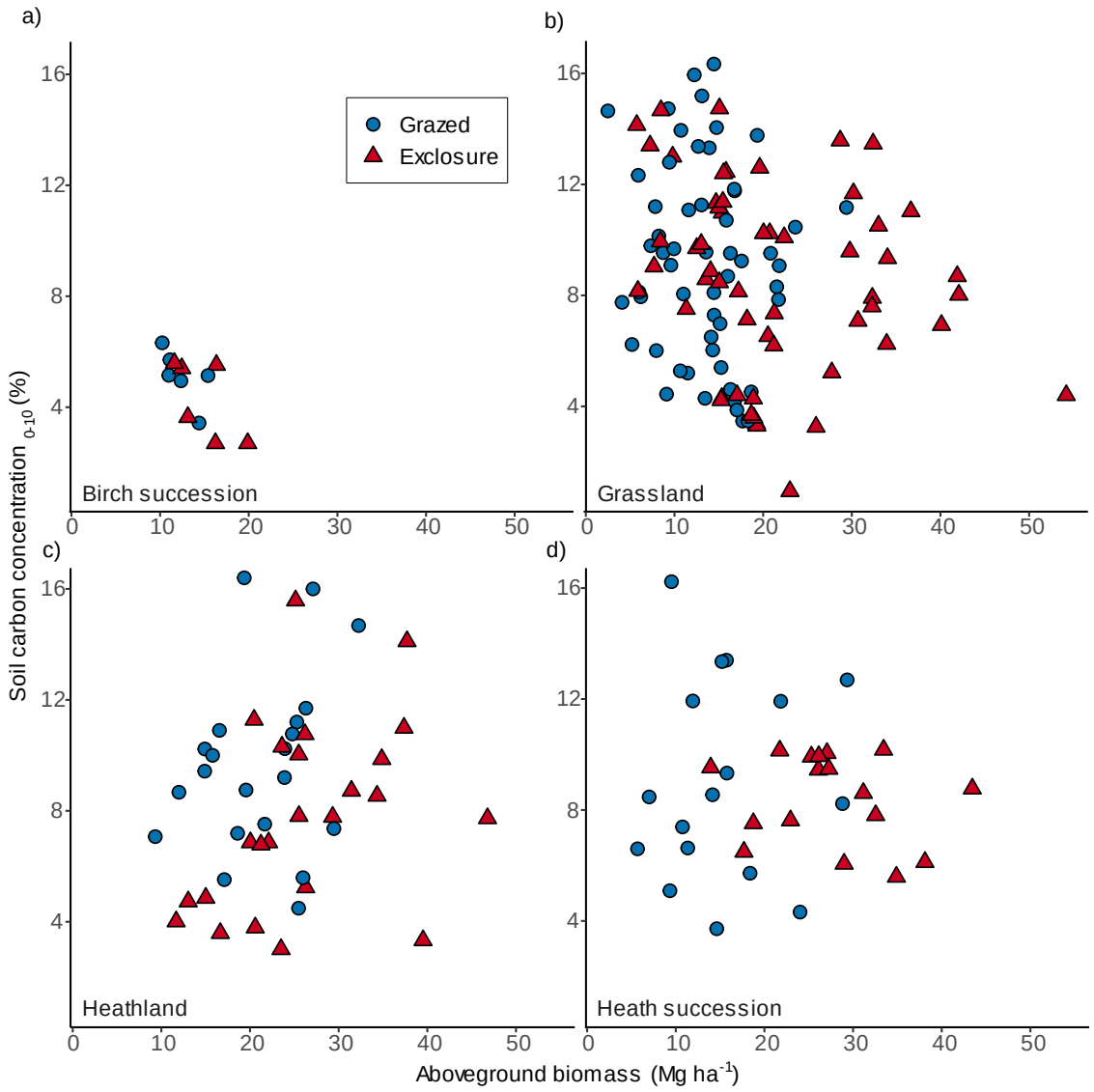

Supplemental Figure 8-25: Scatterplots for above-ground biomass vs. soil carbon concentration in 0-10 cm soil in all four vegetation types of this study. In none of the vegetation types, regardless of grazed or not, above-ground biomass was a predictor for soil carbon concentration.

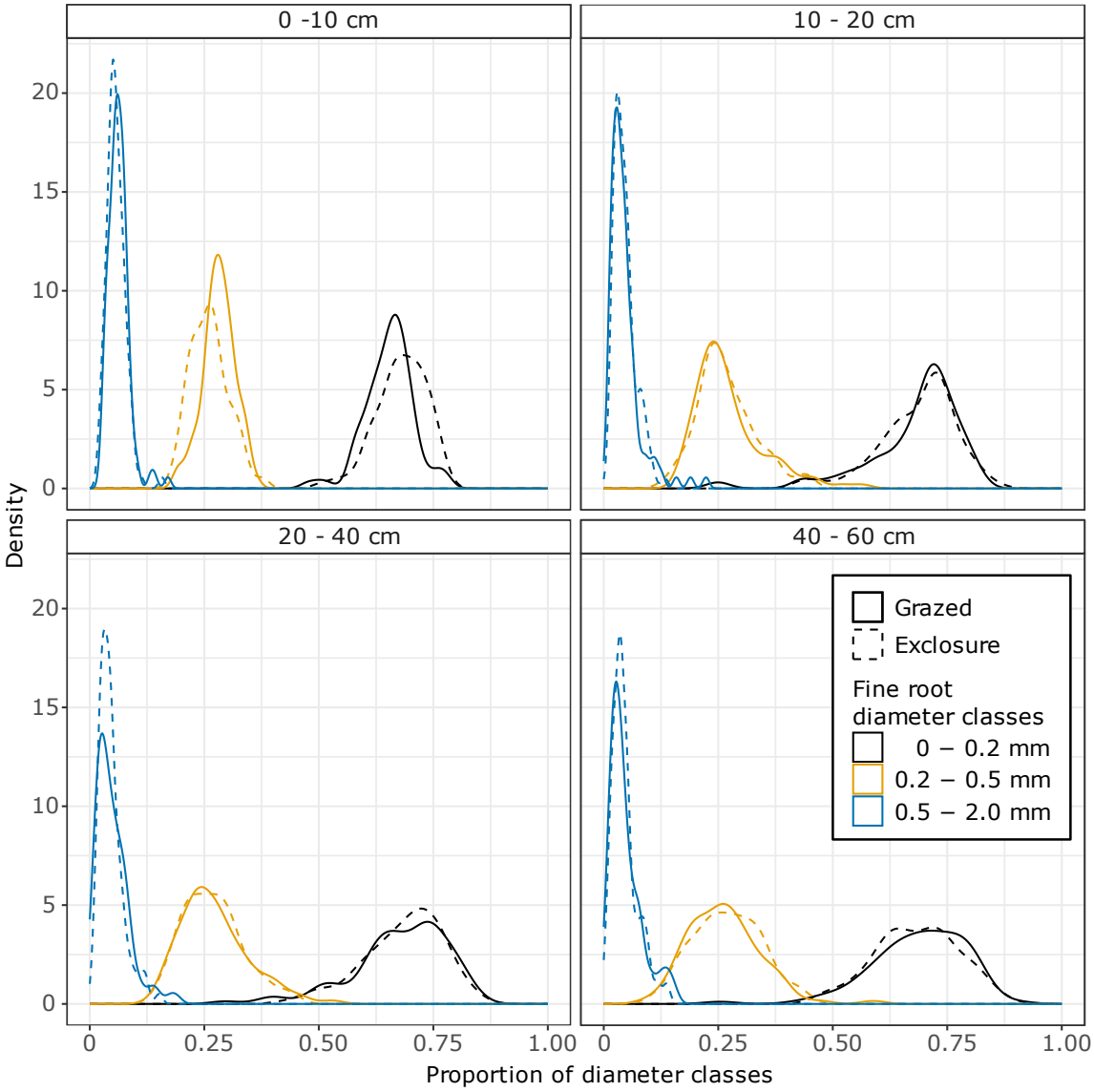

Supplemental Figure 8-26: Density graph of fine root diameter class distribution. Three root diameter classes were separated in the four sampled soil depth intervals and for grazed and exclosure plots, based on root length per diameter class. Density in the y-axis refers to the count of the respective proportion. The smallest fine root diameter class (< 0.2 mm) had consistently the largest proportions across samples in all depth intervals.